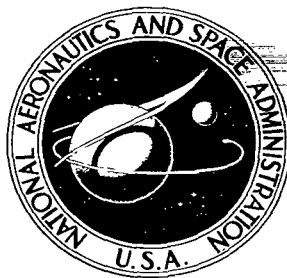


**NASA TECHNICAL  
TRANSLATION**



**NASA TT F-637**

2.1



**LOAN COPY: RETURN TO  
AFWL (DOGL)  
KIRTLAND AFB, N. M.**

NASA TT F-637

# AURORAS

Collection of Articles No. 17

*Edited by S. I. Isayev and Ya. I. Fel'dshteyn*

*"Nauka" Press, Moscow, 1968*



0069170

NASA TT F-637

**AURORAS**

Collection of Articles No. 17

Edited by S. I. Isayev and Ya. I. Fel'dshteyn

Translation of "Polyarnyye Siyaniya. Sbornik Statey, No. 17"  
"Nauka" Press, Moscow, 1968

**NATIONAL AERONAUTICS AND SPACE ADMINISTRATION**

For sale by the National Technical Information Service, Springfield, Virginia 22151  
\$3.00



## ABSTRACT

This collection of papers deals with the planetary morphology of oval auroral zones at varying levels of magnetic disturbances, aurora height in circumpolar areas, the variations of the auroral height with variations of planetary magnetic disturbances, the morphology of U-like auroras, as well as height variations of certain emissions. Auroras observed in years of minimal and maximal polar activity (latitude distribution, auroral motion, the orientation of elongated shapes) are compared. A system for the computerization of visual observation data of auroras, as used by the meteorological network of the USSR, is detailed. Investigation reports, covering a number of geophysical phenomena, which accompany the intrusion of high energy particles into the upper layers of the atmosphere, are included. Variations of x-ray radiation in the stratosphere are described.

This book is intended for students of ionospheric auroras and of the variable magnetic field of the Earth.





# TABLE OF CONTENTS

	<u>Page</u>
A Comprehensive Investigation of the Polar Ionosphere ----- L. S. Yevlashin, S. A. Zaytseva, G. A. Loginov, G. A. Petrova, M. I. Pudovkin, Z. Ts. Rapoport, V. K. Roldugin, N. S. Smirnov, G. V. Starkov, P. Ya. Sukhoivanenko, N. V. Shul'gina	1
The Polar Auroral Band During Magnetic Disturbances----- G. V. Starkov and Ya. I. Fel'dshteyn	28
U-Like Polar Auroral Shapes ----- S. A. Zaytseva	48
The Effect of Magnetic Activity Upon Auroral Heights ----- G. V. Starkov	56
Auroral Pulsations ----- V. K. Roldugin	63
Polar Aurora at the Minimum or Maximum Cycle of Solar Activity ----- Ya. I. Fel'dshteyn, L. V. Kukina, and N. F. Shevnina	72
The Ratio of 1 NGO <sub>2</sub> <sup>+</sup> and 1 PCN <sub>2</sub> Emissions as a Function of Auroral Height----- V. K. Roldugin	87
Ionospheric Processes Associated with Auroral Height Variations ----- P. Ya. Sukhoivanenko	90
The Effect of Quasirhythmicity in Geomagnetic and Aeronomic Phenomena-- G. P. Tsirs	96
The Energy Balance of a Magnetic Storm ----- B. Ye. Bryunelli, M. I. Pudovkin	117
Quiet Solar Day Variations of the Geomagnetic Field During the IGY ----- IV. Variations at High Latitudes A. N. Zaytstev, and Ya. I. Fel'dshteyn	128
Geomagnetic Disturbances at High Latitudes -- June 1965 ----- I. A. Kuz'min, L. L. Lazumin, G. A. Loginov, M. I. Pudovkin, A. I. Charakhch'yan, T. N. Charakhch'yan	146

Dynamics of Magneto-Ionospheric Disturbances in the Polar Auroral Zone -----	161
G. A. Loginov and M. I. Pudovkin	
Latitudinal Variability of Ionospheric Parameters -----	169
A. P. Kolobova, B. P. Los' and Z. Ts. Rapoport	
High Altitude Velocity Distribution of Ionospheric Drift and Strength of the Electric Field in the F2 Layer -----	186
R. S. Sadobnikova	
Problems of Auroral Absorption -----	193
O. I. Shumilov	
Magnetic Activity at High Latitudes of the Northern Hemisphere During the Maximum and Minimum of the Solar Cycle -----	203
R. G. Afonina and Ya. I. Fel'dshteyn	

### Abbreviation List

lg = log

0<sup>h</sup> 0<sup>m</sup> = 0<sup>hours</sup> 0<sup>minutes</sup>

LGT = local geomagnetic time

IQSY = International Year of Quiet Sun

UT = universal time

SPV = short period variation

VLFE = very low frequency emissions

VHF = very high frequency field

TI = tact interval

QR = quasirhythmoid

CG = center of gravity

## A COMPREHENSIVE INVESTIGATION OF THE POLAR IONOSPHERE

L.S. Yevlashin, S.A. Zaytseva, G.A. Loginov, G.A.  
Petrova, M.I. Pudovkin, Z. Ts. Rapoport, V.K. Roldugin,  
N.S. Smirnov, G.V. Starkov, P. Ya. Sukhoivanenko,  
N.V. Shul'gina

The paper presents results of simultaneous observations on a vertical sounding station and by riometers, operating on several frequencies, of the state of ionosphere of the variations of the electromagnetic field of the Earth and of the intensity of the spatial position and spectrum of aurora. The paper discusses the spatial connection of electric currents in the ionosphere, aurora and ionospheric inhomogeneities ( $E_s$  layer and the region of the enhanced radiowaves absorption). The paper analyses the frequency dependence of absorption of cosmic radioemission and its variants depending on the form of aurora and on the depth of penetration of ionizing radiation. The relative intensity of streams of auroral protons and electrons is evaluated. The paper also discusses the microstructure of geomagnetic disturbances connected with active and quiet forms of aurora.

In spite of the large number of reports which establish a close correlation /5\* between auroras and geomagnetic and ionospheric disturbances [1 - 5], the detailed relationship between these phenomena has as yet not been clarified. Notably, auroras, and geomagnetic bays are usually accompanied by the appearance of sporadic formations of the  $E_s$  layer level. However, until now it has not been established whether the regions of auroral glows and increased ionization, which produces the radio echo on the ionograms, do indeed coincide spatially.

It is not entirely clear at what height the region of increased ionization responsible for radio wave absorption in auroral zones during geomagnetic

---

\*Numbers in the margin indicate pagination in the original foreign text.

disturbances is located, nor do we know how this region is related to simultaneously observed auroras and the  $E_s$  layer. The problem becomes considerably complicated because differently shaped auroras are apparently caused by the intrusion of corpuscular streams with different energy spectra, and are accompanied by the emergence of increased ionization at different heights. Moreover, the energy spectrum of the intruding corpuscles and, consequently, their penetration depth, may vary during a single disturbance, the laws governing the variations being unknown.

The investigation of auroral optical spectra reveals the presence of hydrogen emissions. The relative intensity of these emissions indicates that the proton stream is usually much less intense than the electron stream [6]. This conclusion is supported by direct measurements of intruding proton particle streams, using rockets [7, 8]. However, the energy of the intruding protons, computed from rocket data, is at least by one order of magnitude greater than the energy determined from the magnitude of the Doppler shift of hydrogen lines in the auroral spectrum [9]. In view of this, the problem regarding the relative role of the proton and electron streams cannot be considered solved, and additional investigations in this direction are of distinct interest.

#### Experimental Findings

The close relationship and reciprocity of the aforementioned geophysical phenomena determine to a certain degree the methods to be applied in their investigation. Only simultaneous and detailed investigation can further widen our knowledge regarding the character and nature of physical processes in the ionosphere, which are related to the intrusion of corpuscular streams into the upper layers of the Earth's atmosphere. In view of this, the Polar Geophysical Institute initiated the use of the following methods of complex investigation of the disturbed ionosphere. /6

1. Vertical ionospheric sounding, using a panoramic ionospheric station.
2. Measuring radio wave absorption in the ionosphere by the radio-astronomy method A2 at a series of frequencies.

3. Registration of the Earth's electromagnetic field variations, using equipment with varying sensitivity and varying rate of photographic paper processing.

4. Auroral photography, using C-180 cameras.

5. Photography of auroral spectra by SP-48 high-dispersion spectrographs covering the spectral range from 4,100 to 6,800 Å, and by a patrol spectrograph C-180-S.

6. Auroral intensity registration in integral light, using a zenith photometer.

7. Studying the spatial brightness distribution of auroras in the emissions of 4278, 5300, 5577, 5893, and 6300 Å, using a scanning photometer with a 3° angle of vision and the rate of scanning of the celestial hemisphere at 8 seconds per filter.

8. Measuring the auroral height by triangulation as both by photographs taken with C-180 cameras and by using visual sounding of the auroral angular height.

The observation stations were located in Murmansk ( $\phi = 68^{\circ}57' \text{ N}$ ;  $\lambda = 33^{\circ}05' \text{ E}$ ) and in Loparskaya, which is 37 km south of Murmansk. The angular distance between these two stations is 20.4 of the arc of the large circle, rather than 24', as erroneously indicated in [10]. The direction Loparskaya - Murmansk makes a 14° angle westward with respect to the geographic meridian. Theodolites with sighting devices were used for the visual sounding of auroral angular heights. Auroral heights were taken from nomograms, calculated from formulae, as suggested in [10]. The observations were synchronized, using direct radio-telephonic communications between the observation stations.

Two nights were selected for observations: 2-3 and 6-7 March 1965; during the first night, a moderate geomagnetic polar storm took place, whereas a small geomagnetic storm occurred during the second night.

The ionospheric processes during those two nights developed as follows:

On 2 March, auroras became apparent immediately at dusk. At 16<sup>h</sup> 53<sup>m</sup> (here and below, we are referring to world time), an aurora appeared at the northern horizon; it soon took the shape of an arc which began to rise above the horizon. At 17<sup>h</sup> 26<sup>m</sup>, the auroras reached the zenith and, up to 21<sup>h</sup>, while the sky was clouded, there were dynamic radiant auroras with varying brightness reaching a strength of 3. After 21<sup>h</sup>, there was precipitation in the form of snow; however, auroras were still apparent in the northern direction through the clouds.

On 6 March, auroras began at 19<sup>h</sup> 20<sup>m</sup>. In the north a uniform arch formed, which, gradually becoming stronger, approached the zenith. 20<sup>h</sup>, radial shapes became apparent and auroras occupied the major part of the sky. Beginning at 21<sup>h</sup> 40<sup>m</sup>, the auroras became weaker, and by 1<sup>h</sup> 20<sup>m</sup> they were totally extinct. Prior to their disappearance, some pulsating spots were apparent in the sky for a short while. During this day, height measurements of aurora were performed starting only from 20<sup>h</sup> 30<sup>m</sup>. The height of the arc, far in the north (60 - 70° from the zenith), was measured. Meanwhile, weak but extensive diffused surfaces and glows were observed at the zenith.

Figure 1, a shows the curves of the electrophotometric sections of the glow intensity of the Murmansk-Loparskaya direction. The solid curve defines the glow intensity section in the emission 4278 Å (0.1) 1NGN<sub>2</sub><sup>+</sup>. This is an adequately wide band, well centered with respect to the filter's pass band. The dashed line defines the transition to the non-linear region of the scale, /8 where it was difficult to determine its magnitude with sufficient accuracy. The dotted curve defines the auroral intensity section in a filter centered at 5900 Å with a half-width of about 100 Å. There is a relatively strong NaI line in this region, but its intensity should not change notably as a function of auroral activity, and hence, in the presence of aurora, the biggest contribution to the glow in this filter is provided by N<sub>2</sub> bands: (10.6) 1 PG and (8.4) 1 PG. The total intensity of these bands with a glow force of 2 may reach 2 kpel [11 - 13]. These bands are usually excited by electrons and are related to low B-type auroras. Figure 1b shows the relative magnitude of ionospheric absorption of cosmic radio-frequency radiation for four frequencies



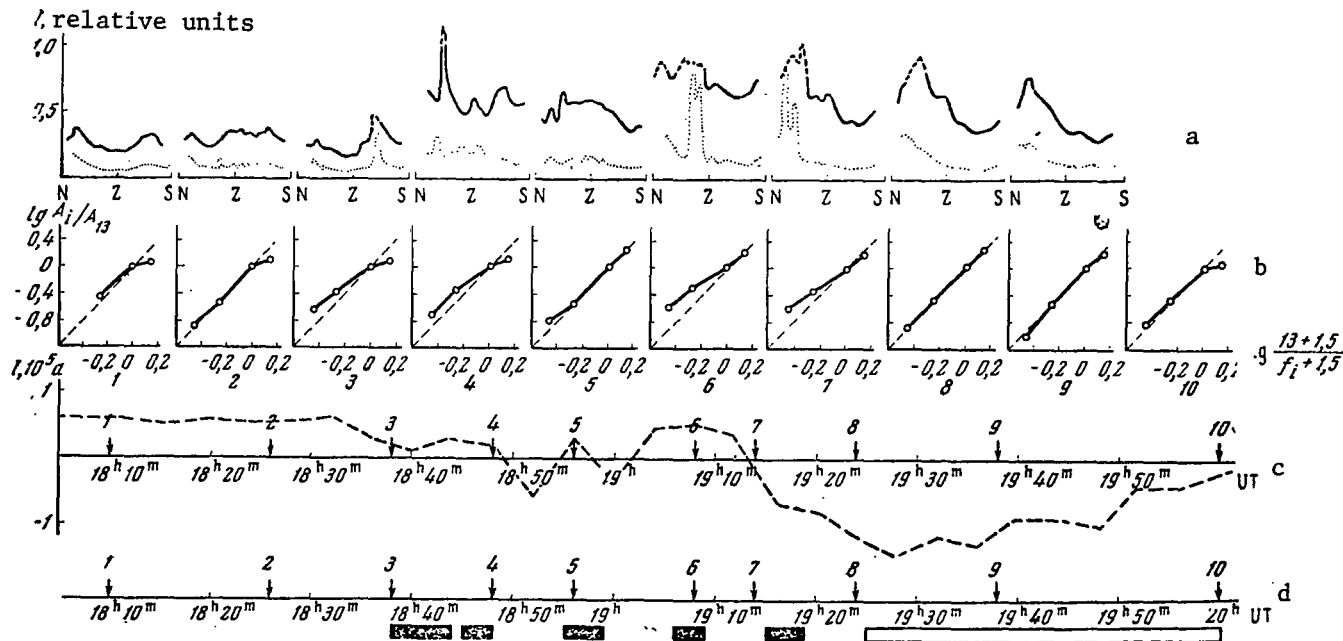


Figure 1. The development of aurora, magnetic and ionospheric disturbances on March 2, 1965 at various times (numeration is Arabic numerals; graphs c and d show the time by arrows).

- a - Auroral brightness distribution along the meridian in filters 4280 Å (solid line), and 5900 Å (dotted line);
- b - Relationship between the riometric absorption and the frequency;
- c - Intensity of electrical currents in the ionosphere;
- d - Observation time of various short-period variations; the blackened rectangles refer to  $P_{12} + P_{1c}$ , the light rectangles refer to  $P_{1l}$ .

(9, 13, 25, and 40 Mc). The dotted line reflects the quadratic frequency relationship. The slope angle of the experimental curve yields the actual index of the extent of the frequency relationship. The frequency of the gyromagnetic electron precession ( $f_H = 1.5$  Mc) was taken into account during the calculations.

Intensity variations of the equivalent electrical current in the ionosphere, obtained from magnetic data, are shown in Figure 1c. In compiling these data, it was assumed that the current flows as a 200 km wide homogenous band, at a height of 100 km.

Short-period variations of various types, observed in the geomagnetic field, are shown on Figure 1d.

At 18<sup>h</sup> 10<sup>m</sup>, the aurora died out, even though remains of radial shapes were still visible in the west. The absorption of cosmic radio interference at a frequency of 9 Mc amounted to about 2 db. This moment is defined by a near-quadratic relationship between the absorption and the frequency, and by weak glow of the 4278 Å emission. This glow goes up somewhat at the horizons, presumably due to the Van Rein effect. By 18<sup>h</sup> 26<sup>m</sup>, the nature of the glow and the frequency relationship still remained practically unchanged, even though at a frequency of 9 Mc the absorption went up to 4 db. Filamentary aurora appeared at the zenith; no 1 PGN<sub>2</sub> bands were observed. This period has a moderate and positive magnetic disturbance with only minute quantitative changes. At 18<sup>h</sup> 38<sup>m</sup>, a radiant arc was formed in the south. At this time in the magnetic field, a transition through zero began in the horizontal component, and a burst of short-period variations was observed. Bands of 1 PGN<sub>2</sub> appeared, and the power index (n) of the frequency relationship of riometric absorption decreased. The absorption itself was relatively small (about 1.5 db for 9 Mc). By 18<sup>h</sup> 48<sup>m</sup>, the value of n, as compared to the previous observations, had changed very little, even though extremely bright glows, encompassing the entire sky, were noted. The absorption meanwhile went up to 10 db. At 18<sup>h</sup> 56<sup>m</sup>, in spite of the fact that the absorption and the glow intensity were still high, n became equal to two. Simultaneously, the 1 PGN<sub>2</sub> glow decreased considerably.

At 19<sup>h</sup> 24<sup>m</sup> and 19<sup>h</sup> 38<sup>m</sup>, the discrete shapes disappeared and only a glow remained in the northern sector of the firmament. While this glow was relatively strong, it had a very weak 1 PGN<sub>2</sub>, and the relationship between absorption and frequency was purely quadratic. The 1 PGN<sub>2</sub> glow, which was gradually dying off, was observed only at the horizon. At this point, the electrical current in the ionosphere reached a considerable magnitude of about  $1.4 \times 10^5$  A. The absorption level also went up significantly: maximum 9 db at a 9 Mc frequency. Simultaneously, the nature of short-range variations of the geomagnetic field also changed. At 20<sup>h</sup>, the current intensity and the absorption decreased ( $A \approx 2.7$  db at a frequency of 9 Mc). Filamentary arc-shaped aurora were concentrated in the northern half of the sky. No scanning photometer data regarding this moment are available. There was some deviation from the quadratic relationship between the absorption magnitude and the frequency.

The data, shown in Figure 1, lead to the conclusion that the exponent of the frequency relationship  $n$  and the micropulsation nature of the geomagnetic field are closely related to the auroral shape and to the relative glow intensity of the first positive N<sub>2</sub> system. For practical purposes, they are independent of the absorption magnitude and of the overall auroral intensity. In two instances (at 18<sup>h</sup> 40<sup>m</sup> and 19<sup>h</sup> 10<sup>m</sup>) during the observation period, there were acute decreases of  $n$ ; they lasted 10 - 15 minutes and were accompanied by a strengthening of the 1 PGN<sub>2</sub> emission. A more detailed analysis of the obtained data is given below. /9

#### The Relationship Between Aurora and Electrical Currents in the Ionosphere

We will now analyze the spatial relationship between auroras and electrical currents in the ionosphere. The central graph in Figure 2 shows the cg position of the current layer with reference to the zenith during the disturbance on 2 March. The cg position of the current system was determined from the slope angle of the vector of the magnetic disturbance. The field of currents, induced in the Earth, was not taken into account due to the low conductivity of the upper Earth layers on the Kola peninsula [14].

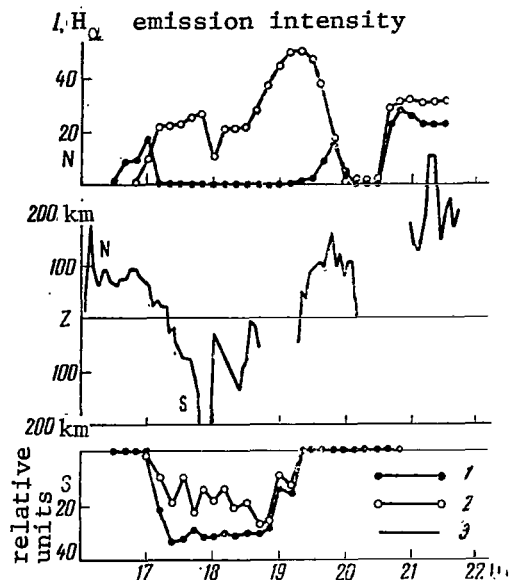


Figure 2. Relationship between aurora and electrical currents in the ionosphere.

1.  $H_{\alpha}$  emission intensity;
2.  $1 \text{ PGN}_2$  emission intensity;
3. Position of electrical currents;

The diagram shows that the time dependence of  $H_{\alpha}$  and  $1 \text{ PGN}_2$  emissions is not always identical. This generally indicates that their excitation is independent. Moreover, it agrees with the generally accepted assumption, i.e., if the presence of hydrogen emission in auroras indicates the intrusion of protons into the ionosphere, then  $1 \text{ PGN}_2$  is usually caused by electron intrusion.

A comparison of the intensity pattern of  $H_{\alpha}$  and  $1 \text{ PGN}_2$  at different points of the firmament fosters specific conclusions regarding the instantaneous position of the intrusion region of proton and electron fluxes, and makes it possible to compare this position with the position of electrical currents in the ionosphere.

As indicated in Figure 2, as of  $16^{\text{h}} 30^{\text{m}}$  and up to  $17^{\text{h}}$ , the  $H_{\alpha}$  emission was observed in the north and was not seen in the south. At the same time, the

It is impossible to determine the position of electrical currents in the ionosphere from the data of one magnetic station without making additional assumptions as to the configuration of the currents. Thus, the calculations were performed with the assumption that the currents flow at a height of 100 km in the form of a 200 km wide band. The results, thus obtained, lead to an approximate estimate of the position of the currents and its variations.

Figure 2 also shows the emission intensities of  $H_{\alpha}$  and of  $1 \text{ PGN}_2$  at a  $30^{\circ}$  angle to the north (N) and to the south (S), obtained with a C-180-S spectral camera.

1 PGN<sub>2</sub> intensity in both directions was small. Simultaneously, the electrical currents in the ionosphere were approximately 70 km north of the zenith. After 17<sup>h</sup>, the hydrogen emission in the north disappeared, and noticeably increased in the southern half of the firmament. Almost simultaneously, the cg of the currents also shifted to the south of the zenith and remained there until 19<sup>h</sup>, in spite of the fact that a rather intensive 1 PGN<sub>2</sub> glow during that time was observed in the north. The appearance of H<sub>α</sub> at 19<sup>h</sup> in the north was also accompanied by a shift of the currents north of the zenith. /10

These findings indicate that at least during the specified day, the electrical currents were spatially connected to the hydrogen emission glow range, whereas in the 1 PGN<sub>2</sub> glow range, there were no noticeable currents. This is also supported by the findings reported in [15]. Such a conclusion appears to contradict the generally-held viewpoint, i.e., that auroras and geometric bays are essentially caused by the intrusion of electrons into the lower atmosphere, rather than of protons [6].

It should be noted, however, that during the evening, H<sub>α</sub> and 1 PGN<sub>2</sub> emissions, as a rule, are observed in auroras of different shape: hydrogen emission is usually found in wide and stable homogeneous and diffused arcs, whereas 1 PGN<sub>2</sub> is associated with short-lived unstable radial shapes which, even though they are bright, are also rather restricted in terms of area.

Thus, the intensity of electric currents is apparently not determined by the stream (proton or electron) that causes the aurora, but by the intensity, of the stream, its length and the area that it occupies in the sky. This conclusion is confirmed by the fact that the intensity of magnetic disturbances reaches its maximum after midnight, even though hydrogen emission at this time is no longer observed. Apparently the essential fact is that auroras associated with electron intrusion lose their radial structure and appear in the form of wide diffused arcs and surfaces.

What then is the energy of the intruding protons? Inasmuch as auroras with hydrogen emission are closely associated with electrical currents in the

ionosphere which can hardly flow above a 120 km level [16, 17], it appears that the initial energy of the intruding protons must be not less than 100 keV [6]. This is supported by the fact that between 17<sup>h</sup> and 20<sup>h</sup> on 2 March 1965, when according to the data of ionospheric station a stable E<sub>s</sub> layer existed at a height of 105 - 120 km, a broad diffused band, containing H<sub>α</sub> was observed south of it at the zenith. If we assume that such a sporadic ionization occurs as a result of a proton stream intrusion it would follow that their energy must be of the order of 100 keV [6]. This agrees with the findings reported in [18].

Thus, the cited magnetic and ionospheric data, obtained from rocket measurements [8], indicate that the initial energy of the intruding protons must be of the order of 100 keV. Lower energy obtained from the shape of the hydrogen emission contour (2 - 5 keV) [9] can be explained, according to [19, 20], by their dispersion and by the direction of motion of the intruding protons.

At the same time, it should be noted that the proton flux intensity apparently is quite negligible. Actually, hydrogen arcs are usually accompanied by small magnetic disturbances [15]. During the day under consideration, the intensity of positive bays, associated with the hydrogen arc, did not exceed 150 γ. Further, ionospheric data also indicate that the maximum ionization density in the E<sub>s</sub> layer and the magnitude of riometric absorption were small, and did not exceed 30% of the corresponding values observed during 1 PCN<sub>2</sub> flares around 19<sup>h</sup>. If we were to neglect the variation of the recombination coefficient with height, and assume that the ionization density in the E<sub>s</sub> layer is proportional to the energy supplied by the ionizing flux per unit time, then we can assume that the maximum density of the energy flux carried by the proton stream between 17<sup>h</sup> and 18<sup>h</sup> was approximately smaller /11 than the density of the electron flux at 9<sup>h</sup> by the factor of three.

Obviously, the intensity ratio of the proton and electron fluxes is

$$\frac{I_p}{I_e} = \frac{n_p v_p}{n_e v_e} = \epsilon \frac{E_e}{E_p},$$

where  $n_e$ ,  $n_p$  are electron and proton concentrations in the stream, respectively;  $v_e$  and  $v_p$ ,  $E_e$  and  $E_p$  are velocity and energy, respectively;  $\epsilon$  is the ratio of the energy flux density in proton and electron streams.

Setting, in accordance with the aforementioned estimates,  $\epsilon = 1/3$ ,  $E_p = 100$  keV and setting conventionally that  $E_e$  is of the order of 6 keV, we find that

$$\frac{I_p}{I_e} = 2 \cdot 10^{-2},$$

This does not substantively contradict the data obtained from rocket soundings [8].

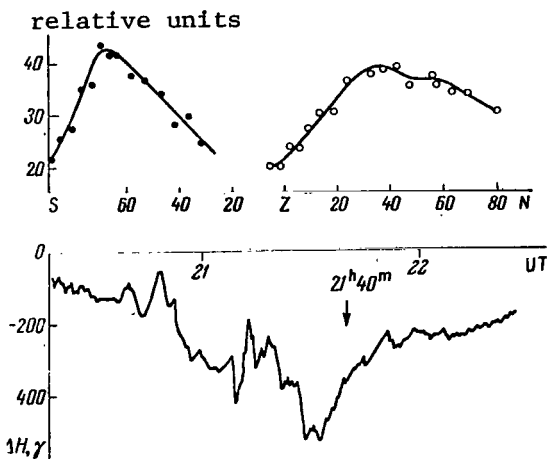


Figure 3. Intensity distribution of the glows of  $H_\alpha$  and 1 PGN<sub>2</sub> emissions along the meridian during a negative bay on 8 February 1959.

1.  $H_\alpha$  emission intensity;
2. 1 PGN<sub>2</sub> emission intensity;
3. Position of electrical currents;

According to the contemporary theories dealing with the emergence of polar magnetic disturbances, the generation of an electrostatic field and electric currents in the ionosphere is caused by charge separation in the corpuscular stream [21 - 23] which initially was neutral. The direction of the current is determined by the (south or north) displacement direction of protons with respect to electrons. The aforementioned data indicate that the intrusion regions of protons and electrons indeed can be scattered considerably. Moreover, between 17<sup>h</sup> and 19<sup>h</sup> when the hydrogen emission is observed south of the intrusion region of

electrons,  $\delta H > 0$ , i.e., the electrical currents in the ionosphere flow eastward. This appears to support the aforementioned point of view. However, a more detailed analysis indicates that positive and negative bays can be observed in any position of the hydrogen emission glow with respect to the  $1 \text{ PGN}_2$  glow region. Thus, Figure 3 (according to the data in [24]) shows a case that took place at  $21^{\text{h}} 40^{\text{m}}$  on 8 February 1959. At this point, the hydrogen emission, as in the given day, was observed south of the electron intrusion region. Yet, in the magnetic field, there was an intense negative bay, rather than a /12 positive bay. Thus, the reciprocal positions of the glow regions of proton and electron aurora apparently do not determine the direction of the electric currents in the ionosphere, nor do they have any bearing upon the sign of the magnetic disturbance.

#### Auroral Shapes and the Height of the Auroral Ionization Region

We will now consider the relationship between auroras and regions of auroral ionization in terms of height. The presence of an intensive  $1 \text{ NGN}_2^+$  emission in the spectrum suggests a high rate of ion formation in glow regions. The relatively small height of auroral arcs and their pronounced lower edge indicate a steep energy spectrum of ionizing corpuscular streams. Thus it is reasonable to assume that the region of auroral altitudinal ionization approximately coincides with the range of auroral glow.

Figure 4 shows the mean heights of polar auroras and the heights of the  $E_s$  layer. These data were obtained from the findings of a vertical sounding station on 2 March 1965. The graph indicates that between  $17^{\text{h}} 45^{\text{m}}$  and  $18^{\text{h}} 5^{\text{m}}$  the heights of the aurora and of the  $E_s$  layer differ considerably, and their variations appear to be independent. This finding to some extent confirms the assumption that the sporadic ionization, observed at this time, is associated with hydrogen glows at the zenith and south of it, rather than with the bright arc in the North. The height of this arc does not exceed  $50^\circ$  above the northern horizon, and the arc itself is a result of the intrusion of an electron stream.



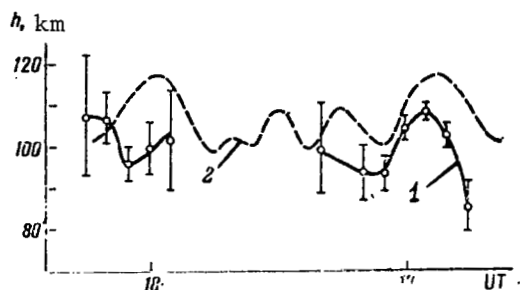


Figure 4. The height of aurora (1) and the height of the  $E_s$  layer (2). Vertical lines denote the mean square error.

step, and their difference does not exceed 10 km. Thus it can be assumed that in this case the heights of the auroral glow regions and the auroral ionization, which forms the  $E_s$  layer, do indeed coincide.

A comparison of the riometric absorption with the data obtained by a vertical sounding ionospheric station leads to the assumption [25, 26] that in some instances, a substantial portion of the auroral absorption of cosmic radio emission takes place on the E layer level. The data that are available to us lead to an estimate of the absorption magnitude of cosmic radio emission. Indeed, aurora were accompanied by the emergence of a sporadic E layer of the r type. In view of this, it was possible to calculate the maximum electron density in the layer  $E_s$  ( $N_{\max}$ ). The shape of  $N_{\max}$  is shown in Figures 5a and 6a.

Using the obtained value of  $N_{\max}$ , we can compute the absorption intensity /13 of cosmic radio emission on a given frequency, using the formula suggested in [27]:

$$A = \frac{0.46 \bar{N}}{(2\pi)^2} v_0 \left(1 - e^{-\frac{h-h_0}{H}}\right) II \text{ dB,}$$

where  $\bar{N}$  is the mean density of ionization in the  $E_s$  layer;  $H$  is the height of the homogenous atmosphere;  $(h - h_0)$  is the layer thickness;  $v_0$  is the collision

At about  $18^h 45^m$ , the hydrogen emission intensity appreciably decreases. The aurora in the north breaks up into a number of radial and diffused forms, becomes stronger and widens, at times reaching the zenith. At that time ( $18^h 45^m - 19^h 15^m$ ), in spite of the fact that the northern auroral boundary (height shown in Figure 4) is still located as previously (about  $40^\circ$  from the zenith), the auroral height and the height of the  $E_s$  layer change almost in

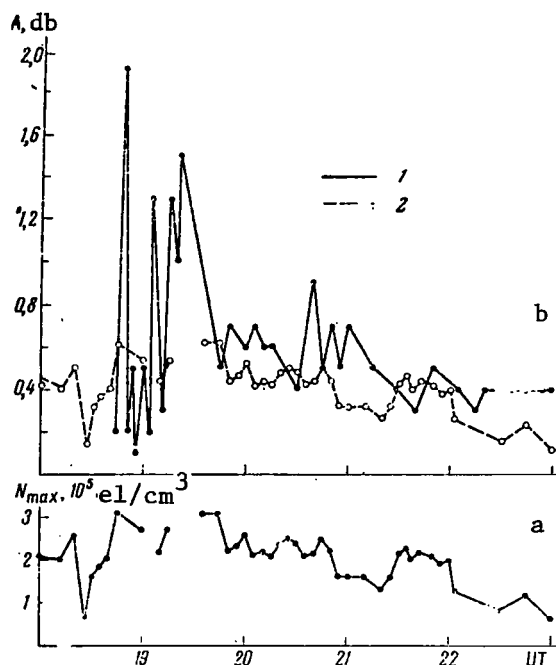


Figure 5. The ionization density in the  $E_s$  layer (a) and the magnitude of rheometric absorption (b), as recorded on 2 March 1965.

1. Experimental curve;
2. Calculated curve.

frequency of electrons at the level of the lower boundary of the absorbing layer.

Thus, it is assumed that the stepped up ionization region is shaped as a homogenous layer, so that the ionization density in it does not depend on the height. Of course, the latter assumption does not reflect the actual altitudinal distribution of the ionization density. Nonetheless, this apparently does not introduce any substantive error into the calculated absorption value inasmuch as the frequency of electron impacts rapidly decreases with increasing height.

Thus, the absorption essentially takes place in the lower range of the  $E_s$  layer where, judging from the altitudinal brightness distribution of the glow [28],  $\bar{N} = N_{\max}$ .

In the calculations, we set  $f = 32$  Mc,  $\nu_0 = 2 \times 10^5 \text{ sec}^{-1}$  which corresponds to the height of the lower aurora edge  $h_0 = 100$  km [29]; the layer thickness was set at 20 km. The calculated absorption magnitude is shown in Figures 5b and 6b. The same diagrams show the actual variations of the rheometric absorption at a frequency of 32 Mc. It is demonstrated in Figure 6b that the absorption patterns, computed on 6 March, coincide quite well in shape and in absolute magnitude. Hence, the assumption that the  $E_s$  layer is to some extent responsible for the auroral absorptions appears to be by and large justified.

The graphs indicate that the experimental and theoretical coincidence between the curves obtained on 2 March is considerably weaker than the coincidence between the curves obtained on 6 March. According to the report of the vertical sounding station, there was a blackout between 19<sup>h</sup> 00<sup>m</sup> and 19<sup>h</sup> 40<sup>m</sup>, and hence no data on the ionization density in the E<sub>s</sub> layer are available for this time. It was only when the blackout was briefly interrupted (19<sup>h</sup> 10<sup>m</sup> — 19<sup>h</sup> 15<sup>m</sup>) that it was possible to record E<sub>s</sub> reflections. In these instances, the computed absorption was noticeably (by a factor of three) smaller than the actual absorption. Such a drastic discrepancy between the calculated and the computed data apparently is caused by the fact that the actual region of increased ionization was below that which was used as a reference in the calculations ( $h_0 = 90$  km). This assumption is supported by the already observed decrease of the frequency relation exponent of riometric absorption (cf. Figure 1). For a more detailed examination of this problem, we show in Figure 7 a curve (solid line) of the variation of the effective exponent of frequency relationships during the examined disturbance. This exponent is taken as a mean of three frequencies, i.e., 9, 13, and 25 Mc. The graph shows that at about 19<sup>h</sup>, the magnitude of  $n$  reaches its minimum, thus indicating the relatively low height of the absorbing region. /14

However, it must be kept in mind that the variation of the effective exponent of the riometric absorption frequency relationship may be caused not just by a height variation of the absorbing layer, but also by its extension in a horizontal direction. Thus,  $n$  may decrease when the increased ionization

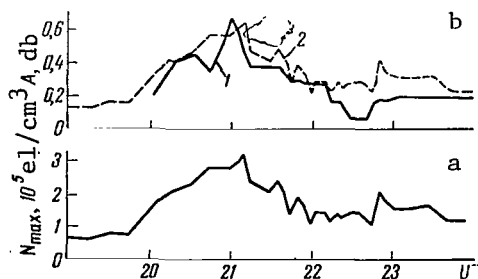


Figure 6. Ionization density in the E layer (a), and the riometric absorption (b), recorded on 6 March 1965. 1-experimental curve; 2-calculated curve.

range does not completely cover the directional diagram of the riometer antenna [30]. Since radial auroras usually occupy a smaller area of the firmament than homogenous arcs and diffuse surfaces, it is entirely possible that the decrease of  $n$ , observed during the flares of bright auroras, is associated with this very effect. Thus it appears to be extremely important that the decrease of  $n$  during the given day was always accompanied by a decrease of aurora height.

Actually, at 18<sup>h</sup> 50<sup>m</sup>, aurora were noted at a height of 90 km. At 19<sup>h</sup> 05<sup>m</sup> a secondary decrease of the aurora height took place, the minimal height being 86 km (Figure 4).

Later, at 19<sup>h</sup> 15<sup>m</sup> the auroral height was no longer measured. There are, however, additional data available on the penetration depth of corpuscular streams into the Earth's atmosphere. Indeed, since  $3_p - 1_D$  [01] is a forbidden transition, (the mean life time of it being only 110 seconds), it follows that the emission intensity  $\lambda = 6300 \text{ \AA}$  must substantially decrease with decreasing aurora height, so that the relative intensity of that emission might serve as an indicator of the aurora height [6]. In figure 7, the dotted line shows that the path of  $I_{6300}/I_{5577}$ . A comparison of the curves indicates that the decrease of  $n$  takes place simultaneously with the decrease of this ratio and consequently with a decrease of the aurora height. This leads to the assumption that a decrease of  $n$  is essentially caused by a decrease of the height of the absorbing layer, rather than by a variation of its configuration, even though the latter does possibly introduce a certain error into the absolute magnitude of  $n$ .

/15

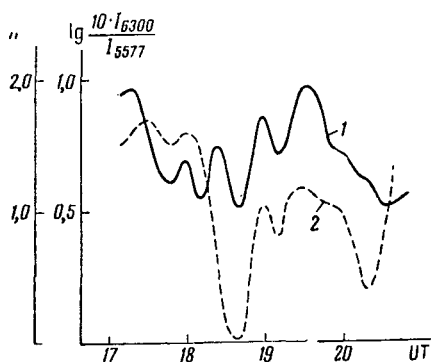


Figure 7. Relationship between the exponent of the riometric absorption frequency relationship  $n$  (1), and the ratio of the emission intensities 6300 and 5577 Å (2).

These data indicate considerable variations of the energy spectrum of electron streams entering the ionosphere. This is applicable from case to case, as well as during individual disturbances. Thus, the variation of aurora height from 110 to 86 km (19<sup>h</sup> 05<sup>m</sup> — 19<sup>h</sup> 15<sup>m</sup> on 2 March) indicates a change in the primary electron energy by at least one order of magnitude. According to [31 - 36], the ratio of the aurora brightness to the riometric absorption intensity must change substantially. This ratio depends on the aurora shape, and on the aurora type, observed during the riometric absorption. The most detailed

classification of aurora absorption was proposed by Z. A. Ansari [35]. He grouped the absorption peaks, observed during auroral flares (both radial and uniform), into group II(SAI). The smooth variations of  $\delta A$ , which are observed after midnight and correlate weakly with the variations of aurora brightness, were grouped into the IV(SVIA) category. Based on the rate of correlation of  $\delta A$  and of  $\delta I$ , Ansari suggested that absorptions of the SAI type are caused by the intrusion of electron streams with energies of the order of  $E \leq 20$  keV into the atmosphere, whereas absorptions of the SVIA type are associated with the electron streams in the energy range of  $E \geq 30$  keV.

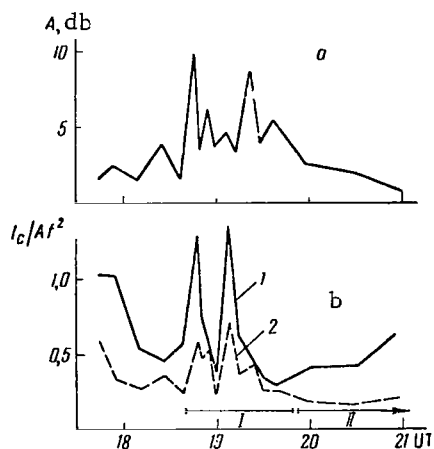


Figure 8. Rheometric absorption (a) and its relationship to aurora intensity (b) on 2 March 1965.

The absorption intensity of cosmic radio emission was measured on the frequencies of 9 (1) and 13 mc (2). Segments with Roman numerals I and II indicate the exposure time of the spectra.

Figure 8,a shows the absorption curve of cosmic radiation at a frequency of 9 Mc; Figure 8b, shows the variation of the ratio  $I_c / A f^2$  during the storm of 2 March 1965. Here,  $I_c$  is the aurora glow intensity (in relative units) according to the data of the zenith photometer;  $A$  is the absorption intensity of cosmic radio interference at frequencies of 9 mc (solid line) and 13 mc (dashed line). For a more convenient comparison of the data obtained from two riometers, the respective absorption magnitudes were multiplied by the square of the appropriate frequency so that the relative shape of both curves indicates the /16 exponent  $n$  of the frequency relationship.

It appears from the graphs that there are two pronounced maximums in the patterns of  $I_c / A f^2$ : at  $18^h 48^m$  and at  $19^h 08^m$ . These maximums coincide in time with the radial-

shaped flares. The growth curve of this ratio can be explained apparently by the small absorption magnitude at this time, and by the fact that it was not determined with precision. The absorption peaks, observed simultaneously with

glow intensity peaks, could be associated with the SAI phase (or the F type, according to the R. Parthasarathy and F. T. Berkey classification [37].) However, a direct measurement of the auroral height (Figure 4) supports the fact that the energy of the intruding electrons at the given moments of time amounts to 30-40 keV, i.e., it is considerably higher than the energy level suggested by Ansari. Moreover, it should be definitely kept in mind that this finding applies only to two specific auroral flares on 2 March 1965. Thus it cannot be applied to all instances of SAI type absorption, nor can it be considered a mean or characteristic value. In spite of the fact that the mean value of exponent  $n$  of the absorbency frequency relation, according to the numerous observations of Parthasarathy and Berky [37], is 1.5, the ionizing corpuscular streams during the SAI phase contain a considerable number of high-energy electrons.

Simultaneously, a relatively large absorption peak with a maximum at  $19^h 24^m$  was not accompanied by any noticeable increase of auroral brightness (Figure 8), suggesting that it belongs to the SVIA type. Nonetheless, it is at this very moment that the frequency relationship of the absorption is closest to a quadratic relationship, i.e., the penetration depth and thus the energy of the intruding electrons are minimal. However, the time of the appearance of this absorption peak (at about  $19^h$  UT, i.e.,  $21^h$  LMT) and its short life contribute to some uncertainty in identifying it with SVIA type absorption.

The considerable penetration depth of corpuscular streams into the atmosphere during the flares of radial aurora is also confirmed by the properties of auroral optical spectra. During the night hours of 2 - 3 March, two auroral /17 spectra were obtained with two SP-48 spectrographs, the total wavelength range being from 4100 to 6800 Å. In both cases the spectrographs were aimed at aurora in the northern half of the firmament. This first spectrum (exposure time  $18^h 40^m - 19^h 50^m$ ) was exposed essentially during the prevalence of bright radial shapes (phase SAI). While the photographing of this spectrum also continued after  $19^h 08^m$ , the auroral intensity at that time was relatively low, so the aurora could not notably distort it.

Wave Length Å	Atom or molecule	Multiplet or band	Spectrum I	Spectrum II
4278	N <sub>2</sub> <sup>+</sup>	1 NG (0.1)	20.2	18.9
4368	OI	5	0.2	0.3
4417	OII	5	0.3	0.3
4709	N <sub>2</sub> <sup>+</sup>	1 NG (0.2)	7.1	7.1
4861	H <sub>β</sub>	1	0.3	1.2
5200	[NI]	Nebular	0.2	0.6
5577	[OI]	Auroral	100.0	100.0
5890 } 5896 }	NaI	1	0.4	0.8
6300	[OI]	Nebular	7.7	18.9
6364	[OI]	Nebular	2.7	5.7
6482	NII	8	0.2	0.1
6545	N <sub>2</sub>	1 PG (7, 4)	2.7	1.3
6563	H <sub>α</sub>	1	0.5	2.5
6624	N <sub>2</sub>	1 PG (6, 3)	4.3	2.2
6705	N <sub>2</sub>	1 PG (5, 2)	6.3	3.2

The entire second spectrum was taken during diffused and pulsed auroras. The exposure time of these two spectra is shown in Figure 8 by segments marked I and II.

Figures 9a, and 9b show the traces, whereas the table shows the relative intensities of the basic emissions for both spectra. The spectra were joined along the 5577 Å (OI) line. The intensities were computed in areas, restricted by the contours of the lines plotted in intensities. In comparing the spectra, it should be kept in mind that the intensity of the green line  $\lambda = 5577$  Å, which is set to be 100 in both spectra, is smaller in the second spectrum, almost by a factor of 3.5, as compared to the first one.

It appears from the traces and from the table that the active radiant auroras have considerably strengthened the molecular bands — this applies to the first positive system of the  $N_2$  molecule, and to the  $O_2^+$  band. Moreover, in the second spectrum, the ratios  $I_{6300}/I_{5577}$  and  $I_{6364}/I_{5577}$  were larger than in the first spectrum by the factor of 2.5. The intensity of hydrogen emission greatly increased. From a currently accepted viewpoint, these data indicate that the first spectrum was exposed during lower auroras than the second spectrum. The increased height of the glow may also account for the growth of the intensity of the forbidden line  $\lambda = 5200 \text{ \AA}$  in the second spectrum, as compared to the allowed emissions. The presence of such emissions as  $6482 \text{ \AA}$  NII in the first spectrum, which is associated with low aurora, is due to the great height of radial shapes. /18

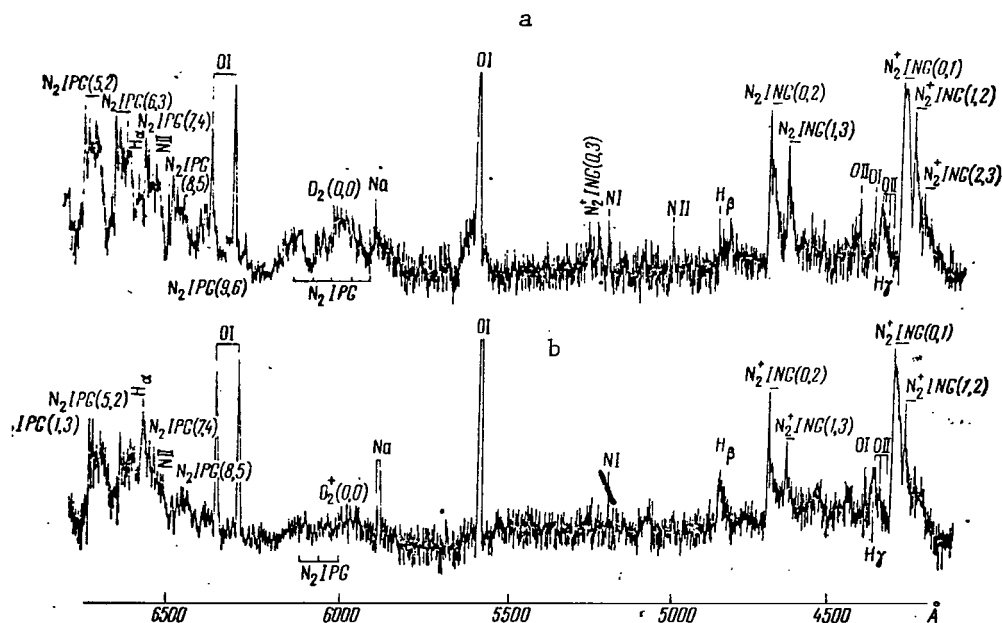


Figure 9. Traces of auroral spectra.

a - Exposure time  $18^h 40^m - 19^h 50^m$ ;

b - Exposure time  $19^h 50^m - 22^h 15^m$ .



## The Microstructure of Magnetic Disturbances

The differing microstructure of geomagnetic disturbances observed at this time also supports the contention of the differing nature of corpuscular streams, associated with different forms of aurora and riometric absorption of varying types. During the nights of the observations, two typical and most characteristic pulsations were observed: the first is a combination of irregular oscillations with a period of 40 - 50 sec and near-sinusoidal oscillations with a period of about 2 seconds (such a combination can be defined by the new classification of short-period variations as  $P_1 2 - P_c 1$ ); the second type includes irregular oscillations with a 5 to 12 seconds period and is denoted by the symbol  $P_1 1$ .

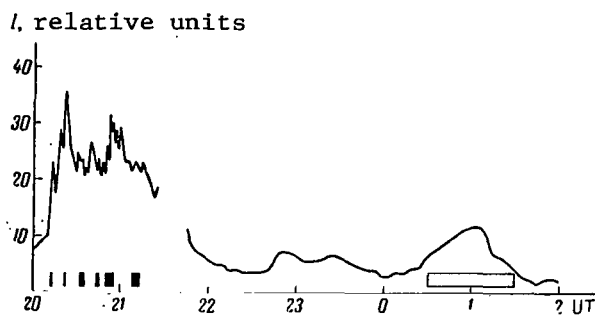


Figure 10. Intensity variations of the polar aurora (solid line) and types of short period variations.

Shaded rectangles represent type  $P_1 2 + P_c 1$ ; the light rectangles are type  $P_1 1$ .

The time of the appearance of short-period variations of the indicated types during the 2 March 1965 disturbance is shown in Figure 1. It appears that pulsations of the first type (i.e.,  $P_1 2 + P_c 1$ ) were observed as a series of separate flares lasting 2 to 5 minutes. The appearance of short-period variations approximately coincides with the moments 3 - 7 when the intensity of the  $1 \text{ PGN}_2$  emission increased, bright radial auroral

shapes appeared, the riometric absorption went up drastically, and the frequency relationship of this absorption deviated from the quadratic relationship. An exception was the flare between  $18^{\text{h}} 55^{\text{m}}$  and  $18^{\text{h}} 59^{\text{m}}$  which did coincide with moment 5, when all of these phenomena were very weakly expressed. It is true that the flare was also of very low intensity. Beginning approximately at  $19^{\text{h}} 24^{\text{m}}$ , recordings of the Earth current fields clearly show pulsations of the second type  $P_1 1$ ; the amplitude of these pulsations changes parallel to the intensity variation of the equivalent electrical current in the

ionosphere. At the same time (moments 8 - 10 in Figure 1), the polar auroral glow intensity diminished and the aurora took on the shape of diffused surfaces, whereas the frequency relationship of the absorption became exactly quadratic.

Figure 10 shows the variations of auroral glow intensity and the time of the appearance of short period variations of the first and of the second type during the night of 6 - 7 March 1965. The graph shows that, as in the preceding night, bursts of short period variations of the type  $P_i2 + P_c1$  were observed simultaneously with flares of radial glows ( $20^h 10^m - 21^h 30^m$ ). /19 Simultaneously, a small negative bay with very pronounced field variations was recorded in the magnetic field. This suggests that the riometric absorption, accompanying these aurora, belongs to the SAI type. However, the penetration depths of the corpuscular streams at that time was apparently insignificant, since the region of increased ionization, responsible for the absorption of the radio waves, as indicated before, was observed at a height of about 100 km.

After a series of micropulsations, the electromagnetic field of the Earth remained quiet approximately until  $0^h 30^m$  on 7 March. At that time, the recordings of Earth currents showed short period variations of the  $P_i1$  type. A relatively smooth increase of auroral glow was observed simultaneously. These auroras were shaped as diffused pulsating spots. The absorption intensity of cosmic radio interference also increased; it was accompanied by a moderate-sized negative geomagnetic bay. All these phenomena gradually ceased at about  $1^h 30^m$ .

Thus, from the aforementioned data it appears that various types of aurora are accompanied by various kinds of short period variations of the electromagnetic field: radial aurora are accompanied by micropulsations of the  $P_i2 + P_c1$  type, whereas homogenous and diffused aurora are accompanied by micropulsations of the  $P_i1$  type. This apparently suggests the existence of different mechanisms of acceleration or discharge of electrons, responsible for these auroras, into the ionosphere.

### Conclusions

Upon analyzing the patterns of a polar magneto-ionospheric storm and of the polar aurora observed at the same time, the following conclusions can be derived:

1. The position of the cg of a current system in space is related to the stable (long-lasting) polar aurora shapes, occupying large areas in the sky, i.e., mostly with hydrogen arcs in the evening, and homogenous arcs and diffused surfaces at night.

2. In regions of auroral glows with hydrogen emission, the protons penetrate the atmosphere up to the  $E_s$  layer, i.e., their initial energy is of the order of 100 keV. The intensity of the proton stream is approximately two orders of magnitude smaller than the intensity of the electron flux that generates bright radial shapes.

3. The direction of electrical currents in the ionosphere, which cause geomagnetic bays, is not determined by spatial separation of the regions of hydrogen and electron auroral glow.

4. Anomalous ionization, responsible for the absorption of radio waves in the ionosphere during polar aurora, is caused by the same particles as polar auroras. At aurora heights of 100 km and more, the glow region, in some instances, apparently coincides with a region of increased ionization.

5. The energy of electrons penetrating the lower ionosphere may change within wide limits from one instance to another, as well as in the case of a separate disturbance. The electron energy causing radial shaped auroras may be considerable as, for example, at 19<sup>h</sup> 8<sup>m</sup> on 2 March 1965 when auroras were observed at a height of 85 km. Only electrons with an energy  $E = 30 - 40$  keV can penetrate to that level.

6. Auroras of various shapes (both radial and diffused) are caused by the intrusion of corpuscular streams into the lower ionosphere. These streams differ from each other not only in terms of energy, but also apparently in terms of structure, inasmuch as they are accompanied by the occurrence of various types of short-period variations of the electromagnetic field of the Earth. This, in turn, suggests that there are different mechanisms for the formation of electron streams that cause differently shaped auroras.

It should be again emphasized that these conclusions are derived from the analysis of isolated cases only, and cannot be considered statistically reliable without additional investigation. However, the demonstrated laws are apparently inherent to these types of phenomena, inasmuch as there are no reasons to believe that these cases are to any extent exceptional.

/20

In conclusion, the authors express their appreciation to the Chief of the NIRFI\* Laboratory, Ye. A. Benediktov and to the Director of the Institute for making available the data on the absorption of cosmic radio emissions at frequencies of 9, 13, 25, and 40 mc. We would also like to thank A. B. Korotin for the useful and stimulating discussions in the course of the preparation of this study, to laboratory assistants P. Ye. Borisov, G. Sh. Zakirova, I. V. Okunev and T. P. Roldugina for help in parallactic observations and data evaluation.

---

\*Translator's note: Scientific Research Institute of Radiophysics

## REFERENCES

1. Meek, J. H. Correlation of Magnetic, Auroral and Ionospheric Variations at Saskatoon. J. Geophys. Res., Vol. 59, No. 1, 1954, p. 187.
2. Heppner, J. P. Time Sequences and Spatial Relations in Auroral Activity During Magnetic Bays at College, Alaska. J. Geophys. Res., Vol. 59, No. 2, 1954, p. 329.
3. Bless, R., C. W. Gartlein, D. S. Kimball, G. Sprague. Auroras, Magnetic Bays and Photons. J. Geophys. Res., Vol. 64, No. 8, 1959, p. 949.
4. Fel'dshteyn, Ya. I. Magneto-ionospheric Disturbances and Aurora on Dixon Island. In: "Issledovaniya polyarnykh siyaniy", No. 4, seriya "Rezul'taty MGG. (Investigation of Polar Aurora) No. 4, Series "Results of the IGY". Academy of Sciences of the USSR Press, Moscow, 1960, p. 29.
5. Oguti, T., T. Nagata. Interrelation Among the Upper Atmosphere Disturbance Phenomena in the Auroral Zone. Rept Ionosphere Space Res. Japan 961, Vol. 15, No. 1, p. 31.
6. Chamberlain, J. The Physics of Polar Aurora and Atmospheric Emissions. Moscow, Foreign Literature Press, (IL), 1963.
7. Davis, L. R., O. E. Berg, L. H. Meredith. Direct Measurements of Particle Fluxes in and Near Auroras. Space Res., No. 1, 1960, p. 721.
8. McIlwain, C. W. Direct Measurement of Protons and Electrons in Visible Aurora. Space Res., No. 1, 1960, p. 715.
9. Gal'perin, Yu. I. Intrusion of Protons in Polar Aurora. In: "Polyarnyye siyaniya i svecheniye nochnogo neba" (Polar Aurora and Night Sky Luminescence", No. 10, Moscow, Academy of Sciences of the USSR Press, 1963, p. 70.
10. Mal'ko, L. N., G. V. Starkov. Certain Features of the Polar Aurora Altitudinal Distribution. Geomagnetizm i aeronomiya. Vol. 5, No. 1, 1965, p. 188.
11. Hunten, D. M. Recent Work at the University of Saskatchewan on Auroral and Night Sky Spectra. Ann. Geophys., No. 14, p. 167.
12. Petrie, W. , R. Small. The Intensities of Atomic and Molecular Features in the Auroral Spectrum. Canad. J. Phys., Vol. 31, No. 5, 1953, p. 911.
13. Khvostikov, I. E. Fizika ozonosfery i ionosfery (The Physics of the Ozonosphere and of the Ionosphere). Moscow, Academy of Sciences of the USSR Press, 1963.

14. Yegorov, Yu. M. Razrabotka ustanovki dlya registratsii variatsiy magnitnogo polya Zemli v shirokom diapazone chastot. (The Development of Equipment for Recording Magnetic Field Variations in a wide Range of Frequencies). Dissertation, Moscow, 1963.
15. Pudovkin, M. I., L. S. Yevlashin. Prostranstvennaya svyaz'polyarnykh siyaniy s elektricheskimi tokami v ionosfere (Spatial Relationship Between Polar Aurora and Electrical Currents in the Ionosphere). Geomagnetizm i aeronomiya, Vol. 2, No. 4, 1962, p. 669.
16. Baker, W. G., D. F. Martyn. Electric Currents in the Ionosphere. Philos. Trans. Roy. Soc., Vol. 246A, No. 913, 1953, p. 281.
17. Cole, K. D. A Dynamo-Theory of Aurora and Magnetic Disturbance. Astral /21 J. Phys., Vol. 13, No. 3, 1960, p. 484.
18. Yevlashin, L. S. Morphology of Hydrogen emission in Aurora. In: Issledovaniye polyarnykh siyaniy, geomagnitnykh vozmushcheniy i ionosfery v vysokikh shirotakh (Investigation of Aurora, Geomagnetic Disturbances and the Ionosphere at High Latitudes), Moscow, Izdatel'stvo "Nauka", No. 11, 1964.
19. Chamberlain, J. W. Theories of the Aurora. Advances in Geophysics, ed. H. E. Landsbery and J. van Meighem. N. Y. Acad. Press, 1958.
20. Bater, D. R. Theory of the Auroral Spectrum. Ann. Geophys., Vol. 11, 1955, p. 253.
21. Akasofu, S. I., S. Chapman. A Study of Magnetic Storms and Auroras. Sci. Rept. Geophys. Inst. Alaska, UAG-R112.
22. Kern, J. W. A Charge Separation Mechanism for the Production of Polar Auroras and Electrojets. J. Geophys. Res., Vol. 67, 1962, p. 2649.
23. Martyn, D. F. The Theory of Magnetic Storms and Auroras. Nature, Vol. 167, 1951, p. 92.
24. Yevlashin, L. A. Space-time variations of hydrogen in Aurora and Their Relationship with Magnetic Disturbances. Geomagnetizm i aeronomiya, Vol. 1, No. 1, 1961, p. 54.
25. Potapov, B. P., Z. Ts. Rapoport, and T. B. Borsuk. Study of Radio Wave Absorption in the Aurora Zone. In: Spektralnyye elektrofotometricheskiye i radiolokatsionnyye issledovaniya polyarnykh siyaniy i svecheniya noch-nogo neba (Spectral, Electrophotometric, and Radar Studies of Aurora and Night Sky Glow), No. 2-3, Moscow, Acad. of Sci. of the USSR Press, 1960 p.42.
26. Pudovkin, M. I. Determination of the Disturbed Ionosphere Parameters in the Aurora Zone. In: Issledovaniye polyarnykh siyaniy, geomagnitnykh vozmushcheniy i ionosfery v vysokikh shirotakh (Investigation of Aurora, Geomagnetic Disturbances and the Ionosphere at High Latitudes),

- No. 49. Moscow, Izdatel'stvo "Nauka", 1964, p. 49.
27. Pudovkin, M. I., R. G. Skrynnikov, and O. I. Shumilov. Magneto-Ionosphere Disturbances, in the Aurora Zone. *Geomagnetizm i Aeronomiya*, Vol. 4, , No. 6, 1964, p. 1094.
  28. Stormer, C. *The Polar Aurora*. Oxford, 1955.
  29. Fligel', D. S. Properties of the Coefficients of Refraction and Damping, and the Transmission Coefficient of the Ionosphere at Low and Ultra-low Frequencies. *Geomagnetizm i aeronomiya*, Vol. 2, No. 5, 1962, p. 886.
  30. Little, C. G., G. M. Lerfald, and R. Parthasarathy. Extention of Cosmic Noise Absorption Measurements to Lower Frequencies, Using Polarized Antennas. *Radio Sci. J. Res. NBS*, Vol. 68D, No. 8, 1964.
  31. Holt, O., and A. Omholt. Auroras Luminosity and Absorption of Cosmic Radio Noise. *J. Atmos. and Terr. Phys.*, Vol. 24, June 1965, p. 467.
  32. Hultqvist, B. On the Height of Auroral Absorption. I. *Planet. Space Sci.*, Vol. 12, No. 11, 1964, p. 579.
  33. Hultqvist, B. On the Height of Auroral Absorption. II. *Planet. Space Sci.*, Vol. 12, No. 11, 1964, p. 1035.
  34. Rees, M. H. Auroral Ionization and Excitation by Incident Energetic Electrons. *Planet. Space Sc.*, Vol. 11, No. 10, 1963, p. 1209.
  35. Ansari, Z. A. The Aurorally Associated Absorption of Cosmic Noise at College, Alaska. *J. Geophys. Res.*, Vol. 69, No. 21, 1964, p. 4493.
  36. Johansen, O. E. Variations in Energy Spectrum of Auroral Electrons Detected by Simultaneous Observation with Photometer and Rheometer. *Planet. Space Sci.*, Vol. 13, No. 3, 1965, p. 225.
  37. Parthasarathy, R., and F. T. Berkey. Auroral Zone Studies of Sudden On-Set Radio Wave Absorptpion Events Using Multiple-Station and Multiple Frequency Data. *J. Geophys. Res.*, Vol. 70, No. 1, 1965, p. 89.

## THE POLAR AURORAL BAND DURING MAGNETIC DISTURBANCES

G. V. Starkov and Ya. I. Fel'dshteyn

**ABSTRACT.** According to the askafilms of the C-180 cameras the position of aurora bands has been determined for four time intervals centered at 20, 04, 08, and 16 hours of local geomagnetic time depending on the level of magnetic activity. The indices  $Q$ ,  $Q_p$  and  $K_p$  were used to characterize magnetic disturbance. The authors obtained the values of changes of the aurora bandwidth at these time intervals with the magnetic activity variations. The paper presents the scheme of the aurora band at different  $Q$ -indices and shows that an evening — morning asymmetry is observed which is expressed in the different width of the corresponding parts of the band and in the different distances of the latter from the pole. This asymmetry is maintained at any level of magnetic activity. A flattening of the aurora band is observed on the day side, which is most prominent during high magnetic disturbances. The paper also indicates that the aurora band during low magnetic activity can have breaks on the morning and evening sides. The probability of such breaks is reduced with the increase of magnetic disturbance. With  $Q \geq 3$  a uniform aurora band can be expected. The presence of the breaks is supported by the synoptic map of aurora.

The position of the auroral oval zone which defines their instantaneous /22 distribution was derived in [1-5] on the basis of statistical data evaluation regarding the polar aurora, without taking into account the variations of the magnetic activity level. In [6,7], the oval zone position was considered in a quiet ( $K_p = 0.1$ ) and disturbed magnetic field ( $K_p \geq 5$ ). Reports [8-10] contain extensive information regarding the position of the equatorial boundary of latitude regions, containing aurora, as a function of the magnitude of the planetary activity index  $K_p$ . The latitude region (auroral band) containing aurora during day (10-14) and night hours, with respect to  $Q$ ,  $Q_p$  and  $K_p$ , was detailed in [11]. This report considers the locations of the northern and southern boundaries of auroral regions in fifteen minute, hourly and three-hour intervals. An analysis of the aurora distribution during day and night hours made it possible to investigate the spatial asymmetry of intruding corpuscular streams in the plane of the noon and midnight meridians.



Auroral distribution was determined for four time intervals centered at 20, 4, 8, and 16<sup>h</sup> local geomagnetic time (LGT). This made it possible to determine the position of the auroral band for all hours of the day, and to investigate its asymmetry in morning and evening hours. The presence of such asymmetry follows from theoretical consideration [12,13] — namely, the differences between the directions of the interplanetary magnetic field, and the motion of the solar wind. The northern and southern boundaries of aurora bands were determined from askafilms of the following stations: Murmansk ( $\phi' = 65.1^\circ$ ), Dixon ( $\phi' = 68.0^\circ$ ), Cape Chelyuskin ( $\phi' = 71.2^\circ$ ), Vize Island ( $\phi' = 73.5^\circ$ ), and Piramida ( $\phi' = 75.3^\circ$ ). As a rule, the data for two seasons of high solar activity (1957 - 1959) were evaluated. The position of the boundaries was compared with the Q-index of the magnetic observatory, located at latitudes of the Fritz Zone at the midnight side of the Earth. All Q-indexes, following the practice suggested in [11], were reduced to the Kieruna observatory ( $\phi' = 64.5^\circ$ ). For pre-midnight and after-midnight hours, the number of readings of  $n$  boundaries of auroral bands for each Q value varies between 20 and 350, when  $2 \leq Q \leq 5$  and  $n > 100$ . For pre-noon and afternoon hours,  $n$  is contained within the range of 10 - 70, for mean values of Q in those hours,  $n \sim 50$ . Auroral heights for pre- and after-midnight hours were set to be 120 km, whereas for pre- and afternoon hours, the estimated height was 140 km.

The stations whose askafilms were used for the determination of the position of auroral boundaries at the respective moments of LGT are shown in the following table. The Q-indexes of magnetic observatories were used for comparison with auroral positions. The intervals of world time at the selected observatories correspond to the investigated interval of LGT.

/23

The mean square deviation of  $\sigma$  within the boundaries amounted to  $1.0 - 1.5^\circ$  latitude, whereas the mean square error of the mean arithmetic time was less than  $0.1^\circ$ , decreasing with increasing number of readings. At the same time when  $n > 20$ ,  $\sigma$  practically did not change. Inasmuch as the mean accuracy of the reading is approximately  $0.3^\circ$  latitude, the constancy of  $\sigma$  indicates that the magnetic activity level does not uniquely determine the position of the auroral band, since an increasing number of observations would lead to a

TABLE

Band Boundary	Station	Magnetic Observatory	LGT	UT
Northern	Piramida	Reykjavik	2 - 6	22 - 2
	Cape Chelyuskin	Kiruna		19 - 23
Southern	Murmansk	Reykjavik		22 - 2
	Dixon Island	Kiruna		20 - 24
	Cape Chelyuskin	Kiruna		19 - 23
Northern	Vize Island	Reykjavik	6 - 10	0 - 4
	Cape Chelyuskin	Reykjavik		23 - 3
Southern	Vize Island	Reykjavik		0 - 4
	Cape Chelyuskin	Reykjavik		23 - 3
Northern	Piramida	Welland	14 - 18	10 - 14
	Vize Island	Yellowknife		8 - 12
	Cape Chelyuskin	Yellowknife		7 - 11
Southern	Piramida	Welland		10 - 14
	Vize Island	Yellowknife		8 - 12
	Cape Chelyuskin	Yellowknife		7 - 11
Northern	Piramida	Tiksi Bay	18 - 22	14 - 18
	Cape Chelyuskin	Welland		11 - 15
Southern	Cape Chelyuskin	Welland		11 - 15
	Dixon Island	Welland		12 - 16
	Murmansk	Tiksi Bay		14 - 18

decrease of  $\sigma$  up to the accuracy level of the reading. Apparently, the parameters of the corpuscular stream which excites the glow change in time. Without an appropriate change in the excitation level of the magnetic field, this at times results in variations of the positions of the auroral bands amounting to approximately  $1 - 2^\circ$ . Moreover, the error in the determination of the indexes, caused by the difficulties involved in the selection of a quiet field level, also becomes pronounced.

It is conceivable that the comparison of the position of the auroral bands with the magnetic activity in the same area will result in a somewhat better

agreement. However, such a comparison excludes the possibility of plotting a planetary distribution of aurora at varying magnetic activity levels. This is caused by the presence of variations of magnetic disturbances in the northern hemisphere in the winter during the IGY [14] with respect to latitude and time. According to [15, 11], the correlation coefficients ( $r$ ) of the  $Q$ -indexes of the northern hemisphere stations vary within rather large limits. For example, at the two magnetic observatories (Murchison - Yellowknife,  $r$  varies from 0.5 to 0.75; i.e., in spite of the reasonably close relationship, we cannot construe this as a unique variation of disturbance intensity at different latitudes during the same hours of world time. Figures 1 and 2 show the variations of the corrected geomagnetic latitude of auroral band boundaries in pre-midnight (18 - 22<sup>h</sup> LGT) and after midnight (2 - 6<sup>h</sup> LGT) hours as a function of  $Q$ ,  $Q_p$ , and  $K_p$ . The data on the auroral band, using planetary indexes  $Q$  and  $K_p$ , were obtained by averaging ten to twenty boundary values and hence have a large  $\sigma$ .

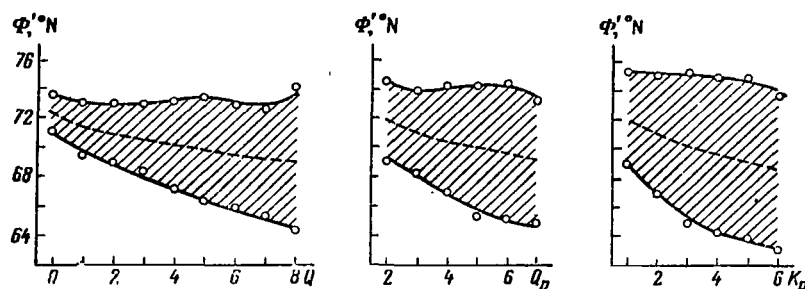


Figure 1. Position of southern and northern auroral band boundaries in pre-midnight hours (20<sup>h</sup>), as a function of  $Q$ ,  $Q_p$  and  $K_p$ .

The broken line indicates the central line of the auroral band; the circles indicate the computed values of  $\phi'$ .

A comparison with  $Q_p$  was performed for the 1957 - 1958 season only. The graphs indicate that the southern boundaries of the band shift southward with an increasing  $Q$ -index. As opposed to the variation of the position of the southern boundary at midnight hours [11], there appears to be no strong increase in the shift at large  $Q$ . On the contrary, the shift velocity decreases with increasing magnetic activity.

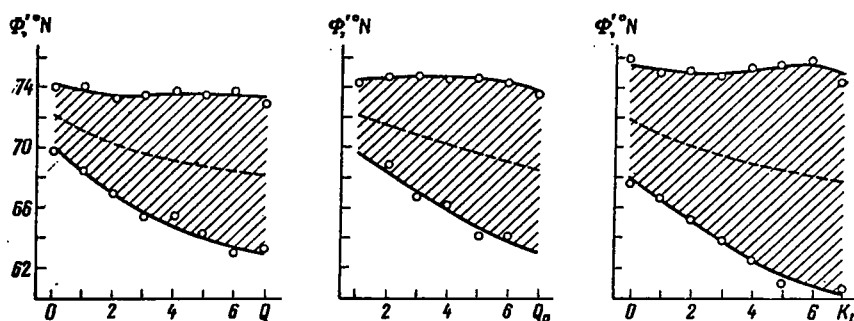


Figure 2. Position of southern and northern auroral band boundaries after midnight hours ( $4^h$ ) depending on  $Q$ ,  $Q_p$  and  $K_p$ .

The broken line indicates the central line of the auroral band; the circles indicate the computed values of  $\phi'$ .

Figure 3 shows the variation of the shift magnitude of the southern boundary with relation to the  $Q$ -index for 20.0 and  $4^h$ . It follows from the graph that during midnight hours the southern boundary rapidly shifts toward the equator in the beginning, whereby the rate of this shift decreases with an increasing  $Q$ : when  $Q = 3 - 4$ , it has a clearly pronounced minimum, and then it again rapidly increases when  $Q \geq 6$ . A rapid shift of the southern boundary of the auroral band toward the equator during intense magnetic disturbances has also been noted in [8].

The nature of the shift in pre-midnight and after-midnight hours is totally different. The boundary shift rate toward the equator decreases monotonically with an increase of  $Q$ ; during after-midnight hours, this rate decreases faster. When  $Q = 6 - 7$ , it amounts to only  $0.4^\circ$ . At pre-midnight hours, the velocity changes relatively little and amounts, on the average, to  $1 - 0.8^\circ$ , when  $Q$  is increased by one unit; i.e., the relationship  $\phi' = f(Q)$  is close to linear. The equatorial boundary during after-midnight hours is systematically located more to the south than in pre-midnight hours. With the exception of periods of weak magnetic disturbance ( $Q = 0; 1$ ), this difference amounts to about  $2^\circ$  latitude. The position of the equatorial boundary of the auroral band in pre-midnight and after-midnight hours always remains closer

to the pole than the southern edge of the band at night hours, even though for both night and after-midnight hours, the difference, at certain Q-values, is very insignificant.

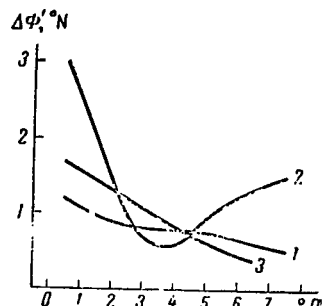


Figure 3. Shift variation of the southern aurora band boundary at different Q values.

- 1 - shift rate for 20<sup>h</sup>;
- 2 - shift rate for 0<sup>h</sup> (from data in [11]);
- 3 - shift rate for 4<sup>h</sup> LGT.

For practical purposes, the position of the northern boundary at 20<sup>h</sup> and 4<sup>h</sup> does not change with varying magnetic activity levels (see Figures 1 and 2). Just as in midnight hours during pre-midnight hours there is a decrease of  $\phi'$  when  $Q = 1 - 2$ . This decrease however, is very insignificant (approximately 0.5°), even though the same tendency is manifested at 20<sup>h</sup> also in the comparison of the northern boundary with  $Q_p$ . The shift amplitude of  $\phi'$  with a Q varying between 0 and 7 at 20 and 4<sup>h</sup> does not exceed 1°; the band boundary is between 73 and 74° northern

latitude. During after-midnight hours, the boundary is located usually somewhat closer to the pole. The constancy of the position of the circumpolar edge of the band is rather remarkable, because at midnight hours, when Q varies from 0 to 8, the position of the northern boundary of aurora changes rather strongly. The shift can take place southward with small magnetic disturbances, as well as northward when  $Q \geq 3$ . The distance between the northern boundary and the pole of an eccentric dipole at midnight hours when  $Q \leq 6$  is greater than at 20<sup>h</sup> and at 4<sup>h</sup>. In view of the relative constancy of the northern boundary position, the central line of the band (dashed line) shifts southward at 20<sup>h</sup> and at 4<sup>h</sup>, is analogous to the shift of the equatorial boundary. This essentially differs from the stable position of the central line of the band at  $\phi' = 67.5$  during night hours.

The nature of the variation of the position of auroral boundaries with reference to  $Q_p$  and  $K_p$  is the same as for the Q-index. The differences in the position of boundaries with reference to Q and  $Q_p$  do not exceed 1° on the

average. For corresponding values,  $K_p \phi'$  of the southern boundary are smaller than for  $Q$  and  $Q_p$ , whereas for the northern boundary they are larger. This leads to a greater bandwidth taken up by aurora which is presumably related to another time and amplitude scale of  $K_p$ . Notably, the scale of the  $K$  index of the Fritz zone stations is more approximate than the scale of the  $Q$  index. The central line of the band shifts southward with increasing magnetic activity, regardless of the indexes used, during pre-midnight as well as after-midnight hours.

In individual instances, there was an absence of aurora with a clear sky (stars showing on the photographs) during 15<sup>m</sup> intervals; the mean position of the aurora band corresponds to the zenith of the observation station. For 20 and for 4<sup>h</sup>, such stations are Cape Chelyuskin and, to some extent, the Piramida Station.

The absence of aurora cannot be explained by a drift of the band from the field of view of the camera. The probability of the disappearance of aurora increases with decreasing  $Q$ . Such instances were not included in the averaging; the median calculation of the data, for practical purposes, does not affect the positions of the boundaries at 20<sup>h</sup> and 4<sup>h</sup>.

Figures 4 and 5 show the southern and northern boundaries at pre-noon (8<sup>h</sup>) and afternoon (16<sup>h</sup>) hours. The askafilms of Cape Chelyuskin and Vize /26 Island stations were processed only for the 1957 - 1958 season. In the determination of the equatorial boundary during strong magnetic disturbances, the southern edge of the band at 8 and 16<sup>h</sup> frequently moves beyond the horizon. For this reason, the same number of the largest  $\phi'$  values was eliminated; the remaining values were averaged. With large  $Q$ , the number of instances of the equatorial boundary shift beyond the horizon exceeded one-half of all readings. It was established that the ratio of such shifts to the total number of measurements increases linearly with an increase of  $Q$ . Thus, it was possible to compute the position of the equatorial boundary even in those instances when the number of shifts of the boundary beyond the horizon exceeded one-half of the total number of readings. In view of the small quantity of data

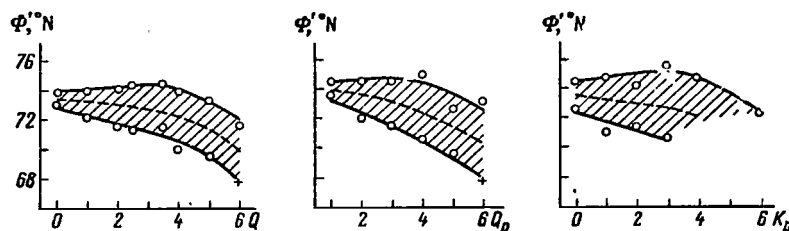


Figure 4. Position of southern and northern aurora band boundaries in pre-noon hours ( $8^h$ ) as a function of  $Q$ ,  $Q_p$  and  $K_p$ .

The dashed line is the central line of the auroral band; the circles indicate the computed values of  $\Phi'$ .

and aurora shift beyond the southern horizon, it is not feasible to determine  $\Phi'$  for large  $K_p$  (Figure 4) and  $Q_p$  (Figure 5).

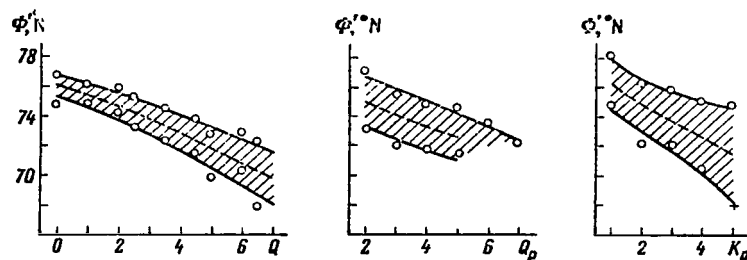


Figure 5. Position of southern and northern aurora band boundaries in afternoon hours ( $16^h$ ) as a function of  $Q$ ,  $Q_p$  and  $K_p$ .

The dashed line indicates the auroras band middle; the circles indicate the computed values of  $\Phi'$ .

In pre-noon hours (Figure 4), the southern boundary withdraws monotonically from the pole; the velocity of this shift increases somewhat with large  $Q$ . The northern boundary, when  $0 \leq Q \leq 3.5$  (fractional values of  $Q$  are obtained in view of the reduction of the indexes of all observatories to the Kiruna Observatory  $Q$  index), somewhat approaches the pole and shifts southward only when  $Q$  is large. The same tendency is manifested for  $Q_p$  and  $K_p$ . When  $Q = 0$ ,

the bandwidth amounts to  $1.2^\circ$  only. This happens to be the smallest of all obtained bandwidth values. The band center withdraws from the pole, and the withdrawal rate goes up with the increase of the magnetic activity index. During afternoon hours (Figure 5), a decrease of  $\phi'$  is observed for the northern as well as for the southern boundaries with a negligible expansion of the band with increasing magnetic disturbance. The nature of the variation in the band /27 position and bandwidth during these hours is very similar to the corresponding variation at noon [11]. The aforementioned laws are also valid for  $Q_p$ . The position of the northern boundary with respect to  $K_p$ , as opposed to  $Q$  and  $Q_p$ , changes nonlinearly. Conceivably, this is related to the inaccuracies in the determination of the boundaries due to insufficient data.

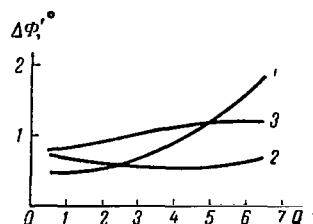


Figure 6. Variation of the rate of shift of the southern aurora band boundary at different  $Q$ . 1, 2 and 3 are the shift velocities for  $8^h$ ,  $12^h$ , and  $16^h$ , respectively.

Figure 6 shows the variation of the rate of shift of the southern boundary for day areas of the aurora band with relation to the magnetic disturbance. Curve 1 defines the velocity variation of the shift in pre-noon hours, Curve 2 applies to day hours, and Curve 3 applies to afternoon hours, Curve 2 was computed from data cited in [11]. Figure 6 indicates that a smooth increase of the rate of shift with increasing magnetic disturbance, which is close to  $2^\circ$  latitude when  $Q = 6 - 7$ , takes place only during pre-noon hours. For  $12^h$  and  $16^h$ , the rate of shift of the equatorial boundary toward the south, for practical purposes, does not change; however, during afternoon hours it is always higher than at noon.

Figure 7 shows the variation curves of auroral bandwidth with relation to the magnetic activity indexes for all four time intervals. At  $20^h$  and  $4^h$ , the auroral bandwidth ( $L^\circ$ ) increases rapidly with increasing activity index, yet the process is slower than on the night side of the earth. During after-midnight hours, the curves for  $Q$  and  $Q_p$  practically coincide. The bandwidth



with relation to  $K_p$  is systematically greater. In pre-midnight hours, the auroral bandwidth varies from  $2 - 3^\circ$  when  $Q = 0$ , to approximately  $8^\circ$  when  $Q = 7$ . In after-midnight hours, the variation interval amounts to  $4 - 10^\circ$ . During before-noon and afternoon hours, the bandwidth is considerably smaller and does not exceed  $5^\circ$  even with  $Q = 7$ . The range of variations is somewhat greater in pre-noon hours. At  $16^h$ , the auroral bandwidth increases only by  $2^\circ$ .

On the basis of the obtained findings and using the data cited in [11], on the position and dimensions of the band in near-midnight and near-midday hours, we can plot the instantaneous distribution of aurora with relation to the magnetic activity level. Figure 8 shows diagrammatically the position of the band in reduced geomagnetic coordinates at various levels of magnetic disturbance in the area of the Fritz zone on the nightside of the Earth. When  $Q = 0$ , the band is narrowest at pre-noon hours. The equatorial boundary is at the greatest distance from the pole at midnight hours, and somewhat more toward the north in after-midnight hours. During pre- and after-midnight hours, the auroral band covers a larger interval of latitudes than at any other time. The bandwidth at  $4^h$  exceeds the corresponding value at midnight almost by the factor of three. The southern boundary during pre-noon hours is closer to the equator than during afternoon hours.

When  $Q = 1$ , these characteristics are still retained, however, due to the rapid expansion of the band during midnight hours; the asymmetry of the nightside of the Earth begins to smoothen out somewhat. A southward shift of the entire aurora band was noted during night hours. The band rapidly moves to the equator also during afternoon hours, yet it still remains considerably closer to the pole than during pre-noon hours.

When  $Q = 2$  and  $3$ , the nature of the expansion of the aurora band is retained. On the nightside of the Earth, the northern boundary begins to shift slowly toward the pole, and asymmetry on the night side of the Earth continues to decrease. Large velocities of the southward shift of the equatorial boundary in pre- and afternoon hours cause the appearance of a flattening of the dayside of the Earth. When  $Q = 4$ , the bandwidth in after-midnight hours is still

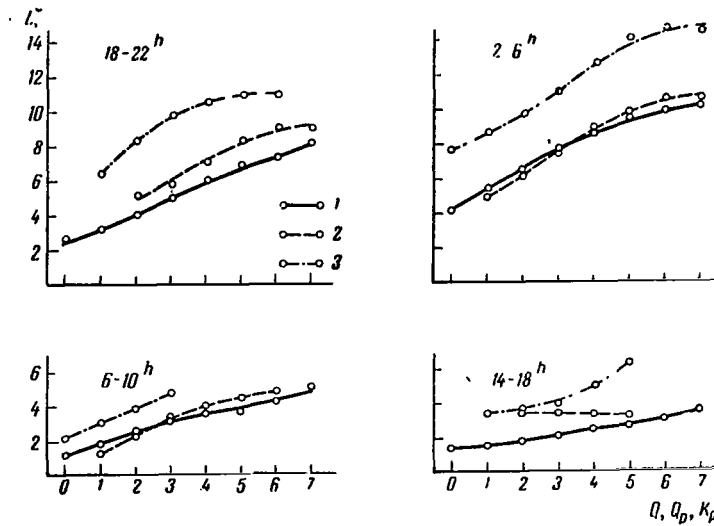


Figure 7. Auroral band variation as a function of the magnetic activity level for four time intervals with relation to  $Q$  (1),  $Q_p$  (2); and  $K_p$  (3).

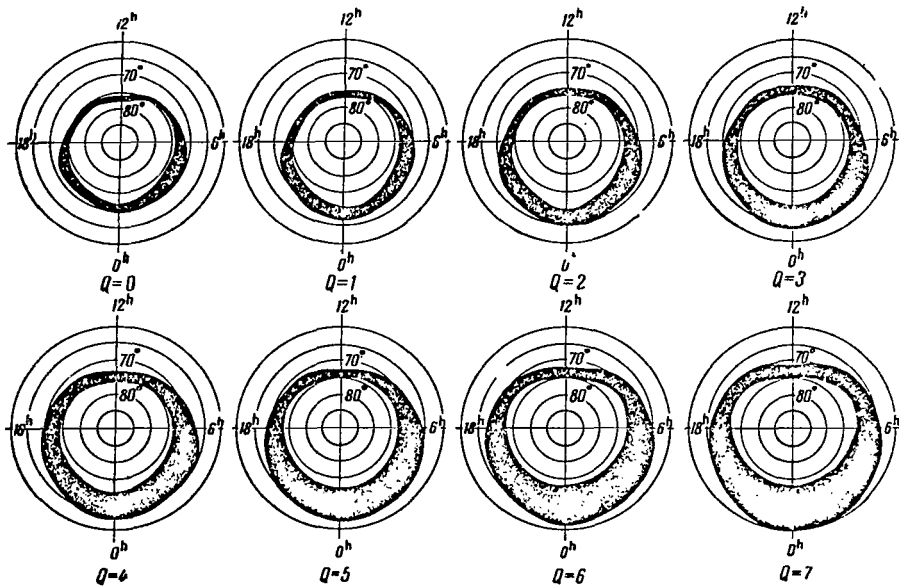


Figure 8. Auroral bands at different  $Q$  (in geomagnetic coordinates).

somewhat greater than in midnight hours, and reaches approximately 1,000 km. At 16<sup>h</sup> the band is still closer to the pole than at 8<sup>h</sup>. The least bandwidth was recorded at noon. The circumpolar boundary is close to a circle whose center is somewhat displaced toward the night side of the Earth. The equatorial boundary of nearly 1/3 of the band is located at  $\phi \sim 65^\circ$ .

With a further increase of magnetic activity, the asymmetry on the night side of the Earth continues to decrease. When  $Q \geq 6$ , the maximum bandwidth was observed at midnight; when  $Q = 7$ , it reaches approximately 1,400 km.

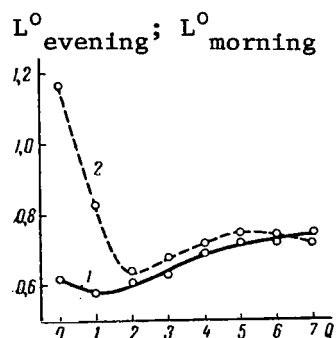


Figure 9. Ratio of the auroral bandwidth in evening (1) and in morning hours (2).

$$1 = \frac{L^0(18-22)^h}{L^0(2-6)^h}, \quad 2 = \frac{L^0(14-18)^h}{L^0(6-10)^h}$$

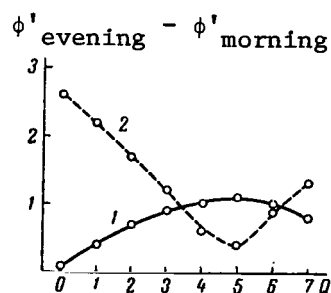


Figure 10. The difference of latitudes of the middle of aurora bands for the evening (1) and morning (2) hemispheres.

$$1 = [\Phi'(2-6)^h - \Phi'(18-22)^h]; \\ 2 = [\Phi'(6-10)^h - \Phi'(14-18)^h]$$

The interval of latitudes occupied by aurora in after-midnight hours is greater than the interval covered by auroras in pre-midnight hours. The more rapid southward shift of the equatorial boundaries at 16 and at 8<sup>h</sup>, as compared to noon hours, distorts the day segment of the aurora band, and causes its flattening.

At low magnetic activity levels, the basic asymmetry of the band is apparent in the larger width in pre- and after-midnight hours, as compared to the midnight hours. This asymmetry disappears gradually with an increasing

Q-index. There appears, however, a flattening on the dayside of the Earth, which increases with increasing magnetic activity. Another interesting feature of aurora bands is the continuous gain of the latitude interval covered by aurora in the morning hours, as compared with the evening hours. The southern boundary of the band is closer to the pole in the evening hours than it is in the morning hours.

To obtain some quantitative characteristics of the band asymmetry, Figure 9 shows the bandwidth ratio variation in evening and morning hours. The solid line indicates the width ratio  $L^\circ$  of the pre-midnight sector to the after-midnight sector; the dashed line shows the ratio of the afternoon to the pre-noon sector. The graph also indicates that only when  $Q = 0$  is the width of  $L^\circ$  at  $16^h$  on the dayside of the Earth greater than at  $18^h$ . It is of interest that when  $Q \geq 2$ , this ratio for day and night hemispheres is practically equal; i.e., the asymmetry between the morning and evening sides of the Earth is retained. When  $Q$  varies from 2 to 7, the width ratio increases from 0.6 to 0.75; i.e., with increasing magnetic activity, the asymmetry decreases somewhat, yet remains reasonably high. However, when  $Q \geq 6$ , an insignificant gain in asymmetry is observed in the day hemisphere. /30

Figure 10 shows the difference in latitudes of the band centerlines for the evening and morning hemispheres. The solid line shows the difference between the reduced geomagnetic latitudes of the pre-midnight and after-midnight sides of the Earth; the dotted line shows the difference between the latitudes of auroral band centerlines in afternoon and pre-noon hours. As we pointed out before, the southern auroral band boundary is further displaced to the equator in morning hours than it is in evening hours. On the basis of the data in Figure 10, it stands to reason that not only the southern boundary, but also the band itself on the morning side, is shifted further from the pole. This shift, as opposed to the curves shown on Figure 9, is not identical for the night and day hemispheres. When  $Q = 0$ , the band middles on the night side of the Earth are practically at the same distance from the pole. On the day side of the earth, we have at the same time a maximum asymmetry, reaching almost  $3^\circ$  in latitude. With increasing magnetic activity, the asymmetry

decreases on the day side of the Earth, going up at the same time on the night side of the Earth. Both curves reach their extremum at  $Q = 5$ . With larger disturbances, the asymmetry changes in the opposite direction. When  $Q = 5$ , maximum asymmetry on the night side and minimum asymmetry on the day side are attained. When  $Q = 3 - 4$  and  $Q = 6$ , the shift of the part of the band in morning hours with respect to the shift of the band in evening hours is approximately the same for the day and the night sides of the Earth. These data appear to indicate that zonal asymmetry takes place at any level of magnetic activity; however, its nature, following the variations of  $Q$ , changes in a rather complex manner. With large magnetic disturbances, this asymmetry is somewhat smaller than with weak disturbances.

Let us consider in more detail the absence of aurora during the 15-minute intervals in the morning and in the evening. These particular instances cannot be interpreted as a shift of the aurora band beyond the field of view on the camera. There is a systematic shift of the aurora band with varying magnetic activity for noon and midnight hours. Thus, with small  $Q$ -indexes, during midnight hours, aurora were seldom recorded in Murmansk, but were regularly observed at Cape Chelyuskin; i.e., the aurora band was always regularly observed by stations whose  $\phi'$  corresponded to the mean latitude of the aurora band.

In isolated instances, the appearance and disappearance of aurora in evening and morning hours takes place very differently. In those instances, the aurora band is in the zenith of high-latitude stations, e.g., Cape Chelyuskin, Vize Island, and Piramida. The absence of a shift with varying magnetic activity level is typical for the northern boundary of the band during pre- and after-midnight hours. Hence the disappearance of aurora during these hours cannot be explained by a band shift from mid-position to the south or to the north. The fact is, it does not shift to the south; this is easily established from the data of low-latitude stations, e.g., Dixon Island. The absence of aurora on Vize station, on the assumption of a northward shift of the band, is possible only with an intermittent shift of the southern boundary up to approximately  $78^\circ$ , and of the northern boundary up to  $80^\circ$ . In view of the relative

constancy of the northern boundary position at that time, this is hardly possible. If auroras do reappear after their disappearance, they appear directly at the zenith, rather than shifting from the horizon, which would have been the case in the event of a band drift beyond the horizon.

In order to perform a more detailed and efficient analysis, we used the askafilms of Vize Island, Cape Chelyuskin, and Piramida stations, which are located at geomagnetic latitudes where the aurora band during these hours is near the zenith. Figure 11 shows the probability of the aurora appearance with relation to LGT; this probability was determined as a ratio of the number /31 of 15 minute intervals with aurora within each hour, to the total number of observations. The probability of aurora appearance was computed in an integrated form for all stations. The smoothing was performed according to the trapezoidal rule.

In the evening hours, when  $Q = 0$ , it was impossible to determine  $P$  due to lack of a sufficient amount of data. The probability of the appearance of aurora strongly increases with increasing  $Q$ , and when  $Q > 3$  aurora practically always appear at these latitudes. For  $1 \leq Q \leq 3$ , the minimal values of  $P$  depend linearly on  $Q$ . Hence, approximating this linear relationship, it is possible to determine the minimum value of  $P$  when  $Q = 0$ , which was 65%. When  $Q = 1$ , we found that  $P_{\min}$  is 77%, and corresponds to 18 - 19<sup>h</sup>. With increasing  $Q$ , the moment of minimum values of the probability of appearance of bands shifts somewhat in the direction of later hours, but it was impossible to determine a clearly defined pattern for this phenomenon.

In the morning hemisphere, the probability of the appearance of aurora at small  $Q$  is considerably less. It goes down to 30% when  $Q = 0^\circ$ ; however,  $P$  grows just as fast with increasing magnetic activity. When  $Q = 0$ , the minimum value of  $P$  is recorded between 8 and 9<sup>h</sup>. With increasing  $Q$ , the probability of occurrence minimum is clearly shifted to earlier hours. When  $Q \geq 4$ , no breaks of aurora bands were observed.

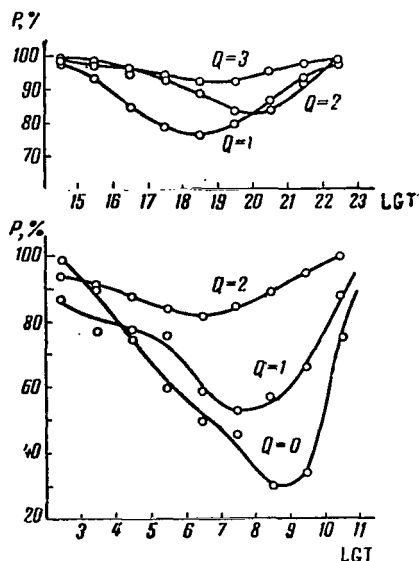


Figure 11. The probability of aurora appearance at Piramida, Vize Island and Cape Chelyuskin stations at evening and morning hours during small magnetic disturbances.

It may be concluded that the aurora band at a low level of magnetic activity is not always a continuous whole phenomenon. We can conceivably assert that the band always exists at day and night side, shifting in latitude with varying magnetic activity. Nonetheless, in the morning, pre-noon and evening sides of the Earth there can be breaks, even though when  $Q = 0$ , the existence of aurora in the form of a single band is possible. The minimal probability of its appearance is approximately 30%. When  $Q = 0$  the aurora band on the night side of the Earth continues from 18 to 7<sup>h</sup>. Moreover, aurora are observed during near-midnight hours. The most probable break occurs between 8 and 9<sup>h</sup>, and at 18<sup>h</sup> LGT.

Notably, aurora occurring at night and day hours are essentially different. For the night hemisphere, we can establish a certain diurnal pattern. During the evening hours and toward midnight, uniform arcs are replaced by radial shapes; toward the morning, we see spots and pulsating surfaces. This pattern may be somewhat modified, depending on the appearance of polar magnetic disturbances of varying intensity; however, its basic characteristics are retained [16, 6]. During day hours, the principal type of aurora in the band are radial arcs of weak intensity; they disappear and reappear without any significantly systematic movements. Their intensity increases with increasing magnetic disturbances; the glow band somewhat widens, simultaneously shifting toward the equator.

Day and night sectors of auroral bands can close into a uniform band with adequately large probability on the evening and on the morning sides, or even on only one of these sides, provided that the magnetic field is quiet. The probability of closure on the evening side, incidentally, is considerably

higher. With an increasing Q index, the region of the most probable breaks is somewhat shifted toward midnight hours with a strong decrease in the break probability; when  $Q \geq 3$ , we can speak about a uniform aurora band.

Band breaks appear at certain moments also on synoptic charts, which show the instantaneous distribution of polar aurora. Figure 12 shows such

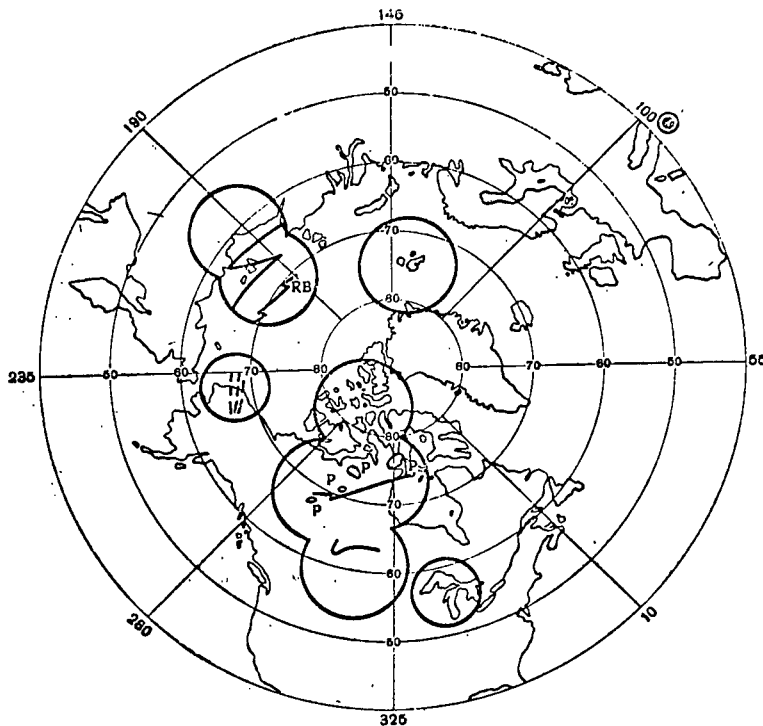


Figure 12. A synoptic chart of aurora plotted at 10<sup>h</sup> 50<sup>m</sup> UT on 13 December 1957.

a chart, plotted at 10<sup>h</sup> 50<sup>m</sup> UT on 13 December 1957. The field of view of the cameras for the entire sky is delimited on the chart by a circle, corresponding to a zenith distance of 85° for 35 mm cameras, and of 80° for 16 mm cameras. The height of the lower aurora boundary is assumed to be 105 km. The direction toward the Sun is denoted by a circle with a dot in the middle. Position and shape of aurora are plotted according to the legend adopted by the International Instructions for Aurora Observations during the IQSY. It follows from Figure 12



that the auroral band has a break in afternoon hours (at the Piramida station, with stars photographed differently, there are no aurora, even though the band should have passed through the camera's field of view).

# REFERENCES

1. Fel'dshteyn, Ya. I. Geographic distribution of Aurora and the Azimuths of Arcs. In: "Issledovaniye polyarnykh siyaniy", No. 4, seriya "Rezul'taty MGG" (Investigation of Aurora, No. 4, series "Results of the IGY"). Academy of Sciences of the USSR, 1960, page 61. /33
2. Khorosheva, O. V. The Diurnal Drift of a Closed Auroral Ring. Geomagnetizm i aeronomiya, Vol. 2, No. 5, 1962, p. 839.
3. Fel'dshteyn, Ya. I. Some Problems of Aurora and Magnetic Disturbance Morphology at High Altitudes. Geomagnetizm i aeronomiya. Vol. 3, No. 2, 1963, page 227.
4. Fel'dshteyn, Ya. I. Auroral Morphology. — Tellus, Vol. 16, No. 2, 1964, p. 252.
5. Khorosheva, O. V. Prostranstvenno-vremennoye raspredeleniye polyarnykh siyaniy (Space-time Distribution of Aurora). Dissertation, Moscow, 1965.
6. Akasofu, S. I. Dynamic Morphology of Auroras. Space Science Rev., Vol. 4, No. 4, 1965, p. 498.
7. Fel'dshteyn, Ya. I. Peculiarities in the Auroral Distribution and Magnetic Disturbance Distribution. — Planet. Space Sci., Vol. 14, No. 2, 1966, p. 121.
8. Isayev, S. I. The Region of Increased Aurora Activity at Mid-latitudes. Geomagnetizm i aeronomiya, Vol. 2, No. 5, 1962, p. 861.
9. Bond, F. R. Motion of the Aurora and Magnetic Bays. Austral. J. Phys., Vol. 13, No. 3, 1960, p. 477.
10. Bryunelli, B. E. Polar Magnetic Disturbances. Geomagnetizm i aeronomiya Vol. 2, No. 5, 1962, p. 801.
11. Starkov, G. V. and Ya. I. Feld'shteyn. The Oval Zone Dynamics of Aurora. Geomagnetizm i aeronomiya, Vol. 7, No. 1, 1967, p. 61.
12. Piddington, J. H. The Magnetosphere and its Environs. Planet. Space Sci., Vol. 13, No. 5, 1965, p. 363.
13. Walters, G. K. Effect of Oblique Interplanetary Magnetic Field on Shape and Behavior of the Magnetosphere. J. Geophys. Res., Vol. 69, No. 9, 1964, p. 1769.
14. Fel'dshteyn, Ya. I. Space-time Distribution of the Magnetic Activity at High Altitudes of the Northern Hemisphere During the IGY. In: "Geomagnitnyye issledovaniya", No. 5, seriya "Rezul'taty MGG" (Geomagnetic Investigations, No. 5, Series "Results of the IGY"). Moscow, Academy of Sciences of the USSR, 1963.

15. Nagata, S., N. Kokubun, Fukushima. Similarity and Simultaneity of Magnetic Disturbance in the Northern and Southern Hemispheres. J. Phys. Soc. Japan, Vol. 17, Suppl. A2, 1962, p. 35.
16. Heppner, J. P. A Study of Relationships Between the Aurora and Geomagnetic Disturbances. Doct. Thesis, Pasadena, 1954.

## U-LIKE POLAR AURORAL SHAPES

S. A. Zaytseva

**ABSTRACT.** The paper discusses the peculiarities of excitation and development of U-like aurora bands and their connection with the level of magnetic activity and configuration of current systems in the lower ionosphere.

The uniqueness of the U-shaped auroras, the patterns which have been determined in their development and motion has attracted the attention of a number of investigators [1 - 5]. In this report, we are attempting to explore and explain certain specific characteristics of this type of shape. Initial data included photographs of the entire sky, taken by a C-180 camera at the following stations:

Murmansk ( $\phi = 65.0^\circ$  N,  $\Lambda = 126.8^\circ$ ) in 1958 - 1960; Dixon Island ( $\phi = 62.8^\circ$  N,  $\Lambda = 165.5^\circ$ ) in 1958; Tiksi Bay ( $\phi = 60.5^\circ$  N,  $\Lambda = 191.4^\circ$ ) in 1958 - 1959; Cape Chelyuskin ( $\phi = 66.1^\circ$  N,  $\Lambda = 176.5^\circ$ ) in 1958 - 1959; data of the appropriate magnetic observatories were also included

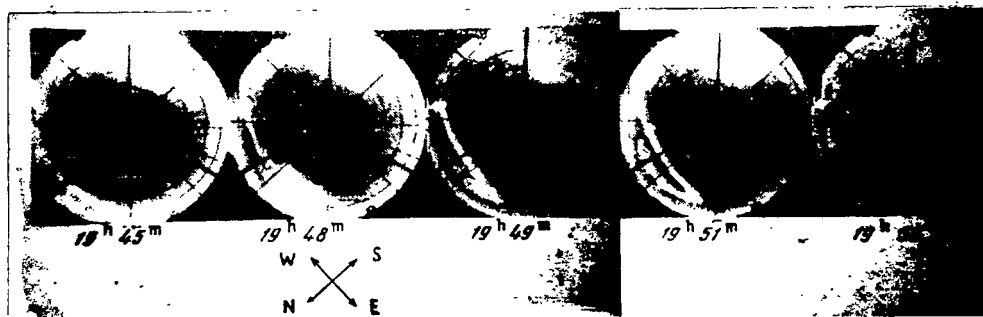


Figure 1. The development of a U-like shape, recorded in Murmansk on 31 March 1958.

Figure 1 shows photographs obtained by a C-180 camera in Murmansk on 31 March 1958 at the following moments:  $19^h 45^m$ ,  $19^h 48^m$ ,  $19^h 49^m$ ,  $19^h 51^m$  and  $19^h 56^m$  UT. These photographs quite adequately illustrate the development

of a U-like shape. As a rule, it appears during evening hours at the northern horizon. Its appearance usually is preceded by a rather narrow arc; the eastern end of the arc gradually deflects to the north, forming a loop which is open in a westward direction. U-like shapes are unstable and disintegrate reasonably fast. For this reason, photographs taken by a C-180 camera do not necessarily reflect all moments of their development. In some instances, the ends of the loop close, forming giant luminescent ovals which sometimes are deformed (Figure 2).

In most instances, the loop is formed on the eastern edge. This occurred in 50 instances of the total of 55 that were examined, and only in five cases were bands observed with a loop that was on the western end and was open toward the east. Apparently, the latter are more unstable. Below, we will /35 examine bands with a loop at the eastern end and open toward the west.

Concerning the structure of U-like shapes, we find among them with equal frequency uniform and radial shapes (35 uniform bands out of a total of 55; the rest were radial). It should be kept in mind that in some instances the phenomenon of an oblique superimposition may occur, resulting in the formation of a pseudo-loop in a band photographed by a C-180 camera. Essentially, this applies to bands with a radial structure.

Of interest is the large drift velocity of U-like shapes in the westerly direction. The height of such a band was determined by a parallax recording at the stations Murmansk-Loparskaya ( $\Phi = 63.7^\circ$ ,  $\Lambda = 126.6^\circ$ ) on 2 March 1965. Its drift rate toward the west was estimated. It turned out to be 970 m/sec, which agrees with the findings reported in [4, 6]. T. N. Davis [4] cites similar values for the drift rate of bands in the easterly direction, apparently including the latter in the category of bands with a loop at the westerly end.

Comparing the time of occurrence for U-like shapes with magnetic data, another characteristic of these shapes was discovered. It appears that they occur near the time of zero transition in the H-component of the  $S_D$ -variation of the Earth's magnetic field. Figure 3 shows the relationship between the



Figure 2. Aurora band in the form of a closed oval, taken at Cape Chelyuskin at 13<sup>h</sup> 3<sup>m</sup> UT on 18 January 1959.

moments of the appearance of U-like shapes and the zero transition time in the H-component. To plot the graph, the data of Murmansk, Dixon, and Tiksi Bay stations were used. In spite of the point scattering, it is obvious that they are grouped near a coincidence line. This is also supported by the findings of Davis [4], who noted the appearance of a loop-like shape at College about 23<sup>h</sup> - 23<sup>h</sup> 30<sup>m</sup> LT (which is approximately the time of zero point in College).

Insofar as the zero transition time at any station is concerned, it is not strictly fixed, but varies within several hours. Along with it, the time of appearance of U-like shapes also varies. However, it should be noted that for early zero points, the band more frequently precedes the beginning of the zero transition, whereas for late zero points it usually lags. Inasmuch as the beginning of the zero transition to some measure is defined by the disturbance intensity [7], we examined the relationship between the time interval  $\Delta t$  (which equals the difference between the time of appearance of a U-like shape and the time of zero point), and the three-hour value of the  $K_p$ -index. The results are shown in Figure 4. Each point was obtained by averaging the data for several days (from 4 to 10). The scatter turned out to be quite substantial; however, it does not affect the nature of the relationship. We can assert with /36 reasonable certainty that with small  $K_p$  indexes, U-like shapes appear later than the zero transition (on the average, 50 minutes later, when  $K_p = 2$ ). With large  $K_p$  values, the U-like shape obviously precedes the appearance of the zero point (approximately one hour earlier when  $K_p = 4$ ).

To some extent, these findings contradict the formation mechanism of U-like auroras, suggested in [4, 8]. According to the latter, U-like forms with

a loop on the eastern or western end are associated with the evening or morning vortex of the  $S_D$  variation, respectively. Thus, the time of appearance of such bands, insofar as the zonal stations are concerned, must be controlled by an  $S_D$  current system. However, during weakly excited days, the  $S_D$ -system between 21 and 9<sup>h</sup> has a meridional orientation, whereas U-like shapes with a loop at the eastern end appear during such days at about 23<sup>h</sup> LT. Hence, it is unlikely that a band, associated with an easterly directed current, according to [4, 8], can be observed after the direction of the zonal current changed from east to west. Further, it is unlikely that aurora, as suggested by Davis [4], duplicate exactly the shape of the currents. Moreover, instances were pointed out [9, 10] where currents and aurora did not coincide spatially.

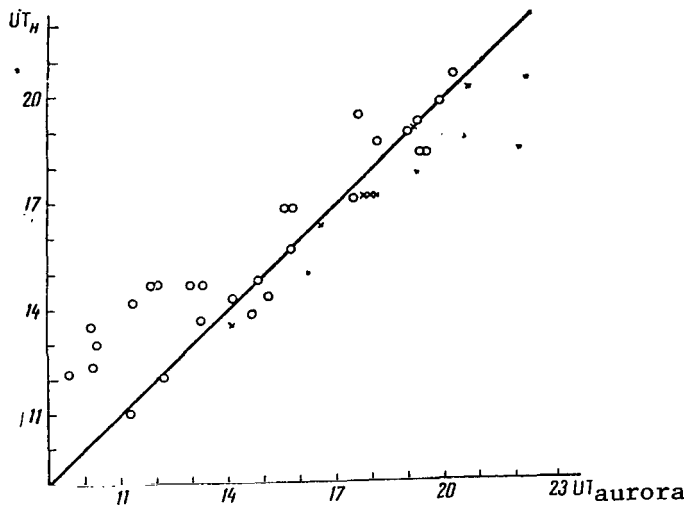


Figure 3. Relationship between the time of appearance of a U-like shape, and the zero transition time of the H-component of the magnetic field.

The circles denote uniform bands; crosses indicate radial shapes. The straight line shows the exact coincidence between the formation of a U-like shape and the occurrence of a zero transition.

Kern [8] assumes the presence of a positive gradient of the magnetic field in the direction of the midnight meridian. This, according to Kern, accounts for the charge separation which, in turn, causes the emergence of currents and U-like

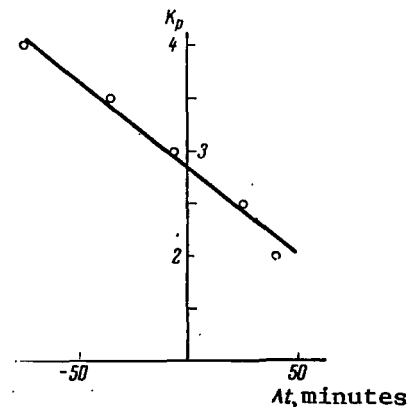


Figure 4. Relationship between  $\Delta t$  ( $\Delta t = t_{\text{comp}}$ ) and the  $K_p$  index.

shapes. This argument is not very convincing. Based on our findings, a somewhat different explanation of the formation of U-like shapes is suggested.

A system of  $S_q^P$  currents, as suggested in [11], is shown in Figure 5. The formation of such a current system, as pointed out by Nagata [11], can be explained by convective vortexes, as suggested by Axford and Hines [12]; a diagram of such vortexes is shown in Figure 6. Axford and Hines explain the vortex formation in the magnetosphere by a viscous interaction between the solar corpuscular stream and surface layers of gases in the magnetosphere. However, they point out that the nature of the process would hardly change if some other interaction mechanism between the corpuscular stream and the plasma captured by the geomagnetic field were assumed to exist. Thus, conceivably the Levi-Danji mechanism could be applicable.

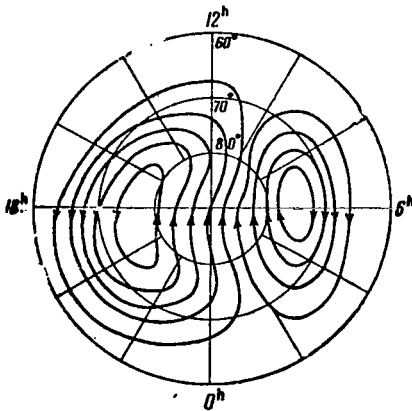


Figure 5. The system of  $S_q^P$  currents [11].

Figure 5 shows that between 23 and 11<sup>h</sup>, the  $S_q^P$ -system has a meridional orientation near the poles. This indicates that the zero point time of the  $S_q^P$ -system approximately coincides with the appearance of U-like shapes at small  $K_p$ -indexes. This

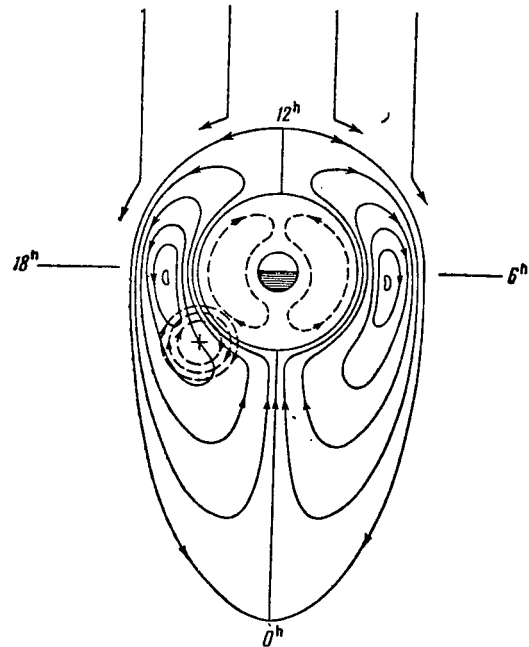


Figure 6. Diagram of plasma motion in the magnetosphere.



leads us to the assumption that the appearance of U-like shapes, north of the auroral zone, during days with a small (but not zero) magnetic activity, is not necessarily associated with the  $S_D$  current system, but rather with the  $S_q^P$  system. This explains the lag of the U-like shape with respect to the moment of zero transition  $\delta H$  at zonal stations. The vortexes at the morning and evening side of the earth can be essentially credited with the formation of auroral shapes with a loop at the eastern and western ends. Due to the rotation of the Earth, the vortex on the morning side is less stable [12]. Apparently this accounts for the instability of the U-like bands with a loop on the western end.

With large  $K_p$ , the  $S_D$  currents affect the time of appearance of U-like bands. The excessive positive charge, formed on the night side, is transmitted into the magnetosphere [13] along the force lines. As a consequence, an additional vortex (clockwise, viewing the North Pole from the top) appears. This vortex, combined with the Axford-Hines evening vortex, leads to a deformation of the latter and shifts toward earlier hours causing the appearance of a U-like shape prior to reaching zero point. /38

Insofar as bands with a loop at the western end are concerned, the positive charge, formed at the evening side of the earth, displaces them from midnight toward the morning. Since the  $S_D$ -system, with increasing activity, becomes reoriented in such manner that its zero point is shifted toward earlier evening hours, it is entirely conceivable that increasing activity has no effect upon the time of emergence of these bands. Nonetheless, it is not feasible to derive any more specific laws from these random data, since not enough bands were observed.

The following conclusions can be derived regarding the U-like shape with a loop at the eastern end:

1. The appearance of a U-like shape is statistically related to the zero transition moment of the H-component of the  $S_D$ -variation of the geomagnetic field.

2. In spite of the time relationship between the U-like shape and the  $S_D$ -current system, the assumption that  $S_D$  currents flow along the U-like shape [4, 8], is erroneous. With small  $K_p$  indexes, the appearance of a U-like shape is controlled by a  $S_q^p$ -system of currents.

3. The emergence of the U-like formation at earlier pre-midnight hours, when  $K_p$  is large, can apparently be explained by the formation of magnetospheric convection vortexes, which are essentially responsible for the  $S_q^p$ -system. Presumably, the deformation is caused by the positive charge formed in the ionosphere on the night side of the earth. This charge is transmitted into the magnetosphere along the force lines.

In conclusion, the author is deeply grateful to M. I. Pudovkin for help in the interpretation of the data obtained.

## REFERENCES

- 1 Störmer, C. The Polar Aurora. Oxford, Clarendon Press, 1955.
2. Nichols, B. Auroral Ionization and Magnetic Disturbances. Proc. Inst. Radio Engrs., Vol. 47, 1959, p. 245.
3. Davis, T. N. The Morphology of the Polar Aurora. J. Geophys. Res., Vol. 65, No. 10, 1960, p. 3497.
4. Davis, T. N. The Morphology of the Auroral Displays of 1957 - 1958. J. Geophys. Res., Vol. 67, No. 1, 1962, p. 59.
5. Akasofu, S. I., D. S. Kimball, Ch. I. Meng. The Dynamics of Aurora. III. Westward Drifting Loops. J. Atmos. and Terr. Phys., 27, 1965, 189.
6. Gartlein, C. W., D. S. Kimball, G. Sprague. The Origin and Morphology of the Aurora. Phys. Dept. Cornell Univ., 1965.
7. Loginov, G. A. Some Findings on the  $S_d$ -Variation at High Latitudes. In: "Issledovaniye polyarnykh siyaniy, geomagnitnykh vozmushcheniy i ionosfery v vysokikh shirotakh" (The Investigation of Aurora, Geomagnetic Disturbances and the Ionosphere at High Latitudes). Moscow, Nauka Press, 1964, p. 71.
8. Kern, J. V. The Charge Separation Mechanism Leading to Aurora and Electrical Currents in the Polar Region. In: "Radiation Belts and Geophysical Phenomena". Moscow, IL, 1963, p. 154.
9. Pudovkin, M. I., and L. S. Yevlashin. The Spatial Relationship Between Auroras and Electric Currents in the Ionosphere. Geomagnetizm i aeronomiya, Vol. 2, No. 4, 1962, p. 669.
10. Meek, J. H. Correlation of Magnetic, Auroral, and Ionospheric Variations at Saskatoon. J. Geophys. Res., Vol. 59, No. 1, 1954, p. 87.
11. Nagata, T. Polar Geomagnetic Disturbances. Planet. Space Sci., Vol. 11, No. 12, 1963, p. 1395.
12. Axford, W. I., C. O. Hines. A Unifying Theory of High Latitude Geophysical Phenomena and Geomagnetic Storms. Canad. J. Phys., Vol. 39, 1961, p. 1433.
13. Bryunelli, B. Ye. Polar Magnetic Disturbances. Geomagnetizm i aeronomiya Vol. 2, No. 5, 1962, p. 801.

## THE EFFECT OF MAGNETIC ACTIVITY UPON AURORAL HEIGHTS

G. V. Starkov

**ABSTRACT.** The paper analyses the results which indicate that the heights of aurora diminish with the increase of magnetic activity. The increase of the vertical stretch with the decrease of magnetic activity is observed for ray forms. The dependence is obtained between the energy of electrons, corresponding to the average value of height of the lower edge of aurora, on the magnitude of the  $K_p$ -index.

Auroral heights are a very important characteristic, since they lead to an /39 estimate both of the energy of particles that cause atmospheric glow and also of their energy spectrum. In view of this, it was deemed of interest to consider the effect of magnetic activity upon polar auroral heights. To establish this comparison, we used height data obtained by C. Störmer in northern Scandinavia [1], and by V. R. Fuller at College [2]. The  $K_p$ -index was taken as a characteristic of the magnetic activity.

In College ( $\phi' = 65^\circ$ ), the lower edge of linearly extended shapes was measured. The observations were performed for two days in January, and for six days in March-April 1932. All measurements were conducted between 9 and 12<sup>h</sup> UT. The  $K_p$ -index varied from 2 to 5. A total of 436 arcs and bands were analyzed. The height measurement data obtained before 1932 were not used, in view of the absence of data on the  $K_p$ -index. Störmer's measurements, conducted in northern Scandinavia ( $\phi' \sim 65.5^\circ$ ), cover March, 1933. The analysis did not include aurora that were illuminated by the Sun. Essentially, the measurements referred to characteristic points of radial formations. A total of 51 height values of uniform arcs and bands were available. The data used refer to seven days of observations, conducted between 21 and 3<sup>h</sup> UT. A comparison with  $K_p$  was possible only for one day for less than six hours.

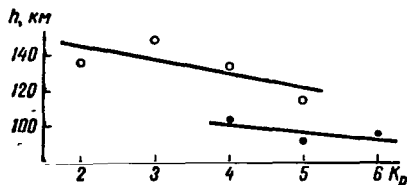


Figure 1. The relationship between the height of the lower edge of homogeneous polar aurora forms, and the  $K_p$ -index. The light circles are data for College; the dark circles are data for the north of Scandinavia.

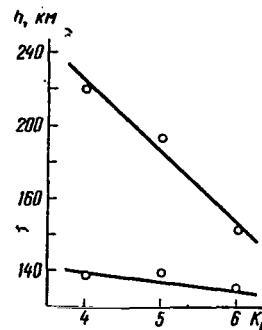


Figure 2. Relationship between the height of the lower and upper edges of radial polar aurora, and the  $K_p$ -index.

Figure 1 shows the measurement data of homogeneous auroral shapes with relation to the magnetic activity. The measurements were performed for College and for Northern Scandinavia. The heights, plotted on the graph, represent the 40 arithmetic mean of all values corresponding to the given  $K_p$ . The straight lines were computed using the least square method. The data cited in [2] are less reliable, since overestimated height values, up to 300 km, were obtained for the arcs. This contradicts numerous findings by C. Störmer [3], as well as some recent results [4, 5]. In spite of this, there is an apparent tendency toward decreasing height with an increase of  $K_p$ .

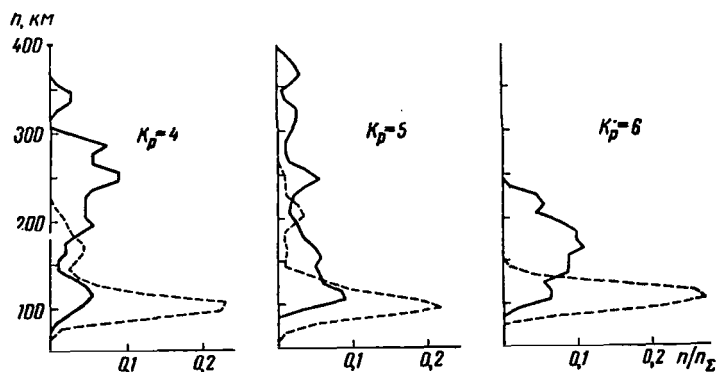


Figure 3. Altitudinal distribution of the upper (solid line) and lower (dashed line) edges of radial aurora with various  $K_p$ -indexes.

Störmer's data for quiet forms turned out to be more limited, both in terms of quantity and in terms of the variation of  $K_p$ ; however, the same patterns are also recurring here. The range of height variation for the Scandinavian Peninsula is considerably smaller than for College. The arcs are at heights which are somewhat lower than the average values, obtained by different authors without taking into account the magnetic activity level. Inasmuch as the mean of  $K_p$ , in presence of quiet aurora forms, amounts to 3 - 4, this again supports the obtained relationship between the mean height of homogeneous arcs, and the magnetic disturbance. An extrapolation of the straight line up to  $K_p = 3$  yields a height of 105 km, which is in good agreement with the mean height values for homogeneous forms.

Figure 2 shows the relationship between the upper and lower edges of radial forms of  $K_p$ , based on Störmer's data. The lower edge was measured 208 times, whereas the upper edge was measured 104 times. It appears that the same relationship of decreasing height with an increasing  $K_p$  prevails. While the height of the lower edge changes insignificantly (approximately by 10 km), the mean height of the upper layers and of the upper ends of the rays changes by 80 km.

Figure 3 shows the altitudinal distribution of the upper and lower edges of radial forms for three values of  $K_p$ . All curves are standardized, i.e., the ratio between the number of arcs with a given height to the total number of cases  $n_{\Sigma}$  is plotted on the abscissa. The diagram shows that the maximum of the altitudinal distribution for the lower edge practically does not change, and is located approximately at the level of about 100 km. An increase of the mean height values (Figure 2) with decreasing  $K_p$  is associated with the appearance of aurora at large heights, i.e., with the appearance of secondary maxima, which are absent when  $K_p = 6$ . The heights of the upper edge of radial arcs and the upper ends of rays, when  $K_p = 4 - 5$ , vary greatly. There are maxima at heights of 110 - 120, and approximately 250 km. The magnitudes of these maxima are redistributed with a transition from  $K_p = 4$  to  $K_p = 5$ . This particular trend is no longer apparent when  $K_p = 6$ , where we deal with only one broad maximum at heights of the order of 170 km. In other words, with stepped up magnetic

activity, there is a decrease not just in the vertical direction of radial formations, but there is also a scatter of probable values.

/41

Figure 4 shows the variation of the mean vertical expanse of rays and of radial arcs with respect to  $K_p$ . The linear decrease of the ray lengths with increasing magnetic activity is clearly apparent. No comparison was performed involving the specific length of radial forms with the  $K_p$ -index. Thus, frequently only the height of the upper and lower edges was measured and the number of indirect measurements was relatively low.

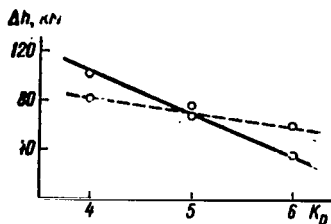


Figure 4. The dependence of the mean vertical direction of radial auroral forms on  $K_p$  (solid line), and the range of heights (dashed lines), for

$$\eta(3914 \text{ \AA}) > 0.1 \eta_{\max}$$

We may assume that radial aurora are caused by electrons whose energy determines the penetration depth. The electron energy for various heights was taken from data reported in [6]. This applied to a monochromatic electron stream, the electrons being distributed isotropically among the pitch angles. The isotropicity of the angular distribution is supported by direct rocket measurements [7]. A decrease of the mean expanse of radial forms with increasing levels of magnetic activity is possible since, according

to [6], a maximum appears with increased electron energy on the excitation efficiency curves of emission  $3914 \text{ \AA}$ ; its intensity increases with increasing energy.

On Figure 4, the dashed line indicates the range of heights within the limits of which  $\eta(3914 \text{ \AA}) > 0.1 \eta_{\max}$ , where  $\eta$  is the number of quanta;  $3914 \text{ \AA} / \text{el:cm} : \eta$  was used for defining the energies of electrons which penetrate to levels corresponding to the lower edge of aurora for data of  $K_p$ -indexes with reference to Figure 2. Obviously, the range of heights with decreasing electron energy increases just like the elongation of radial forms. The

magnitude  $\eta > 0.1\eta_{\max}$  was chosen so that the straight lines coincided (Figure 4) when  $K_p = 5$ . The real spectrum of particles is not strictly monochromatic. However, according to some data, at times a spectrum has been observed that differs very little from a monochromatic spectrum [8].

If the energy distribution of electrons is represented in terms of a power spectrum, it will become apparent that with a decrease of the electron hardness the range of heights, where  $\eta$  is practically constant [6], increases. Thus a decrease of hardness is equivalent to an increase of the number of soft particles and hence of the mean auroral height.

With the aurora edge altitudinal distribution, the following distribution of particles in terms of energies can be plotted. It is conventional to express the energy spectrum in the form of  $\frac{dN}{dE} = \text{const. } E^{-\gamma}$ . According to data in [9],  $\gamma = 5$  for the external radiation belt, and  $\gamma = 6$  for measurements on weather-sounding balloons when the electron spectrum is re-established by X-ray radiation [10]. According to [11],  $\gamma$  varies within large limits, i.e., from 3.4 to 15. According to [12], the magnitude of  $\gamma$  may reach unity.

The energy spectrum of electrons obtained from aurora altitudinal distribution significantly differs from the energy spectrum described in the literature. The presence of an occurrence frequency maximum in terms of aurora height distribution suggests that, at low energies, the number of particles begins to decrease; hence,  $\gamma$  must change its sign. This discrepancy is associated with 42 the fact that until recently only particles with energies starting at 80 eV were registered by rockets and satellites. If we were to construct a differential spectrum for auroral height distribution in power form from the maximum of the frequency of occurrence toward the side of high energies, we would obtain  $\gamma = 2 - 3$ . This closely coincides with the results of other measurements. True, the obtained spectrum would be somewhat harder. The representation of the energy spectrum in exponential form [11] also would yield only a decreasing section near high energies.



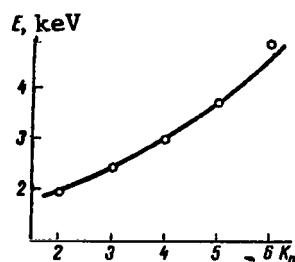


Figure 5. Relationship between the energy of electrons that excite polar auroras, and the  $K_p$ -index. The curve reflects the exponential relationship, the circles are experimental values.

shows the relationship

$$E = 1.31 e^{0.21 K_p}$$

The dots show electron energy values corresponding to heights obtained on Figure 2 (the straight line was extrapolated in the direction of  $K_p$ -indexes). Obviously, during varying magnetic activity, the exponential relationship agrees well with the mean height level of the lower auroral edge.

In conclusion, the author would like to express his appreciation to M. I. Pudovkin for useful consultations, and to G. Sh. Zakirova for data evaluations.

Consider now the relationship between magnetic excitation and the mean energy of the intruding electrons, determined from the auroral height. According to Figures 1 and 2, the height changes linearly with a variation of  $K_p$ . Notably,  $\ln E$  (here,  $E$  is the electron energy) is proportional to  $\ln \rho$  (here,  $\rho$  is the thickness of matter penetrated by one electron until it stops, in  $g \cdot cm^2$  [13]). Since the variation of  $\rho$  for the atmosphere is determined by a barometric formula, we can set  $\ln E \sim H$ . It follows that  $\ln E$  must depend linearly on  $K_p$  or  $E = e^{a+bK_p} = ce^{bK_p}$ . Figure 5

## REFERENCES

1. Störmer, C. Results of the Observation and Photographic Measurements of Aurora in Southern Norway and from Ships in the Atlantic During the Polar year 1932 - 1933, Geophys. Publ., Vol. 18, No. 7, 1953.
2. Fuller, V. R. Auroral Observations at the Alaska Agricultural College and School of Mines for the Year 1931 - 1932. Terr. Magn. Atoms. Electr., Vol. 38, No. 3, 1933, p. 207.
3. Störmer, C. The Polar Aurora. Oxford, 1955.
4. McEwen, D. J., R. Montalbetti. Parallax Measurements on Aurora Over Churchill, Canada. Canad. J. Phys., Vol. 36, No. 12, 1958, p. 1593.
5. Andriyenko, D. A. The Determination of Auroral Heights from Large-Scale Photographs Obtained at the Tiksi Bay Station. Geomagnetizm i aeronomiya, Vol. 5, No. 3, 1965, p. 450.
6. Rees, M. H. Auroral Ionization and Excitation by Incident Energetic Electrons. Planet. Space Sci., Vol. 11, No. 10, 1963, p. 1209. /43
7. McDiarmid, J. B., D. C. Rose, E. Budzinski. Direct Measurement of Charged Particles Associated with Auroral Zone Radio Absorption. Canad. J. Phys., Vol. 39, No. 7, 1961, p. 1888.
8. McIlvain, C. E. Direct Measurement of Protons and Electrons in Visible Auroral. J. Geophys. Res., Vol. 65, No. 9, 1960, p. 2727.
9. Vernov, S. N., A. Ye. Chudakov. The Investigation of Cosmic Rays and of Terrestrial Corpuscular Radiation in Rocket and Satellite Experiments. Uspekhi Fizicheskikh Nauk (UFN) Vol. 20, No. 4, 1960, p. 585.
10. Winkler, D. R. Atmospheric Phenomena, High-Energy Electrons and Geomagnetic Fields. In: Radiatsionnyye poyasa i geofizicheskiye yavleniya (Radiation Belts and Geophysical Phenomena), Moscow IL, 1963, p. 15.
11. O'Brien, B. I., S. D. Laughlin. An Anomalous Large Electron Stream in the Auroral Zone. Ibid, p 143.
12. O'Brien, B. I., S. D. Laughlin, J. A. Van-Allen, and L. A. Frank. The Measurement of Intensity and of Electron Spectra at the Height of 1000 km and at High Latitudes. Ibid, p. 61.
13. Artsimovich, L. A. (editor). Spravochnik po yadernoy fizike (Nuclear Physics Handbook), Physico-Mathematical Press, 1963.

## AURORAL PULSATIONS

V. K. Roldugin

ABSTRACT. Aurora pulsations of the P<sub>1</sub> type, unlike P<sub>2</sub> are caused not by variations of arcs and bands, but by the surrounding background. The diurnal changes of P<sub>1</sub> pulsation intensities differ from the diurnal changes of aurora intensity. Pulsations were observed in the infra-red region which were not accompanied by the glow in the visible region of the spectrum. A conclusion is made about the different mechanisms causing pulsating and non-pulsating auroral forms.

In the investigation of the numerous phenomena which comprise /44  
an ionospheric disturbance (e.g., aurora, absorption of cosmic noises, magnetic and ionospheric storms, x-ray bremsstrahlung), it was found that the registered signals are subject to considerable fluctuations. A variable component is superimposed upon the constant signal; this variable has a period from several fractions of a second to several minutes, and lasts from several minutes to several hours. This phenomenon is defined as pulsation. Notably, pulsations of auroral intensity registered by photometers are associated with short-period variations (SPV) of the magnetic field [1 - 6]. The appearance of auroral intensity pulsations is frequently accompanied by absorption pulsations of the cosmic noise with identical periods. Since most of the studies were concentrated on the SPV morphology of the magnetic field, we will hereafter employ terminology accepted for the description of magnetic pulsations.

An analysis of the photometric recordings at the Loparskaya Station for 1964 - 66 indicates that auroral pulsations occur quite frequently. Their investigations entail certain difficulties. Auroral intensity varies within rather large limits; thus, with increasing intensity, it usually becomes necessary to decrease the sensitivity, whereas with decreasing intensity the

sensitivity must be increased. In the first instance, the absence of pulsations in the recording may be caused by insufficient sensitivity. Thus, in the investigation of pulsations, it is of paramount interest to record the variable component only. This is attained by putting an RC-filter into the amplifying circuit.

Oscillations of the  $P_{i2}$  type with a period of 40 - 120 seconds, which attenuate after several (2 to 5) periods, usually appear after a drastic increase of auroral intensity. Their appearance is associated with a transition of a homogenous arc into a radial arc, accompanied by a gain in intensity. Usually, pulsations of  $P_{i2}$  aurora are observed in pre-midnight hours [6]. Their intensity amounts to about 10% of the overall intensity.

Pulsations with a 5 - 10 second period display a more complex behavior. They are analogous to the SPV of the  $P_{i1}$ -type magnetic field. Their inherent characteristic is that they essentially occur during the decrease of auroral intensity and hardly appear before the maximum is reached. Their share in the total intensity may reach up to 80 - 90 percent. A comparison of auroral recordings made by a conventional photometer, and by a photometer with a RC-filter, shows that there is no direct relationship between the pulsation intensity of this type, and the intensity of general pulsations. During evening hours, even strong pulsations are accompanied by  $P_{i1}$  variations with a small /45 amplitude, whereas in pre-morning hours, aurora may appear with an intensity which, for practical purposes, is caused exclusively by this type of pulsations. The morphology of such aurora, said to be pulsating aurora, has been adequately studied [7]. They appear in a form of scattered wide, low-intensity spots. Some of them become stronger; others become weaker. Visually, it is difficult to establish the frequency and phase relations between them. Sometimes, an intensity variation of adjacent spots is observed with the same period; however, they are out of phase. The general impression is that of the motion of light waves across the sky. The intensity of strong pulsating spots is approximately 500 rel.

Concerning  $P_{i2}$  type pulsations, we can, with sufficient certainty, assert that their intensity is related to the periodic intensity variations of bright auroral types. However, with the appearance of the  $P_{i1}$  type of pulsations with a simultaneous observation of an arc in the sky it is questionable that this type of pulsation is associated with the variation of the intensity of the arc. To compare bright pulsations with background pulsations, a photometer with a  $3^\circ$  angle of view was aimed alternately at the bright (force of 3) uniform arc at a  $30^\circ$  angle over the northern horizon, and at a point in the sky,  $45^\circ$  south of the zenith. At this time, there were no other configurations in the sky with the exception of this arc. Atmospheric transmissivity was good. The signal from the photomultiplier passed through an RC-filter before reaching the amplifier. Intensive variations of the brightness were observed in the arc; at  $45^\circ$  S, they were weaker by 5 to 10 times. Considering that the area of the sky not covered by aurora exceeds the area of the arc by more than a factor of ten, it becomes obvious that the main component of the pulsating intensity is not concentrated in the arc, but rather in the surrounding background. Similar findings for a non-pulsating intensity were reported in [7]. Notably, the pulsations in the arc were chaotic and irregular, whereas pulsations at  $45^\circ$  S had a regular nature.

To understand properly the nature of SPV of auroral intensity, it is important to define with precision the term "pulsations". It can be construed both as short-period outbursts from a constant level, as well as intensity variations with respect to that level. An analysis of  $P_{i1}$  recordings with and without an RC-filter leads us to the definite conclusion that they are outbursts with respect to the fundamental level of the signal which changes slowly. Pulsations of the  $P_{i2}$  type are more suggestive of oscillations than of bursts. In the aforementioned experiment, the intensity variations of the arc took place in the form of outbursts in both directions, whereas at  $45^\circ$  S, the outbursts were directed only toward the side of increasing intensity. The intensity variation of the arc had a noise nature.

Daily variations of the pulsating aurora with reference to local time were plotted from the photometric recordings made by a zenith photometer for

the 1964 - 1965 and 1965 - 1966 seasons. Data for 96 nights were evaluated, regardless of whether aurora did or did not appear at night. The results are shown on Figure 1. The amplification circuit of the photometer did not include an RC-filter, and hence the contribution of very weak pulsations is not taken into account. For comparison purposes, Figure 1, c, shows the daily variations of auroral intensity for the Loparskaya Station for 1963 - 1964, obtained from photometric recordings of the entire sky in the 3914 Å emission.

In plotting the graph, the data for 18 aurora, averaged for 15 minute intervals, were used. There were about 10 aurora for each 15-minute interval. The photometer was standardized for night background. In analyzing the photometric traces obtained at night, in the absence of aurora, it was found that the background intensity at night changes very little, within the limits of about 20%. Repeated standardizing by incandescent lamps, revealed that the background intensity during different moonless nights is sufficiently constant. Thus, standardization of photometric recordings for nocturnal background is acceptable in plotting the daily variations. /46

This daily variation is close to the one described in [8], which was plotted from data obtained with a S-180 camera taking into account aurora activity. In local time, the maximums at 20<sup>h</sup>, 23<sup>h</sup> and 1<sup>h</sup> 30<sup>m</sup> coincide; the morning maximum at Loparskaya Station takes place at 4<sup>h</sup>; at Tiksi Bay, which is geographically north of Loparskaya Station, the maximum occurs at 6<sup>h</sup>.

Figure 1 shows that the maximums of the appearance and of pulsation activity occur between 2 and 3<sup>h</sup> LMT. It is typical that, if there is a smooth broad maximum from zero to 4<sup>h</sup> for the probability of occurrence, then this maximum is more pronounced for pulsation intensities. At about 20<sup>h</sup>, a large maximum of auroral intensity was observed. It is related to homogeneous forms, whereas the corresponding maximum of the occurrence of pulsations is small. The second maximum of auroral intensity (at 23<sup>h</sup>) is caused by the appearance of radial forms. The auroral intensity decreases, and is less after midnight hours than during pre-midnight hours. The pulsation intensity, on the contrary, keeps increasing, and is considerably higher during after-midnight hours than

during pre-midnight hours. In morning hours, there is a second significant increase of both: the probability of the occurrence, as well as of the intensity of the pulsations. However, the elements of this maximum do not lend themselves to tracing due to the onset of daylight.

These diurnal variations differ somewhat from the findings reported in [4,5], The diurnal changes of  $P_{11}$  pulsations, obtained by R. G. Skrynnikov [4], generally are similar to the diurnal changes shown in Figure 1; however, they have a different ratio of the amplitude of the maximum of occurrences. If the probability of occurrence ratio at 3<sup>h</sup> and 21<sup>h</sup> in Figure 1 is approximately 5, then for analogous maximums in [4], this ratio is of the order of 1.2. It is pointed out in [4] that the amplitude of  $P_{11}$  pulsations in the glow maximum is considerably higher than the amplitudes of pre-morning pulsations. Since no data obtained later than 6<sup>h</sup> are given in [4,5], it is impossible to compare the results for the morning maximum. Inasmuch as the findings reported in [4,5] go back to 1961, it is probable that the differences of the diurnal variations are associated with the change of the nature of aurora in years of minimal solar activity. /48

It was pointed out in [9] that almost all fundamental emissions in the visible range are pulsating, with the exception of 6300 Å, whose lifetime is about 2<sup>m</sup>. Photometric observations in the infrared range of the spectrum were performed in the winter of 1964 - 1965 at the Loparskaya Station. Specimen simultaneous recordings of  $P_{11}$  pulsations in the visible and in the infrared ranges made on 4 March 1965 are shown on Figure 2. The intensity variations in both regions of the spectrum are in good agreement with each other. However, during the two and a half months when the photometer was operating in the infrared region, there were three instances noted when radiation appeared which was not accompanied by radiation in the visible range. All three of these instances relate to pulsating auroras: once during pre-midnight hours there appeared  $P_{12}$  type pulsations, and twice during after midnight hours, pulsations of the  $P_{11}$  type were recorded. Unfortunately, since the pass band was too wide (from 8800 to 10,800 Å) it was impossible to determine which emissions cause auroral intensity pulsations in the infrared region.

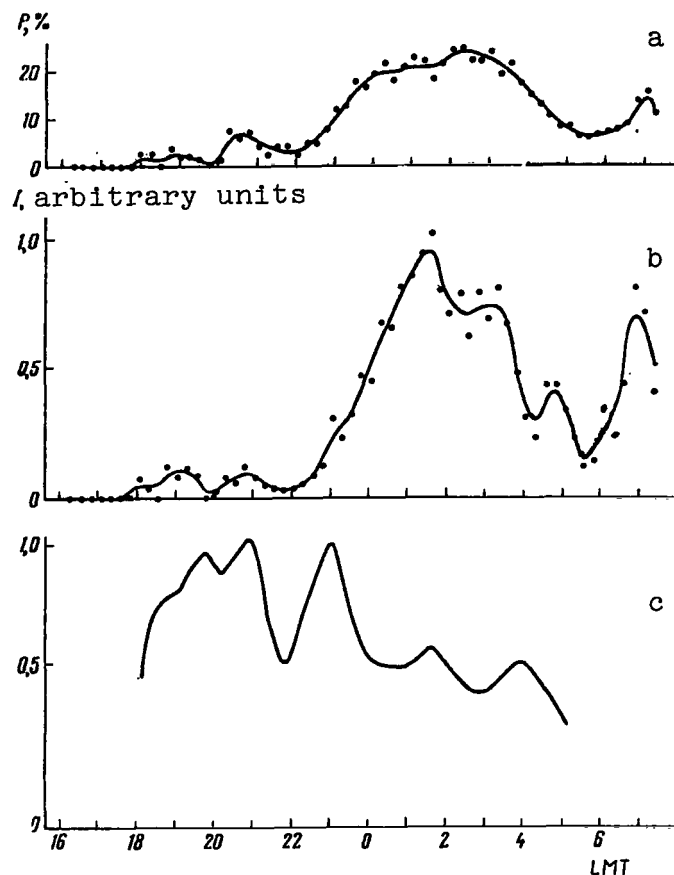


Figure 1. Daily variations of the frequency of occurrence (a), pulsation intensity (b), and auroral intensity (c).

The most characteristic period for pulsations of the  $P_1$  type is the period of 4 to 8 seconds. This agrees with the findings reported in [4,5]. However, variations with a smaller period were also observed. Figure 3 shows a specimen recording of SPV of aurora at 22<sup>h</sup> 30<sup>m</sup> LMT, made on 4 January 1966. Their characteristic feature, outside of the small period (0.5 second), is a regularity of the shape, which is rare for SPV. Variations, approximately with the same period, but, of an irregular nature, were observed before the onset of dawn on 25 December 1965 (Figure 4). It was possible to observe visually only intense short-time flares in the northern hemisphere. Of other



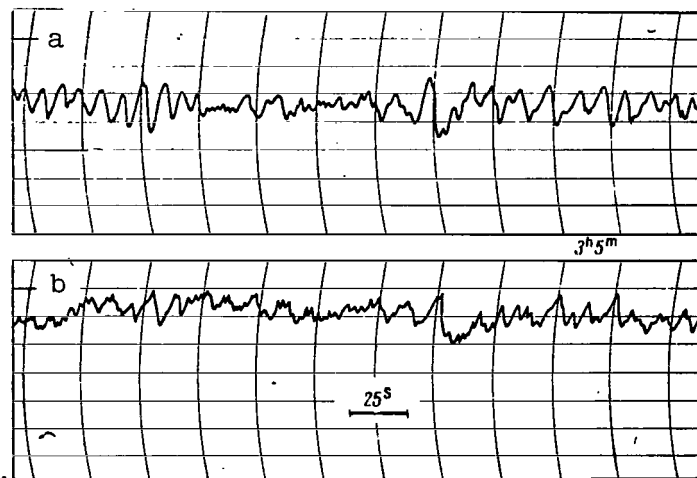


Figure 2. Specimen of a simultaneous recording of auroral pulsations in the visible (a) and infrared (b) region of the spectrum.

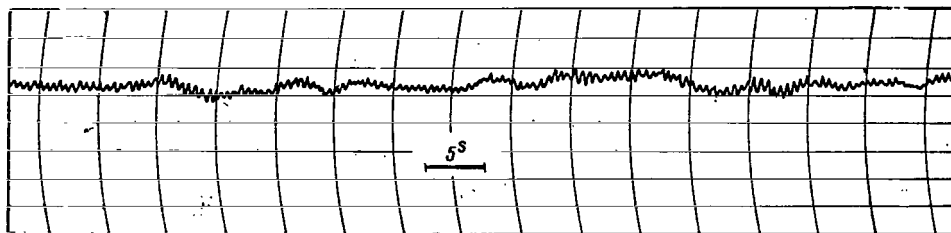


Figure 3. Intensity pulsations of aurora, recorded in the evening of 4 January 1966.

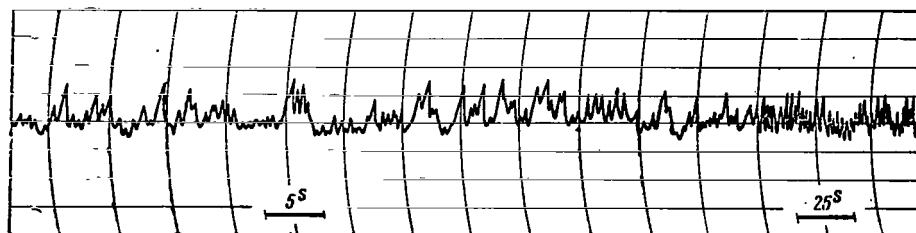


Figure 4. Auroral pulsation intensity, recorded in the morning of 25 December 1965.

forms, only one aurora at the northern horizon was noted which did not hit the angle of view of the photometer, used for recording these pulsations. Pulsations of x-ray radiation for  $E > 60$  keV were reported in [10].

These data indicate that there are different mechanisms at work which are responsible for the occurrence of pulsating and non-pulsating aurora. Apparently, the difference lies, above all, in the energies of the particles involved in non-pulsating and pulsating auroral forms. The conclusions derived from the study of non-pulsating auroral shapes may not be applicable to pulsating shapes. An important step in establishing the nature of pulsating aurora would be a determination of their height. However, direct triangulation methods are rather difficult to apply due to the indistinctness of aurora, and the rapid variations of their shapes.

# REFERENCES

1. Campbell, W. H. Studies of Magnetic Field Micropulsations with Periods of 5 to 30 Seconds. J. Geophys. Res., Vol. 64, No. 11, 1959, p. 1819. /49
2. Korotin, A. B. A Comparison of the Daily Variations with Respect to the Appearance of Hydrogen Emission and Radio Reflections on the Frequency of 72 Mc. In: Spektral'nyye, elektrofotometricheskiye i radiolokatsionnyye issledovaniya polyarnykh siyaniy i svecheniya nochnogo neba (Spectral, Electrophotometrical and Radar Investigations of Aurora and Night Air-Glows), No. 6, Series Rezul'taty MGG (Results of the IGY). Moscow Academy of Sciences of the USSR Press, 1961, p. 31.
3. Troitskaya, V. A., L. V. Al'perovich, and N. V. Dzhordzhio. A Relationship between SPV of the Magnetic Field of the Earth and Aurora. Moscow, Izvestiya Akademii Nauk SSR, Seriya Geofizich., No. 2, 1962, p. 262.
4. Skrynnikov, R. G. Short-Period Variations of Auroral Intensity. Geomagnetizm i aeronomiya, Vol. 2, No. 6, 1962, p. 1080.
5. Skrynnikov, R. G. The Relationship Between SPV of the Electromagnetic Field of the Earth and the Intensity Variations of Auroral Glow at High Latitudes. In: Issledovaniya geofizicheskikh yavleniy v vysokikh shirotakh (Study of Geophysical Phenomena at High Latitudes). Moscow, Ac. of Sci. of the USSR Press, 1964, p. 29.
6. Namgaladze, A. N., O. M. Raspopov, and V. K. Roldugin. On the Relationship Between Geomagnetic Field Pulsations of the  $P_1$  type, and Auroral Intensity Pulsations. In Press.
7. Dzhordzhio, N. V. Electrophotometric Measurements in Auroral Zones. In: Spektral'nyye, elektrofotometricheskiye i radiolokatsionnyye issledovaniya polyarnykh siyaniy i svecheniya nochnogo neba (Spectral, Electrophotometric and Radar Investigations of Aurora and Night Airglow) No. 1, Series Rezul'taty MGG (Results of the IGY). Moscow, Ac. of Sci. of the USSR Press, 1959, p. 30.
8. Nadubovich, Yu. A. Daily Variations of Auroral Activity Recorded from Photoinstrumental Observations at Tiksi Bay. In: Polyarnyye Siyaniya i svecheniya nochnogo neba (Aurora and Night Airglow), No. 7, Series Rezul'taty MGG (Results of the IGY). Moscow, Ac., of Sci. of the USSR Press, 1961, p. 27.
9. Dzhordzhio, N.V. The Laws of Aurora Flickering. In: Polyarnyye siyaniya i svecheniya nochnogo neba (Aurora and Night Airglow). Seriya Rezul'taty MGG (Results of the IGY). Moscow, Ac. of Sci. of the USSR Press, 1962, p. 17.
10. Winkler, J. R., P. D. Bhavsan, and K. A. Anderson. A Study of the Precipitation of Energetic Electrons from the Geomagnetic Field During Magnetic Storms. J. Geophys. Res., Vol. 67, No. 10, 1962, p. 3717.

POLAR AURORA AT THE MINIMUM OR MAXIMUM CYCLE  
OF SOLAR ACTIVITY

Ya. I. Fel'dshteyn, L. V. Lukina, and N. F. Shevnina

ABSTRACT. A comparison is carried out of aurora in the years of the maximum (IGY) and minimum (IQSY) cycle of solar activity. It was found:

1. that, although the level of solar activity has greatly reduced, aurora on the nightside on the latitude of the oval auroral zone continue to appear practically without interval;
2. that the central line of the oval zone during the years of the minimum has only slightly shifted in the night hours towards the pole ( $\sim 1.5^\circ$ );
3. that with planetary magnetic disturbances relatively similar in intensity ( $K_p = 5$ ), the region of latitudes covered by aurora on the night side of the Earth in the years of the maximum stretches to lesser  $\phi'$  than in the years of the minimum;
4. that certain statistical regularities in aurora are in good correlation with the oval form of the auroral zone during the IQSY period; this form is analogous to the one suggested earlier for the IGY period. The regularities mentioned are the diurnal variations in the aurora occurrences  $P\%$  (Figure 4); latitude distribution of the number of aurora occurrences at different hours of local time (Figure 5); diurnal shifts of the aurora region along the meridian (Figure 6); changes of orientation of elongated forms of aurora (Figure 7). Figure 2 shows the map of isoaurora (lines of equal number of occurrences in the zenith for the IQSY period).

Phenomena of the electromagnetic complex of the upper layers of the Earth's 50 atmosphere are closely associated with solar activity and are subject to notable cyclic variations. Observations conducted during the IQSY were followed by an

interpretation of photographic data on aurora, and a comparison with the previously known laws of the IGY<sup>(1)</sup>, to determine the cyclic variations of aurora. To make such a comparison possible, the same method of askafilm evaluation was used in 1963 - 1965 as was used previously during the IGY [1-3]. The frequency of aurora occurrence was used as the index of activity. This index was computed as the ratio of half-hour intervals with aurora at the zenith to the total number of half-hour observation intervals. Daylight and unfavorable meteorological conditions were not included in the analysis. The preliminary results of the analysis of space-time distribution of aurora for the IQSY period, based on photographic observations performed by the observation network of the USSR, follow below. For technical reasons, the most northern observation station was at  $\phi' = 74.5^\circ$ . Thus, for the time being, data on aurora in the circumpolar area are as yet not available to us. In view of this, the data for IQSY, cited below, must be supplemented in the future. This is planned by adding observation data as they become available at the World Data Center.

The latitudinal frequency distribution of aurora for all days, taken during a six hour period, centered for local midnight, is shown on Figure 1. The geomagnetic latitude of observation stations was corrected, taking into account the nondipole distribution terms of the basic geomagnetic field in this series of spherical harmonics [4,5]. Curve 1 defines the distribution probability of occurrence of aurora in 1963 - 1965, whereas Curve 2 reflects the same phenomena in the 1957-1959 period.

In spite of the significant decrease of solar activity (the Wolf numbers decrease approximately by the factor of 13), aurora at Dixon Island and at Cape Chelyuskin were observed almost all the time. Thus, for practical purposes, aurora appear continually on the night side of the Earth near the oval zone latitude. This applies to years of maximum as well as of minimum solar activity. To establish a more precise localization of the position of the maximum in terms of altitudinal distribution in 1963 - 1965, the frequency of aurora occurrence /51 in northern and southern azimuths was computed at zenith angles larger than  $60^\circ$ .

---

(1) i.e., 1957 - 1959.

The computation results for a number of stations are shown in the table.

It follows from the table that near midnight at stations Heiss Island, Cape Zhelaniya, Cape Chelyuskin, the aurora appear with greater frequency in the southern hemisphere, whereas on Dixon Island and Tiksi Bay, they are more frequently seen in the northern hemisphere. At Cape Chelyuskin and Dixon

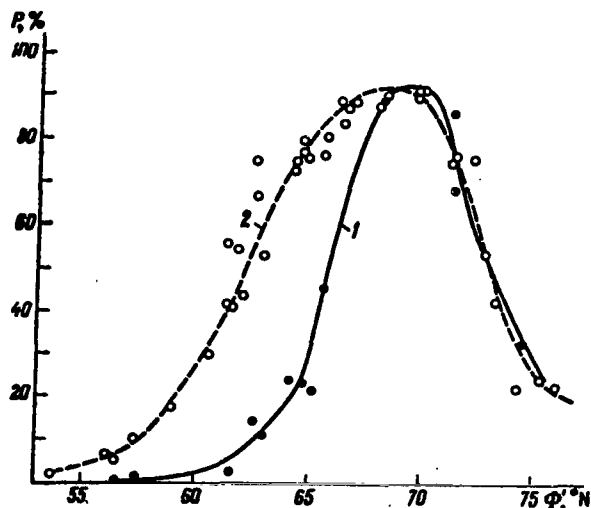


Figure 1. The latitudinal distribution of the frequency of occurrence  $P$  of aurora near midnight for all days.

1 - the IQSY period; 2 - the IGY period.

Island, where aurora appear most frequently at the zenith, the aurora in one half of the hemisphere appear approximately twice as frequently as in the other half. Thus, one could assume that the region of maximum auroral frequency is within the latitudes between Cape Chelyuskin and Dixon Island, approximately at equal distances from these stations. Cape Chelyuskin is at  $\phi' = 71.2^\circ$ , whereas Dixon is at  $68.0^\circ$ . Consequently, aurora during the IQSY most frequently appeared at night hours at  $\phi' \sim 69 - 70^\circ$ . North and south of these latitudes, the probability of occurrence of aurora at the zenith goes down drastically.

The latitudinal distribution during the years of the cycle maximum was obtained by adding the observation data for 1958 - 1959 [7], to the data obtained in 1957 - 1958 [6]. It appears that in 1957 - 1959, aurora latitudinal distribution was more spread out. Aurora most frequently appear in the interval of  $66 - 70^\circ$ . Thus, if the auroral zone is arbitrarily set as the latitude of the center line of the latitude region where aurora appear with maximum frequency then this region, during the IGY, was at  $\phi' \sim 68^\circ$ , whereas during the IQSY it was at  $\phi' \sim 69.5^\circ$ . It follows that the cyclic shift of the auroral zone toward the night side of the Earth amounts to only  $1.5^\circ$ .

TABLE

Observation station	Frequency of occurrence of aurora in the north, %	Frequency of occurrence of aurora in the south, %
Heiss Island	19.2	67.3
Cape Zhelaniya	29.8	40.8
Cape Chelyuskin	44.0	74.6
Dixon Island	80.1	44.9
Tiksi Bay	60.6	11.1

At the circumpolar side of the zone, up to  $\phi' \sim 75^\circ$ , the frequency of auroral occurrence in years of the cycle maximum and minimum is practically the same. However, on the equatorial side, aurora appear with considerably greater frequency during the years of the maximum. Notably, this difference for the equatorial side was obtained from the data of a large number of stations, and thus should be considered reliable. The absence of cyclic variations at  $\phi' > 71^\circ$  is based on data of only one station (Heiss Island), and hence should be considered in conjunction with additional data. The shift of the position of the centerline of the oval zone and the more frequent appearance of aurora at low latitudes in years of the maximum is a consequence of more frequent magnetic disturbances. Moreover, when magnetic disturbances are equal in their intensity, the latitude zone, covered by aurora at the night side of the Earth, extends to lower  $\phi'$  in the years of maximum, than in the years of a minimum [8 - 10].

The minimum of the solar activity during the IQSY was not as deep as in the winter of 1954 - 1955, when hourly visual observations of aurora were performed at 50 stations at longitudes of  $50 - 110^\circ$  E [11]. It was noted then that aurora are observed daily, even during magneto-quiet days ( $\Sigma K < 15$ ). The zone of

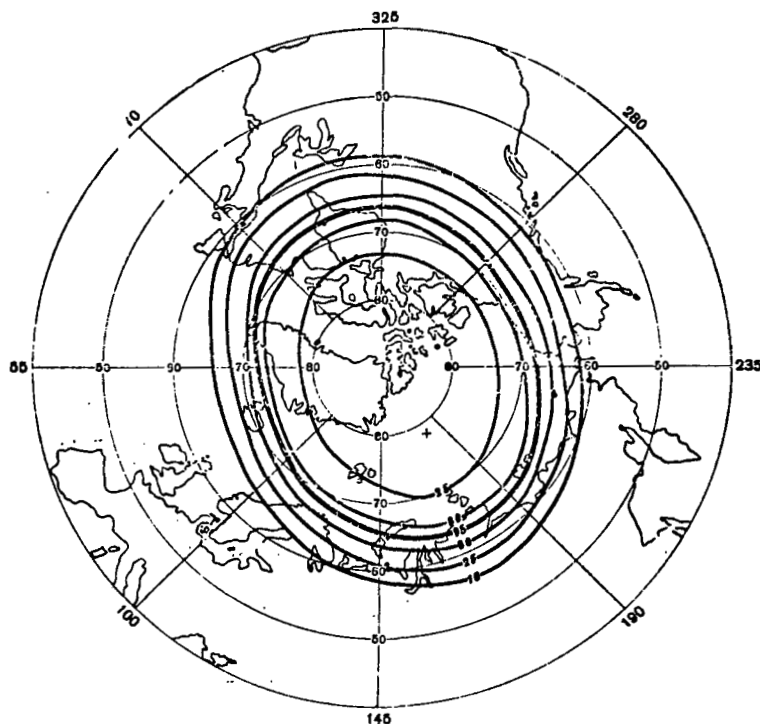


Figure 2. Isoaurora during nighttime hours in 1963 - 1965. The bold line defines the Fritz-Westin zone.

maximum frequency of auroral appearance during all days, including magnetoquiet days, was at the geomagnetic latitude of  $65^\circ$ , which corresponds to  $\phi' \sim 70^\circ$ .

Thus, the practically continuous presence of aurora at  $\phi' \sim 70^\circ$  is typical also for a deeper minimum of the winter 1954-1955 (the sum of the monthly average of Wolf numbers from October 1954 through March 1955 amounted to 72.6, as compared to 123.2 for October - March 1963 - 1964 and 75.7 for 1964 - 1965). /53 According to [12], the auroral zone shift toward the equator from 1954 - 1955 to 1957 - 1958 amounted only to  $2.5^\circ$ . Consequently, cyclic changes in the position of the line outlining the most frequent occurrence of aurora on the night side of the Earth are small, and amount to only  $1.5 - 2.5^\circ$ .

It is assumed that isoaurora (lines on the surface of the Earth, connecting points with equal occurrence of aurora at the zenith) are located during night hours along corrected



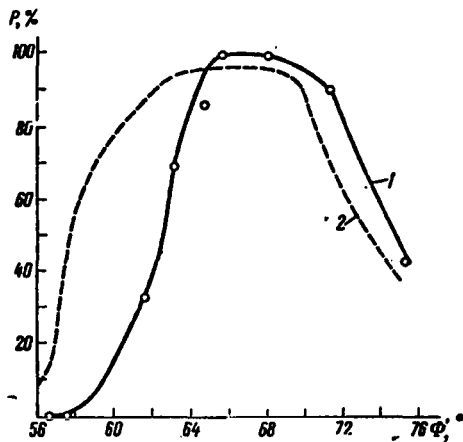


Figure 3. Latitudinal distribution of the frequency of appearance  $P$  of aurora in near-midnight hours when  $K_p = 5$ .  
1 - the IQSY period; 2 - IGY period.

geomagnetic parallels, or along the lines of equal value of the parameter  $L$  [13]. This assumption is reflected in Figure 2, where a family of isoaurora is plotted for a minimum cycle of solar activity. Isoaurora for the maximum cycle are detailed in [14]. The position of the maximum isoaurora (of the Fritz-Westin zone) is shown by a thicker line. In 1963 - 1965, the frequency of appearance of aurora at that zone in the northern hemisphere was the same as in 1957 - 1959; however, the maximum isoaurora was somewhat shifted toward the pole.

It was demonstrated in [9] that when  $K_p \leq 1$ , the latitudinal distributions of the frequency of auroral displays for 1957 - 1959 and 1963 - 1965 practically coincide. When  $K_p \geq 5$ , there are substantial differences in the frequency of auroral displays south of the Fritz-Westin zone. In years of a maximum, a drastic decrease of the probability of auroral displays takes place at  $\phi' \sim 59^\circ$ , whereas in years of a minimum, it takes place at  $\phi' \sim 64^\circ$ . To be able to evaluate the reasons for such a difference with greater certainty, the latitudinal distribution of auroral displays at the zenith were plotted for night hours when  $K_p = 5$ ; the diagram is shown on Figure 3.

The diagram clearly shows the difference in latitudinal distribution at  $\phi' \sim 54 - 65^\circ$ , where, during the maximum of the cycle, aurora appear considerably more often than during the period of the minimum, even at the same level of planetary geomagnetic disturbance. A more frequent appearance of auroral displays at middle latitudes during the IGY, as compared to the IQSY, stems from two causes: 1) a more frequent appearance of intense magnetic disturbances, and 2) expansion of aurora to lower latitudes even at the same level of geomagnetic disturbance.

In processing the IGY data, it was found that instantaneous auroral distribution has an essential asymmetry, and that aurora most frequently appear along the oval zone of polar aurora [2, 15, 16]. The oval zone of the aurora can be used to explain their fundamental statistical laws; the shape of the diurnal frequency variations of auroral displays at different latitudes, the position of the maximum in latitudinal sections as a function of local time, the auroral motion along the meridian, the variations in the orientation of elongated forms observed at the station during the night. The laws stipulated below (for the IQSY) are in very good agreement with the concept of the oval zone of aurora.

Figure 4 shows the frequency variations of auroral displays at the zenith at stations at Cape Zhelaniya, Cape Chelyuskin, Dixon, Murmansk, and Verkhoyansk during a 24-hour period. At the most northern stations (Cape Zhelaniya and Cape Chelyuskin), the near-midnight maximum bifurcates, and auroral displays occur most frequently before and after the geomagnetic midnight. This shape of /54 diurnal variations is typical for points close to the Fritz-Westin zone in the direction of the pole. It is caused by the station passing under the oval zone of aurora before and after midnight during the diurnal rotation of the Earth. Auroral displays on Dixon Island most frequently take place during near-midnight hours; this also supports the concept of the oval zone. In near-midnight hours, the oval zone is located at latitudes of the Fritz-Westin zone, i.e., somewhat north of Dixon. Hence, in the diurnal variation of the frequency of auroral displays, one night maximum is observed at latitudes south of the Fritz-Westin zone. The intensity of this maximum decreases with decreasing distance from the equator. While auroral displays appear at Dixon in a maximum of 96 cases out of a hundred, the ratios for Murmansk and for Verkhoyansk are 25 and 7 out of a hundred, respectively.

The diurnal shift of the zone of the most frequent auroral displays at the zenith becomes especially pronounced when we consider the latitudinal distribution of the frequency of auroral displays at various hours in local time. Figure 5 shows the distribution at 0 - 1, 7 - 8, and 17 - 18<sup>h</sup> LMT, obtained from the

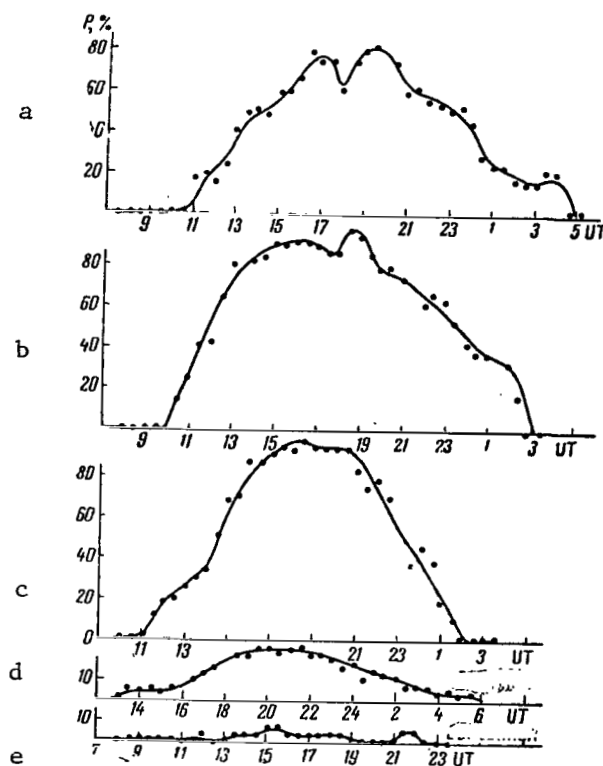


Figure 4. Diurnal variations in the frequency of appearance P of auroral displays during the IQSY.

a - Cape Zhelaniya; b - Cape Chelyuskin;  
c - Dixon Island; d - Murmansk;  
e - Verkhoyansk.

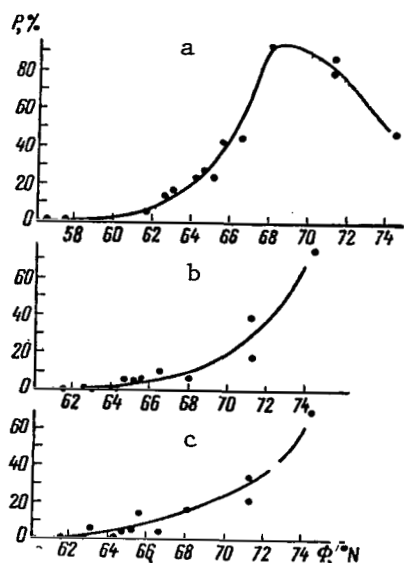


Figure 5. Latitudinal distribution of the frequency of auroral displays P at different hours local time.

(a)- 0 - 1<sup>h</sup>; (b)- 7 - 8<sup>h</sup>; (c)- 17 - 18<sup>h</sup>.

recordings of all S-l80 cameras used in auroral photography during the IQSY. The statistical basis for the values of P (in percent) is different for different stations due to the different duration of darkness allowing auroral photography, as well as due to the differing technical level of the photographic personnel. Unfortunately, the most northern station (Heiss Island) was operating during one season only (1963 - 1964). Thus, the absolute values of P (in percent), obtained at that station, must be approached carefully, taking into account (Figure 5) the tendency for P to vary (in percent) at latitudes above 71.5°.

During near-midnight hours, the maximum of auroral displays is observed in the area of the Dixon Observatory; it decreases toward the pole and toward the equator (Figure 5,a). In the morning and evening hours, the probability of

auroral displays increases monotonically toward the pole; at the latitudes of Dixon, the maximum is definitely absent. Using the data at our disposal at the present time, it appears impossible to determine with accuracy its position in latitudinal sections for morning and evening hours. However, these data (Figure 5) distinctly indicate that the zone of the most frequent auroral displays is shifted toward higher latitudes during morning and evening hours, as compared to night hours. /55

If the zone of the most frequent auroral displays at the zenith is oriented with respect to the Sun in such manner that it is at higher latitudes in day hours than in night hours, then at a given station, one would observe a meridional motion of the aurora toward the equator during pre-midnight hours, whereas during after-midnight hours the motion would be directed toward the pole. The presence of a diurnal auroral shift follows also from the Alfvén [17] theory of aurora. According to this theory, the maximum distance between the pole and the aurora band would be observed at 18<sup>h</sup>, whereas the minimum distance would become apparent at 6<sup>h</sup>.

Shifts in the latitude of auroral displays at stations near the Fritz-Westin zone were known for a long time. It was pointed out in a number of studies that these shifts are not in agreement with what could be expected theoretically from the Alfvén theory. Thus, at a maximum distance from the pole, the auroral band is observed during near-midnight hours, rather than at 18<sup>h</sup> [18, 19]. The existence of systematic meridional movements of aurora during the IGY has been pointed out by Dzyubenko [20]. Such meridional movements agreed with the concept of the oval zone. According to [20], at  $\phi' < 72^\circ$ , auroral displays during evening hours occur at minimal distances from the pole, shift to a maximum distance during near-midnight hours, and shift again toward the northern horizon with the onset of the morning.

Similar methods [20] for the calculation of the shift in latitude of the glow zone were used in the evaluation of observations during the years of minimum solar activity. Figure 6 shows the obtained results. Local midnight is indicated by an arrow. With decreasing latitude of the observation station,

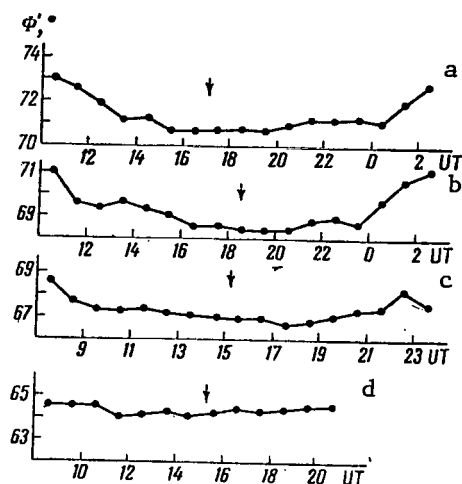


Figure 6. Diurnal shift of the aurora area along the meridian during the IQSY at stations:

a - Cape Chelyuskin; b - Dixon;  
c - Tiksi Bay; d - Verkhoyansk

suggested in [17], were used to explore the diurnal meridional movements.

The movement of aurora along the meridian at Cape Chelyuskin, Dixon and Tiksi Bay corresponds to the shift which can be expected on the basis of the oval zone concept. Maximum distance from the pole is observed during near-midnight hours; during morning and evening hours, the glow zone shifts toward the pole. At about midnight, the computed  $\Phi'$  values for Cape Chelyuskin turned out to be less than the geomagnetic latitude of the station, whereas for Dixon these values were higher. The reason for that, as we pointed out, is that during near-midnight hours aurora at Cape Chelyuskin appeared predominantly toward the south, whereas at Dixon they appeared toward the north. During the IGY, aurora at Dixon were more frequently passing into the southern half of the firmament during near-midnight hours. In view of this, it was reported [20] that during these hours the glow aurora zone was on the average somewhat south of the station.

the amplitude of the computed diurnal shifts becomes smaller. An analogous effect was also noted for the IGY [20], caused presumably by the data evaluation methods.

At southern stations, auroral displays are observed predominantly in the northern half of the firmament. /56 They rarely pass through the zenith and through the southern half. Inasmuch as the absence of aurora is not taken into account in the calculations, this substantially decreases the diurnal drift amplitude. As a result, the computed position of the aurora band at southern stations practically does not change. An analogous circumstance was noted in [19], where the methods,

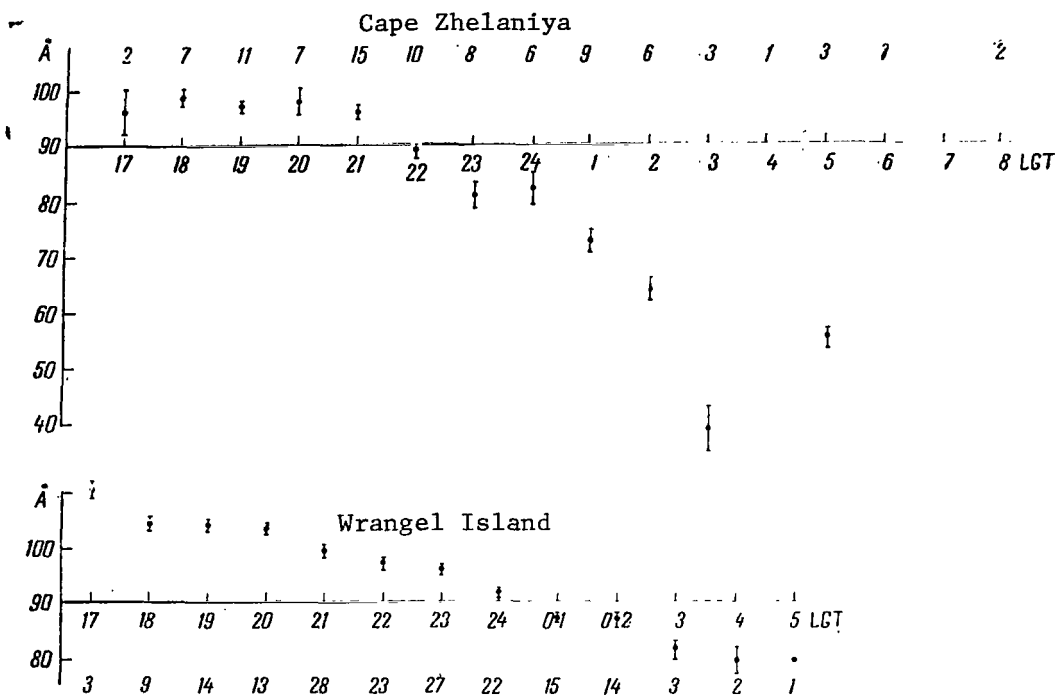


Figure 7. Variations of the orientation of elongated auroral forms in years of minimum solar activity cycle.

Azimuths were calculated east of the geomagnetic pole, taking into account corrections for non-dipole terms. Local geomagnetic time was used. The number of measured azimuths for each hour, from which the mean was determined, is shown in the upper and lower portions of the graph. The mean square deviation is denoted by a vertical line.

Due to an error in camera orientation, the azimuths in Figure 7 for Cape Zhelaniya must be increased by  $20^\circ$

Thus, analyzing diurnal shifts of aurora, we find a clearly pronounced, small cyclic shift of the aurora zone. At Tiksi Bay, aurora during the IGY /57 as well as during the IQSY were located predominantly in the northern half of the firmament. This is an additional confirmation of the small cyclic shift of the oval zone on the night side of the Earth.

As during the IGY, azimuths of elongated aurora are subject to noticeable diurnal variations. Figure 7 shows variations of azimuths, calculated east of

the geomagnetic pole, taking into account the correction for non-dipole terms [21, 12], and with reference to local geomagnetic time. Observation data collected at stations Cape Zhelaniya and Wrangel Island in 1964 - 1965 were used. The method of azimuth determination of elongated auroral displays was similar to the one used in [22].

The characteristics of diurnal variations of azimuths in years of minimum solar activity cycles are analogous to those described in [21 - 23] during the years of maximum activity. Naturally, this can be explained by the different positions of the observation station with respect to the oval auroral zone during the diurnal period.

On Wrangel Island, the azimuths decrease monotonically from evening hours toward the morning hours, amounting to approximately  $90^\circ$  at midnight. This means that elongated aurora in near-midnight hours are located along the line  $L = \text{constant}$ . In morning and evening hours, the azimuths differ from  $90^\circ$ , taking on the values of under  $90$  and over  $90^\circ$ , respectively, with reference to the direction toward the pole. Using the data of this station, it was impossible to determine how the azimuths returned to their initial values, i.e., whether by a leap, according to the Alfvén theory, or by a smooth gain. The reason for that was that the data of this station did not include observations between  $6^h$  and  $8^h$ .

Similar difficulties were encountered earlier during the evaluation of observations at Dixon Island [24] and Tiksi Bay [25]. At Cape Zhelaniya, which is at a higher latitude, the amplitude of diurnal variations of the azimuth increases by more than the factor of two, amounting to approximately  $70^\circ$ . It was pointed out [21, 22], that the increase of the amplitude of variations as the pole is approached at these latitudes is a peculiar characteristic of the IGY period. Despite the relatively small amount of data for morning hours at Cape Zhelaniya, we can definitely assert that the azimuths increase, starting at  $4^h$ . Their growth is not abrupt at a given moment, but gradual. This nature of diurnal variations at  $\phi' \sim 71^\circ$  is analogous to the pattern described in [22] for the IGY period. It is also in better agreement with the concept of the

position of elongated auroral shapes along the oval zone, rather than along the zone which would follow from the Alfvén theory.

The S-180 camera network of the Soviet Union during the IQSY was operating under the direction of Prof. A. I. Lebedinskiy.



# REFERENCES

1. Ann. IGY, 1962, 20, pt. 1. /58
2. Fel'dshteyn, Ya. I. The Geographic Distribution of Aurora and the Azimuths of Arcs. In: Issledovaniya polyarnykh siyaniy (Investigations of Polar Aurora), No. 4, Series "Rezul'taty MGG" (Results of the IGY), Moscow, Academy of Sciences of the USSR Press, 1960, p. 61.
3. Fel'dshteyn, Ya. I. Raspredeleniye polyarnykh siyaniy i magnitnykh vozmushcheniy v vysokikh shirotakh v svyazi s asimmetrichnoy formoy magnitosfery (The Distribution of Aurora and Magnetic Disturbances at High Altitudes With Relation to the Asymmetrical Nature of the Magnetosphere). In Press.
4. Hultquist, B. The Geomagnetic Field Lines in Higher Approximation. Arkiv geofys., Vol. 3, No. 4, 1958, p. 63.
5. Hakura, Y. Tables and maps of Geomagnetic Coordinates Corrected by the Higher Order Spherical Harmonic Terms. Rept Ionosphere Space Res. Japan, Vol. 19, No. 2, 1965, p. 121.
6. Fel'dshteyn, Ya. I. Auroral Morphology. Tellus, Vol. 16, No. 2, 1964, p. 252.
7. Ann., IGY, Vol. 20, 1962, pt. II.
8. Mal'ko, L. N. The Polar Aurora Zone. Geomagnetizm i aeronomiya, Vol. 6, No. 2, 1966, p. 307.
9. Fel'dshteyn, Ya. I, N. F. Shevnina, and L. V. Lukina. Aurora Displays During Magneto-Disturbed and Magneto-Quiet Periods. Geomagnetizm i aeronomiya, Vol. 6, No. 2, 1966, p. 312.
10. Bellerw, W., and S. M. Silverman. The Dependence of Occurrence of mid-Latitude Aurora on the Sunspot Cycle. J. Geophys. Res., Vol. 70, No. 19 1965, p. 4985.
11. Fel'dshteyn, Ya. I. Geographic Distribution of Aurora in the Western Sector of the Soviet Arctic. Problemy Arktiki, No. 4, 1958, p. 45.
12. Fel'dshteyn, Ya. I. On the Variation of the Auroral Zone Position with Relation to the Solar Activity Cycle. Geomagnetizm i aeronomiya, Vol. 2, No. 3, p. 571.
13. McIlvain, C. E. Coordinates for Mapping the Distribution of Magnetically Trapped Particles. J. Geophys. Res., Vol. 66, No. 11, 1961, p. 3681.
14. Fel'dshteyn, Ya. I. Auroral Displays and Geomagnetizm. In: Polyarnyye siyaniya i svecheniye nochnogo neba (Aurora and Night Airglow), No. 10, Series Rezul'taty MGG (results of the IGY). Moscow, Academy of Sciences, of the USSR Press, 1963, p. 121.

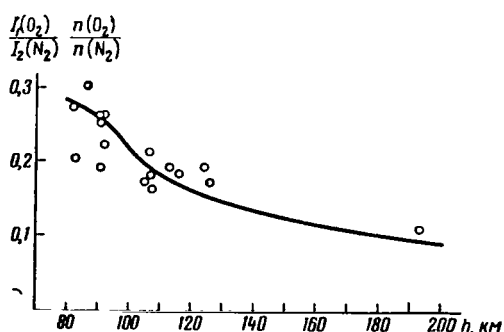
15. Khorosheva, O. V. The Diurnal Drift of a Closed Auroral Ring. *Geomagnetizm i aeronomiya*, Vol. 2, No. 5, 1962, p. 839.
16. Fel'dshteyn, Ya. I. Some Problems of Auroral Morphology and Magnetic Disturbances at High Latitudes. *Geomagnetizm i aeronomiya*, Vol. 3, No. 2, 1963, p. 227.
17. Alfven, Ch. *Cosmic Electrodynamics*, Moscow, IL, 1950.
18. Heppner, J. P. A Study of Relationships Between the Aurora and Geomagnetic Disturbances. *Doct. Thesis*, Pasadena, 1954.
19. Fel'dshteyn, Ya. I. Geograficheskoye raspredeleniye polyarnykh siyaniy. (The Geographic Distribution of Auroral Displays). *Archives of the Aeronavigational Scientific Research Institute of Dixon Island*, 1956.
20. Dzyubenko, N. I. The Diurnal Drift of Aurora by Latitude. *Geomagnetizm i aeronomiya*, Vol. 3, No. 2, 1963, p. 240.
21. Hultquist, B. On the Orientation of Auroral Arcs. *J. Atmos. Terr. Phys.*, Vol. 24, No. 1, 1962, p. 17.
22. Starkov, G. V., and Ya. I. Fel'dshteyn. Oriyentatsiya polyarnykh siyaniy i yeye svyaz' s formoy mgnovennoy zony polyarnykh siyaniy (Auroral Orientation and Its Relationship to the Shape of the Instantaneous Auroral Zone). *In Press*.
23. Davis, N. T. The Morphology of the Auroral Displays of 1957 - 1958. *J. Geophys. Res.*, Vol. 67, No. 1, 1962, p. 59.
24. Starkov, G. V., and Ya. I. Fel'dshteyn. Azimuths of Auroral Arcs., as Observed on Dixon Island. In: *Issledovaniya polyarnykh siyaniy (Investigations of Polar Aurora)*, No. 4, series Rezul'taty MGG (Results of the IGY). *Academy of Science of the USSR Press*, 1960, p. 56.
25. Dzyubenko, N. I. East-West Auroral Movements and Quiet Arc Azimuths from the Observation data Collected in Tiksi Bay. *Geomagnetizm i aeronomiya*, Vol. 4, No. 659, 1964.

# THE RATIO OF $1 \text{ NGO}_2^+$ AND $1 \text{ PGN}_2$ EMISSIONS AS A FUNCTION OF AURORAL HEIGHT

V. K. Roldugin

**ABSTRACT.** The change of ratio of  $1 \text{ NGO}_2^+$  emissions, registered by scanning photometer, to  $1 \text{ PGN}_2$  has the same form, depending on the height of aurora, as the change of concentration ratio  $\text{N}(\text{O}_2)$  to  $\text{N}(\text{N}_2)$  in the atmosphere.

On 2 - 3 March 1965, scientists of the Polar Geophysical Institute performed a determination of heights of the lower edge of aurora at the Loparskaya and Murmansk Stations [1]. In the same plane in which the heights were determined, the "sections" of the sky were scanned by a scanning photometer with automatic replacement of filters. The scanning time from one horizon to another in one filter was 8 seconds; the angle of view of the photometer was  $3^\circ$ .



The ratio of intensities  $1 \text{ NGO}_2^+/1 \text{ PGN}_2$  in arbitrary units (circles), and the ratio of concentrations  $\text{O}_2/\text{N}_2$  (curve) as a function of the height of the lower edge of the aurora.

Among the filters used were two interference filters centered at 5,300 and 5,900 Å with a width of about 150 Å [2] for half of the maximum pass band. The aurora zones of the sky in those filters essentially coincided with the aurora zones of emissions 4278 and 5577 Å. Roughly, the intensities can be estimated at 5 *krel* in the 5300 Å filter, and at 3 *krel* in the 5900 Å filter. On the other hand, the intensity of 5577 Å was of the order of 15 *krel*. Thus, it can be postulated that the intensity, registered by the photometer

in these filters, was not caused by a solid continuum and Na, but rather by 5200 NI, 522281  $\text{NGN}_2^+$ , 1  $\text{NGO}_2^+$  in filter 5300 Å, and by 1  $\text{PGN}_2$  in filter 5900 Å. A spectrum, photographed by S. A. Zaytseva using photometer SP-48 in the 5300 Å region, revealed only the line 5200 Å and did not show 5228 Å. The intensity of 5200 NI is one order of magnitude weaker than that of 1  $\text{NGO}_2^+$  [3]; moreover, it is in the decay region of the transmission band of the filter. Thus, its contribution to the overall signal may be neglected.

The ratio of the intensities 1  $\text{NGO}_2^+$ /1  $\text{PGN}_2$  with reference to the auroral height is shown by circles on the diagram above. Readings were taken at heights corresponding to the maximum intensity. In view of the approximation of the absolute value, relative values were used. It is apparent that the ratio decreases with increasing height of the lower auroral edge.

The solid curve on the same diagram shows the ratio of concentrations  $\text{O}_2/\text{N}_2$  as a function of height, taken from [4]. It is apparent that its altitudinal pattern is analogous to the altitudinal pattern of 1  $\text{NGO}_2^+$ /1  $\text{PGN}_2$ . The results indicate that both emissions are excited in a similar manner. It follows that their ratio can be used to estimate the auroral height. /60

#### REFERENCES

1. Yevlashin, L. S. et al. Comprehensive Investigation of the Polar Ionosphere. Article in this Collection. p. 1.
2. Dzhordzhio, N. V. Electrophotometric Measurements in the Polar Aurora Zone. In: Spektral'nyye, elektrofotometricheskiye i radiolokatsionnyye issledovaniya polyarnykh siyaniy i svecheniya nochnogo neba (Spectral, Electrophotometric and Radar Investigations of Polar Aurora and Night Glow). No. 1, Series Rezul'taty MGG (Results of the IGY). Academy of Sciences of the USSR Press, 1959, pp 30 - 40.
3. Chamberlain, J. The Physics of Polar Aurora and Atmospheric Emissions. Moscow, IL, 1963, p. 227.
4. ibid., p 652.

## IONOSPHERIC PROCESSES ASSOCIATED WITH AURORAL HEIGHT VARIATIONS

P. Ya. Sukhoivanenko

**ABSTRACT.** The paper makes a comparison of the height of aurora during several hours in March 1965 with the intensity of emission  $\lambda$  4278 Å, radio wave absorption at a frequency of 32 Mhz and Earth current pulsations.

In March 1965, the Polar Geophysical Institute conducted a program involving a rapid determination of auroral height by triangulation methods [1].

Observation stations were located in Murmansk, and in Loparskaya, 37 km south of Murmansk. The observations were performed with theodolites equipped with sighting devices; observers were in radio-telephone communication with each other. The visual observations of heights were supplemented and controlled by photographic observations. As a rule, the discrepancies for a given auroral shape, observed by both methods at the same physical moment of time, were within the limits of 0 to 10 km.

The objective of this study was to investigate the height variation of a given auroral shape during the observation time period, and to compare the findings with other geophysical phenomena. The auroras were observed by a scanning photometer in the  $\lambda = 4278 \text{ Å}$  ( $1 \text{ NGN}_2^+$ ) emission. The half width of the light filter pass band was 120 Å. The field of view of the photometer amounted to a  $3^\circ$  solid angle. The scanning time of the sky from the northern horizon (toward Murmansk) to the southern horizon was eight seconds. The light filter period of rotation amounted to about two minutes (the photometer was equipped

with five filters). In addition, data obtained by the magnetic observatory and rheometric studies from the Loparskaya Station were used, as well as Earth currents data from the Lovozero Station.

As indicated on Figure 1 [2], the decrease of height of the lower auroral edge during the night of 2 - 3 March 1965 was accompanied by a brightness gain at the emission  $\lambda = 4287 \text{ \AA}$  and by a growth of the ionospheric absorption of radio waves at the 32 Mc frequency. Short-period variations of the geomagnetic field of the Earth of the type  $P_{12} + P_c$  appear during periods of increased intensity of auroral glow at heights under 100 km. This glow is accompanied by ionospheric absorption of radio waves at the 32 Mc frequency, if the aurora, observed at such height, are within the directional diagram of the rheometer.

The investigated time interval coincides with the transition through zero (Figure 2) of the H-component of the magnetic disturbance field. Thus, even in presence of bright auroral displays (up to the force of 4 on the international scale), the absolute deviations of the H-component from the non-disturbed level are relatively small. However, during moments when the lower auroral edge descended to heights below the 100 km level, the recording showed brief (2 - 3 minutes) flares amounting to tens of gammas: /62

Time . . . . .	18 <sup>h</sup> 43 <sup>m</sup>	18 <sup>h</sup> 48 <sup>m</sup>	19 <sup>h</sup> 2 <sup>m</sup>	19 <sup>h</sup> 12 <sup>m</sup>
h, km . . . . .	82	86	99	100
$\Delta H$ , $\gamma$ . . . . .	80	70	45	60

No less typical is the relationship between the ionospheric absorption level and the electron energies causing auroral displays, especially if we bear in mind that the height of the lower auroral edge was determined within an accuracy of 10 km. Radial auroral forms, as a rule, did not fill out the entire directional diagram of the rheometer. Thus, one would have to expect a qualitative correlation of the graphs in (Figures 1b and c) rather than a quantitative correlation. This was confirmed by experimental data.

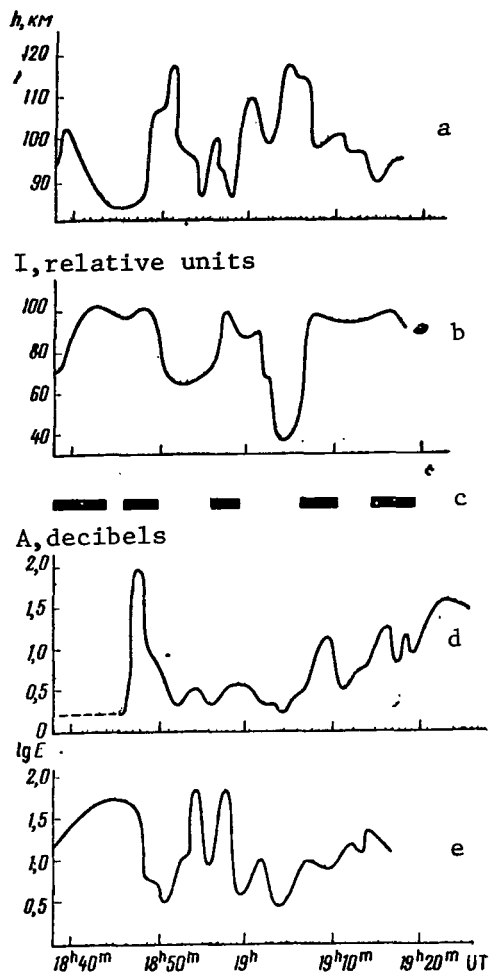


Figure 1. Variations of the lower auroral edge in time (a) and of the monochromatic light flux (in relative units) of the emission  $\lambda = 4278 \text{ \AA}$  (b); the calculation was performed from the lower auroral edge whose height above the reference surface of the Earth was determined at the given moment; the appearance of pulsations of the type  $P_{i2} + P_{c1}$  (c); absorption of cosmic noise at a frequency of 32 Mc (d); the directional diagram of the rheometer is oriented at the North star. The width of the directional diagram for half of the power is  $60^\circ$  along the meridian and  $50^\circ$  along the parallel; temporal pattern of the energy of electrons capable of reaching auroral heights (e).

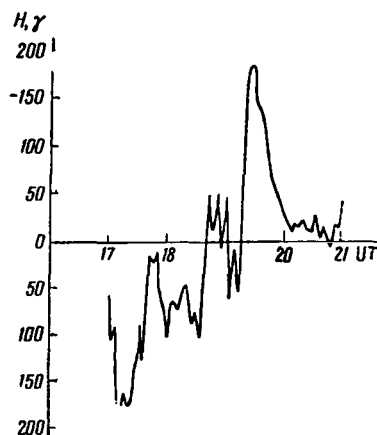


Figure 2. Variations of the horizontal component of the geomagnetic field during the nights of 2 - 3 March 1965.



Actually, on 2 March 1965 at 18<sup>h</sup> 54<sup>m</sup> and 18<sup>h</sup> 58<sup>m</sup>, aurora reached heights of 86 km; however, they were accompanied by a weak absorption. At these heights, they existed for a short time only. Hence, it can be assumed [3] that the variation of the ionospheric absorption during flares of radial auroral forms is associated not only with the intensity variation of the corpuscular stream, but also with the variation of the energy of electrons which penetrate into the upper atmosphere of the Earth.

Between 18<sup>h</sup> 38<sup>m</sup> and 18<sup>h</sup> 46<sup>m</sup>, auroral displays were beyond the directional diagram of the rheometer. Naturally, for this period of time there is no correlation between the aurora height and the absorption of radio waves. From 19<sup>h</sup> 18<sup>m</sup> on, the aurora became diffused and blurred. From this point on, it became impossible to determine its height. However, radio wave absorption continued to increase up to 19<sup>h</sup> 24<sup>m</sup> and slowly diminished only after that moment. The recording of the H-component for this time shows a large negative /63 bay of about 200 $\gamma$  (Figure 2). Considerable absorption after 19<sup>h</sup> 18<sup>m</sup> apparently can be explained by the ionization in the current layer which at that time was still sufficiently high; auroral glow occupied a large area in the sky and adequately filled the directional diagram of the rheometer.

According to the data of the survey camera C-180-S in Murmansk, there was no hydrogen emission H $\alpha$  in the auroral display during the given period of time. Typical for the aurora was the presence in the spectrum of the first positive system 1 PGN<sub>2</sub>. In its total intensity, this system exceeded the emission  $\lambda$  4278 Å. The intense glow leads to the assumption that it may be excited by electrons.

If we interpret auroral glows at heights of under 100 km as the penetration of electrons into the Earth's atmosphere with energies of over 10 keV (we will refer to them as "hard electrons") [3], then it would appear to follow that the intrusion of such electrons takes place over a short period of time (no more than several minutes). The data used in [1] suggest that auroral displays have a quasi-periodic nature with periods of three to seven minutes. For a certain time, auroral displays glow only at heights over 100 km above sea level.

Consequently, the Earth's atmosphere is penetrated by electrons with energies of under 10 keV (or soft electrons).

Radial arcs are less than 30 km in height [4]. Therefore, we could stipulate that, regardless of the height of the lower auroral edge, during the entire existence of the auroral display the glow takes place at heights of over 100 km. During the entire existence of aurora, the Earth's atmosphere is penetrated by soft electrons.

Since not enough height measurements were performed in [1], these conclusions must be considered as preliminary.

The author is extremely grateful to M. I. Pudovkin for the meaningful discussions during the preparation of this study.

#### REFERENCES

1. Yevlashin, L. S., and S. A. Zaytseva, et al. Kompleksnoye issledovaniye polyarnoy ionosfery (A Comprehensive Investigation of the Polar Ionosphere). Article in this Collection. p. 1.
2. Rees, M. H. Auroral Ionization and Excitation by Incident Energetic Electrons. Planet. Space Sci., 1963, Vol. 11, No. 10, 1963, p. 1209.
3. Ansari, Z. A. The Aurorally Associated Absorption of Cosmic Noise at College, Alaska. J. Geophys. Res., Vol. 69, No. 21, 1964, p. 4493.
4. Chamberlain, J. The Physics of Polar Aurora and Atmospheric Emissions. Moscow, IL 1963.

THE EFFECT OF QUASIRHYTHMICITY IN GEOMAGNETIC  
AND AERONOMIC PHENOMENA

G. P. Tsirs

ABSTRACT. Bursts of ultra-low frequency emissions, bursts of some geomagnetic disturbances, bursts of auroral absorption and bursts of ultra-high frequency field, observed with the rheometer, often form successions (quasirhythmoids), so that the greatest ratio of the neighboring intervals between the commencements of bursts is within 1.00 - 1.12, or 1.38 - 1.74. The paper briefly discusses the problem of the physical meaning of this empirical effect.

In this study, we analyze the time distribution of the beginnings of /64 significant intensity increments with reference to the following phenomena:

- 1) very low frequency emissions (VLFE) at 725 Hz;
- 2) magnetic field pulsations with quasiperiods from 20 to 600 seconds;
- 3) storm-type variations of the magnetic field;
- 4) auroral absorption of cosmic noise at 32 MHz;
- 5) very high frequency field (VHF) at 32 MHz, observed rheometrically.

The study is essentially based on observations performed in September and October, 1965, at the Loparskaya and Lovozero stations (recordings of magnetic field pulsations), as well as on some literature data.

On a continuous trace, increments of intensity frequently form single bursts; their beginnings can be objectively and precisely studied, especially if the larger bursts have a steep forward front. If the forward front is not steep, the beginning of the burst is determined by the moment of its intersection with the envelope of insignificant (random) oscillations. In this manner, the length

of the time interval between the beginnings of successive bursts, known as the tact interval (TI), can be determined.

Obviously, this study relates to the exploration of the reciprocal relationship of consecutive TI or, in other words, the reciprocal relationship of the bursts with a view to the aftereffect of these phenomena. It is easy to understand that in statistical laws, e.g., the distribution of the TI, must be associated with the observed dynamic effects or laws, e.g., with the periodicity of the phenomena, with the shape of the bursts, with the nature of their associations, etc.

#### Quasirhythmoids of VLFE Bursts

According to some studies [1 - 5], VLFE<sup>(1)</sup> at  $700 \pm 100$  Hz form a certain maximum in the spectrum. It was also pointed out [1 - 3], that they are associated with the micropulsations of the magnetic field and with the auroral absorption [3]. Moreover, these frequencies are empirically identical to proton gyrofrequencies in the ionosphere up to a height of approximately 1,000 km [1, 2, 3, 5]. However, there exist theoretical difficulties involving the explanation of the discharge of cyclotron emissions of protons from the region of the normal Doppler effect [3, 5], or its narrow band in the region of the anomalous Doppler effect [5]. Mc Arthur, Murcray et al., [6, 7], assumed, and Murcray and Pope [8] considered the excitation of chorus-type VLFE by low- and medium-energy protons (auroral protons) in the region of the anomalous Doppler effect. Notably, choruses correlate positively with magnetic activity indexes [9, 10]. Moreover, they are active after negative bays [9], and are closely related with moderate absorption [11, 12], especially during morning hours [12]. However, there is a negative correlation with polar aurora activity [11]. In [13], chorus-type resonances of up to 1500 Hz are referred to as "polar chorus". /65

---

(1) Rather than using the term "very low frequency" (VLF), we are employing a more concise definition: "Very low frequency emissions" (VLFE), [12].

In [8], the relationship of the observed proton emission frequency during its approach to Earth was computed with respect to time, recorded from the beginning of the reception for the range of radial velocities of 500 - 3000 km/sec. Notably, the reception begins at a frequency of 500 Hz. In time, the frequency gains so that the reception length in the constant band  $\Delta f$  decreases with the gain of  $f$ . This indicates that the maximum of the spectrum of average intensity is shifted to 500 Hz. The latter is caused by the selective distribution of the  $N/f_p$  parameter in height, where  $N$  is the electron density, and  $f_p$  is the proton gyrofrequency.

The observed radiation at  $f = 750$  Hz may produce protons with a velocity of 10 km/sec at a height of two Earth's radii, where the gyrofrequency  $f_p < 100$  Hz [8]. The smaller the radial velocity, the higher is the reception time of the emission in the range of lower frequencies. When the region of mirror points is reached, the combination of a small radial velocity with large pitch-angles does not yield effective radiation across the magnetic field [8].

The protons reach the mirror points region with a greater velocity; however, their emission is more intensive. For this reason, one can expect a broader band of observed radiation. /66

The reception of VLFE at the Loparskaya Station was performed with a vertical frame (height 10m) located in the plane of the geomagnetic meridian. The amplified and detected signals were averaged and recorded on an automatic recorder with a paper velocity of 60 mm/hr. Even though the integration by an RC-circuit with a time constant of 20 seconds does strongly suppress the registration of discrete signals, it appears, judging from the oscillograms, that VLFE of about 725 Hz more likely consist of a multitude of discrete signals, rather than a continuous noise. For the average burst in October, the spectral flux intensity was estimated at  $3 \times 10^{-13} \text{ W/m}^2 \cdot \text{Hz}$ , which is in agreement with a number of estimates [4, 14, 15, 16].

A visual analysis of the reciprocal distribution of individual bursts in time, with a characteristic duration of 10 - 20 minutes, frequently

identical in shape, revealed that their sequences appear quite frequently. These sequences are at the beginning of the bursts, located at almost equal intervals (Figure 1, curves for 8 and 9 July). This "periodicity" is often disrupted, while the type of bursts remains unchanged. Frequently, the appearance of a sequential burst is accelerated or retarded in a certain relationship. This led us to the formulation of the following effect of quasirhythmicity.

Substantial bursts are statistically related in such a manner that, when the probability is greater than with an exponential distribution of TI, sequences between the beginnings of the forward fronts of bursts can be distinguished, out of three or more bursts with the largest ratio of the adjacent TI within the limits of 1.00 - 1.2, or 1.38 - 1.74. Such a sequence shall be subsequently referred to as a quasirhythmoid (QR). Three types of two-interval QR were distinguished:

- 1) Adjacent TI are approximately equal;
- 2) The subsequent TI is approximately smaller than the preceding TI by the factor of 1.5;
- 3) The subsequent TI is larger than the preceding TI by the factor of 1.5 on the average.

We will demonstrate that such TI frequently appear in numerous geomagnetic and aeronomic phenomena. Figures 1 and 2 (quoted from [16]) show specimen QR of VLFE. It is of interest that sometimes a VLFE "storm" can be represented by a superposition of overlapping QR, whose bursts are determined from their shape, duration, etc., as shown on Figure 3. Analyzing VLFE recordings taken over a 25-day period in October, 1965, and measuring the TI, we separated 101 dual-interval QR, containing a total of 140 TI. Of all these QR's, 50% were QR's of type I, 30% of type II, and 20% of type III. The averages of the ratios of successive QR's were 1.04, 1.56 and 1.55, respectively. Since the characteristic duration of a burst was 10 - 15 minutes, and no QR was distinguished when the length of significant excesses exceeded 25 minutes, it could be assumed that the TI distribution would have a maximum at 15 - 25 minutes. However, the principal maximum is at 30 - 40 minutes (Figure 4).

/67

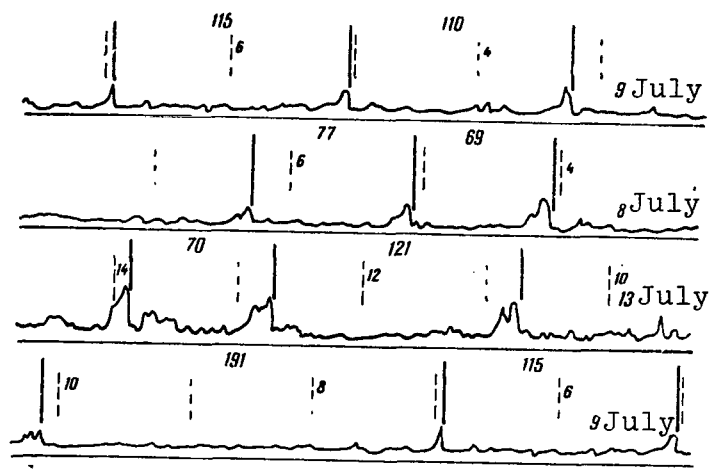


Figure 1. Quasirhythmic emissions of very low frequency at 725 Hz. Bold vertical lines denote the beginnings of the bursts; the numerals between them denote the durations of the intervals (in minutes); thin dashed lines are the time traces; the numerals next to them denote the LMT (30° E)

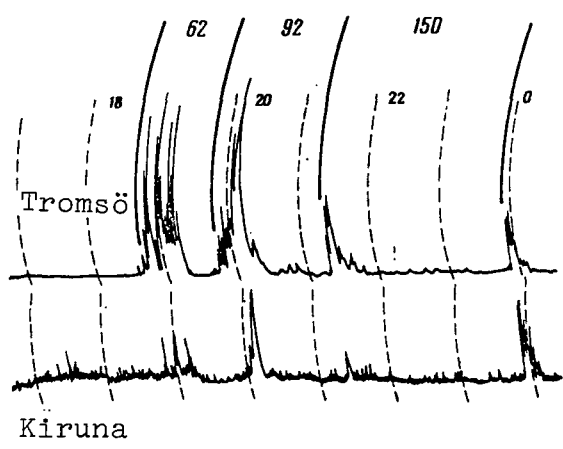


Figure 2. A QR of VLFE at 8 KHz [6], recorded on 14 February 1964. Notation same as in Figure 1.

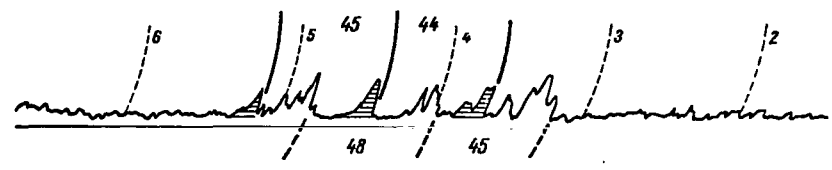


Figure 3. Superposition of quasirhythmic emissions during a VLFE storm on 13 November 1965. The beginnings of the bursts of the second QR are denoted by bold broken lines; the remaining notations are the same as in Figure 1.



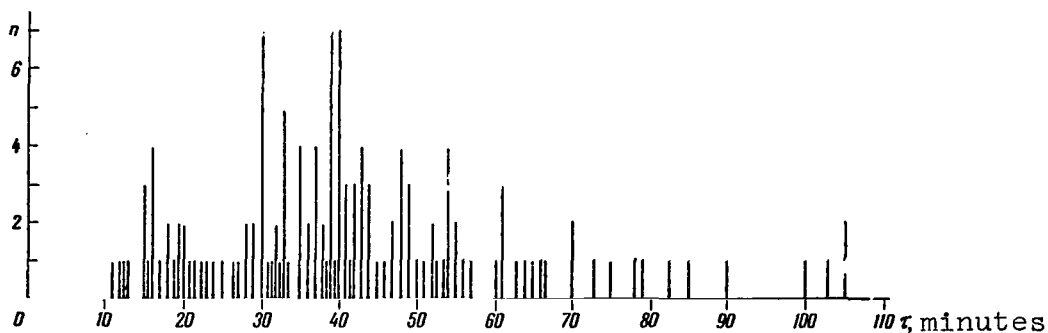


Figure 4. The distribution of tact intervals of isolated VLFE quasirhythms.

Thus, one could assume the existence of a mode of TI QR's of the order of 30 - 40 minutes.

#### Quasirhythms of Magnetic Field Pulsation Bursts

QR of pulsation bursts were separated from magnetograms with a velocity of 90 m/hr. A classification of the pulsations within the bursts was not taken into account. The commencements of the bursts were determined from the burst of the envelope, and from the moment of the change in the oscillations at the commencement of the burst. Some activity was noted somewhat earlier than the beginning. A typical QR, which developed during the storm of pulsations, is shown in Figure 5; a storm of pulsations is usually associated with a bay-like disturbance. A QR consisting of weak  $P_{13}$  was isolated between 7 - 8<sup>h</sup> UT on 4 October 1965 (Figure 6); at 16 - 18<sup>h</sup> UT, a QR was noted that consisted of individual sharp bursts on a relatively quiet background.

The table shows moments (UT) at which pulsations appeared in October, 1965, and the intervals (in minutes) between them (in parentheses). The isolated QR are separated by semicolons.

During the remaining days of October, 1965, it was difficult to separate the individual pulsation outbursts because of the large disturbances. Obviously, the TI of the pulsation bursts have a large range of values. The

QR appear with a considerable frequency. It is of interest to isolate the effect for micropulsations. Empirically, this is associated with the fact (as emphasized in [17]) that the ratio of TI between the "pearls"  $P_c 2$  (CP1p) to the TI between "pearls"  $P_c 1$  (PP) is  $190/120 = 1.56$ . This phenomenon is interpreted in [17] as the ratio of the oscillation times between the mirror points for slow protons (exciting the  $P_c 2$ ), and the fast protons (exciting  $P_c 1$ ).

/70

TABLE

Date	Bursts of pulsations, grouped into quasirhythms
1	9 <sup>h</sup> 7 <sup>m</sup> (226), 12 <sup>h</sup> 13 <sup>m</sup> (150), 15 <sup>h</sup> 28 <sup>m</sup> , 19 <sup>h</sup> 25 <sup>m</sup> (120), 21 <sup>h</sup> 25 <sup>m</sup> (190)
2	0 <sup>h</sup> 35 <sup>m</sup> , 0 <sup>h</sup> 35 <sup>m</sup> (358), 6 <sup>h</sup> 46 <sup>m</sup> (498), 15 <sup>h</sup> 0 <sup>m</sup> (350), 20 <sup>h</sup> 50 <sup>m</sup>
3	17 <sup>h</sup> 41 <sup>m</sup> (267), 22 <sup>h</sup> 8 <sup>m</sup> (273)
4	2 <sup>h</sup> 41 <sup>m</sup> , 6 <sup>h</sup> 38 <sup>m</sup> (53), 7 <sup>h</sup> 31 <sup>m</sup> (36), 8 <sup>h</sup> 7 <sup>m</sup> 16 <sup>h</sup> 24 <sup>m</sup> (46), 17 <sup>h</sup> 10 <sup>m</sup> (27), 17 <sup>h</sup> 37 <sup>m</sup>
5	1 <sup>h</sup> 14 <sup>m</sup> (88), 2 <sup>h</sup> 42 <sup>m</sup> (63), 3 <sup>h</sup> 45 <sup>m</sup> , 22 <sup>h</sup> 56 <sup>m</sup> (190)
6	2 <sup>h</sup> 6 <sup>m</sup> (127), 4 <sup>h</sup> 13 <sup>m</sup>
7	7 <sup>h</sup> 3 <sup>m</sup> (57), 9 <sup>h</sup> 0 <sup>m</sup> (80), 10 <sup>h</sup> 20 <sup>m</sup>
9	1 <sup>h</sup> 30 <sup>m</sup> (240), 5 <sup>h</sup> 30 <sup>m</sup> (367), 11 <sup>h</sup> 37 <sup>m</sup> (350), 17 <sup>h</sup> 27 <sup>m</sup> 19 <sup>h</sup> 27 <sup>m</sup> (44), 20 <sup>h</sup> 11 <sup>m</sup> (31), 20 <sup>h</sup> 42 <sup>m</sup> , 20 <sup>h</sup> 42 <sup>m</sup> (236)
11	4 <sup>h</sup> 13 <sup>m</sup> (247), 8 <sup>h</sup> 20 <sup>m</sup> (224), 12 <sup>h</sup> 4 <sup>m</sup> (216), 15 <sup>h</sup> 40 <sup>m</sup> (191), 18 <sup>h</sup> 51 <sup>m</sup>
13	0 <sup>h</sup> 51 <sup>m</sup> (46), 1 <sup>h</sup> 37 <sup>m</sup> (67), 2 <sup>h</sup> 43 <sup>m</sup> , 12 <sup>h</sup> 6 <sup>m</sup> (128), 14 <sup>h</sup> 14 <sup>m</sup> (121), 16 <sup>h</sup> 15 <sup>m</sup> (72), 17 <sup>h</sup> 27 <sup>m</sup>
14	1 <sup>h</sup> 44 <sup>m</sup> (43), 2 <sup>h</sup> 27 <sup>m</sup> (48), 3 <sup>h</sup> 15 <sup>m</sup> (49), 4 <sup>h</sup> 4 <sup>m</sup> (70), 5 <sup>h</sup> 14 <sup>m</sup> 13 <sup>h</sup> 0 <sup>m</sup> (120), 15 <sup>h</sup> 0 <sup>m</sup> (120), 17 <sup>h</sup> 0 <sup>m</sup>
16	5 <sup>h</sup> 30 <sup>m</sup> (365), 11 <sup>h</sup> 35 <sup>m</sup> (390), 18 <sup>h</sup> 5 <sup>m</sup>
19	12 <sup>h</sup> 0 <sup>m</sup> (240), 16 <sup>h</sup> 0 <sup>m</sup> (225), 19 <sup>h</sup> 45 <sup>m</sup>
26	15 <sup>h</sup> 16 <sup>m</sup> (274), 19 <sup>h</sup> 50 <sup>m</sup> (175), 22 <sup>h</sup> 45 <sup>m</sup>

/68

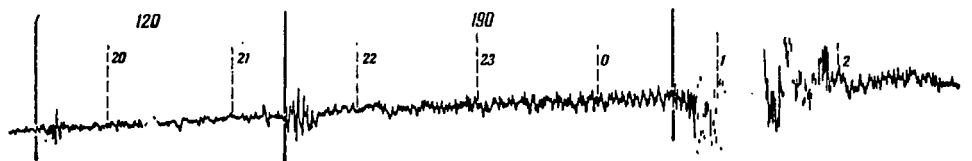


Figure 5. A QR of the pulsations of the geomagnetic field, recorded on 2 October 1965. Notations same as on Figure 1.

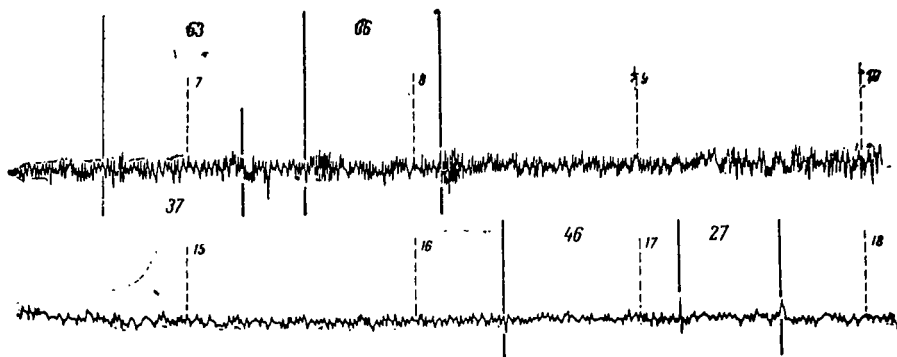


Figure 6. A QR of weak pulsations and of intense bursts of the geomagnetic field, recorded on 4 October 1965.

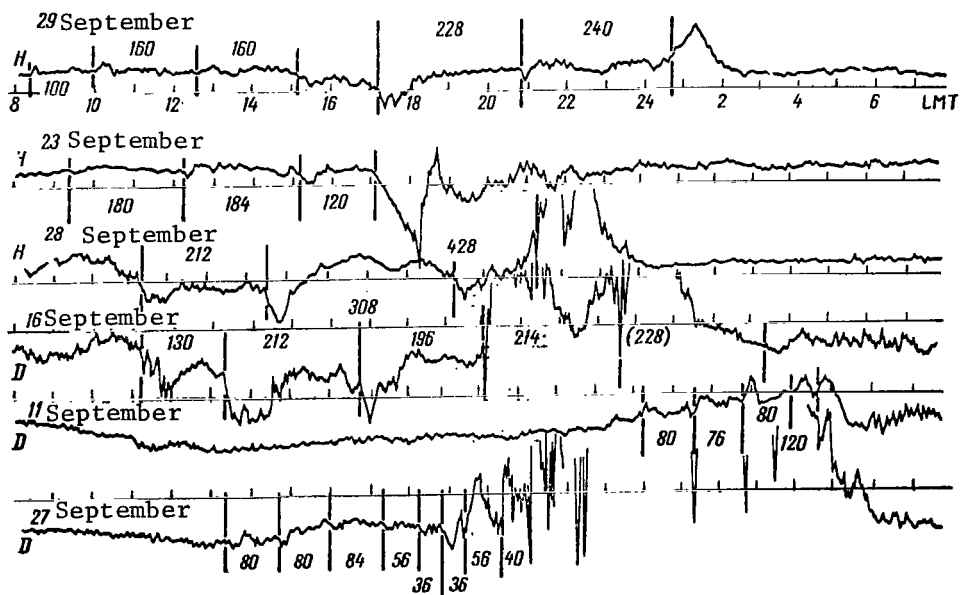


Figure 7. Quasirhythmoids of bay-like disturbances of the geomagnetic field, recorded in September 1965.

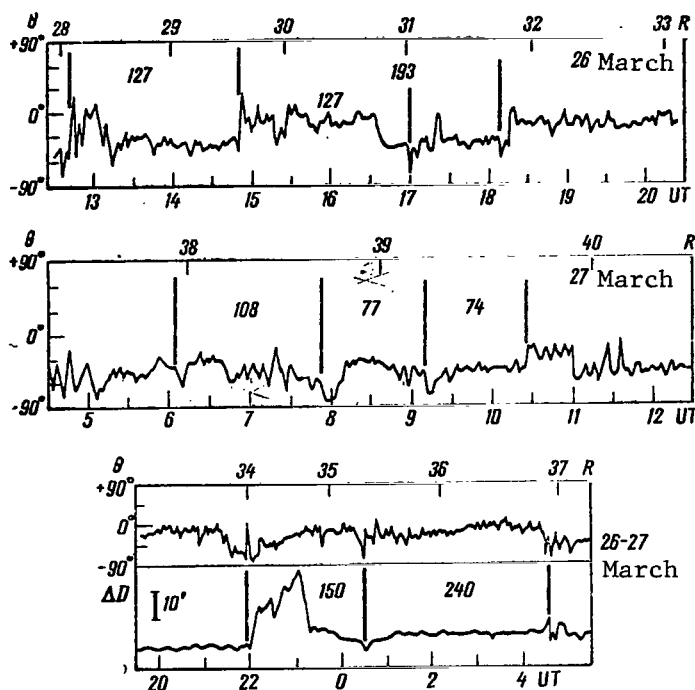


Figure 8. Quasirhythmoids of magnetic field disturbances, beyond the magnetosphere, recorded in March 1965 [18].

The upper scales show the geocentric distance in Earth radii, the lower scales indicate the UT. The satellite was on the evening side of the Earth; the straight line, connecting the satellite with the center of the Earth, made a  $25^\circ$  angle with the Earth-Sun plane, which is normal to the ecliptic, and a  $35^\circ$  angle with its projection upon the plane of the ecliptic. The lower QR correspond to QR of bay  $\Delta D$  at Murmansk.

magnitude) correlate with approximately equal (in amplitude) bursts of the field beyond the magnetosphere. This, conceivably, could be caused by the drift of Murmansk upon the morning side of the Earth. This example further emphasizes the importance of the moments of commencement of bursts, at least in magnetic field phenomena.

### Quasirhythmoids of Bay-Like Disturbances of the Magnetic Field.

Specimen QR, identified from magnetograms taken in September 1965, are shown in Figure 7. When the bursts had no steep forward front, their commencement was determined from the intersection of their magnetogram with the magnetogram of the quietest day of the month. During strongly disturbed days, the bays overlap, the trace becomes undecipherable, and the QR cannot be identified.

In Figure 8, the QR are defined with respect to the deviation of the  $\Theta$ -vector of the magnetic field from a plane that is parallel to the plane of the ecliptic beyond the magnetosphere, according to the data supplied by "Explorer X" [18]. The graph indicates that the commencements of different bays (in terms of

### Quasirhythmoids of Bursts of Auroral Absorption of Cosmic Noise

In Figure 9, we show two QR of a total of 12 that were isolated and that cover the majority of absorption bursts that took place in October, 1965. On 23 and 24 October, the QR bursts are superimposed upon lengthy and small anomalous absorption. An extensive QR, covering small anomalous absorptions, was isolated on 17 - 18 October. These absorptions are associated with VHF bursts and their natural causes will be discussed below. A similar QR had a TI of approximately 144 minutes. With a rapid recording, and under the condition that separate disturbances do not cause an absorption-like effect on the rheometric recording, we can isolate QR of small absorption bursts with short intervals — i.e., on the order of an hour, as for example, took place on 17 - 18 November, 1965 (Figure 10). Figure 11, from [19], shows the absorption traces in the morning hours in College, based on a number of frequencies and absorption recordings in adjacent areas; there appear QR with TI of several hours.

Notably, x-ray radiation in the stratosphere, caused by electron intrusion, is frequently associated with anomalous absorption in the auroral zone. Figure 12 (from [20]) shows the QR of x-ray microbursts with energies of the order of  $\geq 100$  keV.

### The Quasirhythmoids of Bursts of the Very High Frequency Field

Some studies [21 - 26] report irregular bursts of the VHF field, registered by radar and rheometric observations during geomagnetic storms, anomalous absorption of  $E_s$ , and diffusion in the F region at high latitudes. In [16], the relationship between the bursts of the VHF and VLFE is emphasized. It is pointed out that they arrive from northern directions, and have a noise-like nature and a wide range. Even though some investigators who used rheometric traces and radar interpret such VHF field bursts as actual disturbances, no particular attention was paid to them otherwise. Some authors discuss possible forms of long-range propagation of disturbances (atmospheric, industrial as well as signals of VSW and SW radiostations), emphasizing the role of auroral ionization, of  $E_s$  scattering in the propagation, and of the

/73

distortion of the signals. On the other hand, the natural mechanisms of excitation are also mentioned: e.g., Cherenkov excitation [21], synchrotronic excitation [22, 23], plasma emissions [21, 24, 25], as well as emission by electrons that are ejected from molecules [26]. It is pointed out that it is possible to transform the frequency of an SW radiostation due to the rapid variation of the ionization density [27]. We should also keep in mind the scattering by meteorite traces, or the reflection from them, whereby the latter may be also elongated along the force lines of the magnetic field, [28 - 30].

It was suggested in [31], that VHF bursts, observed rheometrically during radio-synchrotron anomalies and during geomagnetic storms with a sudden commencement, may well be a consequence of the "porosity" of the absorbing region, or they may be bursts of solar radio emission. The first assumption appears somewhat artificial; the second assumption is not unfeasible during the day in years of maximum solar activity, and during the night when VSW( $\sim 50$  MHz) changes to high latitudes as a result of the reflection from the F2 layer. As to minimum years, it is difficult to visualize the reception of solar radio-emissions at a frequency of 32 MHz at nighttime. At low latitudes, VHF bursts after a nuclear explosion are quantitatively interpreted as a synchronous emission of captured electrons [32, 33].

At high latitudes, [23], the required electron stream with energies over 500 keV with an energy power spectrum index of  $\approx 2$ , (yielding a burst of UHF at a frequency of 30 MHz, which is 0.4 dB higher than cosmic noise), has been estimated at  $2.5 \times 10^7 \text{ cm}^{-2} \cdot \text{sec}^{-1}$  [23]. In the magnetosphere, a stream of such electrons was registered on the force line  $L \sim 6$  at  $5 \times 10^5 \text{ cm}^{-2} \cdot \text{sec}^{-1}$  [34]. It is assumed that for special perturbations, the fast electron stream can reach the required magnitude. It is a typical feature of synchrotron emission that it propagates within a narrow cone; the axis of the cone coincides with the direction of the electron velocity and is almost normal with respect to the magnetic force line.

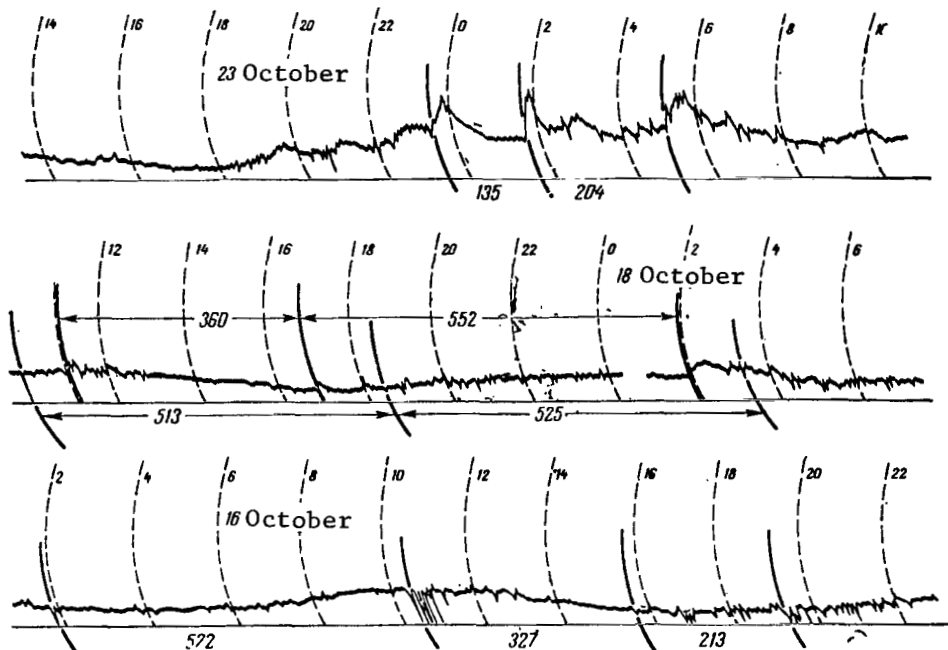


Figure 9. Quasirhythmoids of auroral absorptions of cosmic noise on a archeometric trace on 23 and 18 October, and the QR's of VHF bursts (32 MHz, 16 October). Notations same as in Figure 1.

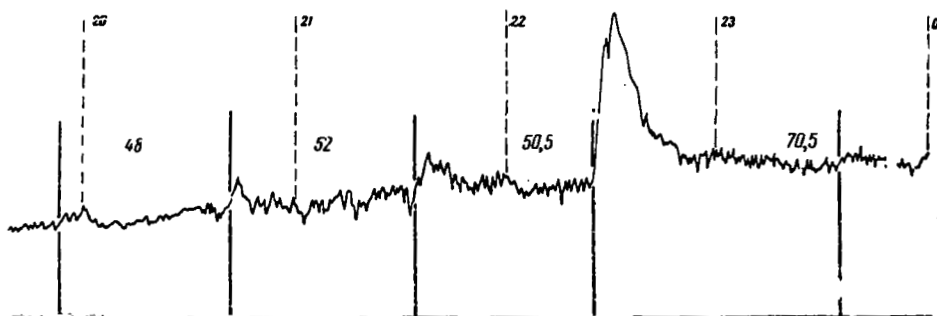


Figure 10. Quasirhythmoids of auroral absorptions, recorded on 17 November 1965 with intervals of approximately 50 to 70 minutes. Notations same as in Figure 1.

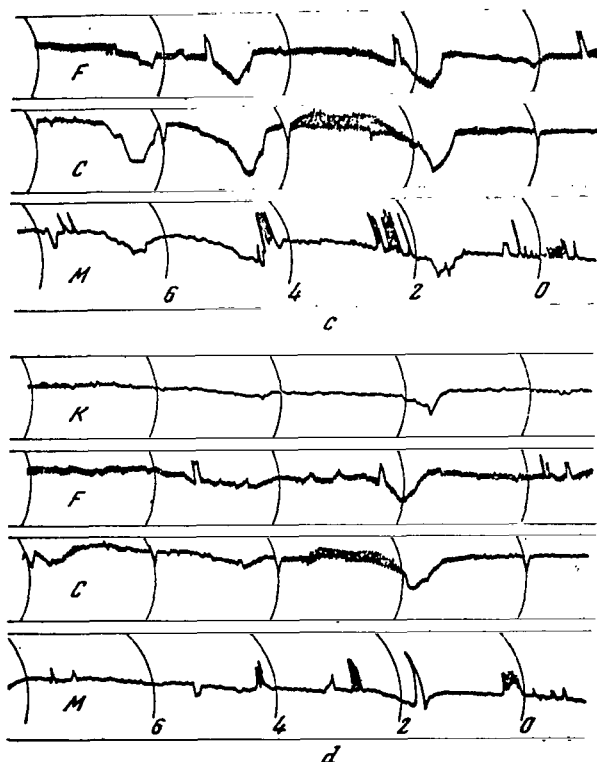


Figure 11. Quasirhythmoids of auroral absorptions and VHF field bursts in conjugate areas [19]. Time: (LMT 150° W). M - Makuori Island; K - Kotzebue; C - College; F - Fort Yukon.

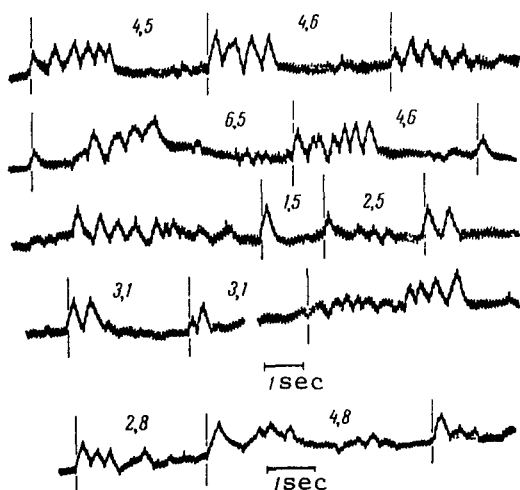


Figure 12. Quasirhythmoids of a group of x-ray bursts in the stratosphere for energies  $E \geq 100$  keV [20].

Obviously, without detailed studies of the burst intensity of the VHF field, the directions of their arrival, their distribution in terms of frequency and amplitude, as well as their relationship to other phenomena, the problem of the exciter of UHF field bursts cannot be resolved. /73

The rheometer antenna at the Loparskaya Station (a four-element wave channel) was beamed at the North Star; this does not preclude reception from other directions. Typical specimens of UHF field bursts are shown in Figure 13. Bursts were observed that range from several seconds and more, which frequently form a close group ("forest" of bursts), or else solid excesses of the apparent cosmic noise (or "interferences") lasting several hours. /74

Most frequently, bursts appear prior to and after anomalous absorption. Short bursts in the maximum of anomalous absorption are rare. Longer lasting excesses of the VHF field on a background of considerable anomalous absorption do take place; however, they are interpreted as a rapid reduction of the cosmic noise absorption. Figure 13 shows traces for April and June 1965, when remote passages of SW - VSW were



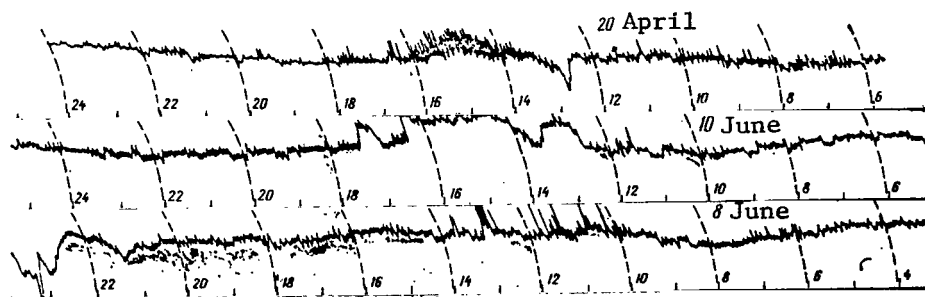


Figure 13. Typical bursts of the VHF field (32 MHz) on a rheometric trace. Notations same as in Figure 1.

observed at the Kola Peninsula at a frequency of approximately 30 MHz, due to reflection from summer-type  $E_s$  at subpolar latitudes. The typical phenomena involving the VHF fields are observed at any time of the year or of the day; this suggests reasons other than  $E_s$  for solar radio emission at subpolar latitudes. The almost simultaneous appearance of short ( $\sim 1$  min.) bursts of the VHF fields at Cape Chelyuskin and at Dixon Island (the distance between the two points being  $\sim 750$  km) on 26 September 1963 was noted in [35].

Figure 11 shows bursts of the VHF field in the decay of anomalous absorption (after 2<sup>h</sup> LMT, 150° W) in adjacent areas.

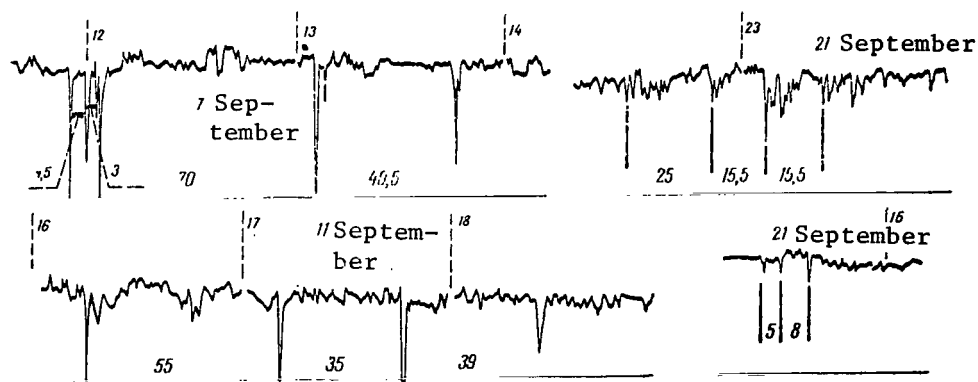


Figure 14. A VHF QR (32 MHz) with intervals from several minutes to approximately 50 to 70 minutes, recorded in September 1965. Notations same as in Figure 1.

The relationship between bursts of the VHF field at a frequency of 28 MHz and VLFE at a frequency of 8 KHz was reported in [16]. We also pointed out a number of instances when, increasing with the beginning of anomalous absorption, the activity of VLFE at a frequency of 725 KHz continued after the absorption maximum. It decreased with the bursts (18 June and 27 October 1965, etc.). A long QR of VHF field bursts on 16 and 18 October 1965 is shown in Figure 9; the TI were close to those of the absorption. Figure 14 shows shorter QR of the VHF field. On 7 September, the first closed group of bursts is a short QR with TI of the order of several minutes. Figure 11 shows QR of VHF emission bursts, recorded on Makuori Island; they are identical to the QR of absorption in terms of the duration of their TI; however, (in the first 154 minutes), they began earlier. Thus we see that the relationship between bursts of the VHF field with anomalous absorption and VLFE in time affords the possibility of isolating QR with TI of similar orders of magnitude. All told, this indicates that the principal share of the analyzed bursts of the VHF field is not due to local disturbances or meteoric ionization, but is related to the activity of charged particle streams at high latitudes, where QR are frequently isolated.

If we were to assume that bursts of the VHF field are actually bursts of solar radio emission, it would be difficult to explain the mechanism of their relationship with VLFE and the relationship of QR of the VHF field with QR of the auroral absorption. Notably, the occurrence of an electron outburst at the moment of the arrival of the radio frequency radiation of chromospheric bursts was predicted in [36]. The question also arises regarding the probability of QR of the solar radio frequency radiation. Traces of the latter were not examined; however, a QR was discovered [37] (see Figure 15). /75

Thus, in the five analyzed types of phenomena which are typical for the activity of charged particle streams in MHD waves or sporadic ionization above the observation area at high latitudes, there are frequent QR of significant bursts of characteristic magnitudes. Quantitative estimates of the probability

of their occurrence and the feasibility of using these phenomena for short-range forecasting requires additional statistical analyses, with a consideration of the magnetic and solar activity.

In the interpretation of the physical meaning of these phenomena, two approaches are feasible:

- 1) The significant probability of QR observation is a statistical consequence of the TI distribution among homogenous events; this distribution is caused by general physical conditions of random mechanisms;
- 2) A QR reflects the structure that is typical for a single mechanism which appears at random, but frequently.

If we accept the second interpretation, we could assume, as in [38], that moving in the magnetosphere, captured and drifting about the Earth, is a quasistable multitude ("cloud") of geoactive corpuscles. This "cloud", passing over the observation area, causes bursts of QR of these phenomena. Obviously, this problem should be resolved in the framework of the dynamics of space-time distribution of different phenomena at high latitudes. It is necessary to consider the numerous effects of periodicity of associated geophysical phenomena [39], as well as the presently existing interpretation.

The strong probability of occurrence of QR indicates that the TI distribution has more probable or, in other words, modal values of the TI. It could be expected that with two modal intervals, or two peaks in the energy spectrum, the intensity of the phenomenon, the ratio of the frequencies or periods, corresponding to the neighboring peaks of the energy spectrum, will lie between 1.38 - 1.74. Actually, quasiperiods obtained by harmonic analysis of the activity of  $E_s$  in [40] are 162 hours 102 minutes. The quasiperiods of polar aurora [41]; 6, 9, 14 (weakly pronounced), 22, 36, 54, and 90 minutes. The quasiperiods of minimums in the spectrum of Earth currents [42]: 15.5; 9.25; 6.0; 3.63; 2.60 minutes. The strongest eigen vibrations of the Earth [43, 44] have the following periods: 53.5; 35.6; 25.8; and 16.1 minutes, and 43.6; 28.2; 21.6 and 15.4 minutes. The frequency of the peaks of the energy spectrum of the electromagnetic field in the "Earth-Ionosphere" cavity [45]: 0.8; 1.3;

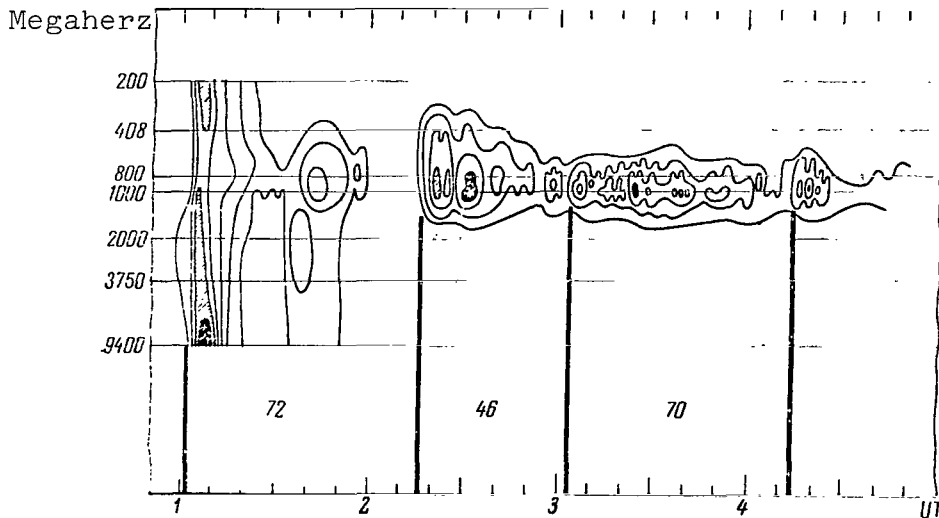


Figure 15. A QR of solar radio frequency radiation, recorded on 3 September 1960 [37]. Lines of equal intensity are shown.

1.8 Hz. It appears that QR can be characteristic for the magnetosphere, as well as for the atmosphere of the Earth itself; they can be interpreted as spherical oscillating systems. It follows from [46] that the simplest types of standing waves in the spherical cavity have frequencies of the first three harmonics such that about  $2/3$  of the ratios of the second to the first and third to the second are within 1.38 - 1.75. It is difficult to judge whether this is also true for the hydromagnetic oscillations of the entire magnetosphere and its individual cavities [47].

Using very general considerations, it appears that an identical relationship between the modal frequencies in the energy spectrum can also occur during the excitation of parametric oscillations, if the parameter that determines the frequency of the system's eigen vibrations is modeled with a frequency that is smaller than the eigen vibration frequency by approximately a factor of 1.5. Then both the parametric eigen vibrations and vibrations with a pumping frequency can be excited. Apparently the superposition of several mechanisms in one phenomenon cannot be ruled out.

## REFERENCES

1.   Aarons, J. G. Gustavson, and A. Egeland. Correlation of audio-frequency electromagnetic radiation with auroral zone micropulsations. *Nature*, Vol. 185, No. 4707, 1960, p. 148.
2.   Gustavson, G., A. Egeland, W. Barron, and J. Aarons. Band emissions at gyro-frequencies of ionospheric ions and Trill frequencies. *Propagation of radio waves at frequencies below 300 kc/s.* Pergamon Press, Oxford - London, N.Y., Paris, 1964, p. 175.
3.   Egeland, A., G. Gustavson, S. Olsen, J. Aarons, and W. Barron. Auroral zone emissions centered at 700 cycles per second. *J. Geophys. Res.*, Vol. 70, No. 5, 1965, p. 1079.
4.   Gurnett, D. A., and B. J. Brien. High latitude geophysical studies with satellite "Injun 3" very low frequency electromagnetic radiation. *J. Geophys. Res.*, Vol. 69, No. 1, 1964, p. 65.
5.   Hultquist, B. On the amplification of VLF emissions by charged particles in the exosphere, with the special reference to the frequency band around the proton cyclotron. *Planet Space Sci.*, Vol. 13, No. 5, 1965, p. 391.
6.   MacArthur, J. W. Theory of the origin of very low frequency radio emissions from the Earth's exosphere. *Phys. Rev. Letters*, No. 2, 1959, p. 491.
7.   Murcray, W. B., J. H. Pope. Doppler shifted cyclotron frequency radiation from protons in the Earth's exosphere. *Phys. Rev. Letters*, Vol. 4, 1960, p. 5.
8.   Murcray, W. B., and J. H. Pope. Radiation from protons of auroral energy in the vicinity of the Earth. *J. Geophys. Res.*, Vol. 65, No. 11, 1960, p. 3569.
9.   Pope, J. H. An investigation of whistlers and chorus at high latitudes. *Sci. Rept. Geophys. Inst. Alaska*, 1959.
10.   Hachiroe, T. VLF emissions and geomagnetic disturbances at the auroral zone. Part I. Chorus bursts and preceding geomagnetic disturbances. *J. Geomagn. and Geoelectr.*, Vol. 14, No. 1, 1962, p. 33.
11.   Tadanori, O. VLF emissions and geomagnetic disturbances at the auroral zone. Part II. Chorus increases and geomagnetic pulsations at the auroral zone. *J. Geomagn. and Geoelectr.*, Vol. 14, No. 2, 1962, p. 86.
12.   Ecklund, W. L., J. K. Hargreaves, and J. H. Pope. On the relations between auroral radio absorption and very low frequency emissions. *J. Geophys. Res.*, Vol. 70, No. 17, 1965, p. 4285.

177

13. Ungstrup, E., and I. M. Juckerott. Observation of chorus below 1500 cycles per second at Godhavn, from July 1957 to December 1961. J. Geophys. Res., Vol. 68, No. 8, 1963, p. 2141.
14. Tadanori, O. The ionospheric absorption of the VLF emissions at the auroral zone. J. Geomagn. and Geoelectr., Vol. 15, No. 2, 1963, p. 90.
15. Iwane, K. Amplification of the VLF electromagnetic wave by a proton beam through the exosphere an origin of VLF emissions. Rept. Ionosphere Space Res. Japan, Vol. 15, No. 2, 1961, p. 171-191.
16. Harang, L., and R. Larsen. Radio wave emissions in the VLF band observed near the auroral zone. I. Occurrence of emissions during disturbances; II. The physical properties of the emissions. J. Atmos. and Terr. Phys., Vol. 27, No. 4, 1965, p. 481.
17. Yanagihara, K. Geomagnetic micropulsations with periods from 0.03 to 10 seconds in the auroral zone with special reference to conjugate point studies. J. Geophys. Res., Vol. 68 No. 11, 1963, p. 3383.
18. Heppner, J. P., N. F. Ness, C. S. Searce, and T. L. Skillman. "Explorer 10" magnetic field measurements. J. Geophys. Res., Vol. 68, No. 1, 1963, p. 1.
19. Parthasarathy, R. and F. T. Berkey. Multiple-frequency investigation of radio-wave absorption during the dawn-breakup phase of aurora. Radio Sci. J. Res. NBS, Vol. 69D, No. 3, 1965, p. 415.
20. Anderson, K. A. and D. W. Milton. Balloon observations of x-rays in the auroral zone. 3. High time resolution studies. J. Geophys. Res., Vol. 69, No. 21, 1964, p. 4457.
21. Hartz, T. R. Auroral radiation at 500 Mc. Canad. J. Phys., Vol. 36, No. 6, 1958, p. 677.
22. Egan, R. D. and A. M. Peterson. Auroral noise at HF. J. Geophys. Res. Vol. 65, No. 11, 1960, p. 3830.
23. Hower, G.L., A. M. Peterson. Synchrontron radiation from auroral electrons. J. Geophys. Res., Vol. 69, No. 19, 1964, p. 3995.
24. Benediktov, Ye. A., V. O. Rapoport, and V. Ya. Eydman. Plasma wave emission in the ionosphere. Geomagnetizm i aeronomiya, Vol. 2, No. 4, 1962, p. 708 - 711.
25. Forsyth, P. A., Win. Petrie, and B. W. Curie. On the origin of 10 cm radiation from the polar aurora. Canad. J. Phys., Vol. 28, No. 3, 1950, p. 324.

26. Rapoport, V. O. and V. Ya. Eydman. Radio-frequency radiation, generated in the ionosphere during ionization by corpuscular streams. *Geomagnetizm i aeronomiya*, Vol. 5 No. 5, 1965, p. 930 - 931.
27. Barry, G. H., and P. R. Wides. The effect of a solar flare on the frequency of high-frequency back-scatter. *J. Geophys. Res.*, Vol. 67, No. 7, 1962, p. 2707.
28. Walter, B. F. Possible effects on magnetic field alignment of meteoric ionization. *J. Geophys. Res.*, Vol. 66, No. 9, 1961, p. 3065.
29. Heritage, J. L., S. Weisbrod, and W. J. Fay. Evidence that meteor tails, produce a field aligned scatter signal at V. H. F. *J. Geophys. Res.*, Vol. 67, No. 3, 1962, p. 953.
30. Heritage, J. K., S. Weisbrod, and W. J. Fay. Evidence for a 200-megacycle per second ionospheric forward scatter mode associated with Earth's magnetic field. *J. Geophys. Res.*, Vol. 64, No. 4, 1959, p.1235.
31. Keppler, E., A. Ehmert, G. Pfozter. Sudden increase in radiation intensity coinciding with a geomagnetic storm sudden commencement. *J. Geophysical Res.*, Vol. 67, No. 13, 1962, p.5343.
32. Ochs, G. R., D. T. Farley, and K. L. Bowles. Observations of synchrotron radio noise at the magnetic equator following the high-altitude nuclear explosion of July 9, 1962, *J. Geophys. Res.*, Vol. 68, No. 3, 1963, p. 701.
33. Peterson, A. M., and G. L. Hower. Synchrotron radiation from high-energy electrons. *J. Geophys. Res.*, Vol. 68, No. 3, 1963, p. 723.
34. Frank, L. A. A survey of electrons E 40 kev beyond 5 Earth radii with "Explorer 14". *J. Geophys. Res.*, Vol. 70, No. 7, 1965, p.1593.
35. Driatskiy, V. M., et al. Issledovaniye pogloshcheniya radiovoln v ionosfere vysokikh shirot (Investigation of radiowave absorption in the high-latitude ionosphere). Archives of AANII (Astronomic-Astrogeophysical Institute of Scientific Research), 1964.
36. Tsytovich, V. N. Electron acceleration in the radiation belts of the Earth. *Geomagnetizm i aeronomiya*, Vol. 3, No. 4, 1963, pp. 616-625.
37. Wincler, J. R., and P. D. Bhavsar. The time variations of solar cosmic rays during the September 3, 1960, event. *J. Geophys. Res.*, Vol. 68, No. 8, 1963, p. 2099.
38. Pudovkin, M. I. and N. S. Smirnov. Two types of corpuscular intrusions into the polar zone. *Geomagnetizm i aeronomiya*, Vol. 6, No. 1, 1966, p. 166 - 168.

39. Tsirs, G. P. Effekty periodichnosti v ryade geofizicheskikh yavleniy. (The effect of periodicity in some geomagnetic phenomena). Review. Archives of the Polar Geophysical Institute (PGI), 1966.
40. Bennett, S. M., and T. M. Noels. Antarctic research and data analysis of an electron bombardment theory of high latitude sporadic. Res. and Advanc. Developm. Div. Avco. Corp. Wilmington, Vol. 48, 1964.
41. Roldugin, V. K. O periodichnosti vspyshek polyarnykh siyaniy (On the periodicity of auroral bursts). In press.
42. Horton, C. W., and A. A. J. Hoffman. Power spectrum analysis of the telluric field at Tbilisi, USSR, for periods from 2.4 to 60 minutes. J. Geophys. Res., Vol. 67, No. 9, 1962, p. 3369.
43. Nowroozi, A. A. Eigenvibrations of the Earth after the Alaskan Earthquake. J. Geophys. Res., Vol. 70, No. 20, 1965, p. 5145.
44. Winch, D. E., B. A. Bolt, and L. Slaucaitajs. Geomagnetic fluctuations with the frequencies of torsional oscillations of the Earth. J. Geophys. Res., Vol. 68, No. 9, 1963, p. 2685.
45. Hyqhes, H. G. Power spectral analyses of modulated Earthionosphere cauty resonances. J. Geophys. Res., Vol. 69, No. 21, 1964, p. 4709.
46. Mors, F. M. and G. Feshbach. Methods of theoretical physics. Moscow, Foreign Literature Press, 1960, pp. 534 and 799 - 803.
47. Watanabe, T. On the origin of geomagnetic pulsations. Sci. Rept. Tohoku Univ., Vol. 13, No. 3, Ser. 5, 1961, p. 127.



## THE ENERGY BALANCE OF A MAGNETIC STORM

B. Ye. Bryunelli, M. I. Pudovkin

**ABSTRACT.** The paper analyses the total energy and its dissipation rate at different stages of development (DCF, DR and DP) of the magnetic storm. Evaluations are made of the energy expenditure of the solar corpuscular stream, associated with the formation of current systems in the magnetosphere of the Earth and beyond it.

A geomagnetic storm occurs as a result of the interaction between solar corpuscular streams and the magnetosphere of the Earth. The mechanism of this interaction is known only in very general terms. Thus, it is of interest to examine the energy balance of a magnetic storm; this permits us, without going into the details of any specific mechanism, to develop an estimate of its probability. /79

A storm is created by current systems which occur beyond, as well as within, the Earth. Chapman [1] pointed out that when the screening effect of the conductive layers of the Earth is taken into account, the energy of a magnetic storm appears to be equal to the energy of the corresponding current systems. The component, corresponding to the interaction energy of the current systems with the main field of the Earth, is not included in the expression for the total energy. Further, it was demonstrated [2], that the effect of the Earth's conductivity upon the energy losses by the corpuscular stream and upon the generation of a magnetic storm is insignificant. Thus, variations of the magnetic moment of the Earth can be neglected in calculating the energy of the stream. Actually, a magnetic storm can be modelled by a

system of three interacting contours: the first corresponds to the main field of the Earth, the second represents the extra ionospheric current system of the storm, and the third corresponds to currents induced in the Earth, which screen its interior layers from the effects of the external magnetic field. The energy of such a system is

$$W_m = \frac{1}{2} L_{11} I_1^2 + \frac{1}{2} L_{22} I_2^2 + \frac{1}{2} L_{33} I_3^2 + L_{12} I_1 I_2 + L_{13} I_1 I_3 + L_{23} I_2 I_3. \quad (1)$$

For the case of nonconductive Earth  $I_3 = 0$ , the magnetic energy of the entire system is

$$W_m = \frac{1}{2} L_{11} I_1^2 + \frac{1}{2} L_{22} I_2^2 + L_{12} I_1 I_2, \quad (1a)$$

i.e., it contains the component  $L_{12} I_1 I_2$ , which corresponds to the interaction energy between the current system of the storm and the main field of the Earth.

However, as pointed out in [2], with a constant magnetic moment of the Earth, the magnetic interaction energy  $W_{in} = L_{12} I_1 I_2$  is generated not due to the energy of the flux, but due to the sources of the main field of the Earth. Actually, with an arbitrary shift of the contour  $L_2$  and with a variation of the force of the current  $I_2$  in this contour, the sources which maintain the current in the first contour perform the work

$$\delta P = -I_1 \delta(I_2 L_{12})$$

and when  $I_1 = \text{constant}$ ,

$$\delta P = -\delta(L_{12} I_1 I_2) = \delta W_{in}$$

Thus, when the conductivity of the Earth is zero, and the magnetic moment of the Earth during the storm is retained, then the mutual energy of interaction  $W_{in} = L_{12} I_1 I_2$  is entirely produced by the sources of the main field. The energy of the corpuscular stream is only consumed for the generation of self-

induction energy

$$W_m = \frac{1}{2} L_{22} I_2^2. \quad (2)$$

This is a consequence of the commonly known fact that the constant (in time) magnetic field does not perform any work; hence, the kinetic energy of contour  $L_2$  can only be converted into its own energy of self-induction.

If, on the other hand, the conductivity of the interior layers of the Earth is sufficiently high, then the magnetic flux through contours  $L_1$  and  $L_3$  does not change during the storm, i.e.,  $L_{12} I_2 + L_{13} I_3 = 0$ . The sources of the main field do not perform any work. The magnetic energy of the system

$$W_m = \frac{1}{2} L_{11} I_1^2 + \frac{1}{2} L_{22} I_2^2 + \frac{1}{2} L_{33} I_3^2 + L_{23} I_2 I_3 \quad (1b)$$

as pointed out by Chapman [1], does not contain the term that corresponds to the interaction energy between the system of the storm's currents and the main geomagnetic field.

Obviously, in the calculation of the energy losses of the stream, the mutual energy  $L_{12} I_1 I_2 = (\vec{M} \cdot \Delta \vec{I})$  should not be taken into account, regardless of the conductivity of the Earth.

The emergence of three extra terms in expression (1b), as compared to (2), reflects the fact that, with a high conductivity of the Earth, the energy of the corpuscular stream is consumed for generating currents, beyond as well as within the Earth. However, quantitatively this variation of energy  $W_m$  is rather insignificant. In fact, as pointed out in [1, 2], the energy of self-induction of currents, flowing on the surface of a sphere, is proportional to the square of the radius of this sphere. Since the radius of the sphere upon which the currents  $I_3$  are flowing does not exceed the radius of the Earth ( $r_3 \approx 0.8 R_E$ ), and the radius of the sphere  $r_2$  upon which DR and DCF currents are flowing is of the order  $3R_E$  and  $6R_E$ , respectively, it follows that  $L_{22} I_2^2 / L_{33} I_3^2 \gg 10$ . The interaction energy of current systems  $I_2$  and  $I_3$  equals

$L_{23}I_2I_3 = -2L_{33}I_3^2$  [2]. Thus, it also does not exceed the energy of self-induction of current system  $I_2$  by the factor of 0.2.

Accordingly, in estimating energy losses of the stream, the energy of currents inducted in the Earth may be disregarded, and the magnetic moment of the Earth may be considered constant. In this instance, it is easy to demonstrate that the self-induction energy of the extra ionospheric current ring is connected by a simple relationship to its interaction energy with the main magnetic field of the Earth. Indeed, if the approaching contour is regarded as superconductive, then the magnetic flux through the surface that is bounded by the contour must remain constant, i.e.,

$$L_{22}I_2 + L_{12}I_1 = 0. \quad (3)$$

The magnetic energy generated at the end of the motion due to the corpuscular stream is

$$W = \frac{1}{2}L_{22}I_2^2 = -\frac{1}{2}L_{12}I_1I_2. \quad (4)$$

With respect to the Earth, this means that the energy of the initial phase of the storm is

$$W_1 = -\frac{1}{2}(\vec{M}_E \Delta \vec{H}_e), \quad (5)$$

where  $\Delta H_e$  is the field increase in the initial phase which is attributable to external causes only. /81

Assuming that the observed field is larger than the external field by the factor of 1.5, we get

$$W_1 = \frac{1}{3}M_E \Delta H \approx 2.5 \cdot 10^{20} \Delta H \gamma, \quad (6)$$

where  $\Delta H$  is the observed increase.

Energy of  $2 \times 10^{22}$  erg corresponds to a storm with a gain of  $70\gamma$ .

In the main phase of the storm, the energy of the stream is consumed for the generation of magnetic energy of the current system, and for an increase of the kinetic energy of the captured particles. The energy of a current system, as indicated before, amounts to the self-induction energy of a system, for which an estimate has already been made [1, 2]:

$$W_1^{(1)} \approx \frac{1}{4} r_R^2 (\Delta H_e)^2, \quad (7)$$

where  $r_R$  is the radius of the current ring and  $\Delta H_e$  is the magnitude of field decrease during the main phase of the storm.

In [2], the increment of the kinetic energy was computed; it was pointed out that the field of a current which is static equilibrium with the captured plasma, i.e., satisfying condition

$$\frac{1}{c} [\vec{j} \times \vec{H}] = -\text{grad } p, \quad (8)$$

creates a field that is proportional to the total energy of the particles. If the current is in a dipole field with moment  $M$ , then the disturbance  $\Delta H_2$ , created by it, relates to the total energy of the particles as

$$W_1^{(2)} = \frac{1}{2} M \Delta H_2, \quad (9)$$

provided that the pressure included in (8) is isotropic. The presence of anisotropy can be taken into account by the introduction of a correction factor; for experimentally obtained distributions [3], its magnitude will not differ greatly from unity.

The requirement that the energy density of the captured particles be less than the energy density of the main magnetic field of the Earth imposes restrictions upon possible values of radius  $r_R$  [4]. In view of this restriction,  $W_2^{(1)}$  is always smaller than  $W_2^{(2)}$ , and the latter can be used as the estimated energy of the main phase. Interpreting  $\Delta H_2$  as the observed field, we rewrite (9) similarly to (6)

$$W_2 = \frac{1}{3} M_E \Delta H_2 \approx 2.5 \cdot 10^{20} \Delta H_2 r. \quad (10)$$

Thus, we find that an energy of  $4 \times 10^{22}$  erg corresponds to a storm with an observed drop of the field of  $150\gamma$  during the main phase.

Apart from the absolute magnitude of the energy of a magnetic storm, the rate of its variation is also of distinct interest because it is this magnitude which is determined directly by the parameters of the solar corpuscular stream and by the effectiveness of the mechanism involving the energy transfer from the stream to the magnetosphere.

As far as the first phase of a magnetic storm is concerned, it follows from the above calculations that

$$p_1 = \frac{W_1}{\Delta t} = \frac{2,5 \cdot 10^{22}}{100} = 2,5 \cdot 10^{20} \text{ erg/sec,}$$

where  $\Delta t = 100$  sec is the duration of the growth of the field during sudden commencement of the storm.

/82

The magnitude thus obtained coincides with the findings reported in [5] indicating that the growth rate of magnetic energy during the initial phase of the storm is rather high. In terms of order of magnitude, it is comparable to the total energy flux carried by the corpuscular stream to the boundary of the magnetosphere ( $p_{\text{flux}} = 5 \times 10^{20} - 10^{21}$  erg/sec, according to [6]). The latter indicates that the effectiveness of the mechanism which converts the kinetic energy of the translational motion of the corpuscular stream into magnetic energy must be rather high. This is in full agreement with the generally accepted model of the initial phase of the storm.

The estimation of the rate of energy input into the magnetosphere of the Earth during the main phase of the storm is somewhat more complex, because this phase is associated with the formation of electrical currents in radiation belts, where different dissipative processes can take place. The decay of the ring current and the dissipation of the accumulated energy during storms of moderate intensity take place relatively slowly, i.e., over several days. During intense storms, on account of the aforementioned approach of the current to the

Earth, the decay takes place faster, and the field, as a rule, grows within five to ten hours. The activity during the storm changes rather rapidly as is evidenced from the graphs of  $A_p$  for some storms, cited in [7]. If we assume that rapid variations of  $A_p$  correspond to equally rapid variations of the energy flux, then the course of the flux during the storm can be approximated by a rectangular impulse, included at the beginning of the field drop and eliminated upon reaching the minimum. The dissipation time can thus be estimated from the field reduction pattern. Based on the regeneration of the field, one can estimate the dissipation time. Using the field diagram cited in [8] for the storm of 13 September 1957, the curve can be defined as  $\exp(-t/\tau)$ , where  $\tau = 10$  hours. The rate of energy loss for a storm with a decrease of 150 $\gamma$  will be

$$\frac{dW_3}{dt} \sim \frac{W_3}{\tau} \sim 10^{18} \text{ erg/sec}$$

and will exponentially decrease with time. During the growth phase, provided it lasts the same ten hours, the rate of energy input must be twice as large, i.e., of the order of  $2 \times 10^{18}$  erg/sec; with shorter growth periods, it will have to be accordingly higher.

It is pointed out in [8] that, empirically, it is not feasible to isolate field variations caused by a change of the energy input from variations proper which are determined by the dissipation time. For this reason, one could justifiably assume the existence of small values of dissipation time. It is further pointed out that when a very small time  $\tau$  (for example, 0.5 hour) is assumed, this brings about a drastic increase in the estimates of the flux (by one order of magnitude). While this is correct, however, empirical findings and examples cited in [8] do not justify the assumptions of small  $\tau$ . The assumption that the regeneration rate of H is determined by the process itself leads, as was pointed out, to an estimate of  $\tau = 10$  hours, and to estimates of the dissipation rate as cited above.

In [1], a value of  $W_3 = 10^9$  erg was derived for the energy of a polar magnetic disturbance. This is considerably lower than  $W_1$  and  $W_2$ , and for

this reason, polar disturbance was excluded from further analysis. However, a polar disturbance associated with a current in the ionosphere causes high energy losses.

The current density in the zone is of the order of 1000 amp/km. This current is generated by the electric field in the meridional direction; its magnitude can be estimated from the velocity of motion of heterogeneities in aurora, registered by radar and optical methods. If these movements are determined by the electric drift, then  $E = vH/c$ . Observed velocities of 0.5 - 1 km/sec [9] correspond to fields of the order of 25 - 50 watt/km. These values of the field and of the current are in agreement with the total Hall conductivity [10] obtained by direct calculation.

/83

Hall's current is not accompanied by heat emission. However, the existence of conductivity and of Hall current is impossible without the simultaneous existence of Pedersen conductivity and current along the electric field. In the region where the frequency of electron collisions is low the relation between Pedersen and Hall conductivity is

$$\frac{\sigma_p}{\sigma_H} = \frac{\omega_i}{\nu_i} \quad (11)$$

where  $\omega_i$  is the gyrofrequency of ions. Auroral ionization, and the current stream created by it, occur within a relatively narrow height interval (100-120 km). Near the upper edge of this region is the boundary between regions of short and long ionic mean free paths. Inasmuch as the distance between the center of the current and this boundary does not exceed the height of the homogenous atmosphere, the ratio (11) apparently is smaller than two (a value of 1.5 was reported for this ratio in [10]). It follows that, simultaneously with the Hall current, there must exist a direct current with a strength that is smaller than that of the Hall current only by the factor of 1.5 - 2. The existence of a direct current leads to a release



of heat. The power lost per 1 km<sup>2</sup> can be estimated as

$$W' = \frac{\omega_i}{v_i} jE \sim 2,5 \cdot 10^4 \text{ watt/km}^2.$$

The area covered by the disturbance can be estimated by an arc 5,000 km long and 500 km wide [11]. The total energy loss in an arc of a polar aurora should amount to

$$\frac{dW_s}{dt} \sim 6 \cdot 10^{17} \text{ erg/sec.}$$

While energy losses must also exist beyond the boundaries of this arc, and the suggested mechanism is not unique, even though the most significant [12], this estimate may be increased to  $10^{18}$  erg/sec. It should be pointed out that the values used in the computation are not limiting values. Larger values of current density (corresponding to disturbances exceeding 600γ), as well as larger values of the electric field leading to high rates of drift, were observed. Studies [12, 13] cite movements with a velocity of 3 to 5 km/sec rather than the accepted velocity of 0.7 km/sec. Hence the aforementioned estimate may be increased by several orders of magnitude, and it may amount to several units of  $10^{18}$  erg/sec.

The dissipation rate of Joule heat in the ionosphere is close to the dissipation rate of energy in the magnetosphere. It should, however, be kept in mind that the currents responsible for the main phase of the storm flow in the region with  $L \sim 3$ , whereas auroral disturbances are associated with processes in the region  $L \sim 5 - 6$ . In both instances, the energy is derived from different magnetic shells; this suggests that the obtained coincidence of the estimates is a random occurrence. Apparently, a polar storm requires its own sources of energy in order to sustain itself.

The results of the analysis of the energy balance of a magnetic storm are summarized in the table which gives the total energy, the rate of arrival, and the energy dissipation rate at different stages of development.

Phase	W, erg	P, erg/sec	P, dissipation erg/sec
Initial	$2.5 \cdot 10^{22}$	$2.5 \cdot 10^{20}$	—
Main	$4 \cdot 10^{22}$	$2 \cdot 10^{18}$	$10^{18}$
Polar storm	$10^{19}$	—	$(1 - 5) 10^{18}$

# REFERENCES

1. Chapman, S. The energy of magnetic storms. Geophys. J. Roy. Astron. Soc., Vol. 8, No. 5, 1964, p. 514. /34
2. Bryunelli, B. Ye., and M. I. Pudovkin. Energiya geomagnitnoy buri (The Energy of a Geomagnetic Storm). Geomagnetizm i aeronomiya, Vol. 6, No. 6, 1966, p. 1083.
3. Fan, S. I., R. Meyer, and I. A. Simpson. The dynamics and the structure of the external radiation belt of the Earth. In: "Radiation Belts of the Earth". Moscow, IL, 1962.
4. Bryunelli, B. Ye. The field of currents in a radiation belt. Geomagnetizm i aeronomiya, Vol. 6, No. 6, 1966, p. 1076.
5. Chapman, S. and J. Bartels. Geomagnetism. Oxford, 1940.
6. Shabanskiy, V. P. The hydromagnetic and thermodynamic profile of a magnetic storm. Kosmicheskiye issledovaniya, Vol. 2, No. 4, 1964, p. 595.
7. Akasofu, S. I., and S. Chapman. Magnetic storms: the simultaneous development of the main phase (DR) and of polar magnetic substorm (DP). J. Geophys. Res., Vol. 68, No. 10, 1963, p. 3155.
8. Akasofu, S. I., and S. Yoshida. Growth and decay of the ring current and the polar electrojets. J. Geophys. Res., Vol. 71, No. 1, 1966, p. 231.
9. Boström, R. A model of the auroral electrojets. J. Geophys. Res., Vol. 69, No. 23, 1964, p. 4983.
10. Leadabrend, R. L., J. C. Schlobohm, and M. J. Baron. Simultaneous very high frequency and ultra-high frequency observations of the aurora at Fraserburgh, Scotland. J. Geophys. Res., Vol. 68, No. 6, 1963, p. 1667.
11. Akasofu, S. I. The dynamical morphology of the aurora polaris. J. Geophys. Res., Vol. 68, No. 6, 1963, p. 1667.
12. Bryunelli, B. Ye. The electric field of a polar magnetic disturbance. Geomagnetizm i aeronomiya, Vol. 3, No. 5, 1963, p. 929.
13. Harang, L. and J. Troim. Studies of auroral echoes. Planet. Space Sci. Vol. 5, No. 1, 1961, p. 33.
14. Unwin, R. S. Movement of auroral echoes and the magnetic disturbance current system. Nature, Vol. 183, No. 4667, 1959, p. 1044.

## QUIET SOLAR DAY VARIATIONS OF THE GEOMAGNETIC FIELD DURING THE IGY

### IV. VARIATIONS AT HIGH LATITUDES

A. N. Zaytsev, and Ya. I. Fel'dshteyn

**ABSTRACT.** The paper discusses the variations of the magnetic field at high latitudes on exceptionally magneto-quiet days of the winter season of the IGY. The form and the amplitude of variations indicate a close relation between  $S_q^0$  of high latitudes and  $S_q$  variations in middle and low latitudes (Figures 1 and 2). The magnitude and direction of the variation vector  $S_q^p + DP$  are calculated for five international magneto-quiet days of the summer season of the IGY for the observatories of the American and Europe - Asia longitude sectors (Figure 5a, b). The magnitude of the excluded component of the variation field  $S_q^0$  was determined in deviations from the midnight values of the field which physically is better proved than in the commonly applied methods when the deviations are determined by the average diurnal values.

Figure 7 presents the current system  $S_q^p$  for the five international magneto-quiet days of the IGY summer season in the northern hemisphere. The current lines are drawn through 10 thousand ampere. The  $S_q^p$  variation is caused by a vortex with the focus on  $\phi \sim 80^\circ$  and on the  $15^h$  meridian. The direction of the current is counterclockwise. The  $S_q^p$  system corresponds to the closed circulation of matter on the boundary of the magnetosphere around a neutral line. The statistical current system  $S_q^p$  is confirmed by the distribution of the variation field at separate hours of Universal Time (Figure 8).

Research conducted in recent years has shown that even in exceptionally /85  
quiet periods when the daily sum of  $\Sigma K_p$  planetary indexes is only several  
units, there are observed on the polar cap disturbances of the Earth's magnetic  
field which have an irregular character in time [1 - 3]. The magnetic field at

latitudes  $65 - 67^\circ$  does not experience notable changes at that time. The complexity of completely isolating disturbances in circumpolar regions and the sparseness of data have prevented an accurate determination of the morphology of phenomena or an explanation of their connection with the well-researched  $S_D$  and  $S_q$  fields. Moreover, according to the method accepted in the literature for studying disturbed fields, disturbances in circumpolar regions are included in  $S_D$  if  $S_D$  is calculated as the deviations of the field on disturbed days from its magnitudes on quiet days.

Data from IPY II (conducted during the minimum of the solar activity cycle) were analyzed in [4] to determine if  $S_q$  exists at high latitudes. The analysis showed that the principal part of the variation field at high-latitude stations on days when  $\Sigma K_p \leq 2$  is a simple continuation of the  $S_q$  field from low and middle latitudes ( $S_q^0$ ). Irregular disturbances decreased in amplitude with the decrease of  $\Sigma K_p$ , and on exceptionally quiet days their contribution to the variation field was small.

Observations at high latitudes during the IGY made it possible to distinguish a supplementary component  $S_q^P$  from the variation fields at high latitudes on international magneto-quiet days [5,6]. The quantity  $S_q^P$  is clearly observed on the magnetograms of individual observatories during the summer in daylight hours (even on extremely magneto-quiet days). As five international magneto-quiet days a month during the maximum solar activity cycle are not free from bay disturbances  $DP$ , which are most intensive in the early morning hours at  $65 - 67^\circ$  latitudes, changes of the magnetic field at high latitudes for five magneto-quiet days can be given in the form

$$S = S_q^0 + S_q^P + DP. \quad (1)$$

Detailed research of  $S_q^P$  was completed using data from thirteen high-latitude observatories in the northern hemisphere and seven in the southern [6]. The daily mean value for five international quiet days for each season individually was taken as a standard of magnitude readings for the variation field. Equivalent current systems for summer and winter, which are responsible /86

for the observed space-time distribution of the variation field, are cited in [6]. The current systems in the northern and southern polar caps are completely alike. The exclusion of  $S_q^0$  was accomplished by graphic deduction from the total current system of part of the field, due to the flow of  $S_q$  currents from middle latitudes to high latitudes.

The  $S_q^0$  field was calculated for five magneto-quiet days by calculating the daily mean value of the field for stations with geographical latitudes from 55°N to 55°S and extrapolating it to high latitudes on the basis of data from a spherical analysis of  $S_q$ . In [7, 8] it was mentioned that the amplitude and form of  $S_q$ -variations at middle and low latitudes during the IGY are not determined simply by geographical latitude. Therefore, extrapolation to high latitudes on the basis of spherical analysis data, which was conducted with the variables "geographical latitude-local time," is hardly valid. The DP field was not eliminated, as it was assumed that it is small on magneto-quiet days.

The resulting  $S_q^P$  current system [6] for local summer is characterized by two vortexes, similar and of approximately equal intensity, with no condensation of current lines, which are symmetrical relative to the pole and limited by a circle of latitude 65°. The circumpolar region within the limits of  $\phi \geq 80^\circ$  is covered by a uniform current layer with an overall intensity of 150,000 amps, flowing from the nighttime side of the Earth to the daytime, parallel to the 23- and 11-hour meridians. Foci of both vortexes are at  $\phi \sim 78^\circ$  on the 6- and 18-hour meridians. The current system during local winter is similar to summer, but its intensity is three times less. Having compared the current system obtained by a statistical method and the specific disturbance of 12<sup>h</sup> UT, 24 May 1958 [9], we see an agreement between the average current system by field distribution in an individual case. However, current directions on the polar cap are somewhat varied. A physical interpretation of these results is given in a diagram of magnetospheric circulation [10].

The characteristics of geomagnetic variations for five international quiet days during the IGY were also studied in [11] in terms of the deviations

from daily mean values. To explain the differences between  $S_q$  variations in winter and summer, it is assumed that some kind of supplementary mechanism causes systematic changes in the Earth's magnetic field in polar regions, in addition to the continuous mechanism. This supplementary mechanism generates a zonal current system which becomes stronger during the daylight hours in circumpolar regions [12], and which flows from west to east. When the intensity and location of current vortexes is similar [6, 9, 11], the current system [11] for summer is significantly different from [6, 9]:\* vortexes on the periphery are characterized by a condensing of current lines at  $64 - 68^\circ$  latitudes in the post-midnight hours and at  $69 - 73^\circ$  in the post-noon hours. Evidently this is caused by a more complete utilization of observational materials (sixteen observatories compared with seven in [6]), and by the possibility of more detailed calculation of DP disturbances. These attain greatest intensity at  $\phi \sim 64 - 68^\circ$  in post-midnight hours and undoubtedly appear in the five international quiet days. Thus, the assumption about the lack of DP during the international magneto-quiet days, which lies at the basis of the isolation of the  $S_q^P$  field in [5 - 6], is not corroborated.

During research of  $S_D$ -variations at high latitudes during the IGY [13, 14], it becomes evident that the field distribution observed in local summer cannot be explained by a current system connected only by electrojet streams. On the polar cap in the summer there is a supplementary disturbance field where  $S_q^P$  could have a somewhat different intensity compared with the  $S_q^P$  of quiet days. This stimulated the investigation of magnetic field variations at high latitudes and on magneto-quiet days. Besides this, their characteristics on very quiet days in the circumpolar region are of general interest, as  $S_q^P$ -variations can theoretically be used to study the circulation of matter in remote parts of the magnetosphere. The determination of the variation field from the daily mean values is physically not sufficiently valid [7, 15]. Therefore, it is possible that the  $S_q^P$  current system changes essentially, if the reading is taken from nighttime levels [7, 15, 16] and not as is done in [5, 6, 11]. Besides, field variations of the DP type were not excluded in

/87

---

\*Translator's note: There is an apparent omission in Russian text.

[5, 6]. Therefore, the  $S_q^P$  current system obtained in these works is, in fact, the sum of  $S_q^P + DP$ .

A direct survey of magnetograms on exceptionally quiet days of summer on the polar cap showed that changes of the field can be divided into two types, according to their nature: smooth  $S_q^0$  variations with a period of solar days [4], which is no doubt a continuation at high latitudes of the middle- and low-latitude part of the  $S_q$  current system, and quite irregular  $S_q^P$  changes which reach a maximum amplitude in the hours around noon. Moreover, even in such exceptionally magneto-quiet days brief bay-type disturbances are observed which are connected with the oval current zone (polar electro-current) and the maximum intensity at early morning hours.

In winter, as is seen from the magnetograms, on quiet days  $S_q^P$  does not contribute greatly to the change of the magnetic field, as it depends essentially on the season. Therefore, choosing exceptionally quiet days in the winter months, it can be assumed that changes of the field after the elimination of brief bay disturbances will be basically determined by  $S_q^0$ , which is a continuation of the middle and low latitude  $S_q$  current system at high latitudes. Certain variations in X-, Y-, Z-components of the geomagnetic field must be observed at high latitudes; their amplitude must decrease as the pole is approached. This decrease is connected with the fact that in the winter in the circum-polar regions the ionosphere at the E-layer level has no illumination from solar rays all day long; and consequently, there are no variations which are caused by a change of illumination of the E-layer during a 24-hour period.

To isolate  $S_q^0$  at high latitudes, it is necessary to use exceptionally quiet periods to decrease the influence of brief disturbances as much as possible. During the IGY, magnetic disturbances at high latitudes were almost continuously observed, and such quiet intervals were an infrequent occurrence. During the period November 1957 - February 1958 and November - December 1958, the days of November 30 and December 1, 1958, were an exceptionally magneto-quiet interval. Their daily sum of  $K_p$ -indexes was  $3_+$  and  $4_+$ .



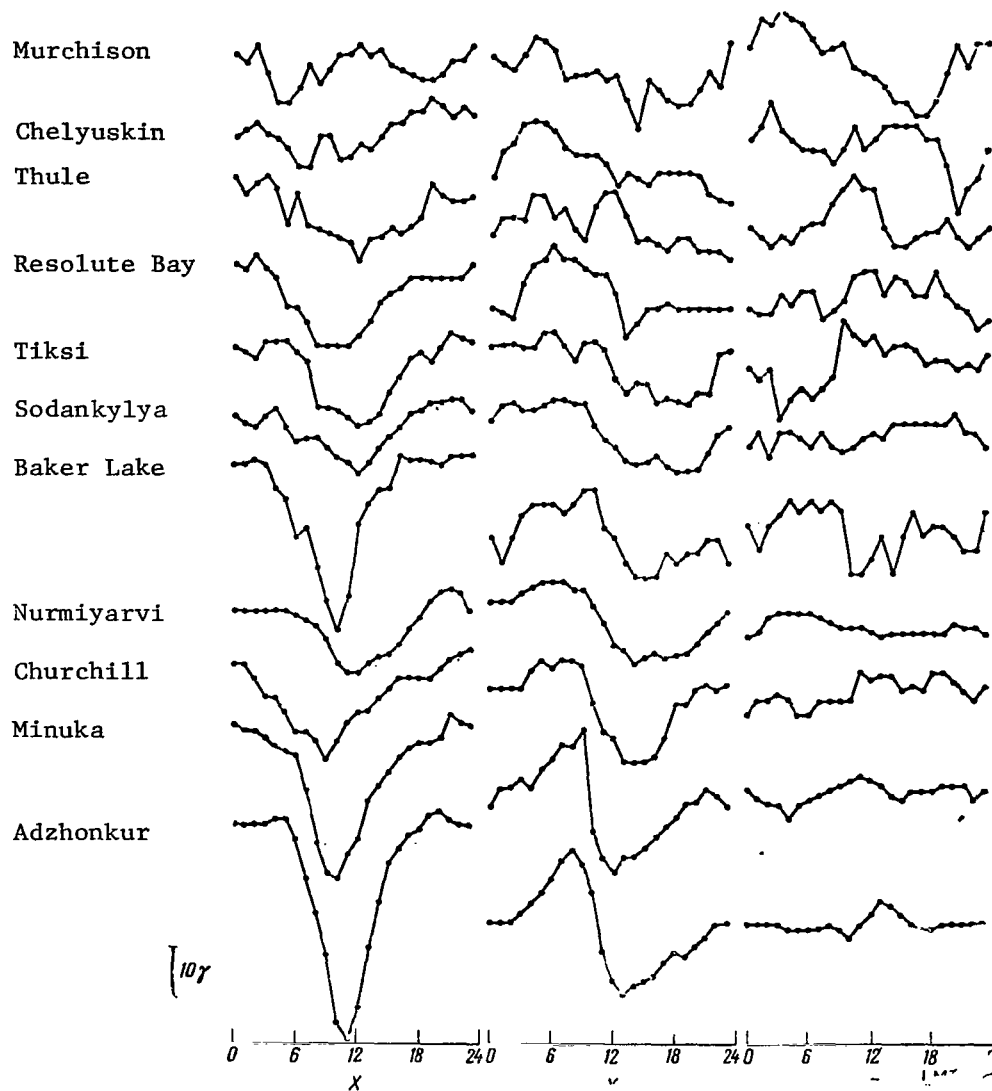


Figure 1. Variations in local time of the X-, Y-, Z- components of the geomagnetic field at high altitude stations for the period November 30 - December 1, 1958. Stations are arranged in decreasing order of geographical latitude.

In Figure 1 the daily changes (according to local time) of X-, Y-, and Z-components of the variation field are shown for these two days. Brief disturbances observed at individual stations are excluded. The scale, which

is the same for all three elements, is given in the lower left hand corner. The stations are arranged in decreasing order of geographical latitude. At  $\phi \sim 80^\circ$ , regular changes of the magnetic field of the  $S_q$  middle-latitude type in X- and Y-components are absent, and the magnitude of the variations is small. At  $\phi \sim 70 - 73^\circ$ , P-type variations are observed in X- and Y-components, these variations are typical for middle-latitude stations located near the pole from the focal point of the  $S_q$ -current system. Maximum deviations of  $X$  from night-time values are observed in the hours around noon. In the pre-noon hours the northern component increases, and it decreases in the post-noon hours. Thus, the /88 character of magnetic field variations in exceptionally quiet intervals at high latitudes to  $\phi \sim 73^\circ$  is analogous to the middle latitude ones. Nearer to the pole, systematic variations of the middle latitude  $S_q$  type are practically non-existent.

It should be stressed that a change of the variation form (appearance of characteristic middle latitude type and the absence of systematic variations in the circumpolar region) is controlled more by geographical latitude than by geomagnetic latitude or inclination. This is revealed clearly when data from eastern and western hemisphere stations are compared, for which there is a maximum difference between geomagnetic and geographical latitudes is maximum. The Murchison-Baker Lake and Cape Chelyuskin-Churchill stations are located at approximately the same geomagnetic latitudes, but their geographical coordinates differ by  $\sim 15 - 19^\circ$ . At Baker Lake and Churchill, located at lower geographical latitudes, quiet solar day variations are observed just as they are at middle latitudes. systematic variations are absent at the Murchison and Cape Chelyuskin station. 9

The close connection between the field variations at high latitudes on November 30 - December 1, 1958, and the  $S_q$  variations at middle and low latitudes also results from the wide distribution of  $\Delta T_{hor}$  -- maximum value of the variation vector in a horizontal plane, shown in Figure 2. Data for low and middle latitude stations are taken from [16] and pertain to the winter of 1957 - 1958. As is seen, the amplitude of  $\Delta T_{hor}$  decreases monotonically from low latitudes to high latitudes, and dispersion at high latitudes due to inclination.

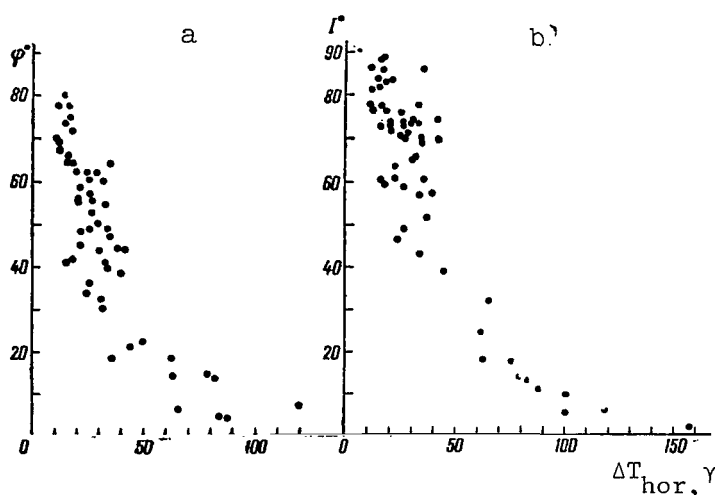


Figure 2. Distribution of the variation vector amplitude in a horizontal plane for winter 1957 - 1958 at middle and low latitudes of the northern hemisphere and for November 30 - December 1, 1958, at high latitudes, geographic latitude (a) and direction (b).

Analyzing the change of the field in exceptionally quiet periods makes it possible to determine the existence of  $S_q^0$ -variation at high latitudes, which is due to the extension of the middle and low latitude  $S_q$  current system at high latitudes. Therefore, the reasons for the necessity of an  $S_q$ -variation field determination from values obtained in the hours around midnight, which are physically more valid, naturally, extend also to the high latitudes. Moreover, this analysis showed a lack of type  $S_q^p$  variations in the circumpolar region in winter, by more than  $10\gamma$ .

It is impossible to isolate the summer  $S_q^0$  variation by using the method utilized for winter. In fact, the quietest intervals in the summer of 1958 were May 23 and May 24 when the daily sum of  $K_p$  was  $8_0$  and  $4_+$ , respectively. A survey of magnetograms from high latitude observatories for these days showed /90 that in summer as well as in winter there are smooth changes of the  $S_q^0$  field and  $S_q^p$  variations, appear mostly in daylight hours.

If  $S_q^0$  in summer is also an extension to high latitudes of the middle and low latitude  $S_q$  system, then the magnitude of  $S_q^0$  at high latitudes in summer can be determined from the ratio

$$S_{q\text{summer}}^0 = K S_{q\text{winter}}^0, \quad (2)$$

where  $K$  is the coefficient, allowing for a change of intensity in the  $S_q$  current system in the transition from winter to summer;  $S_{q \text{ win}}^0$  is the X-, Y-, Z-variations at high latitude stations in exceptionally quiet intervals in winter (see Figure 1).

The coefficient  $K$  is determined according to the change of intensity of the middle latitude current system. In [17, 8] it is shown that in the transition from winter to summer the intensity of the current system at middle latitudes increases 1.7 times, according to data from stations in the American longitudinal sector, and 2.6 times according to data from stations in Europe and Asia. These values were also taken for the value of  $K$  in (2).

$S_q^0$  variations both in winter and in summer were measured from values of the field in the hours around midnight in exceptionally magneto-quiet periods: November 30 - December 1 for the winter, and May 23-24 for summer. The  $S_q^P$  contribution to the variation of the field is minimal during these hours, but using the quietest intervals eliminated a possible contribution from the DP field. However, the midnight field magnitudes differ somewhat in winter and in summer. Changes in their level were analyzed for low and middle latitude stations in [18]. It was shown that the difference in the hours around midnight of the D- and Z-components does not change systematically with latitude, but in the H-component the field is greater in summer than in winter, and  $|\Delta H|$  decreases with a decrease of geographical latitude. In Figure 3,  $|\Delta H|$  according to middle and low latitude observatories from [18] are supplemented by high latitude stations.

The tendency recorded earlier toward a monotonic increase of  $|\Delta H|$  toward high latitudes is corroborated by supplementary data. The regular change of  $|\Delta H|$  connects it with changes of the solar illumination of the E-layer of the ionosphere. This is especially significant on the polar cap, as illumination in winter is absent for the whole day, but whereas in summer there is illumination all day long. Such an interpretation of the change in the level of the field in the hours around midnight attributes them to seasonal variations in the intensity of the  $S_q^0$  current system from winter to summer.

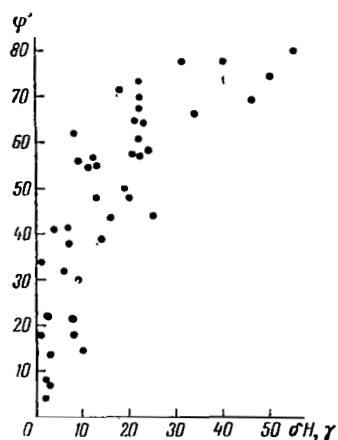


Figure 3. Variation with geographic latitude of the difference between the horizontal component in quiet periods at hours around midnight in summer and winter.

In Figure 4, vector diagrams of daily variations are shown in a horizontal plane for the Thule, Resolute Bay, Godhavn, Churchill, and College stations for five international quiet days during the period of May-August, 1958.  $S_q^0$  variations calculated for the summer by the above-mentioned method are excluded. The letter N indicates the direction toward the point at which the line of force comes from infinity [19, 20]. At the circumpolar stations of Thule and Resolute Bay, the variation vector rotates clockwise, and its magnitude exceeds 100  $\gamma$  at individual times. In the Godhavn observatory, its magnitude /91 is somewhat less but rotation changes during the day. From 22 to 11<sup>h</sup> UT it is clockwise; the remainder of the day, it is

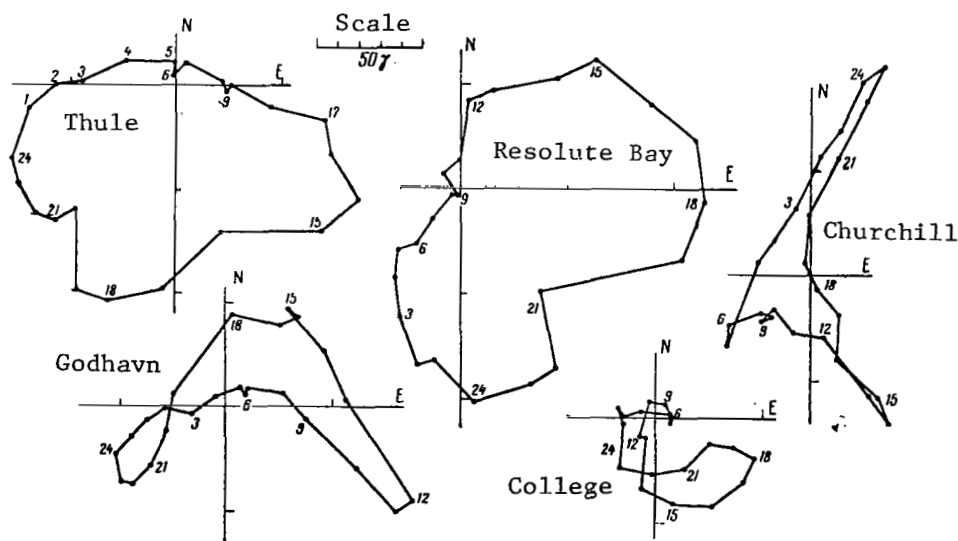


Figure 4. Vector diagrams of daily variations in a horizontal plane at observatories at Thule, Resolute Bay, Godhavn, Churchill and College. UT time.

counterclockwise. Variations of X- and Y-components are approximately the same at all three observatories. Changes of the field at the Churchill station are due to a basic variation of X-components which are greatest in the evening and are directed toward the pole at these hours. The direction of vector rotation is primarily counterclockwise. At the College station, located at latitude  $64.9^\circ$ , variations of the X- and Y-components of the field are insignificant. In the morning hours, primarily negative changes of the X-components are observed.

Such vector diagrams were calculated for seventeen high latitude stations in the northern hemisphere. Differing only in details from those presented in Figure 4, they basically remain the same, particularly regarding changes in form and intensity of variations with latitude. It can be concluded from an analysis of data from all seventeen observatories that  $\Delta T_{\text{hor}}$  for five international quiet days is most intense in circumpolar regions, and decreases with increasing distance from the pole. It must be noted that the values of  $\Delta T_{\text{hot}}$  calculated according to formula (1) represent the sum of  $S_q^P$  and the DP fields.

In plotting the space-time distribution of the variation vector components in horizontal and vertical planes in polar coordinates (corrected geomagnetic latitude -- time of the eccentric dipole) using observational materials from all stations, some difference between variations was revealed in observations from American and Eurasian longitudinal sectors. This difference consisted of a shift of approximately 2 "hours" in the variation phase of post-noon hours at  $\phi \sim 70^\circ$  and a different variation vector in the morning hours at  $\phi \sim 65^\circ$ . Therefore, the space-time distribution of the variation vector was studied separately for each sector, but the circumpolar station at Thule was included in both sectors.

The distribution of vectors for the American sector is given in Figure 5a, /92 and for the Eurasian sector in Figure 5b. The direction of the variation vector in the horizontal plane is shown by arrows. The length of the arrow corresponds to the magnitude of  $\Delta T_{\text{hor}}$ , without separating the field of external

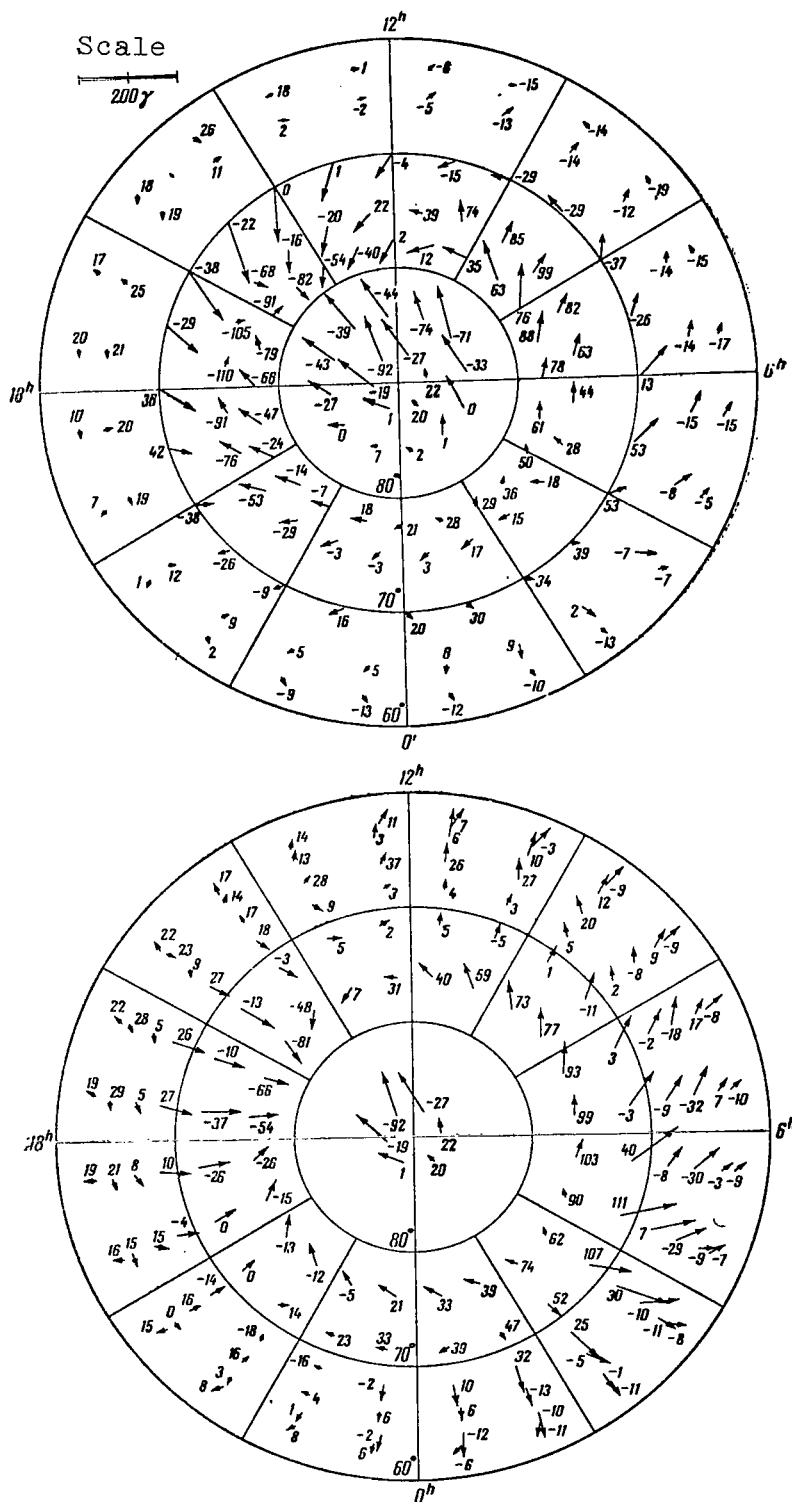


Figure 5. Space-time distribution of vector variation  $S_H^D + DP$  for five international magneto-quiet days of summer of IGY.

(a) American sector (observatories at Thule, Resolute Bay, Godhavn, Baker Lake, Churchill, College, Minuka);

(b) Eurasian sector (observatories at Thule, Murchison, Cape Chelyuskin, Dixon, Tiksi Bay, Sodankylä, Welland).

The arrows characterize magnitude and direction of the  $\Delta T_{hor}$  vector. Figures at the base give magnitude of  $\Delta Z$ . System of coordinates — corrected geomagnetic latitude and corrected geomagnetic time according to [19,20]. Scale is given in the upper left hand corner.

and internal sources. The numbers at the base of the arrow give the value of  $\Delta Z$  at the corresponding hour of local geomagnetic time, taking account of the sign for the vertical component change. Negative values correspond to the  $\Delta Z$  vector, directed toward the zenith. The direction and value of  $\Delta T_{\text{hor}}$  and  $\Delta Z$  indicate the presence of an intense closed current (in terms of ionospheric current systems) at latitudes  $70 - 90^\circ$  in daytime post-noon hours, and of a current with a westerly direction along the oval zone of the aurora polaris, which is most intense in the post-midnight hours at  $\phi \sim 65^\circ$ .

The existence of  $\Delta T_{\text{hor}}$  directed toward the equator in the morning hours at  $\phi \sim 65^\circ$  indicates the presence of DP-disturbances in field variations during the five international quiet days. The most important characteristic of these disturbances is the westerly-directed electrocurrent at all longitudes within the oval zone of the aurora polaris [13, 14, 21]. The difference of  $\Delta T_{\text{hor}}$  in the two longitudinal sectors in the post-midnight hours at  $\phi \sim 65^\circ$  is evidently caused by a different level of planetary magnetic disturbance when the observ- /93 atories in the American and Eurasian longitudinal sectors reach the post-midnight side of the Earth. In fact, calculations have shown that the sum of  $a_p$ -indexes for twenty international magneto-quiet days during the summer at  $21 - 24^{\text{h}}$  UT is 134, but at  $6 - 9^{\text{h}}$  it is 85. The approximate method described in [22] was used to calculate the intensity of the current system which is responsible for the observed distribution of the variation field on the surface of the Earth. In visual form, this current system gives a generalized schematic representation of the value and direction of the variation vector.

The exterior source current system for the American longitudinal sector for quiet days in summer is given in Figure 6. The current system consists of two vortexes on the night/morning and afternoon/evening sides of the Earth. The American longitudinal sector was selected because the DP field on quiet days during the IGY was considerably smaller at the American stations than at the Eurasian stations. Therefore, with the subsequent elimination of the DP part from the  $S_q^P + \text{DP}$  resulting current system, the error in the  $S_q^P$  current system will be smaller for the American sector than for the Eurasian. The current vortex which results from negative changes of  $\Delta T_{\text{hor}}$  at latitudes  $65^\circ$



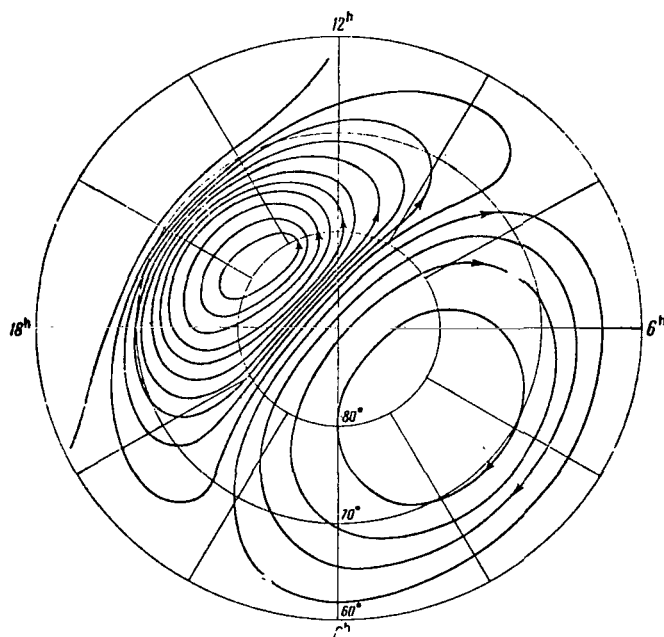


Figure 6. Current system, giving a schematic representation of the magnitude and direction of variation vector  $S_q^P + DP$  on the Earth's surface on five international magneto-quiet days of the summer of the IGY for the American longitudinal sector.

The current lines are drawn through 10,000A. Arrows indicate current direction. The portion of currents indicated in the Earth is taken into account.

corresponding with optically observed aurora, showed that the oval zone of the aurora actually is the same in summer as in winter [23, 24] and its position experiences analogous daily variations.

The  $S_q^P$  current system is represented in Figure 7. The  $S_q^P$  system, according to our data, is essentially different from the one obtained in [5, 6], and in no event can it be explained by the system of convective movements in the magnetosphere proposed by V. I. Oxford and K. O. Heinz. The system of

in the morning hours is a consequence of the small intensity of the DP-disturbances. These occurred during the IGY even on international magneto-quiet days. The current vortex in circumpolar regions is strictly an  $S_q^P$ -variation of the magnetic field, which reaches considerable intensity even on quiet days in summer. The condensation of the current lines in Figure 6 corresponds to the greatest values of  $\Delta T_{hor}$  and to the sign change of  $\Delta Z$ . Due to  $S_q^P$ -variations, the focal point of the current vortex is located at  $\phi \sim 80^\circ$  on the 15-hour meridian for the American longitudinal sector and on the 17-hour meridian for the Eurasian longitudinal sector.

Assuming that the electrocurrent of the DP current system is located along the oval zone of the aurora polaris in both summer and winter, the current system was separated into parts (Figure 6) which correspond to  $S_q^P$  and DP. Radar observations of reflections from regions of unusual ionization,

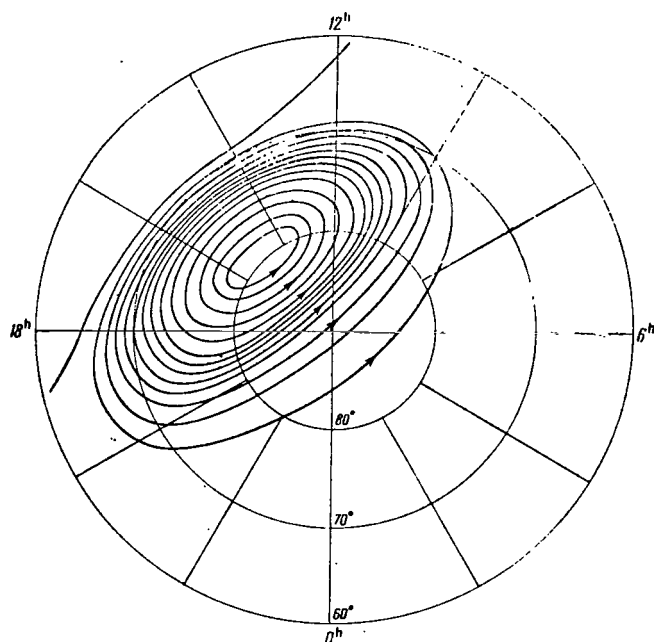


Figure 7. Current system  $S_q^D$  for five international magnetoquiet days of the summer during the IGY. Current lines pass through 10,000 A. Arrows show the direction of the current.

Rather it is formed by a hypothetical zonal system of currents. According to Figure 7, by comparing the vector distribution [11] of the  $S_q^P$  current system, it is possible to detect a remote analogy between them, despite a cardinal difference. Considering the results of [11, 12], it can be assumed that the geomagnetic effect of a solar chromosphere flare at high latitudes consists of a brief intensification of  $S_q^P$  (in the same way as occurs from  $S_q$  at middle latitudes). However, the zonal current system according to [11] differs from that presented in Figure 7, both in direction and in location of the currents.

The average  $S_q^P$  current system (see Figure 7) is verified also by the distribution of the variation field at individual hours of exceptionally

currents corresponds more to a closed circulation, analogous to the movement of matter on the edge of the magnetosphere around a neutral point [25]. The location of the neutral point at  $\phi \sim 80^\circ$  is explained by the corresponding relationship of static and dynamic pressure in the solar plasma [26].

/95

The study [11] gives the field vector distribution at high latitudes of the southern hemisphere at 1<sup>h</sup>6<sup>m</sup> UT on the magneto-quiet day December 12, 1958, during a chromosphere flare. It is noted that the variation distribution of the magnetic field at the moment is connected neither with the middle latitude nor with the high latitude well-known current systems which are responsible for  $S_q$ -variations.

magneto-quiet days. The distribution of  $\Delta T_{\text{hor}}$  and  $\Delta Z$  for May 24, 1958, at 11 - 12<sup>h</sup> UT is presented in Figure 8, according to data from seventeen magnetic observatories. At all stations, with the exception of the Churchill observatory during these hours, field variations are determined by typical brief bay disturbances. From the data cited, it follows that the direction and magnitude of  $\Delta T_{\text{hor}}$  and  $\Delta Z$  can be explained by the existence of one current vortex in the circumpolar region on the post-noon/evening side of the Earth.

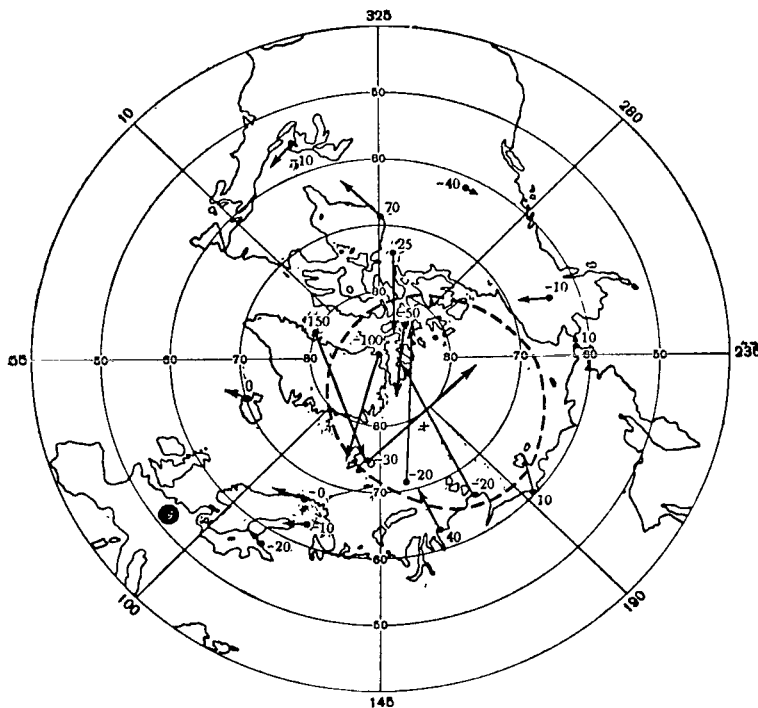


Figure 8. Distribution of variation vector of  $\Delta T_{\text{hor}}$  and  $\Delta Z$  for May 24, 1958, at 11 - 12<sup>h</sup> UT. The direction toward the Sun is marked by the black circle. The dotted line shows the approximate location of maximum intensity of currents responsible for the observed field distribution. Arrows and figures at their bases denote the same as in Figure 5.

In its general features, it corresponds with the  $S_q^0$  current system represented in Figure 7. It can be concluded from a survey of magnetograms from high latitude observatories for May 23 - 24, 1958, that the  $S_q^P$ -field experiences appreciable irregular variations in intensity from hour to hour and from day to day. The variability of  $S_q^P$ , both in form and in intensity, shows a possible connection with solar wind and with the direct entry of wind particles in the circumpolar region in the vicinity of the neutral line. /96

## REFERENCES

1. Mayaud, P. N. Activity of magnetism in polar regions. Scientific results. Terrestrial magnetism Antarctic expeditions Adelie Coast 1951-1952. Section II, Paris, 1955. /97
2. Bobrov, M. S. General planetary map of geomagnetic disturbances of corpuscular origin. In: "Solnechnyye korpuskulyarnyye potoki, lokalizatsiya ikh istochnikov i svyaz' s geomagnitnymi vozmushcheniyami" (Solar corpuscular fluxes, localization of their sources and connection with geomagnetic disturbances), No. 1, series "Resultati MGG" (Results of IGY), Moscow, USSR Academy of Sciences Press, 1961, p. 36.
3. Fukushima, N. Morphology of magnetic storms. J. Phys. Soc., Japan, Vol. 17, Suppl. A-1, 1962, p. 70.
4. Nagata, T. and H. Mizuno. Sq-field in the polar region on absorption quiet days. J. Geomagn. and Geoelectr., Vol. 7, No. 3, 1955, p. 69.
5. Nagata, T. Polar geomagnetic daily variation on quiet days. Proc. Benedum Earth Magn. Sympos., 1962, p. 31.
6. Nagata, T. and S. Kokubun. An additional geomagnetic daily variation field ( $S_q^P$ -field) in the polar region on geomagnetically quiet day. Rept Ionosphere Space Res. Japan, Vol. 16, No. 2, 1962, p. 256.
7. Price, A. T., and G. A. Wilkins. New methods for the analysis of geomagnetic fields and their application to the Sq-fields of 1932, 1933. Philos. Trans. Roy. Soc., Vol. 256, No. 1066, 1963, p. 31.
8. Fatkulín, M. N. and Y. I. Fel'dshteyn. Basic characteristics of planetary distribution of S -variations at middle and low latitudes. Geomagnetizm i aeronomiya, Vol. 5, No. 5, 1965, p. 858.
9. Kokubun, S. Dynamic behavior and North-South conjugacy of geomagnetic bays. Rept. Ionosphere Space Res. Japan, Vol. 19, No. 2, 1965, p. 177.
10. Axford, W. I., and C. O. Hines. A unifying theory of high latitude geophysical phenomena and geomagnetic storms. Canad. J. Phys., Vol. 39, No. 10, 1961, p. 1433.
11. Mansurov, S. M. and L. G. Mansurova. Some characteristics of geomagnetic variations in polar regions. Geomagnetizm i aeronomiya, Vol. 5, No. 4, 1965, p. 740.
12. Mansurova, L. G. and S. M. Mansurov. Some results of the investigation of the Antarctic variable geomagnetic field. XIII General Assembly IUGG in Berkeley, California, 1963.
13. Fel'dshteyn, Ya. I. and A. N. Zaytsev. Disturbances of solar day variations at high latitudes during the IGY. Geomagnetizm i aeronomiya, Vol. 5, No. 3, 1965, p. 477.

14. Fel'dsteyn, Ya. I. and A. N. Zaytsev. Current system of  $S_D$ -variations at high latitudes for the winter of the IGY. *Geomagnetizm i aeronomiya* Vol. 5, No. 6, 1965, p. 1123.
15. Fatkulin, M. N. and Ya. I. Fel'dshteyn. The relationship of  $S_q$ -variations with parameters of the ionosphere (preliminary report). *Geomagnetizm i aeronomiya*. Vol. 4, No. 4, 1964, p. 802.
16. Fatkulin, M. N., and Ya. I. Fel'dshteyn. The relationship of  $S_q$ -variations with parameters of the ionosphere. *Geomagnetizm i aeronomiya*. Vol. 5, No. 2, 1965, p. 312.
17. Price, A. T. and D. J. Stone. The quiet day magnetic variations during the IGY. *Ann. IGY*, Vol. 35, 1964, p. 65,
18. Fatkulin, M. N. and Ya. I. Fel'dshteyn. Acyclic variations on magneto-quiet days. Seasonal changes in field values in nighttime hours. *Geomagnetizm i aeronomiya*, Vol. 5, No. 4, 1965, p. 735.
19. Hultquist, B. The spherical harmonic development of the geomagnetic field epoch 1945, transformed into rectangular geomagnetic coordinate system. *Arkiv geophys.*, Vol. 3, No. 4, 1958, p. 63.
20. Hakura, Y. Tables and maps of geomagnetic coordinates corrected by the higher order spherical harmonic terms. Rept. Ionosphere Space Res. Japan, Vol. 19, No. 2, 1965, p. 121.
21. Akasofu, S. I., S. Chapman, and Ch. I. Meng. The polar electrojet. /98  
*J. Atmos. and Terr. Phys.*, Vol. 27, No. 11-12, 1965, p. 1275.
22. Chapman, S. and J. Bartels. *Geomagnetism*, 1, 2, Oxford Univ. Press, 1940.
23. Bates, H. F. The determination of the diurnal variation of the auroral belt by radio means. *Sci. Rept. Geophys. Inst. Alaska*, 1965, UAG R-170.
24. Bates, H. F., A. E. Belon, G. J. Romick, and W. J. Stringer. Tracking the aurora by a multifrequency HF backscatter sounder. *Sci. Rept. Geophys. Inst. Alaska*, 1965, UAG R-169.
25. Pletnev, V. D., G. A. Skuridin, V. P. Shalimov, and I. N. Shvachunov. Dynamics of the geomagnetic trap and passage of the Earth's radiation belts. *Geomagnetizm i aeronomiya*. Vol. 5, No. 4, 1965, p. 626.
26. Slutz, R. J., and J. R. Winkelman. Shape of the magnetospheric boundary under solar wind pressure. *J. Geophys. Res.*, Vol. 69, No. 23, 1964, p. 4933.

## GEOMAGNETIC DISTURBANCES AT HIGH LATITUDES — JUNE 1965

I. A. Kuz'min, L. L. Lazumin, G. A. Loginov, M.I.  
Pudovkin, A. I. Charakhch'yan, T. N. Charakhch'yan

**ABSTRACT.** The paper presents results of the electron currents, precipitating into the lower ionosphere, which are registered by the decelerating x-ray emission with counters on balloons, and of their relations with geomagnetic disturbances and rheometric absorption. The paper discusses the spatial connection of the region of electron precipitation with the electric currents in the ionosphere and with the region of anomalous absorption. The paper shows two types of electron precipitation, associated with quiet and active forms of aurora.

Recently completed studies of geomagnetic disturbances in the auroral zone /99 have determined quite a close connection between polar aurora, absorption of cosmic radio noise, magnetic bay disturbances, micropulsation of the magnetic field, and penetration into the atmosphere of electron streams. These streams were recorded by Bremsstrahlung at sounding-balloon altitudes. We can assume that, at least for nighttime disturbances, electron streams cause ionization in the upper atmosphere. This, in turn, influences the transmission of radio waves, which is recorded by the absorption of cosmic radio noise on a rheometer. Ionization also creates the conditions which produce currents responsible for magnetic bay disturbances.

In a series of articles, a statistical analysis was conducted to show the connection between certain phenomena, for example, between magnetic bays and absorption [1 - 6], polar aurora and absorption [7 - 10], pulsation in the

magnetic field and in the polar aurora [11 - 12], etc. A smaller portion of the work studies individual specific disturbances from a group of different observations. Such study is especially important for its examination of large geomagnetic storms, which are usually excluded from statistical analysis because of their complexity [13].

In this article an attempt at such complex research has been made according to observations of the magnetic storm of June 15 - 18, 1965. This magnetic storm was one of the strongest of the whole IQSY period. This period was chosen because several successful radiosonde flights were conducted at that time at Apatity and Olyenya. Instruments were at a considerable altitude during substantial disturbances. Magnetograms from the Loparskaya station, data from rheometers operating at a frequency of 32 mc. in Apatity and Loparskaya, and records of micropulsations of Earth currents at the Lovozero station were used for the analysis. Observational data from various phases of the storm are cited in Figure 1-7 (universal time).

Sonde Observations. The magnetic storm began on June 15 about 11<sup>h</sup>. That day, in the evening, absorption appeared on the rheometers which had the form of four regular bays. There was increased amplitude and a recurrence period of about one hour. The radiosonde launched at Apatity at the beginning of absorption, was at a high altitude during the interval between the two bays of absorption and no excessive radiation was recorded. The next instrument was launched in five rubber coatings and hovered at an altitude of more than /101 30 km (for four hours). In Figure 1b, the time pattern of the number of discharges in a single Geiger counter and the atmospheric pressure during the flight are presented.

During the flight the neutron monitor at the Apatity station registered a considerable lowering of cosmic ray intensity (Forbush effect), connected with the beginning of the magnetic storm. If we assume that at 23<sup>h</sup> - 23<sup>h</sup>40<sup>m</sup>, when absorption was minimal on the rheometer, the radiosonde registered the intensity of galactic cosmic rays with no x-rays, then the intensity decrease /102

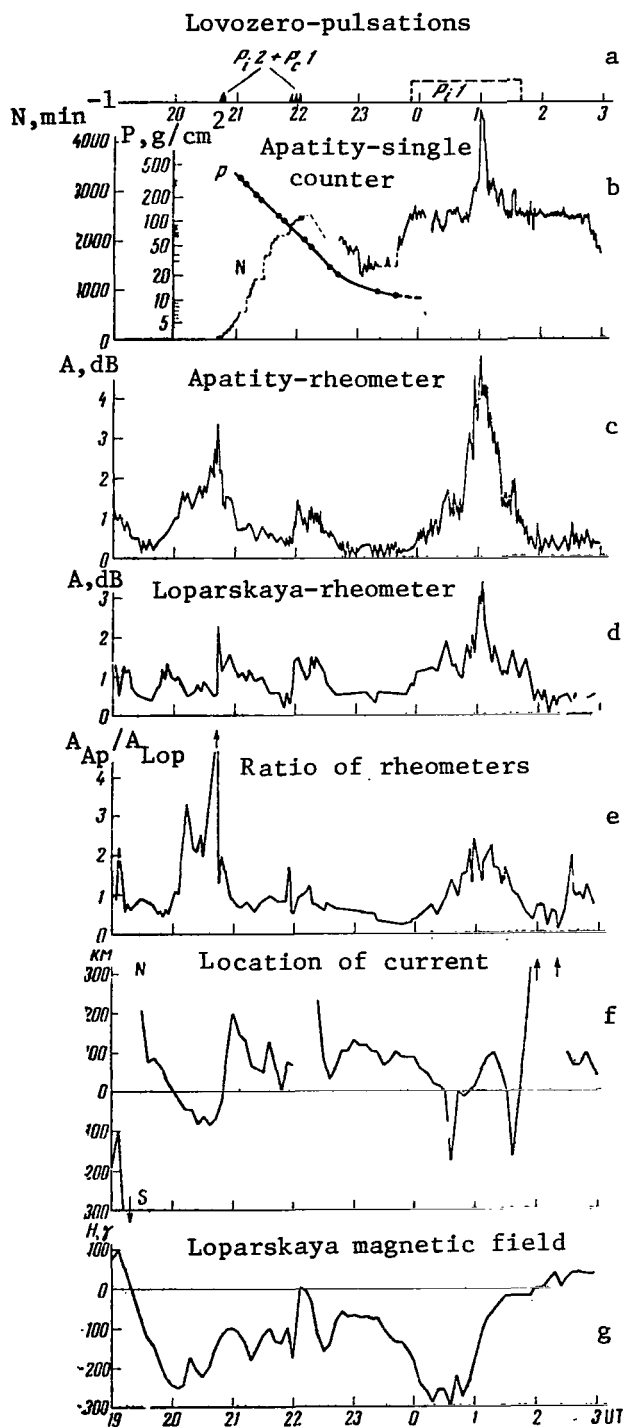


Figure 1. Geomagnetic disturbances the night of June 15 - 16, 1965. /100

- a. Micropulsations at the Lovozero Station; the black triangles indicate  $P_{12} + P_{11}$  bursts, the lines indicate  $P_{11}$ ; dotted line is used where the amplitude (M) cannot be measured in the tracing because of overlapping of notation;
- b. P is the atmospheric pressure in g/cm<sup>2</sup> and N is the number of discharges in an STS-6 counter per minute during the flight of the radiosonde at Apatity;
- c. Absorption of cosmic radio noise in decibels, measured by a rheometer at a frequency of 32 mc at Apatity;
- d. The same as above, at the Loparskaya Station;
- e. Ratio of absorption magnitudes at Apatity and Loparskaya;
- f. Location of the current causing magnetic disturbances; above the line — north of Loparskaya Station; below — south;
- g. The H-component of the magnetic field at the Loparskaya Station.



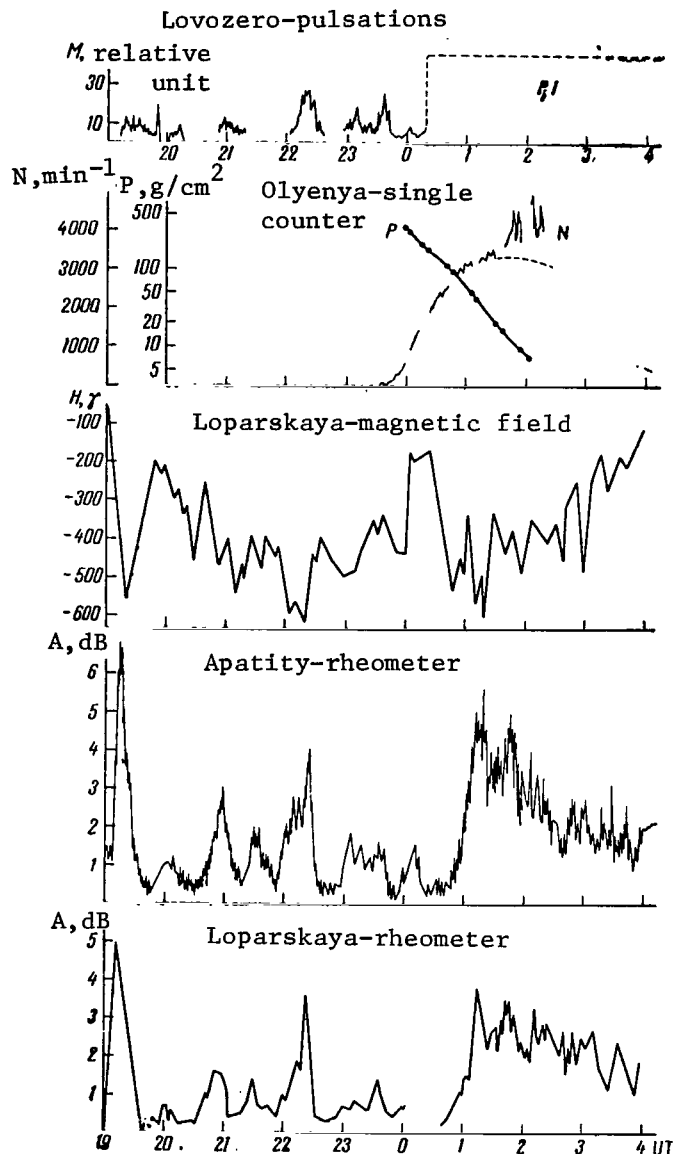


Figure 2. Geomagnetic disturbances the night of 16-17 June. In the diagram of the radiosonde flight, the normal rate of the counter at a given altitude is indicated by a dotted line. The remaining notation is the same as in Figure 1.

of the cosmic rays in the stratosphere was 40% in comparison with the normal background. It must be pointed out, however, that for technical reasons the possibility of such a sharp decrease cannot be completely eliminated. Even though the Forbush effect had a smaller amplitude, the abrupt jump in the recording at 21<sup>h</sup>23<sup>m</sup> at an altitude of 80 g/cm<sup>-2</sup> is connected with the appearance of a supplementary flow of photons. This is verified by the rapid increase of cosmic noise absorption beginning at the same time.

The next powerful burst of absorption was accompanied by x-rays at an altitude of 10.5 g/cm<sup>-2</sup> while the instrument was hovering. The peak of burst at 1<sup>h</sup>2<sup>m</sup> coincided on the rheometer and in the stratosphere within 1 - 2 minutes. The supplementary flux had a magnitude of 2 - 3 cm<sup>-2</sup>·sec<sup>-1</sup>. In converting the given photon flux into electron flux on the edge of the atmosphere, we obtained  $(1 - 1.5) \times 10^7$  cm<sup>-2</sup>·sec<sup>-1</sup>.

During the night of June 16 - 17 the flight over the Olyenya Station

again registered a photon flux during high absorption and a negative magnetic bay. The time pattern of this flight and charts of the rheometers, the

H-component of the magnetic field and micropulsations are noted in Figure 2. This flight is interesting because during the first maximum peak of absorption in the stratosphere, at an altitude of  $50 \pm 30 \text{ g/cm}^{-2}$  no x-rays were recorded. The instrument only began to register it at a level of  $18 \text{ g/cm}^{-2}$ . If it is assumed that during this period the electron flux spectrum did not change very drastically, the upper limits of photon energy can be determined (and, consequently, the electron generations).

In the next (morning) flight from Olyenya (Figure 3), x-ray radiation appeared at an altitude of  $8.5 \text{ g/cm}^{-2}$ , but at a level of  $20\text{--}12 \text{ g/cm}^{-2}$  it was not observed, although absorption on the rheometer at Apatity was more than 2 dB. Evidently, toward morning the electron flux spectrum became weaker. The time pattern of the x-ray radiation in this flight also correlates very well with the absorption pattern. The intensity decrease at  $9^{\text{h}}43^{\text{m}}$  agrees with the absorption decrease at Apatity with an accuracy allowed by the recording.

The time of the sonde flight matched the zero point of magnetic field variations at Loparskaya. Nevertheless, a noticeable negative peak is observed in the recording of the H-component of the magnetic field at the moment when the absorption bay begins. /103

Rheometer Observations. One characteristic of the June disturbances is a significant quantity of sharp bursts of absorption of a very large magnitude. Definite conclusions about the dynamics of incoming electron fluxes can be reached from studying these bursts.

In Figure 4, we see data from various recording instruments during the large negative bay (above  $500\gamma$  in the H-component) on the night of June 17 - 18: the time patterns of micropulsations, absorption of rheometers at Apatity and Loparskaya, the ratio of rheometer readings  $A_{\text{Ap}}/A_{\text{Lop}}$ , the location of fluxes responsible for magnetic disturbances north and south of Loparskaya, and finally, the H-component of the magnetic field at Loparskaya.

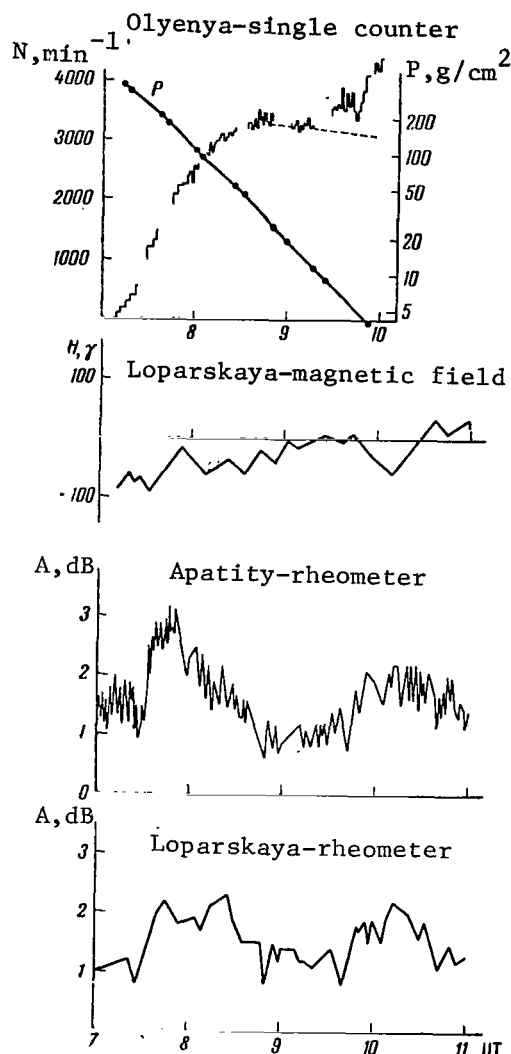


Figure 3. Geomagnetic disturbances during the day June 17, 1965. Notation, the same as in Figure 1.

system also shifts south, although most of the time the ionization region is found to the north.

2. The typical time of these movements is ten minutes; the movement is comparatively smooth.

The antennae of both rheometers are directed at Polaris and have similar directional diagrams. The instruments are identical, and the data were processed by the same method. Therefore, the comparative magnitudes of absorption on the rheometers indicate that the basic ionization region (and, consequently, the maximum of the incoming electron flux) is closer to one of the stations. The time pattern of the ratio of the instrument readings can serve as an indication of the movement of the electron precipitation region. On the other hand, we can track the movements of the ionization region by the position of the system of currents causing magnetic disturbances, which is determined by the ordinary method using three components of the magnetic field. By comparing these data, the following characteristics of the movement of incoming currents and their time aspects can be distinguished.

1. As soon as the ratio of rheometer readings ( $A_{Ap}/A_{Lop}$ ) becomes greater than unity, i.e., the region of absorption shifts toward Apatity, the current

3. The drift south of the current system is observed principally during intensification of the electron flux (increase of absorption). It is like a supplementary flux, entering farther south, being superimposed on the total electron flux which is produced all during this period. The ionization caused by this flux also forces the current system to be shifted south. When the supplementary flux stops, the center of gravity of the currents is again shifted to the north.

4. It can be noted that in the current shift from north to south the peak of the supplementary absorption burst begins several minutes earlier at the Loparskaya station than at Apatity. Vice versa, in the return movement of the current from south to north, the peak of the burst begins earlier at Apatity.

5. The forms of absorption bursts at Apatity and Loparskaya do not agree in detail. The same can be said about their amplitude, which as a rule was greater at Apatity than at Loparskaya during short bursts. Usually, the shorter the bursts, the greater the difference. Consequently, locations of surges are mutually connected in time and space.

It is evident from Figure 4 that absorption occurs simultaneously with a negative magnetic bay. As a rule, the same thing is also observed in other nighttime and evening disturbance periods [1-6]. There are also exceptions. One of them is shown in Figure 1. Here absorption at 20 - 21<sup>h</sup> June 15 is accompanied both by a negative bay and movement of the precipitation region to the north. But absorption, with a peak at 1<sup>h</sup>2<sup>m</sup> June 16, began at the time when the negative bay had already developed, so that during peak absorption (and penetration of particles according to stratospheric data) the magnetic bay had already ended. It is interesting to note that in this case also a shift of the current systems to the south did not occur, if two momentary surges at the beginning and at the end of absorption are not considered. Thus, the magnetic bay and the currents it caused were connected with penetration of particles in the north. This was also reflected on the rheometers (to a greater degree on the Loparskaya rheometer), but the powerful burst at 1<sup>h</sup>

/105

caused ionization south of the primary precipitation region and absorption on the rheometers which was not connected with the formation of an electric current in the ionosphere. This last circumstance indicates that the region of increased ionization is either extremely localized or is below the conductive layer (i.e., below 80 km).

Daytime disturbances. Much research has been devoted to the nature, morphology and other characteristics of night and morning disturbances which indicate indisputably that electron fluxes are the cause of these disturbances. A great deal still remains unclear about daytime disturbances. Distinct types of disturbances have not been isolated, and even the spectrum of particles causing them is not known. In particular, in articles [14, 15] it is assumed that a specific type of positive magnetic bay is connected with proton fluxes that drift from the nighttime side of the Earth.

In the period we studied, radiosonde flights were made during two-day positive magnetic bays. In neither case was a supplementary (on the background of the cosmic rays) radiation recorded. Data from the first flight (June 15), the H-component of the magnetic field, and rheometer readings are given in Figure 5. The radiosonde reached altitudes of  $5 \text{ g/cm}^{-2}$  during the peak of the bay (its magnitude in the H-component was  $230\gamma$ ). In the second flight, on June 17 (Figure 6), during a bay of  $200\gamma$  the sonde rose to an altitude of  $15 \text{ g/cm}^{-2}$ . Rheometer absorption in both cases did not exceed 0.5 dB.

We conclude by the cases cited that if an electron flux was the agent causing the magnetic disturbances, then the spectrum of this flux must be soft (electron flux with energy of 20 keV not more than  $10^6 \text{ cm}^{-2} \cdot \text{sec}^{-1}$ ). Or it might actually be protons which the radiosonde is not able to record. In both cases, the agent responsible for these positive bays must have a qualitatively different nature from the night and morning fluxes. On the other hand, ordinary electron disturbances are nevertheless observed in daytime and early evening hours. This is known from direct observations on sondes [16 - 18]. It should therefore be assumed that two disturbance

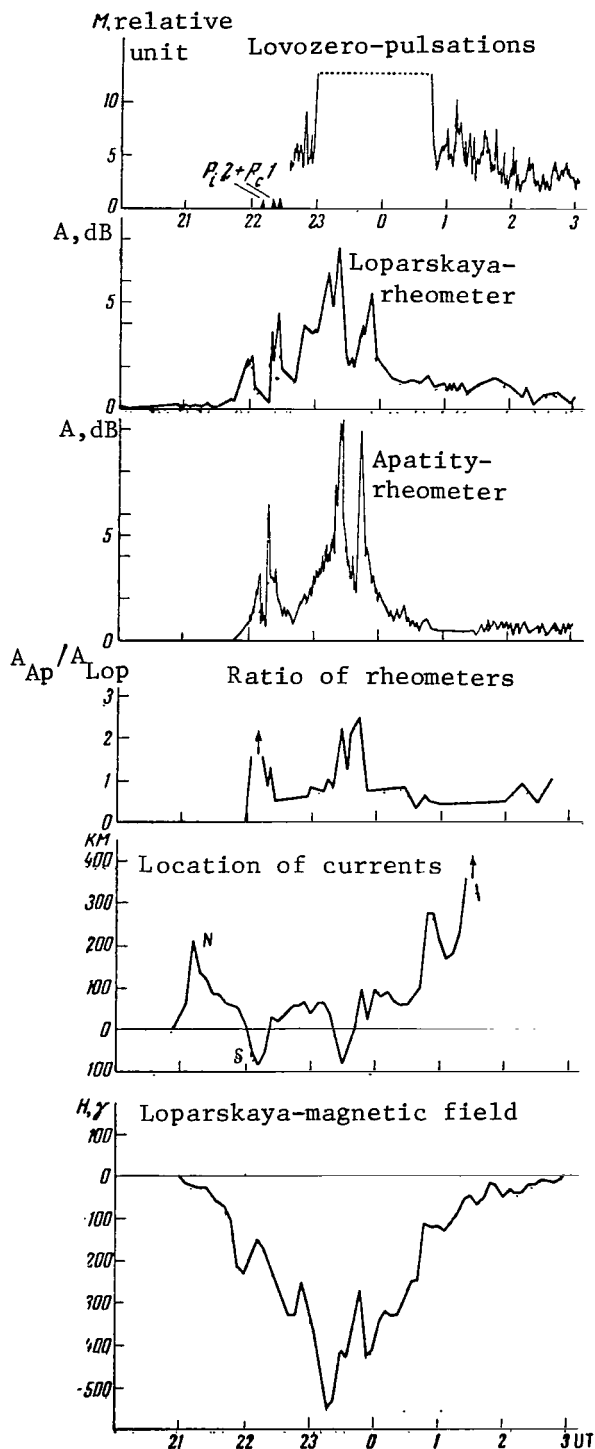


Figure 4. Geomagnetic disturbances the night of June 17 - 18, 1965. Notations the same as in Figure 1.

mechanisms are observed in daytime, both of which can act either independently or together

Micropulsations. In comparing the character of micropulsations with the phenomena in the upper atmosphere of the Earth (enumerated in this article), several definite connections arise which are essential in determining the nature of micropulsation mechanisms and geomagnetic disturbances. In Figure 7, we can see the relation between cosmic radionoise absorption and the character of micropulsations during the storm of June 16, 1965.

A tellurogram analysis shows that a series of bursts of the fluctuating  $P_{12} + P_{1C}$  type are observed in the late day and evening hours. In the diagrams these bursts are marked by a shaded triangle with no indication of amplitude. We conclude from the rheometer data presented here from Apatity and Loparskaya that each such burst is accompanied by a peak of absorption. Deviations from this synchronism do not exceed 1 - 2 minutes, which is within the accuracy limits of time determination in rheometer readings.

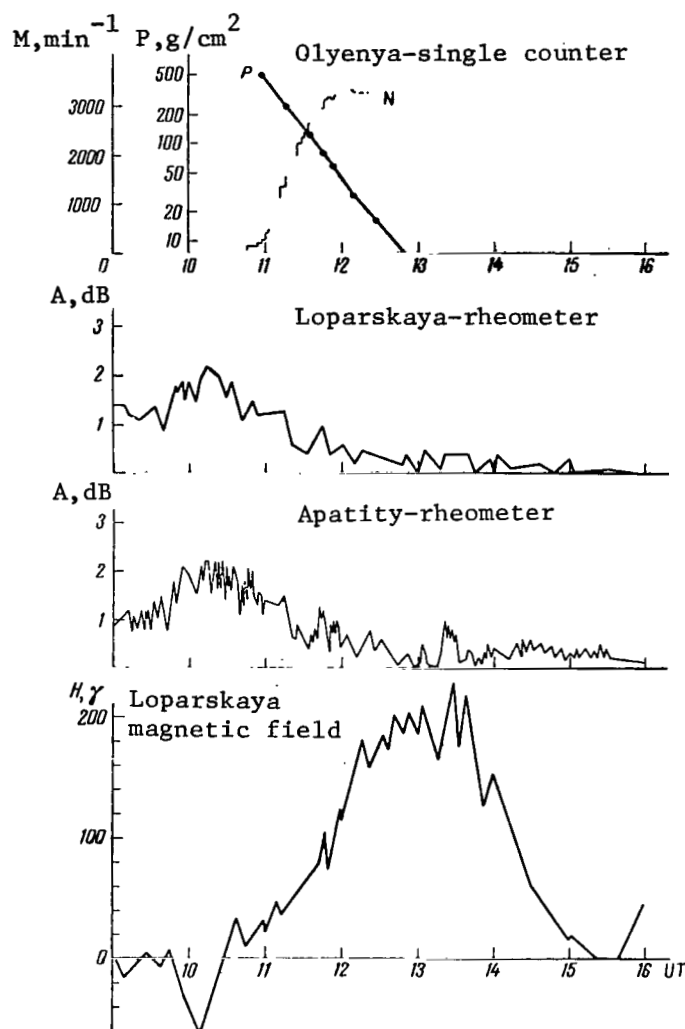


Figure 5. Lack of x-rays in the stratosphere June 15, 1965 during a positive magnetic bay. Notations the same as in Figure 1.

Earlier [19] it was noted /106 that  $P_{i1}$ -type micropulsations are only observed during night-time negative bays, with their amplitude fairly well repeating the pattern of  $\delta H$ . It can be seen from Figure 2 that  $P_{i1}$ -type fluctuations develop after the zero point in the  $H$ -component. It appears that the magnitude of the continual peak amplitude of these fluctuations changes parallel with the absorption magnitude at both Loparskaya and Apatity (see Figure 7). Thus, the amplitude of micropulsations is determined not so much by an increase of the electric field as by an increase in the intensity of the ionizing flux. In observing irregular pulsations of the intensity of x-ray radiation in the stratosphere (intervals between bursts of 7.8 - 8.8 sec) simultaneously at Makuori Island and at

College [18], we conclude that fluctuations of the Earth's electromagnetic field with the same  $P_{i1}$  period are determined by pulsations within the same electron stream penetrating the atmosphere. This is also verified by the agreement of the periods and the character of the fluctuations in the Earth's electromagnetic field and in the intensity of auroral radiation [12]. /107

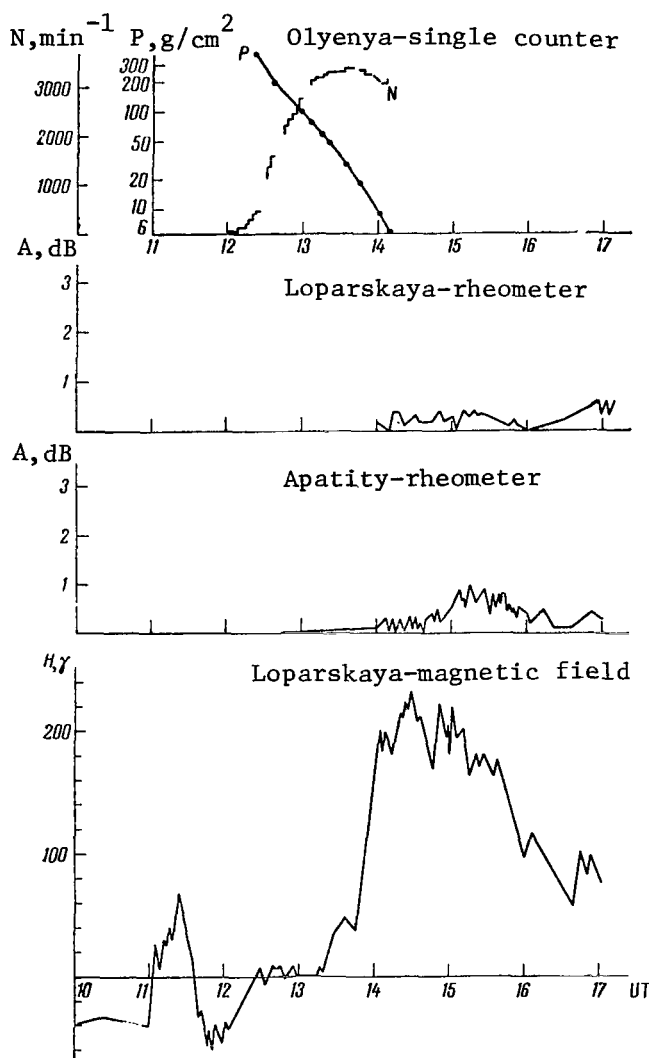


Figure 6. Lack of x-rays in the stratosphere June 17, 1965 during a positive magnetic bay. Notations the same as in Figure 1.

The characteristics exhibited in the relation of micropulsations with the magnetic field and absorption on the evening of June 16 are confirmed by other ion disturbances. In Figure 1-4 we see that an absorption peak corresponds to each  $P_{\perp 2} + P_{\perp 1}$  burst. After the bursts,  $P_{\perp 1}$ -type micropulsations begin, whose amplitude repeats in general the pattern of  $\delta H$  and absorption. Unfortunately, in those cases when the disturbance reached a great magnitude, the standard micropulsation reading was too complex for any accurate detailed analysis. /108

An analysis of the microstructure of daytime positive disturbances revealed a definite class of these disturbances which are not connected with any kind of micropulsations, showing that during such bays the rheometer registered very weak absorption of cosmic radionoise. The two cases of positive bay disturbances cited earlier correspond

completely to this class. A lack of any kind of micropulsation at this time also confirms the conclusion that the usual electron flux recorded during the night and morning hours is absent here.



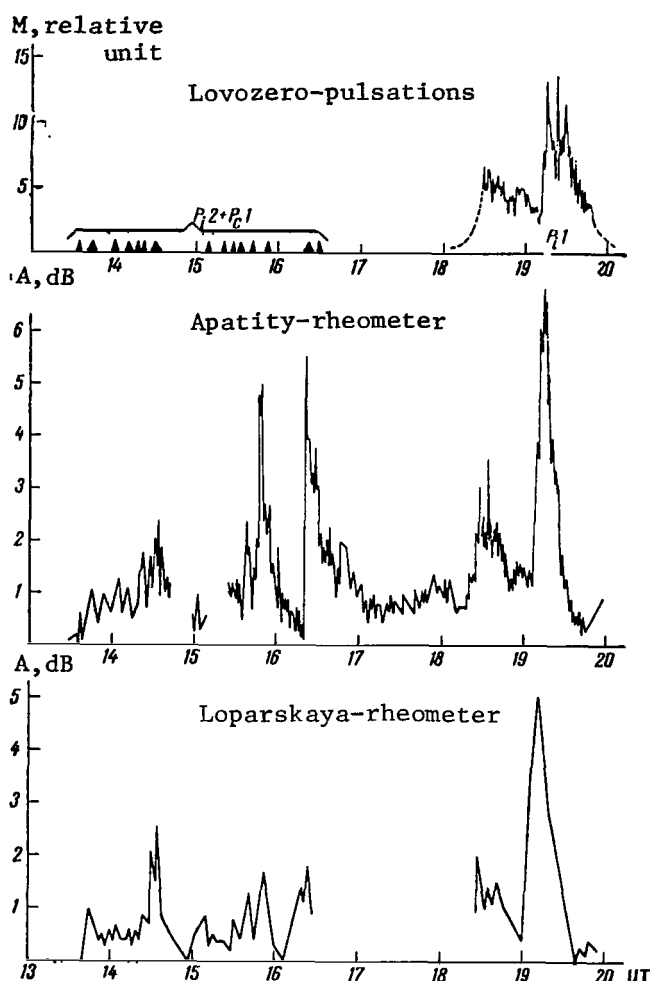


Figure 7. Micropulsations of the electromagnetic field and absorption of cosmic radio noise June 16, 1965. Notations the same as in Figure 1.

Discussion of Results. A complete examination, using various kinds of observations, reveals several relationships in the complex picture of a magnetic storm. /109 Two kinds of electron fluxes can be distinguished. Those of the first kind last several hours, change quite smoothly, and are observed principally after midnight; their center of gravity is located somewhat north of Loparskaya. These streams are accompanied by  $P_{11}$ -type micropulsations of the Earth's electromagnetic field. In earlier hours, in the evening and at local midnight, fast impulses (bursts of absorption) are observed, with the beginning more abrupt than the beginning of the decline. In character they resemble the F-type observed by R. Partasarathy and F. T. Berkey [8], or the SAI-type, according to Z. A. Ansari [10]. Ansari has discovered that SAI is usually connected with the disintegration phase of the aurora polaris and that it has a limited ionization field (90 km in latitude and 200 km in longitude).

Our observations supported this, and it can be concluded that such absorption impulses are observed not only individually, but also in groups during several hours. Principally, they originate south of the main precipitation,

which is usually present during this time. The fast bursts or groups of bursts in the south can also be accompanied by a drift southward of the current stream responsible for negative bay magnetic disturbances.

It is important that in several cases the impulse can be so localized and momentary that the current system does not drift south, i.e., in the precipitation of the supplementary electron flux the current system cannot develop. This can evidently explain the weak connection this type of absorption impulses (F-type) has with the negative bursts in the magnetic field (obtained by Partasarathy and Berkey [8]). In micropulsations of this kind, the impulses are accompanied by "flares" (type  $P_{i2} + P_{c1}$ ). The time characteristics of these flares and the intensity pattern indicate their connection with the incoming flux.

The times of day in which the two types of fluxes occur are divided: fast bursts occupy several hours before midnight, but smoother and wider ones occur after midnight until morning. Then the latter are also "pulled" into the daytime side of the Earth. It is true that disturbances of another kind can also be observed on the daytime side -- positive bays in the H-component of the magnetic field. These are not connected with ordinary electron precipitation and are not, therefore, accompanied by x-rays in the stratosphere or by absorption of cosmic radio noise or micropulsations.

## REFERENCES

1. Oguti, T. Geomagnetic bay disturbance and simultaneous increase in ionospheric absorption of cosmic radio noise in the auroral zone. Rept. Ionosphere Space Res. Japan, Vol. 17, No. 4, 1963, p. 291.
2. Brown, R. R. and W. H. Campbell, An auroral zone electron precipitation event and its relationship to a magnetic bay. J. Geophys. Res. Vol. 67, No. 4, 1962, p. 1357.
3. Barcus, J. R. and R. R. Brown. Electron precipitation accompanying ionospheric current system in the auroral zone. J. Geophys. Res. Vol. 67, No. 7, 1962, p. 2673. /110
4. Brown, R. R. and J. R. Barcus. Day-night ratio for auroral absorption events associated with negative magnetic bays. J. Geophys. Res. Vol. 68, No. 14, 1963, p. 4175.
5. Pudovkin, M. I., R. G. Skrypnikov, and O. I. Shumilov. Magneto-ionospheric disturbances in the polar auroral zone. Geomagnetizm i Aeronomiya Vol. 4, No. 6, 1964, p. 1094.
6. Pudovkin, M. I., and O. I. Shumilov. Intensity of auroral absorption with regard to time of day and type of geomagnetic disturbance. In Press.
7. Berkey, F. T. and R. Partasarathy. The investigation of selected types of cosmic radio noise absorption in the auroral zone. Sci. Rept. Geophys. Inst., Alaska, 1964, UAG-R 151.
8. Partasarathy, R. and F. T. Berkey. Auroral zone studies of sudden onset radio wave absorption events using multiple-station and multiple-frequency data. J. Geophys. Res., Vol. 70, No. 1, 1965, p. 89.
9. Brown, R. R. Day-night ratio of auroral absorption for break-up events. J. Geophys. Res., Vol. 69, No. 7, 1964, p. 1429.
10. Ansari, Z. A. The aurorally associated absorption of cosmic noise at College, Alaska. J. Geophys. Res. Vol. 69, No. 21, 1964, p. 4493.
11. Campbell, W. H., and M. H. Rees. A study of auroral coruscations. J. Geophys. Res., Vol. 66, No. 1, 1961, p. 41.
12. Skrypnikov, R. G. The connection of short-cycle fluctuations of the Earth's electromagnetic field and variations of intensity of polar auroral radiation. In: "Issledovaniya geofizicheskikh yavleniy elektromagnitnoy kompleksa v vysokikh shirotakh" (Studies of geophysic phenomena of the geomagnetic complex at high latitudes). Moscow, "Nauka" Press, 1964.

13. Dorman, L. B. Variatsii kosmicheskikh luchey i issledovaniye kosmicheskogo prostranstva (Variations of cosmic rays and study of outer space). Moscow, 1964.
14. Pudovkin, M. I. and N. S. Smirnov. Two types of corpuscular precipitation into the polar zone. Geomagnetizm i Aeronomiya, Vol. 4, No. 1, 1966, p. 166.
15. Loginov, G. A. and M. I. Pudovkin. Dynamics of magneto-ionospheric disturbances in the polar auroral zone. In press.
16. Campbell, W. H. A study of geomagnetic effects associated with auroral zone electron precipitation observed by balloons. J. Geomagn. and Geoelectr., Vol. 16, No. 1, 1964, p. 41.
17. Brown, R. R. and J. R. Barcus. Balloon observations of auroral zone x-rays in conjugate regions. I. J. Geophys. Res., Vol. 70, No. 11, 1965, p. 2579.
18. Brown, R. R., J. R. Barcus, and N. R. Parsons. Balloon observations of auroral zone x-rays in conjugate regions, II. J. Geophys. Res., Vol. 70, No. 11, 1965, p. 2599.
19. Loginov, G. A. Microstructure of the excited solar diurnal variation of  $S_D$ . In press.

DYNAMICS OF MAGNETO-IONOSPHERIC DISTURBANCES IN THE POLAR  
AURORAL ZONE

G. A. Loginov and M. I. Pudovkin

ABSTRACT. The paper analyses the connection of the magneto ionospheric disturbances observed in Murmansk in daytime with the corresponding phenomena in Alaska. It is shown that the lagging time of disturbances in Murmansk relative to the disturbances in Alaska is different for absorption bays and for bays in the geomagnetic field, i.e., the regions of enhanced ionization and the electric currents in the ionosphere may not coincide spatially.

In article [1] it was observed that the region of anomalous radio wave /111  
absorption at high latitudes sometimes includes a very significant longitude range. Maximum absorption at stations located at various longitudes is not reached simultaneously; this difference in time can reach one hour or more. The authors of [1] explained the observed lag as a shift of the absorption region along a parallel in a westerly direction primarily. However, as data from only two stations were used in [1], and these stations were separated from each other by  $160^\circ$  of geomagnetic longitude, this does not seem to be the only possible direction of the movement.

A study of polar magnetic disturbances using data from four points located in the polar auroral zone showed that the maximum of magnetic disturbances of a specific type was reached at various times [2]. It was also discovered that the region of maximum  $\delta H$  moves along the auroral zone from east to west. According to data in [1], the speed of the western drift is approximately the same as the speed of the absorption maximum.

Such coincidence of direction and speed of drift of the region of maximum  $\delta H$  and  $\delta A$ , together with the close relationship between the ionization region and electric currents in the ionosphere at night [3 - 5], leads to the assumption that the correlation in the daytime between geomagnetic bays moving along the auroral zone and rheometer absorption must be quite high. However, this assumption has not yet been successfully proven experimentally. In article [1], only rheometer data were used and in [2] only geomagnetic data. It is therefore interesting to trace the relationship between the phenomena mentioned, even though for a small number of individual disturbances. Data of several magneto-ionospheric disturbances, observed in February - March, 1964, were chosen for this analysis. There is detailed information about their course from stations in Alaska [6] and at Murmansk. The geomagnetic coordinates of these stations are given in the table.

Figure 1 shows the intensity of geomagnetic disturbances  $\delta H$  at College and Lovozero and the pattern of rheometer absorption  $\delta A$  at a frequency of about 30 MHz at College and Loparskaya during the storm of February 26, 1964. As /112 the magnitude of rheometer absorption changes very rapidly with the latitude of the observation point, absorption at the Kotzebue and Apatity stations is also included in Figure 1. The charts show that in this case the disturbance, magnetic as well as ionospheric, was observed almost simultaneously at stations approximately  $120^\circ$  geomagnetic longitude apart. The form of the curves  $\delta H$  and  $\delta A$  is basically the same everywhere. Thus, peaks observed at the Murmansk station can be confidently identified with peaks at the Alaska stations. For example, it can be assumed that the small positive bays at Lovozero at  $11 - 12^h$  and  $12 - 13^h$  UT correspond to the intensive negative bays in Alaska with maxima about 11 and  $12^h$ . Although the maxima of  $\delta H$  at Lovozero are expressed indistinctly so that it is impossible to determine their time delay relative to corresponding  $\delta H$  peaks at College, a tendency toward a general delay of bays on the whole at Lovozero is expressed clearly.

During this time there were also two peaks of rheometer absorption at Loparskaya and Apatity ( $11 - 12^h$  and  $13 - 14^{h30m}$  UT). These are evidently connected with disturbances in Alaska but are considerably delayed in relation to

them. It is noteworthy that peaks of absorption at Loparskaya and Apatity are shifted in time not only in relation to corresponding peaks in Alaska, but also in relation to maxima of  $\delta H$  at Lovozero. This shift is already noticeable for a peak of  $\delta A$  at 11 - 12<sup>h</sup> and clearly marked for a peak of  $\delta A$  at 13<sup>h</sup> - 14<sup>h</sup>30<sup>m</sup>. In this last case, the absorption bay begins after the bay in the magnetic field has ended.

TABLE

Station	$\Phi$ , °N	$\Lambda$ , °
College	64.6	256.5
Kotzebue	63.5	242.4
Loparskaya	63.7	126.6
Lovozero	62.8	127.3
Apatity	63.0	125.4

Figure 2 shows a graph of  $\delta H$  and  $\delta A$  at the Alaska and Murmansk stations for February 28, 1964. The amplitude of the magnetic disturbances at Lovozero on that day is small. Their form differs markedly from the form of the  $\delta H$  curve at College. Therefore, it is very difficult to identify the  $\delta H$  curve at Lovozero with  $\delta H$  peaks at College. The peaks of  $\delta A$  at

Loparskaya and Apatity (in particular, the double peak during the period of 13<sup>h</sup>20<sup>m</sup> - 14<sup>h</sup>30<sup>m</sup>) have a form which is considerably closer to the form of  $\delta A$  at College. As on February 26, the  $\delta A$  peaks at Loparskaya lag notably in relation to  $\delta A$  and  $\delta H$  peaks at College. Also on that day the absorption bays at Loparskaya did not coincide in time with the geomagnetic bays at Lovozero. For example, the peak of  $\delta A$  at 13<sup>h</sup>25<sup>m</sup> is accompanied by a very weak positive bay, and the peak of  $\delta A$  at 11<sup>h</sup>50<sup>m</sup> is not accompanied by any magnetic disturbance.

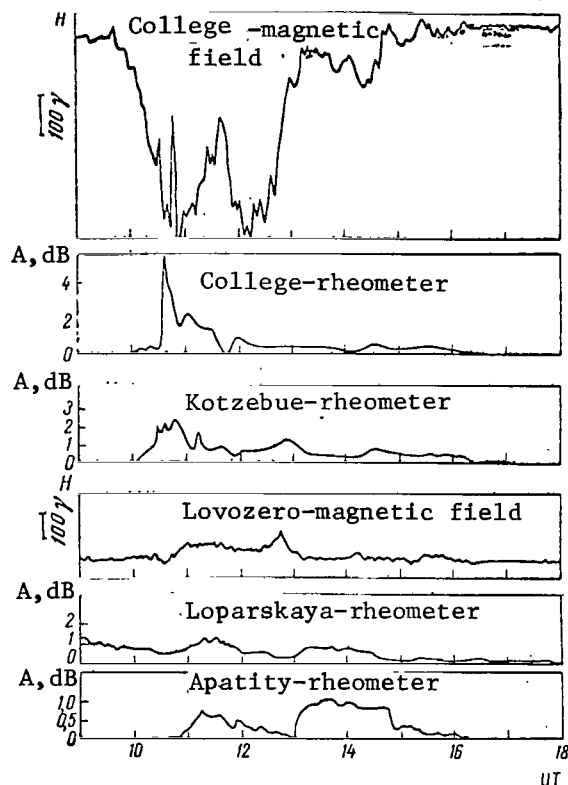


Figure 1. Intensity of geomagnetic disturbances and absorption of cosmic noise at stations in Alaska and the Kola peninsula February 26, 1964.

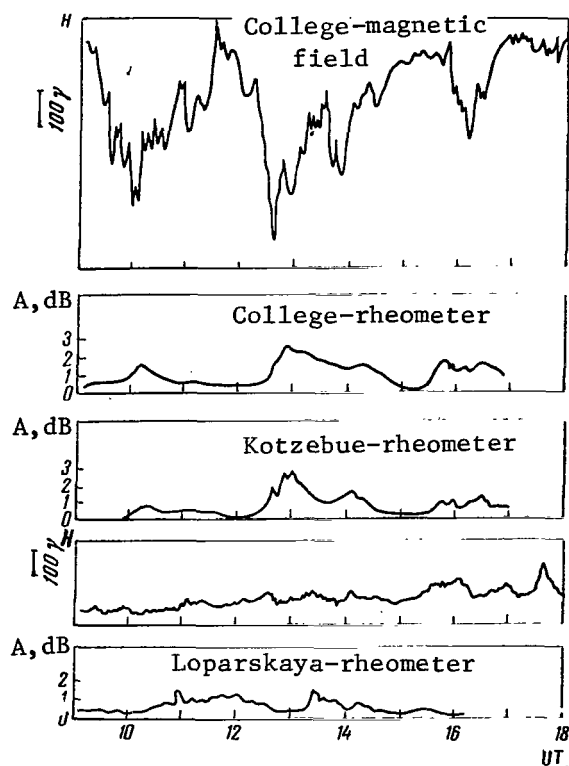


Figure 2. Intensity of geomagnetic disturbances and absorption of cosmic noise at stations in Alaska and the Kola Peninsula, February 28, 1964.

An analogous pattern is also observed on March 5, 1965, (Figure 3). An intensive bay in  $\delta H$  and  $\delta A$  on that day at College at 12 - 13<sup>h</sup> caused only a small variation in  $\delta H$  at Murmansk, as it was not accompanied by a simultaneous increase of radio wave absorption. But approximately an hour after the beginning of the disturbance at College, a rather intensive bay in  $\delta A$  was observed at Apatity. This in turn was not accompanied by a magnetic disturbance.

The examples cited are too few to indicate some kind of regularity in the flow of magnetic ionospheric disturbances. However, these examples (corresponding to data in [1, 7]) show that absorption bays, similar to geomagnetic bays, on the daytime side of the polar auroral zone can lag significantly in relation to phenomena connected with them on the

nighttime side of the zone. But their delay time can differ considerably from the delay time of corresponding bays in the geomagnetic field. Thus, electric currents in the ionosphere and in the region of auroral absorption appear to a large extent to be spatially separated on the daytime side of the polar auroral zone. Evidently, it is just this circumstance which explains the fact that the magnitude of the ratio  $\delta H/\delta A$  in the daytime is equal to 700γ dB at the moment of  $\delta H$  maxima [5] and 60γ dB at the moment of  $\delta A$  maxima [8].

The spatial separation of electric currents and regions of increased radio wave absorption in the ionosphere indicates that their sources move around the Earth with various speeds or along various paths. From this circumstance, we



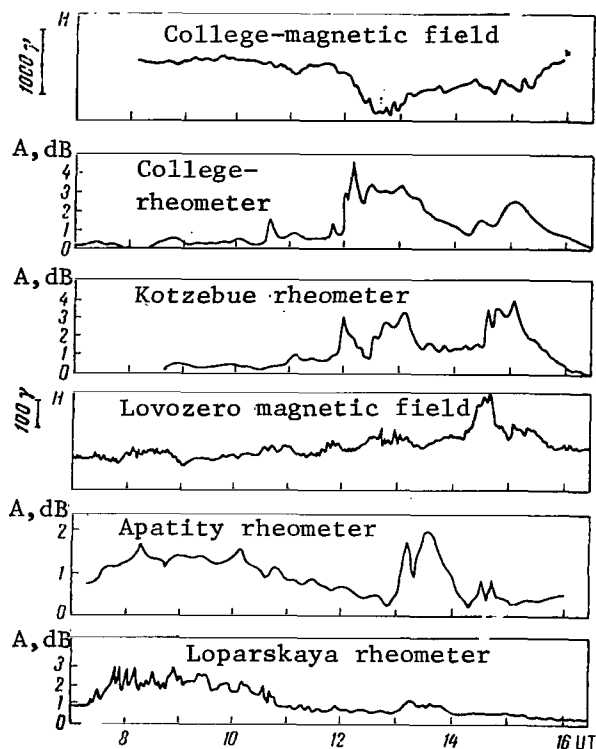


Figure 3. Intensity of geomagnetic disturbances and absorption of cosmic noise at stations in Alaska and the Kola Peninsula March 5, 1964.

can assume that on the dayside of the polar auroral zone electric currents in the ionosphere and regions of increased radio wave absorption are caused by various sources, evidently by streams of corpuscles distinguished by their energy spectrum or even by their nature.

As has already been said, the source of the delayed magnetic bays moves around the Earth from east to west with a speed about 6 km/sec. It can be assumed from this that the source is protons with an energy of about 150 - 200 keV [2]. As data from only four stations were used in [2], it is impossible to determine accurately /114 the zone along which the region of maximum  $\delta H$  moves. It can only be assumed that the movement does not take place along the oval of the polar aurora, obtained in [9, 10], as only negative bays are observed there [11, 12]. In this case the question is

positive magnetic disturbances. On the other hand, the ratio  $\delta Z/\delta H < 1$  is characteristic for delayed bays. This shows that the sources of the daytime delayed bays move approximately along the main auroral zone.

The speed with which the absorption region moves along the auroral zone can be judged by Figure 1, where obviously a series of  $\delta A$  peaks was observed on February 26, 1964, both in Loparskaya and in Alaska. Maxima of  $\delta A$  are observed at Loparskaya at approximately the same time that minimums of  $\delta A$  are noted at Kotzebue. The alternation of peaks seems so clear and

regular, it gives the impression that they are always caused by the same source of ionization passing over the station. This seems to move along the polar auroral zone with an almost constant speed of about one revolution every two hours. Judging by the number of peaks observed, the ionization source completed no less than three revolutions around the Earth during this disturbance. Evidently on March 5, 1964, (see Figure 3) the same ionization source, moving along the auroral zone, successively caused an absorption peak at College ( $12 - 13^h$ ), then at Apatity ( $13 - 14^h$ ), and in half an hour -- once more at College. In this case the speed of the ionization source was one revolution every 2.5 hours.

Lack of necessary experimental data makes it impossible as yet to draw conclusions about the nature of ionizing radiation. The fact that delayed absorption bays are accompanied by anomalously small magnetic disturbances indicates, evidently, that the region of increased ionization is formed below the current layer, i.e., below 80 km. Consequently, if a stream of corpuscles is the ionizing agent, these particles can be either protons with an energy of  $E > 2$  MeV [13], or electrons with an energy of  $E > 50$  keV [14]. However, precipitation of protons with the indicated energy into the polar auroral zone is not supported by experimental data. Protons with an energy of 2 MeV would complete a revolution around the Earth in approximately one minute [15], so that it would be impossible to notice the delay of absorption peaks at Murmansk in relation to absorption peaks in Alaska. For electrons with an energy of 80 keV, revolution around the Earth would take 2.2 hours [14]. This is quite close to the magnitude obtained. But in this case the drift of maximum absorption must occur in a west-to-east direction. Unfortunately, lack of data from intermediate stations prevents determining the direction of this movement. /115

## REFERENCES

1. Eriksen, K. W., C. S. Gillmar, and J. K. Hargreaves. Some observations of short duration cosmic noise absorption events in nearly conjugate regions at high magnetic latitudes. *J. Atmos. and Terr. Phys.*, Vol. 26, No. 1, 1964, p. 77.
2. Pudovkin, M. I., and N. S. Smirnov. Two kinds of corpuscular precipitation in the polar zone. *Geomagnetizm i Aeronomiya*, Vol. 4, No. 1, 1966, p. 166.
3. Barcus, J. R., and R. R. Brown. Electron discharge connected with the ionospheric current system in the polar auroral zone. In: *Radiation belts and geophysical phenomena*, Moscow, IL, 1963, p. 216.
4. Brown, R. R., and V. H. Campbell. Electron discharge in the polar auroral zone and its connection with bay disturbances of the magnetic field. In: *Radiation belts and geophysical phenomena*, Moscow, IL, 1963, p. 195.
5. Pudovkin, M. I., and O. I. Shumilov. Intensity of auroral absorption according to time of day and type of geomagnetic disturbance. In Press.
6. Brown, R. R., J. R. Barcus, and N. R. Parsons. Balloon observations of auroral zone x-rays in conjugate regions. I. *J. Geophys. Res.*, Vol. 70, No. 11, 1965.
- 8.\* Oguti, T. Geomagnetic bay disturbance and simultaneous increase in ionospheric absorption of cosmic radio noise in the auroral zone. *Rept Ionosphere. Space Res., Japan*, Vol. 17. No. 4, 1963, p. 291.
9. Fel'dsteyn, Ya. I. Geographic distribution of polar aurora and arc azimuths. In: *"Issledovaniya polyarnikh siyaniy"* (Studies of polar auroras). No. 4, series "Resultati MGG" (Results of the International Geophysical Year), Moscow, USSR Academy of Sciences Press, V1962, p.61.
10. Khorosheva, O. V. Daily drift of the closed ring of polar aurorae. *Geomagnetizm i Aeronomiya*, Vol. 2, No. 5, 1962, p. 839.
11. Sibsbee, H. B. and E. H. Vestine. Geomagnetic bays, their frequency and current systems. *Terr. Magn. Atmos Electr.* Vol. 47, 1962, p. 195.

---

\* Translator's note: Number 7 was omitted in the original foreign text.

12. Fel'dsteyn, Ya. I. and A. N. Zaytsev. Disturbed solar diurnal variations at high latitudes during the IGY. *Geomagnetizm i Aeronomiya*. Vol. 5, No. 3, 1965, p. 477.
13. Bates, D. R. Theory of the auroral spectrum. *Ann. geophys.*, Vol. 11, No. 3, 1955.
14. Chamberlain, J. Physics of polar auroras and radiation of the atmosphere. Moscow, IL, 1963.
15. Akasofi, S. I., and S. Chapman. Current ring, geomagnetic disturbances and radiation belts. In: *Radiation belts of the Earth*, Moscow, 1962, p. 149.

# LATITUDINAL VARIABILITY OF IONOSPHERIC PARAMETERS

A. P. Kolobova, B. P. Los'  
and Z. Ts. Rapoport

**ABSTRACT.** The paper analyzes the data of ionospheric stations in Murmansk, Rugozero and Leningrad for 1962-1963. The critical frequencies of the regular layers ( $f_0F2$  and  $f_0E$ ) at these stations in the day hours change in accordance with the change of the zenith distance of the Sun and increase with the decrease of latitude. In the night time the  $f_0F2$  variations are less regular than during the day; the inhomogeneity of the ionosphere increases and the ionization changes irregularly in the layer E level ( $\sim 100$  km), as well as the radiowave absorption. The  $E_s$  layer of the r-type in the auroral zone is caused by corpuscular radiation. The energy spectrum of particles, causing this layer, is wide, and as the latitude decreases it becomes narrower. The number of occurrences of  $E_s$  of the f type increases with the decrease of latitude. During ionospheric magnetic disturbances phenomena typical for the auroral zone are observed at lower latitudes and shift in the E and F layers to lower latitudes than in the D layer. The paper discusses connections between the geomagnetic disturbance and the ionospheric variations over Murmansk, Rugozero and Leningrad.

This paper analyzes data from three ionospheric stations:

/116

Station	$\varphi$ , °N	$\lambda$ , °E	$\Phi$ , °N	$\Lambda$ , °
Leningrad . . .	59°57'	30°42'	59.3°	116.7°
Rugozero . . .	64°5'	32°47'	59.6°	121.4°
Murmansk . . .	68°57'	33°3'	64.1°	126.5°

The stations are situated on nearby longitudes. Rugozero is near the midpoint of the orthodrome connecting Murmansk and Leningrad. We can expect that the material from the observations made at these stations will allow further clarification of the features of the subpolar ionosphere, and especially the boundaries of the region where anomalous absorption and other phenomena

characteristic of the ionosphere at high latitudes occur. It is possible that their analysis will allow formulation of theories regarding the corpuscular fluxes that are responsible for anomalous phenomena in the ionosphere at high latitudes. In contrast to [1-4] we have used data obtained in 1962 and 1963, when solar activity was lower. The average annual relative number of sunspots was 46.3 in 1962 and 34.3 in 1963.

A correct analysis of the data from different ionospheric stations can be performed only by taking the technical characteristics of the installations into account. A number of ionospheric parameters (for example,  $f_{\min}$ , diffusivity,  $fE_s$  — types of 1 and f) depend on the resolving power of the ionospheric station, which, in turn, depends upon the transmitter power, the antenna efficiency, the sensitivity of the receiver, etc. It would be desirable if all the stations in the world network had identical technical characteristics and were stable in their operation. This is not the case in reality, and it must be taken into account in an analysis.

In our case, too, the technical characteristics of the stations were different. A type Sp-3 station, built in the German Democratic Republic, was operated in Leningrad. Its frequency range was 0.5-20 MHz, and the pulse length was about 100  $\mu\text{sec}$ ; the peak power in the given frequency range (for the antenna equivalent) was approximately 15 to 20 kW, the sounding frequency was 30  $\text{sec}^{-1}$ , and the scanning time of the station frequency range was 30 sec. Rhombic antennas suspended at a height of 38 m were used; the length of the side of the large rhomb was 62 m, that of the small, 34 m.

A modernized station built by the "Cossor" firm was used at Rugozero. Its frequency range was 1-18 MHz, the pulse length was 60  $\mu\text{sec}$ , and the pulse repetition frequency was 50  $\text{sec}^{-1}$ . The pulse power varied from 2-5 kW. The scanning time of the frequency range was about 15 sec. Rhombic antennas were used, suspended on a 27-meter central mast and 15-meter side masts; the distance between the side masts was about 100 m.

A station built at the Leningrad Electrotechnical Institute of Communications imeni Prof. M.A. Bonch-Bruyevich [5] was used at Murmansk. Its frequency

range was about 1-20 MHz, the pulse length was about 100  $\mu$ sec, the pulse repetition frequency was 50  $\text{sec}^{-1}$ , the pulse power was 0.5-5 kW, and the scanning time for the frequency range was approximately 30 sec. A rhombic antenna was used, suspended on a 26-meter mast; the side of the large rhomb was about 34 m, and the small — about 23 m. The receiver of the Leningrad station was much more sensitive than the receivers at Rugozero and Murmansk.

From these data we can conclude that the ionospheric station at Leningrad had a significantly greater resolving power than the stations at Rugozero and Murmansk (the difference between the latter is slight). This is immaterial in comparing the variability of critical frequencies and heights of regular layers, but the technical capabilities of the stations must be kept in mind when considering the frequency of occurrences of several types of  $E_s$  (1,f), anomalous absorption, or diffusivity.

Let us consider the variability of the parameters of the F2 layer. Figure 1 shows the change in the  $f_0F2$  medians at Murmansk, Rugozero, and Leningrad in the course of 24 hours for various seasons in 1963. It is apparent from the curves that the nature of the changes in the  $f_0F2$  medians is similar, but that the absolute median values are also very close at the equinox and in summer. In summer, during the hours preceding midnight, the  $f_0F2$  at Leningrad is greater than at Murmansk, while the reverse is true after midnight. The  $f_0F2$  maximum is observed at Leningrad at about 21<sup>h</sup>. The reason for this maximum is not clear, but the increase in  $f_0F2$  at Murmansk after midnight can probably be explained by the conditions of illumination of the F2 layer. There is a polar day there in June. Rugozero occupies an intermediate position nearly everywhere. In December, the quantitative differences in  $f_0F2$  at the three stations are much greater than in winter and at the equinox. There is a clearly pronounced maximum at noon at all three stations, although it is polar night at Murmansk at this time, and the solar radiation passes through the denser layers of the atmosphere before it reaches the F2 layer. During the daylight hours (8<sup>h</sup>-17<sup>h</sup>) the  $f_0F2$  at Leningrad is higher than at Rugozero, and higher in the latter location than at Murmansk. At 18<sup>h</sup>-24<sup>h</sup> the  $f_0F2$  at Murmansk is higher (and at Leningrad lower) than in Rugozero. After midnight, the  $f_0F2$  at Leningrad and

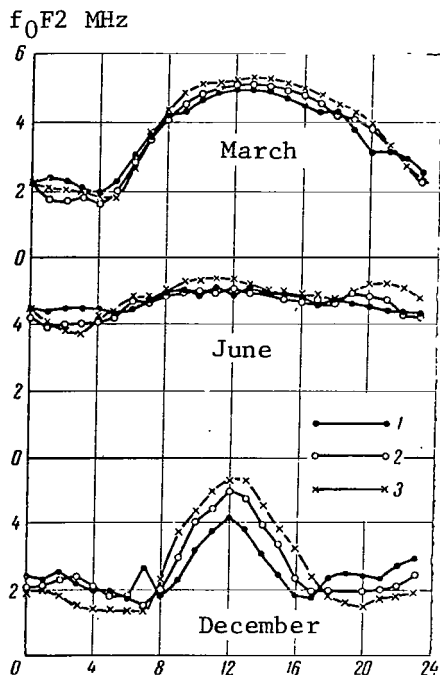


Figure 1. Diurnal variation  $f_0F2$  during various seasons in 1963 (according to monthly medians).  
Time: LMT (30°E)

1. Murmansk; 2. Rugozero;
3. Leningrad.

Murmansk differ only slightly, but they are lower at Leningrad until 7<sup>h</sup>.

Obviously the solar wave radiation is decisive for the  $f_0F2$  at all seasons during daylight hours. The corpuscular factor is apparent during the hours of darkness. It does not appear as regularly as the effect of the wave radiation, but it seems to us that it is the sole explanation for the increase in  $f_0F2$  during the night with increasing latitude. /118

Figure 2 shows the diurnal variation of the height of the maximum electron density of the F2 layer, assuming a parabolic distribution of this density with height (hpF2). In March, 1963, the hpF2 was definitely lower at Rugozero during the daylight hours than at Leningrad and Murmansk. No such regularity was observed in summer. In many instances, the hpF2 at Rugozero during the winter nights exceeded the hpF2 at Leningrad and Murmansk.

However, the major portions of the curves are not marked by any regularity, and it is difficult to confirm any uniformity for the hpF2 curve. /119

Figure 3 shows the diurnal variation of the frequency of occurrence of diffuse reflections in the F2 layer. There is no doubt that the technical capacities of the ionospheric stations exert an influence on the numerical values of  $P(F)$ . The nature of the diurnal variation of  $P(F)$  is also significant, however. It is apparent from the graph that the diurnal variation is clearly evident in summer (May-July) and at the equinox (February-April), with a maximum occurring during the hours near midnight. During daylight hours, the frequency of occurrence of diffusivity is greatest at Murmansk. From November to January



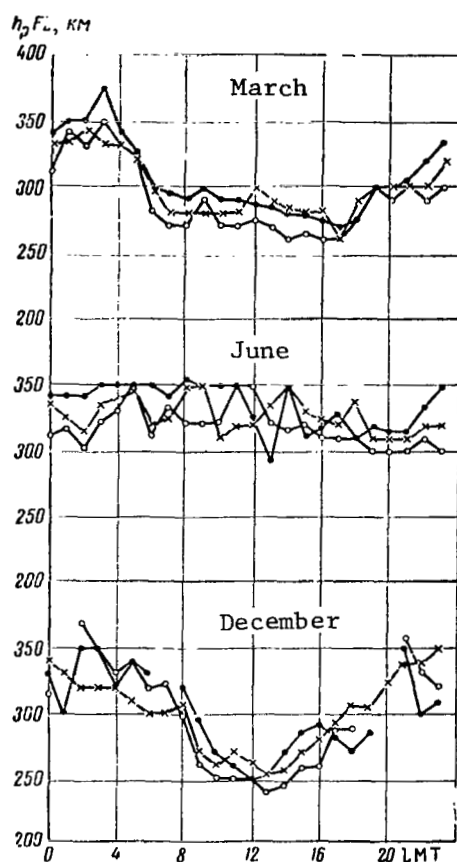


Figure 2. Diurnal variation of  $h_p F_2$  during various seasons in 1963 (according to monthly medians). Time: LMT ( $30^\circ E$ ). Notation the same as in Figure 1.

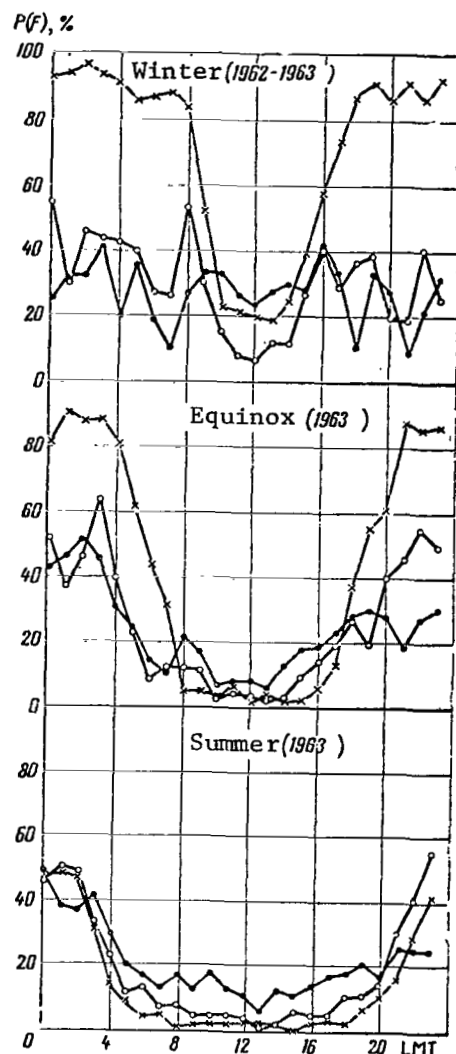


Figure 3. Diurnal variation of frequency of occurrence of diffusivity  $P(F)$  in the  $F_2$  region at various seasons. Time: LMT ( $30^\circ E$ ). Notation the same as in Figure 1.

the  $P(F)$  at Murmansk is higher during daylight hours than in Rugozero; it is approximately the same at Murmansk and Rugozero at night. At Leningrad, the  $P(F)$  exceeds 80% during the night and falls sharply (to about 20%) in the day. The diffusivity of the pulses reflected from the ionosphere is explained by the inhomogeneity of the ionosphere at this time. Inhomogeneity increases during

the dark hours of the day and toward higher latitudes; it is therefore natural to relate it to the influx of corpuscular radiation, as well as to processes in the ionosphere itself. The sharp drop in diffusivity during the daylight hours can be explained by the influence of solar wave radiation that smooths out the inhomogeneities and leads to formation of an ionosphere that is more homogeneous in the horizontal direction.

Figure 4 shows the median values of  $f_{\min}$  (a) and  $f_0E$  (b) for March, June, and December, 1963. The influence of the height of the sun above the horizon is obvious in the case of  $f_0E$ . The curves indicate an increase in this parameter with decreasing latitude, and this is especially notable in the evening and morning hours in summer (in June) and in the hours near noon in winter (in December). The effect of corpuscular radiation on  $f_0E$  is also not excluded at the high zenith distances of the sun in June. The seasonal variations are quite pronounced: while the E layer was detected at all stations in June at all hours of the day (with the exception of 23<sup>h</sup> at Leningrad), the time of its occurrence in December was limited to the hours near noon. Hence, as the latitude increases, the time interval when the E layer is observed grows narrower. The variability of the medians for  $f_0E$  is quite regular in March and June; the maximum occurs at noon or at sunset and sunrise. In December, however, the diurnal variation of  $f_0E$  is less regular, especially at Murmansk; corpuscular radiation appears when the Sun is low in the sky.

The variability of  $f_{\min}$  is less regular during the day than is that of  $f_0E$ . This is probably related to some degree to the fact that the resolving power of the ionospheric stations differs within the limits of the frequency range of  $f_{\min}$  variation. On the other hand, the irregular variability of  $f_{\min}$  itself (and the absorption of radio waves in general) is a characteristic feature of the ionosphere at high latitudes. It is clear from the figure that in March and June, 1963, the changes in the median  $f_{\min}$  at Leningrad and Rugozero were comparatively regular and small, with the maximum occurring in the hours around noon. The changes in the median  $f_{\min}$  in December at Rugozero proceed quite slowly (not changing markedly from one hour to the next); the maximum is observed at noon and during the hours near midnight. The variability of  $f_{\min}$  at

Leningrad in December, 1963, (with minimum values during the hours near noon and marked changes during the evening and night hours) is difficult to explain, however. It may possibly be the result of unstable operation of the instruments, but we have no data that would support this categorically. The variations of  $f_{\min}$  are most irregular at Murmansk. This is especially noticeable in June and December. Here the difference between the variabilities of the median  $f_0E$  and  $f_{\min}$  is greatest; this can be explained by the nature of the spectrum of the corpuscular radiation that penetrates to the height of the D layer and does not produce any significant ionization in the regular E layer.

Figure 5 shows the frequency of occurrence of the sporadic  $E_s$  layer at different seasons: in winter (November-January), at the equinox (February-April), and in summer (May-July). The technical capabilities of the ionospheric stations are reflected in the absolute values of the frequency of occurrence of  $P(E_s)$ , but the variability of  $P(E_s)$  during the day is highly characteristic. /120

At Leningrad,  $P(E_s)$  is higher in the daylight hours and lower at night at all seasons of the year. The absolute values of  $P(E_s)$  during the daylight hours reach 90 and 100% (they are higher in summer and at the equinox).

The curves of  $P(E_s)$  at Leningrad and Murmansk in winter and at the equinox are mirror images of one another. The minimum  $P(E_s)$  is observed at Murmansk in the hours near noon, and the maximum occurs near midnight. In summer there are two maxima: one (smaller) near noon and the other near midnight. The nature of the diurnal variation of  $P(E_s)$  at Rugozero in winter is the same as at Murmansk, but in summer it is the same as at Leningrad. It is interesting to note that the minimum at 15<sup>h</sup> occurs simultaneously at all three stations. At the equinox, however, the diurnal variation of  $P(E_s)$  at Rugozero differs from that at Leningrad and at Murmansk; at this time,  $P(E_s)$  at Rugozero is small in absolute values at all hours of the day and changes slightly from one hour to the next. The equinox at Rugozero is the time when the nature of the diurnal variation changes from high-latitudinal (in winter) to middle-latitudinal (in summer).

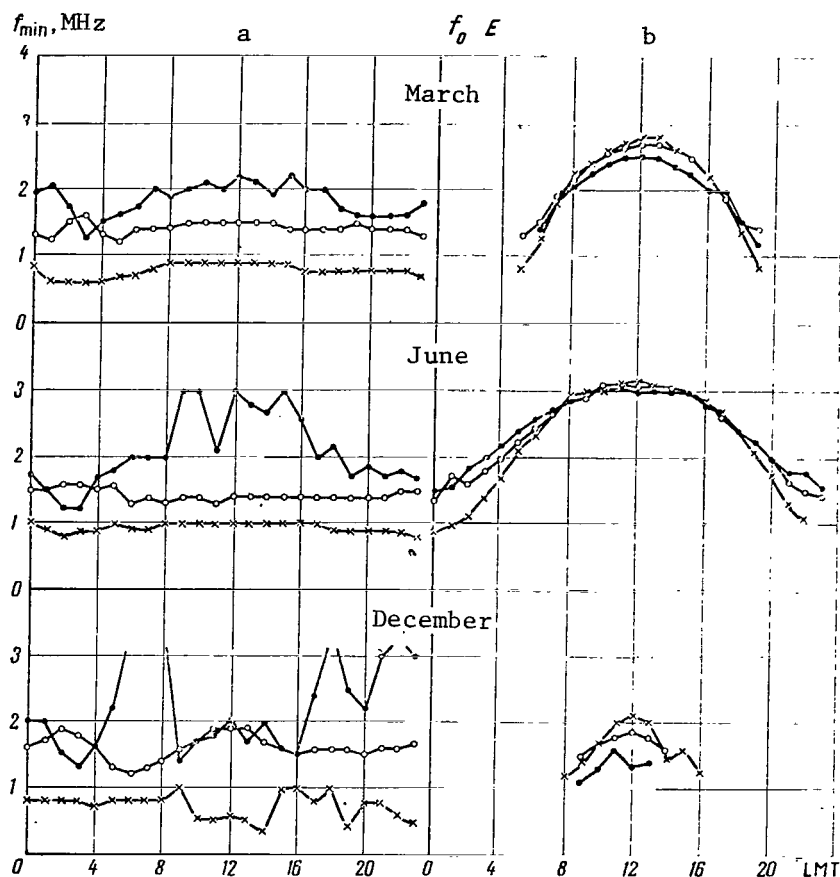


Figure 4. Diurnal variation of  $f_{\min}$  (a) and  $f_o E$  (b) at various seasons in 1963 (according to monthly medians). Time: LMT ( $30^\circ E$ ). Notation the same as for Figure 1.

Figure 6 shows the diurnal variation of the frequency of occurrence of  $E_s$  of different types during the same seasons. The total number of cases of occurrence on the ionograms of the  $E_s$  layer is taken as 100%. It is clear that Type r appears at Leningrad only in isolated instances and only at night. It is encountered most often at Murmansk, but the frequency of occurrence of the Type r  $E_s$  is significant at Rugozero, especially in winter and at the equinox. The minimum in the diurnal variation of the frequency of occurrence of the Type r  $E_s$  is observed in the hours near noon, while the maximum occurs near midnight. The graph in Figure 6 emphasizes once again that the  $E_{sr}$  is a phenomenon characteristic of the auroral zone. At Rugozero the  $E_{sr}$  occurs at all seasons, but an  $E_{sr}$  layer of this type is practically never observed at Leningrad during moderate solar activity. /121

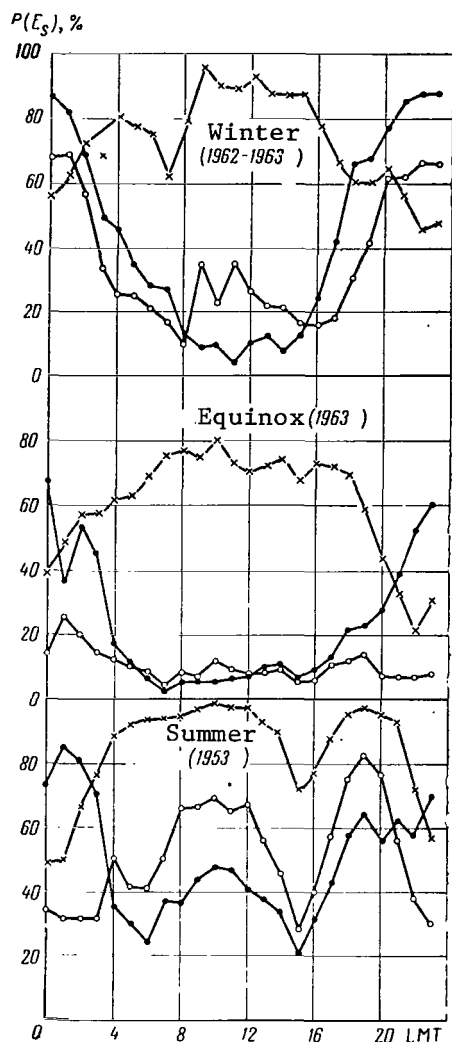


Figure 5. Diurnal variation of the frequency of occurrence of the sporadic E layer at various seasons. Time: LMT (30°E). Notation same as for Figure 1.

Types  $\lambda$  and  $f$  are similar in structure and the use of one symbol or the other depends on the time of day: the symbol  $f$  is used for the dark part of the day, and  $\lambda$  for the daylight portion. This is a flat layer; the limiting frequency of reflection from it depends on the resolving power of the ionospheric station. It is evident from the graph that the frequency of occurrence of  $E_s$  (Types  $\lambda$  and  $f$ ) during the dark part of the day is very high (nearly 100%) and decreases during daylight hours. It is true that a slight maximum is observed in summer during the hours after noon. In summer, the diurnal variation of  $P(E_s)_{f+\lambda}$  is similar at all three stations. This cannot be said at other seasons. The maximum  $P(E_s)_{f+\lambda}$  in winter at Murmansk is observed at 8<sup>h</sup>, and the  $P(E_s)_{f+\lambda}$  values during the hours of darkness are definitely smaller than during the daytime. The diurnal variation of  $P(E_s)_{f+\lambda}$  in winter is similar at Rugozero and Leningrad, although the difference between the daytime and nighttime values is not so significant here. At Murmansk,  $P(E_s)_{f+\lambda}$  is much greater in the daylight hours at the equinox than at night, but the variability of this value from one hour to

the next is very great. Moreover, this does not provide a basis for far-reaching conclusions, since the total number of cases when  $E_s$  is observed during this time is relatively small. At Rugozero, the variability of  $P(E_s)_{f+\lambda}$  from one hour to the next is also great, but the frequency of occurrence of the  $E_s$  of these types has a minimum in the evening hours and a maximum near midnight.

Evidently,  $E_s$  (types  $\lambda$  and  $f$ ) can be produced by both wave and corpuscular /122

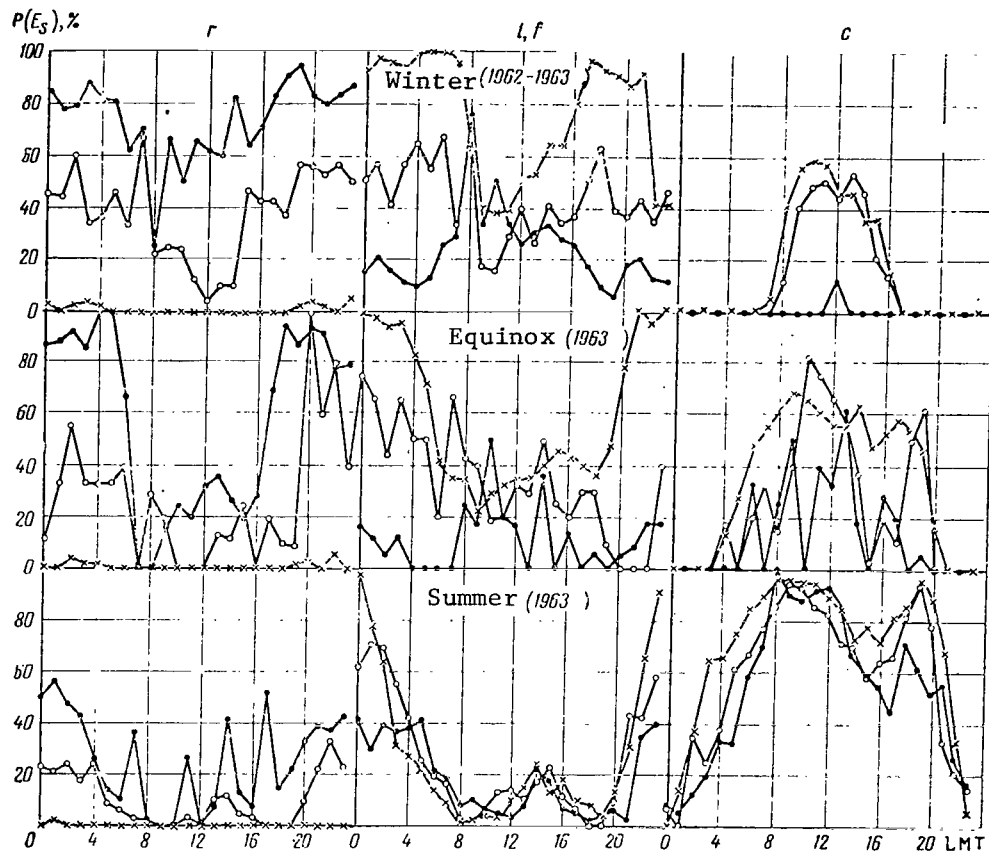


Figure 6. Diurnal variation of the frequency of occurrence of the sporadic  $E_s$  layer (Types r, l, f, and c) at different seasons. Time: LMT ( $30^\circ E$ ). Notation same as for Figure 1.

radiation from the sun. The diurnal variation of  $P(E_s)_{l+f}$  changes with latitude: at the latitude of Leningrad,  $E_s$  of these types occur primarily at night. At the latitude of Rugozero in summer,  $E_{sl}$  and  $E_{sf}$  are also encountered primarily at night, but at the equinox and in winter they can be encountered with the same frequency in the day as in the night. At this time,  $P(E_s)$  varies quite sharply and irregularly from one hour to the next. At Murmansk,  $E_{sl}$  and  $E_{sf}$  are also encountered primarily at night in summer [the maximum  $P(E_{sl})$  is observed during the hours near midnight], but the frequency of occurrence of  $E_s$  (types l and f) is much higher during daylight hours at the equinox and especially in winter. (It should be emphasized that the general frequency of occurrence of  $E_s$  at Murmansk and at Rugozero in winter and at the equinox is very low; see Figure 5).

The value  $P(E_{sc})$  is maximum in the day and equal to zero at night. It is obvious that the occurrence of  $E_s$  (Type c) is related to the solar wave radiation.

The lack of reflections from the ionosphere on the ionograms ("blackout", B) is a phenomenon that is typical of the auroral zone. As we can see (Figure 7) no blackouts were observed in 1962 - 1963 at Leningrad, and they were very rare at Rugozero. In summer and at the equinox, cases of B at Rugozero were scattered and occurred only at night. At Murmansk, however,  $P(B)$  exceeded 20 and 30% at certain hours. B could be observed at all hours of the day and night, but  $P(B)$  was minimal in summer during the afternoon (14 - 19<sup>h</sup>). The maximum  $P(B)$  was observed near midnight. The reason for the lack of reflections (auroral absorption) can naturally be found in the penetration of energetic particles into the lower ionosphere. The southern boundary of the zone of auroral absorption with moderate solar activity ( $W \approx 30 - 50$ ) rarely drops (at a given longitude) to the south of  $64^\circ$ , and is located to the north of that latitude in the majority of cases. /123

Figure 8 shows three examples of ionospheric-magnetic disturbances that occurred on 5 July, 19 September 1962, and 31 January 1963. The graph shows the hourly values for  $f_{min}$  and the amplitude of the variations of the horizontal component of the geomagnetic field  $R_H^Y$  according to the data of the variation station at Loparskaya (near Murmansk). In the first instance (5 July)  $R_H$  does not even reach 100  $\gamma$ . At Leningrad,  $f_{min}$  is about 1 MHz during the entire excited period, and is somewhat higher at Rugozero (a station with a lower resolving power) but does not exceed 2 MHz. One may conclude that the lower ionosphere was not disturbed here. At Murmansk, however, at the same time anomalous absorption or a high value of  $f_{min}$  (above 3 MHz) was observed during most of the period.

On 19 September  $R_H$  exceeded 100  $\gamma$  for most of the excited period. It is interesting that  $f_{min}$  was somewhat higher at Leningrad, while at Rugozero it was more than 2 MHz and in some cases even reached 3 MHz. At Murmansk there

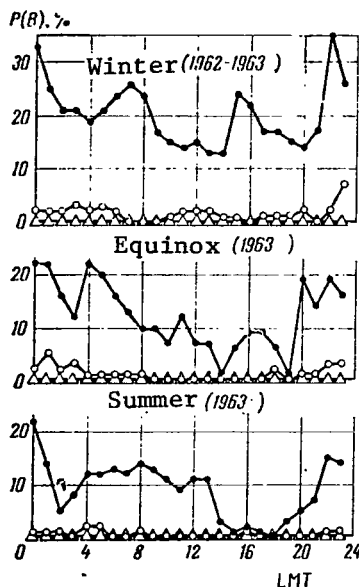


Figure 7. Diurnal variation of frequency of occurrence of anomalous absorption  $[P(B)]$  at different seasons. Time: LMT ( $30^\circ E$ ). Triangles: data for Leningrad; Other notation, same as Figure 1.

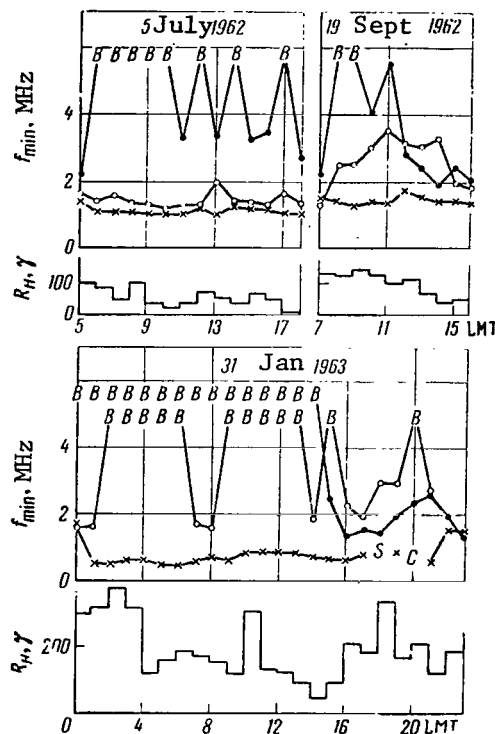


Figure 8. Variation of  $f_{\min}$  during ionospheric disturbances.  $R_H$ : according to data from the magnetic variation station of the polar Geophysical Institute at Loparskaya. Notation, same as Figure 1.

were no reflections, and increased values of  $f_{\min}$  were observed. However, the  $f_{\min}$  at Murmansk fell below 3 MHz beginning at  $12^h$ . This drop in  $f_{\min}$  roughly corresponds to the drop in  $R_H$  at Loparskaya. Note that  $f_{\min}$  is higher /124 at Rugozero than at Murmansk from  $12^h$  to  $14^h$ .

On 31 January 1963, the magnetic disturbance at Loparskaya was particularly strong:  $R_H$  was systematically higher than 100  $\gamma$  and in a number of cases exceeded 200 and 300  $\gamma$ . No disturbance whatsoever occurred in the lower ionosphere at Leningrad;  $f_{\min}$  was below 1 MHz on almost all days. At Rugozero at this time, the lower ionosphere was severely disturbed, increased  $f_{\min}$



values were recorded, and in a number of cases there was anomalous absorption as well. The value of  $f_{\min}$  underwent sharp variations from one hour to the next, which is also characteristic for a disturbance in the lower ionosphere in the auroral zone. No reflections were recorded at the ionospheric station at Murmansk from 0 to 14<sup>h</sup>, but from 18<sup>h</sup> to 24<sup>h</sup>  $f_{\min}$  fell and did not reach 3 MHz. From 15<sup>h</sup> to 21<sup>h</sup>,  $f_{\min}$  was again higher at Rugozero than at Murmansk.

In this article, we have considered some of the features of the ionosphere in the sub-auroral zone (Rugozero). They were compared with the ionosphere in the auroral zone (Murmansk) and at lower latitudes (Leningrad). Note once again that we are dealing with a period of moderate solar activity: in 1962 - 1963 the average monthly values of  $\bar{W}$  varied from 13.7 to 62.9 [6].

There is scarcely any need for a detailed comparison of the features of the variability of the ionospheric parameters at Rugozero and Salekhard, which were analyzed in [1-4]. These papers dealt with material for years of high solar activity. The observation points were located at different geographic and geomagnetic latitudes ( $\varphi_P = 64^\circ 05'N$ ;  $\varphi_P = +59.6^\circ$ ;  $\varphi_c = 66^\circ 32'$ ;  $\varphi_c = +49.9^\circ$ ). In addition, it was quite clear from the data given that many of the regularities that are characteristic of the ionosphere of the subauroral zone during a period of high solar activity [1-4] also occur during lower activity.

Of the regular features of ionospheric parameter latitudinal variability that occur during the period of moderate solar activity, we should like to call attention to the following. The critical frequencies of the regular layers  $f_0F_2$  and  $F_0E$  change regularly during daylight hours (increasing with decreasing zenith distance and having their maximum approximately at noon) and increase with decreasing latitude. A maximum for  $f_0F_2$  has also been recorded at noon at a station in the auroral zone during winter, although the solar wave radiation passes through the denser layers of the atmosphere before it reaches the F2 layer. The difference between the absolute values of the parameters in question is greater in winter than at other seasons. The changes in  $f_0F_2$

are not as regular at night as in the day, but in the majority of cases  $f_0F2$  increases with increasing latitude. Hence, at the latitudes in question, the variability of  $f_0F2$  is determined mainly by solar wave radiation (the zenith distance of the sun) during the day and by corpuscular radiation at night. The influence of the corpuscular radiation makes itself felt (at all the stations mentioned) both by a significant increase in ionospheric inhomogeneities at night (as revealed by the diffuseness of reflected signals) and in the irregular variation of the absorption of radio waves in the ionosphere.

The  $E_s$  layer can be produced by both the and corpuscular radiation from the sun. The critical factor for the  $E_s$  (type r) layer in the auroral zone is the solar corpuscular radiation. This layer occupies a rather extensive range of altitudes, and it is therefore possible to assume that the spectrum of the particle flux that produces  $E_{sr}$  is quite broad and contains components with different energies. At the latitude of Leningrad,  $E_{sr}$  is encountered only on isolated occasions. The  $E_s$  (type f) layer is evidently also produced by corpuscular radiation. However, the spectrum of the particles that produce the  $E_{sf}$  is very narrow, since this layer occupies a very limited range of heights. The frequency of occurrence of the  $E_s$  (type f) layer increases with decreasing /125 latitude. We can conclude that the energy spectrum of the particles of the corpuscular flux that produce ionization at the level of the E region grows narrower as the latitude decreases. Therefore, the value of  $P(E_{sf})$  may be affected by the instrument parameters, and the last reading must be considered as preliminary. A layer similar to the  $E_{sl}$  may probably be produced by solar wave radiation as well. The cause of the appearance of the sporadic  $E_s$  layer (type c), as far as we can determine from the available data, is solar wave radiation.

Anomalous absorption of radio waves in the ionosphere, indicated by an absence of reflections in the ionograms, is caused by fluxes of particles penetrating the D region of the ionosphere. This phenomenon is characteristic of the auroral zone, and rarely appears before the latitude of Rugozero during moderate solar activity, while it is never encountered at all at the latitude of Leningrad (once again we shall not be categorical in this regard, keeping in mind the differences in the technical characteristics of the ionospheric stations).

The energy spectrum of the corpuscular radiation is highly variable with time, while the spectrum in the auroral zone, as a rule, has a predominance of components that produce additional ionization in the E and D regions (at heights of 100 km and below). The energy spectrum of the particle fluxes that cause anomalous absorption is highly irregular in space (the D region at lower latitudes is sometimes subjected to a more intense action of the flux than at the usual latitudes of the auroral zone). This too, it seems to us, can be explained by variations in the spectrum of the particle flux.

A shift to lower latitudes of the regions where phenomena typical of the auroral zone are observed (in particular, the anomalous absorption of radio waves), i.e., a shift of the southern limit of the auroral zone, is closely linked to the excitability of the geomagnetic field in the auroral zone. At an amplitude of the horizontal component  $R_H$  exceeding  $100\gamma$ , the excitation in the D region can reach the latitude of Rugozero (the increase in  $f_{min}$  can be observed at the latitude of Leningrad as well), and at  $R_H$  greater than  $200 - 300 \gamma$ , it can in all probability, reach still farther south.

Thus, in the case of the longitudinal interval under consideration, during moderate solar activity, a tendency toward shifting of the southern boundary of the zone of anomalous absorption during magnetic disturbances has been confirmed — a tendency which was studied previously.

In talking about the southern boundary of the auroral zone, we shall keep in mind this limit of anomalous absorption. If we determine the limit of the auroral zone on the basis of phenomena in the E region (the appearance of the  $E_{sr}$  or  $E_{sf}$  layers), we come to the conclusion that it can sometimes shift down to the latitude of Leningrad or even farther south. On the basis of the F2 region, however, it evidently moves to still lower latitudes. If we are talking about an averaged characteristic, then on the basis of an analysis of the diurnal variations of  $f_{min}$ ,  $P(B)$ , and  $P(F_s)$  at different seasons, we can come to the conclusion that the southern boundary of the auroral zone varies with the seasons. It extends farther south in winter than in summer; it extends farther north in the day than at night. We must also point out

that the critical frequencies of the F2 layer in the auroral zone are quite stable during moderate solar activity. Cases of a significant (above 20%) deviation of  $f_oF2$  from the median values are nearly nonexistent.

We should also point out in this regard the seasonal effect that was observed in [9]. At the same magnetic storm intensity, the currents of the zone of luminescence in winter shift toward lower latitudes than in summer, and this difference increases with an increase in the intensity of the storm. This is yet another indication of the interaction of phenomena in the auroral zone. A more detailed study of the variability in time and space of ionospheric parameters in the auroral and sub-auroral zones, as well as a study of the relationship of this variability to the geomagnetic excitability, would be of /126 great interest.

The authors express their gratitude to the directors of the Leningrad Branch of IZMIRAN (The Institute of Terrestrial Magnetism, the Ionosphere, and Radio Wave Propagation of the USSR Academy of Sciences) for making available the data from the Leningrad Ionospheric Station (Voyeykovo) and also to G. N. Shchegol'kova and I. N. Berezin of the Polar Geophysical Institute for their assistance with calculations and formulating the work.

## REFERENCES

1. Bogacheva, N. A. The ionosphere above Salekhard during the IGY, In: Ionosfernyye Issledovaniya, No. 6 Seriya "Rezultaty MGG" (Ionospheric Investigations, No. 6, Series "Results of the IGY"). Moscow, Academy of Sciences of the USSR Press, 1961, pp. 75 - 81.
2. Potapova, N. I. The E at middle-latitude and circumpolar stations, In: Ionosfernyye Issledovaniya, No. 10, Seriya "Rezultaty MGG" (Ionospheric Investigations, No. 10, Series "Results of the IGY"). Moscow, Academy of Sciences of the USSR Press, 1962, pp. 34 - 47.
3. Glushkova, Ye. P. Preliminary results of a study of magnetic-ionospheric disturbances at Voyeykovo. In: Ionosfernyye Issledovaniya, No. 6, Seriya "Rezultaty MGG" (Ionospheric Investigations, No. 6, Series "Results of the IGY"). Moscow, Academy of Sciences of the USSR Press, 1961, pp. 46 - 51.
4. Ibid. Some features of magnetic-ionospheric disturbances in the transition zone. In: Ionosfernyye Issledovaniya, No. 14, Seriya "Rezultaty MGG" (Ionospheric Investigations, No. 14, Series "Results of the IGY"). Moscow, Academy of Sciences of the USSR Press, 1965, pp. 104 - 116.
5. Ryzhkov, Ye. V., L. M. Shur, and A. I. Rakin: Automatic panoramic ionospheric station. "Elektrosvyaz", No. 5, 1956, pp. 18027.
6. Kosmicheskiye Dannyye (Cosmic Data). IZMIRAN. Moscow, "Nauka" Press, 1964-1965.
7. Gorbushina, G. N. Geographic distribution of anomalous absorption in the Northern Hemisphere. Geomagnetizm i Aeronomiya, Vol. 2, No. 2, 1962, pp. 267 - 274.
8. Shchuka, T. I. The shift of a region of anomalous absorption according to rheometric observations. Geomagnetizm i Aeronomiya, Vol. 5, No. 5, 1965, p. 941 - 942.
9. Glushkova, Ye. P. Distribution of current in the auroral zone as a function of storm intensity, Geomagnetizm i Aeronomiya, Vol. 5, 1965, p. 942 - 943.

HIGH ALTITUDE VELOCITY DISTRIBUTION OF IONOSPHERIC  
DRIFT AND STRENGTH OF THE ELECTRIC FIELD IN THE F2 LAYER

R. S. Sadobnikova

ABSTRACT. The paper discusses the dependence of the velocity of ionospheric drifts in the auroral zone on height: with the increase of height, the drift velocity diminishes. As the drift in the F2 region is carried out mainly under the effect of the electrostatic fields perpendicular to the geomagnetic field, a conclusion is made that the electric field is formed in the dynamo-region. The paper presents the evaluations of the strength of the electric field at the height of 200 km, as well as the sizes of inhomogeneities causing the creation of the electric field which brings about the drifts in the F region.

It is universally recognized that, since the F2 layer is a region of mean free paths for both electrons and for ions, the movement of the ionized gas component in F2 takes place essentially under the influence of electrostatic fields perpendicular to the geomagnetic field.

/127

With respect to the origin of the electric field in the ionosphere, there are two points of view [1]. On the one hand, it is assumed that the electric field arises as a result of the interaction of the solar wind with the lower parts of the magnetosphere and is transported to the ionosphere because of high conductivity along magnetic lines of force. According to the theory of Martin, it originates in the dynamo region. The neutral gas in the lower part of the ionosphere moves under the influence of the tidal forces, taking with it the ionized component. A current is produced which is accompanied by an electric field at the boundaries of the conductivity inhomogeneities. Reaching region F, the electric field produces an inhomogeneous drift ("Motor" effect).

The speed of the drift  $v = cE/H$  [1, 2]. In this expression, the geomagnetic field strength may be taken to be constant, since even for strong disturbances it changes by about 1%. Since the magnetic field changes with altitude as  $R^{-3}$ , where  $R$  is the distance from the center of the Earth in the F layer (200 - 400 km), this change will be about 8%. In order to avoid complicating the problem, we will take  $H = \text{const}$ . If the altitude distribution of the drift velocity  $v$  in the F region (and possibly in E) is known one can calculate where the electric field originates -- higher or lower than the region under consideration.

Based on the drift velocity of very small scale inhomogeneities made at the Polar Geophysical Institute at Loparskaya in 1958 - 1964, graphs were compiled of the dependence of the drift velocity on the altitude in the F2 layer (Figure 1). As can be seen in the figure, with an increase in height, the speed, and consequently the electric field, decreases. This fact shows that at high latitudes, an electric field is produced below the F2 layer, apparently in the dynamo region (layer E).

In Figure 2, histograms are presented of the distribution of the number of observations in a day for altitudes  $< 300$  and  $> 300$  km. It can be seen that in the daytime there were more frequent observations of reflections from lower altitudes and, on the other hand, during the night there were reflections from  $> 300$  km. Graphs for day and night observations (Figure 3) were compiled separately, in order to establish whether the altitudinal drift velocity distribution shown in Figure 1 is a reflection of the altitudinal diurnal pattern of the reflecting region. It may be seen from the graphs that the drift velocity decreases with altitude during both the night and the day. Therefore, it may be assumed that the dependence  $v(h)$  shown in Figure 1 corresponds to an altitudinal drift distribution, and not to a time distribution. It is even possible that the diurnal pattern of the drift velocity is due to its altitudinal distribution: during the daytime, observations were performed at low altitudes, and therefore, the drift velocity is greater in the daytime.

/128

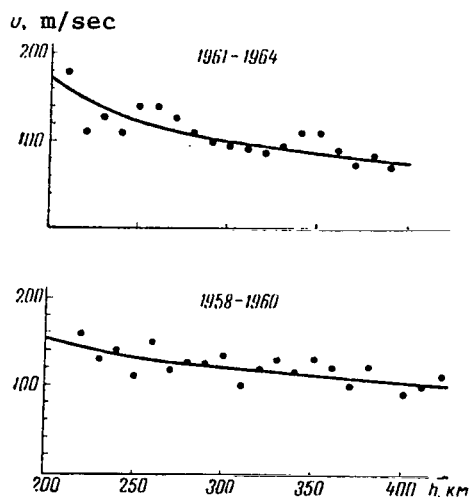


Figure 1. Dependence of drift velocity on altitude.

If the ionosphere conductivity along the magnetic force lines and perpendicular to them is known, we may calculate the electric field strength  $E$  as a function of altitude [4, 5]. Let us assume that an electric field arises at the boundaries of the inhomogeneities having the form of the horizontal layer with the width  $l$  and extended along the parallel. In the region  $F$  this field produces a horizontal electromotive force equal to  $E_0$  at an altitude of 200 km. Let us investigate the electric linear diagram (Figure 4). The resistance of sections  $A_0A_1, B_0B_1, \dots, A_nA_{n+1}, B_nB_{n+1}, \dots$  equals  $R$ . The resistance of the leakage, i.e., sections  $A_1B_1, \dots, A_nB_n, \dots$ , equals  $r$ .

The distance  $A_0B_0, \dots, A_nB_n, \dots$  equals  $l$ .

Let us introduce the current profiles as shown in Figure 4. The Kirchhoff equation for the section  $A_{n-1}A_n B_{n-1}B_n$  will have the form

$$i_{n-1} + i_{n+1} = 2 \left( 1 + \frac{R}{r} \right) i_n.$$

This linear difference equation of second order has two linearly independent solutions  $e^{\alpha n}$  and  $e^{-\alpha n}$ , where  $\alpha$  is determined for the equations

$$\operatorname{sh} \frac{\alpha}{2} = \frac{1}{2} \sqrt{\frac{2R}{r}}, \text{ т. е. } \alpha = \sqrt{\frac{2R}{r}}$$

within an accuracy of small terms of the third order, since the conductivity along the magnetic force line is greater than it is perpendicular to it ( $r \gg R$ ). Since the field decreases with altitude, the solution of  $e^{\alpha n}$  does not satisfy the condition  $i_n$ , for  $n \rightarrow \infty$ .



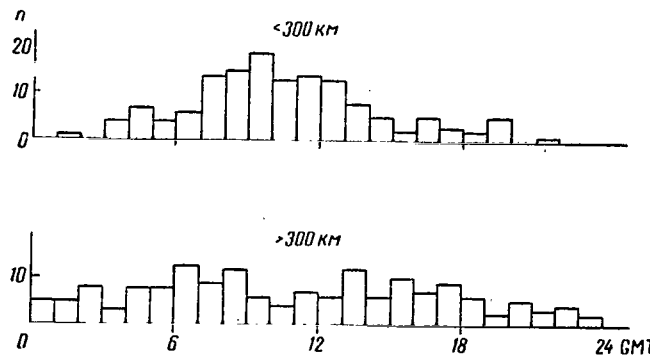


Figure 2. Histogram of the number of observations for the reflection altitudes  $<300$  km and  $>300$  km (1961-1964).

/129

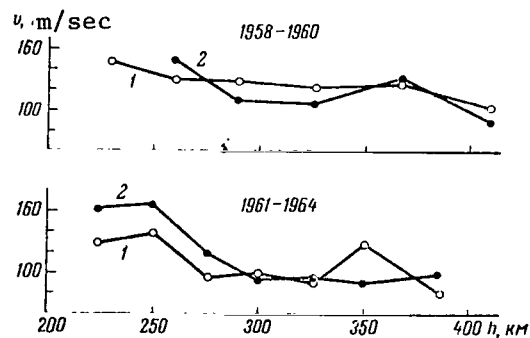


Figure 3. Dependence of drift velocity on altitude for day (1) and night (2) observations.

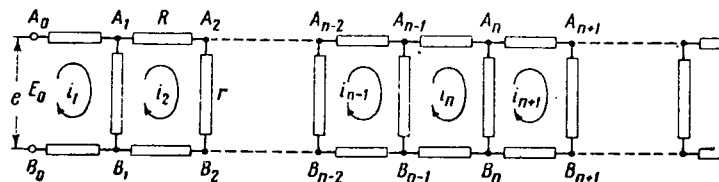


Figure 4. Altitudinal distribution of the electric field in the ionosphere .

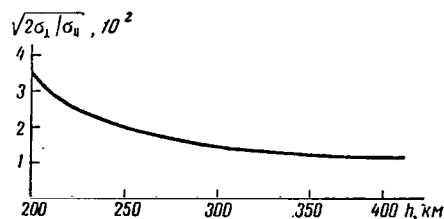


Figure 5. Dependence of  $\sqrt{2\sigma_{\perp}/\sigma_{\parallel}}$  on altitude.

We thus have

$$E_n = ri_n = Ae^{-zn}.$$

The coefficient A may be determined from the condition that the initial field equals  $E_0$

$$E_n|_{n=0} = Ae^{-zn}|_{n=0}.$$

Since  $A = E_0$ , we have

$$E_n = E_0 e^{-zn}. \quad (1)$$

Let us now turn to the case with continuously distributed leakage. Since the current flows along the entire thickness  $l$ ,  $R = dx/\sigma_{\parallel} l$ , where  $\sigma_{\parallel}$  is the conductivity along the magnetic force line. The leakage resistance  $r = l/\sigma_{\perp} dx$ , where  $\sigma_{\perp}$  is the conductivity perpendicular to the magnetic force lines, and  $n = \frac{z}{dx}$ . Substituting these values in Equation (1), we obtain /130

$$E = E_0 e^{-\frac{x}{l} \sqrt{\frac{2\sigma_{\perp}}{\sigma_{\parallel}}}}.$$

If the value of  $\sigma_{\perp}/\sigma_{\parallel}$  changes with altitude, we may assume

$$E = E_0 e^{-\frac{1}{l} \int_{x_0}^{x_1} \sqrt{\frac{2\sigma_{\perp}}{\sigma_{\parallel}}} dx}$$

or

$$v = v_0 e^{-\frac{1}{l} \int_{x_0}^{x_1} \sqrt{\frac{2\sigma_{\perp}}{\sigma_{\parallel}}} dx}$$

The values of  $\sigma_{\parallel}$  and  $\sigma_{\perp}$  were taken from data in [6].

Figure 5 shows the dependence of  $\sqrt{2\sigma_{\perp}/\sigma_{\parallel}}$  on altitude. Figure 6 gives graphs showing the dependence of  $v_0/v$  on altitude for various values of  $l$ .

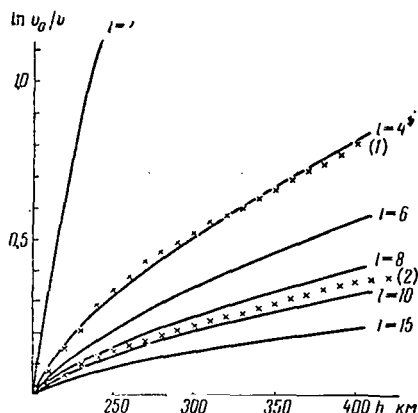


Figure 6. Dependence  $\ln v_0/v$  on height  $h$  for different values  $l$ . Solid line, calculated curve. Crosses, experimental data.

$0.8 \cdot 10^{-4}$  V/cm, which closely coincides with results obtained by S. J. Akasofu and S. Chapman [7]. This value is the same during years of maximum and minimum solar activity. The fact that the drift velocity in the E layer does not change with an increase of the K-index of magnetic activity, while it increases in the F2 layer [8], may be explained by the fact that the dimensions of the inhomogeneities are greater and the velocity change with altitude is less during great activity.

## CONCLUSIONS

The drift velocity in the F2 layer decreases with increase in altitude. Consequently, the electric field decreases in an upward direction, i.e., it apparently rises in the dynamo region. The inhomogeneities producing it are several kilometers in size. The inhomogeneities increase in size when the magnetic activity increases.

In conclusion, I would like to thank M. I. Pudovkin for valuable advice in this work.

The crosses plot curves obtained from experimental data for years of minimum (1) and maximum (2) solar activity. It may be seen from graphs that the experimental curves coincide quite well with the theoretical ones. The electric field is produced by inhomogeneities which are several centimeters in size. When the solar activity increases, the inhomogeneities increase in size, since during years of a maximum the electric field decreases more slowly with altitude than it does during the years of a minimum. The electric field calculated from experimental data was found to be

#### REFERENCES

1. Bostrom, R. A model of the auroral electrojets. J. Geophys. Res., Vol. /131 69, No. 23, 1964, p. 4983.
2. Frank-Kamenetskiy, D. A. Lektsii po fizike plazmy (Lectures on plasma physics) Atomizdat 1964.
3. Sadovnikova, R. S. Dreyf neodnorodnostey v sloye F2 po nablyudeniya v Loparskoy (Drift in inhomogeneities in region F2 based on observations at Loparskaya). In press.
4. Smith, V. Electrostatics and Electrodynamics. Moscow, IL, 1954.
5. Batygin, V. V. and N. I. Toptygin. Sbornik zadach po elektrodinamike (Collection of problems in Electrodynamics). 1962.
6. Mitra, S. K. The upper atmosphere. Moscow, IL, 1955.
7. Akasofu, S. J., and S. Chapman. A study of magnetic storms and auroras. Sci. Rept. Geophys. Inst. Alaska, 1961, UAG-R112.
8. Mikrotan, S. F., and Yu. V. Kushnerevskiy. Non-uniform structure and movement in the ionosphere. In: Ionosfernyye issledovaniya (Ionospheric Studies), No. 12. Series MGG Results. Moscow, "Hauka" Publishing House, 1964.

## PROBLEMS OF AURORAL ABSORPTION

O. I. Shumilov

**ABSTRACT.** The paper analyses about 100 bays of auroral absorption according to the materials of rheometric absorption from December 1963 till December 1964, obtained at the station Loparskaya ( $\phi = 68^{\circ}37'$ ,  $\lambda = 35^{\circ}17'$ ). The paper also shows that the subtypes of auroral absorption recognized earlier by different authors are connected with each other. The diurnal pattern of the rate of changes of the ionization agent intensity is probably responsible for the diurnal changes of the form in separate cases of auroral absorption.

Studies with the help of noise absorption rheometers of cosmic radio /132  
sources in the lower ionosphere were initiated in 1956 [1]. The efforts of many researchers have made it possible at the present time to distinguish between four types of anomalous radio wave absorption in the ionosphere [2, 3]. One of these is auroral absorption, which has been given this name due to its relationships with the visible aurora polaris. This absorption is observed at latitudes close to the zone of aurora polaris. Its maximum is located somewhat to the south [4]. Auroral absorption is very irregular, and its individual peaks are separated by several minutes, although it may continue for several hours. It changes greatly from month to month along the zone of the aurora polaris and is related to local magnetic disturbances. The term "auroral absorption" is used when anomalous absorption is studied at latitudes of the aurora polaris zone during the daytime, i.e., when visual observations of aurora polaris are impossible in general [5].

Many works have been published recently which have attempted to distinguish between the individual subtypes of auroral absorption. These studies may be divided into two groups depending on which criterion they use as a basis for classifying cases of absorption. The first classification group uses the

different connection between auroral absorption and the accompanying geophysical phenomena "auroral polaris, local magnetic disturbances" [6 - 8]. The second group distinguishes between the subtypes of absorption on the basis of external indices: smooth or sharp increase, large or small extension, monotonic or pulsing nature [5, 9-11]. For example, three types of auroral absorption F, S, P, were distinguished in [9]. Type F are absorption bursts reaching a maximum in several minutes. They are primarily observed at night, and are related to aurora flares having a radial form. Type S represents the case when the absorption increases in approximately 30 minutes. They are observed primarily in the morning hours and are much longer than absorption of type F. R. R. Brown [11] has called the same phenomenon slow absorption events. Type S is especially interesting, since there is a maximum in the diurnal absorption pattern in the morning hours, as Bassler has shown [4].

Type P is pulsing absorption, which is usually superimposed on S-absorption. Brown [11] also studied it. Figure 1 presents examples of absorption of type F and S observed on February 13, 1964. The local time ( $30^{\circ}$  E) is plotted along the abscissa; the absorption in decibels is plotted along the ordinate axis. As Ansari has shown [5], S-absorption, observed in the late morning hours (near noon) is much longer than the usual S-events, [9, 11]. It may thus be characterized as a special type, since it has several distinguishing features (Figure 1; absorption, May 1, 1964.). /133

At first glance, it makes a great deal of sense in physical terms to distinguish between individual subtypes of auroral absorption, making use of their differing relationship with visible auroral polaris and local magnetic disturbances, since the "criterion of form" is somewhat formal. However, this is not absolutely correct. In all studies pertaining to the second group, after the subtype was identified with the formal characterization, its relationship with the visible aurora polaris and local magnetic disturbances was steady. It was found that no matter which basis of classification was used, several subtypes developed by different authors arose; namely phase SAI (sudden absorption increase) [6] corresponds to type F [9]; and phase SVIA (slowly varying intense absorption) [6] corresponds to type S [9]. Classification by form

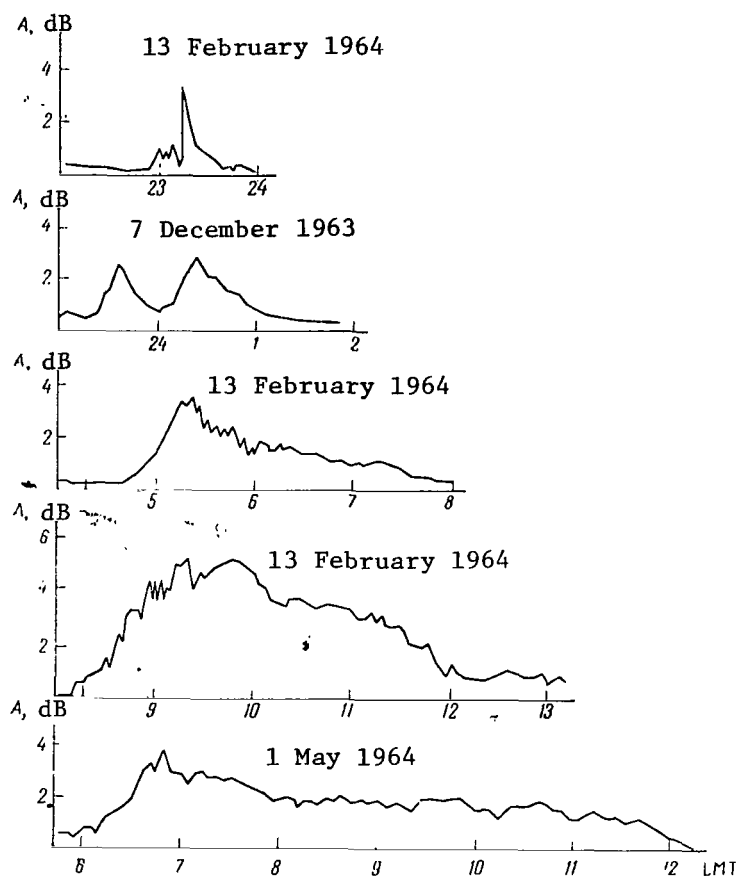


Figure 1. Examples of auroral absorption.  
Time LMT (30°E).

which pertain only to it. The relationship between each of the subtypes or auroral absorption is not clear: whether they are special phenomena or whether they can be combined and explained by a certain physical process which is responsible for changes in the auroral absorption during one day. The purpose of this study is to answer this question.

Analysis was made of data derived from measuring absorption of cosmic radial emission obtained at Loparskaya at the Polar Geophysical Institute base ( $\varphi = 68^{\circ}37'N$ ,  $\lambda = 35^{\circ}17'E$ ) from December 1963 to December 1964. The rheometer operated at frequency of 32 MHz. The antenna—a wave channel having five

has several advantages over classification employing the, differing relationships between auroral absorption and the visible aurora polaris /134 and local magnetic disturbances. This is due to the fact that such factors as a zero point in the diurnal pattern of magnetic disturbances ( $20.8 - 10^h$  LMT) [8, 12] and the impossibility of visual observations of the aurora polaris during the daytime have no influence upon this type of classification.

Each of the types F, S, of the S-diurnal type is most clearly observed at a specific local time, and is characterized by several features

elements—was directed toward the pole of the sea. Elementary cases were studied during the analysis (for example, Figure 1). It was found that the time pattern of absorption preceding and after the maximum may be represented in the form of the following expressions:

$$A_t = A_{\max} e^{-\frac{t-t_0}{\tau_d}}, \quad A_t = A_{\max} e^{+\frac{t-t_0}{\tau_{in}}}, \quad (1)$$

where  $A_{\max}$  is absorption at the maximum for a given elementary absorption event;  $A_t$  is absorption at a given moment of time when absorption increases or decreases;  $t_0$  is time of absorption maximum;  $\tau_d$ ;  $\tau_{in}$  is characteristic time of decrease or increase in absorption. It is clear from Figure 1 that  $\tau_d$  does not equal  $\tau_{in}$ .

All absorption events which satisfied the following conditions conditions were analyzed.

1. Absorption at the maximum must be no less than 2 decibels. This value was chosen for the following considerations: Brown [11] showed that the majority of absorptions of S have the amplitude of 2 decibels. It was noted in [12] that the maximum of type S absorption is observed in the zone of the aurora polaris. Therefore, by studying  $A \geq 2$  decibels, we excluded with great probability those absorption events which could have been recorded by the side lobes of the rheometer directional pattern.

The absorption level preceding and after the event in consideration could not be greater than 0.5 decibels. The only exception was those April events of extremely great absorption, when the level of the "background" equals 1 decibels.

3. During the day under consideration, if the given type of absorption had two, three, or more maxima of approximately equal magnitude with intermediate minima amounting to no less than half the maxima, then  $\tau_{in}$  was selected before the first maximum, and  $\tau_d$  after the last maximum.



About 100 events were studied in all. The overwhelming majority (85%) had a "correct" form which satisfied expression (1) quite well.

Figure 2 shows the diurnal pattern of  $\tau_d$  for all the absorption events studied. The local time ( $30^\circ\text{E}$ ) of the maximum is plotted along the abscissa axis, while the  $\tau_{in}$  values are plotted in minutes along the ordinate axis. In spite of the great scatter of the points, it is apparent that, after local midnight, there is a clear increase in the values of  $\tau_{in}$  before  $11^{\text{h}}$  LMT. At  $11 - 15^{\text{h}}$  LMT the scatter of the points is so great that no conclusion may be reached at this time regarding the behavior of  $\tau$ . Therefore, all events in the crosshatched time interval were excluded from the overall investigation./135

The diurnal pattern of the values of the  $\tau_d$  averaged over one hour is shown in Figure 3. It is interesting to note that the scatter of  $\tau_d$  is comparatively small. This means that in the analyzed intervals there is a continuous increase in the values of average of  $\tau_d$ . From 3 - 11 hours there is a linear increase in the values of  $\tau_d$  depending on the distance of the stations from the northern meridian.

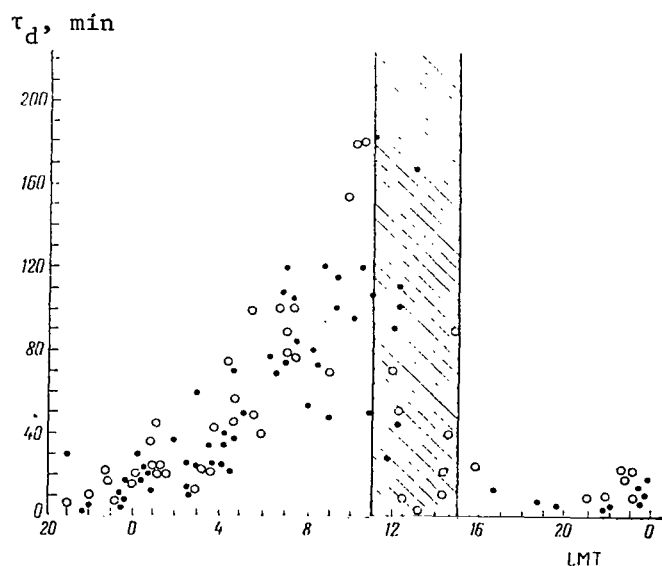


Figure 2. Diurnal pattern of  $\tau_d$  for all the studied absorption events. LMT ( $30^\circ\text{E}$ ) time.

circles - absorption observed in the summer and partially in months of the equinox (April, September); dots - in winter months. The crosshatched section - the time interval encompassing the events not investigated.

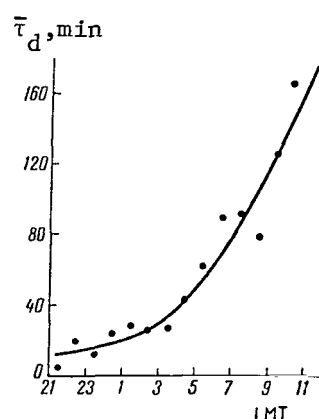


Figure 3. Diurnal pattern of LMT (30°E) time. Averaging interval - 1 hour.

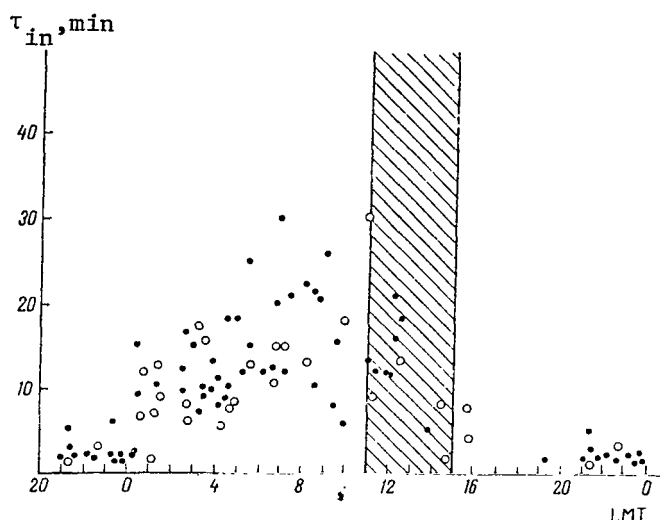


Figure 4. Diurnal pattern of  $\tau_d$  for all absorption events studied. LMT (30° E) time. Notation, same as in Figure 2.

Since the majority of authors upon classifying the subtypes of auroral absorption analyzed the absorption increase rate up to the maximum [9 - 11], while in [5, 9, 11] this characteristic determines the type of absorption. Figure 4 gives the diurnal pattern of  $\tau_{in}$  for all the absorption events considered. Just as previously, the crosshatched region is excluded in the investigation. Figure 5 presents the values of  $\tau_{in}$  averaged over one hour. It may be seen that from 0 to 11h LMT  $\tau_{in}$  increases almost linearly as the distance of the station from the northern meridian increases.

Thus, we may reach the conclusion that, for local events of auroral absorption, there is a gradual but continuous increase in  $\tau_d$  and  $\tau_{in}$  depending on the local time (or depending on the distance of the station from the northern meridian) in the 1 - 11<sup>h</sup> LMT interval.

It is interesting to note that a change in  $\tau_d$  and  $\tau_{in}$  depending on local time (Figures 3 and 5) closely coincides with the results obtained by different authors; namely type F[6, 9, 10], which is characterized by an absorption

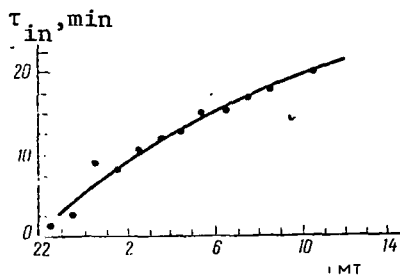


Figure 5. Diurnal pattern of  $\tau_{in}$ . LMT (30° E) time. Averaging interval - 1 hour.

increase in several minutes, is observed at close to local midnight, while type S (increase in 30 minutes) is observed approximately at 4 - 6<sup>h</sup> LMT [6, 9, 11]. Finally, the absorption type introduced by Ansari [5] which has a still longer duration, is observed in the early morning (around noon) hours. However, as these data have shown, all types of absorption (F, S, S-diurnal) are interrelated. If we use the criterion of form for classification, it may be noted that type F

absorption which is observed at midnight gradually—and not abruptly—changes into type S absorption in the early morning hours. Then around noon it changes to type S-diurnal absorption. It may therefore be assumed that all these absorption types are determined by a single physical process whose diurnal pattern is responsible for the change in the absorption form. Such processes may be the diurnal pattern of the recombination coefficient and the diurnal pattern of the rate at which the intensity of the ionizing flow changes.

Actually, if it is assumed that the main flow of intruding particles is stopped or almost stopped at the absorption maximum, then the absorption decrease may be represented as a recombination process following the law [13]:

$$\frac{dN_e}{dt} = -\beta N_e, \quad (2)$$

where  $N_e$  is the electron density;  $\beta$  is the constant coefficient which depends on 137 atmospheric density and not on electron concentration. Expression (2) holds when the concentration of free electrons decreases due to their adhesions to neutral atoms, as a result of which many negative ions are formed.

The diurnal pattern of the absorption form could possibly be explained by investigating the separation of electrons from negative ions as the ionospheric illumination increases (based on the position of the crosses and circles in Figures 2 and 4; this is very difficult to represent). However,

by analyzing the rapidly and smoothly changing events of auroral absorption, we reach the conclusion [14, 15] that the relationship  $N_e \gg N^-$  holds for them (i.e., the concentration of negative ions is small as compared to the electron concentration). Since we do not know any other recombination process which can explain the observed change in the local absorption form as a function of local time, we must then investigate the second possibility -- namely, that the diurnal pattern of the rate at which change occurs in the intensity of the intruding particle (electron) flow (which is responsible for the auroral absorption). This explanation is even more possible since direct measurements of the rate at which the electron flow intensity changes on balloons [16] closely coincide with the results obtained in this study. The values of  $\tau_d$  calculated with data from [16]  $\tau_d$  for the decrease in the electron flow intensity lie closely along the absorption curve of  $\tau_d$  shown in Figure 3. However, it must be noted that close to local midnight  $\tau_d$  of local events of auroral absorption can be determined by the rate of recombination, as was done in [8]. This is due to the fact that at this time the rate at which the electron flow changes is greater than the recombination rate. However, as the station recedes from the northern meridian, the reason for the change in form of individual events of auroral absorption may more and more be found in the diurnal pattern of the rate at which the intensity of the ionizing agent (electrons) changes.

## CONCLUSIONS

1. It is impossible to draw a distinction between individual subtypes of auroral absorption introduced by several authors, if the rate at which absorption increases in each individual case is used as the classification criterion. It decreases smoothly in the 1 - 11<sup>h</sup> LMT interval, which leads to a gradual change in the form of absorption.

2. The diurnal pattern of the rate at which the intensity of the ionizing agent (electrons) changes is apparently responsible for the diurnal pattern of the auroral absorption form.

The authors are indebted to B. M. Yanovski and M. I. Pudovkin for valuable advice and interest in this work.

# REFERENCES

1. Little, C. G. Some measurements of high-latitude ionospheric absorption /138  
using extraterrestrial radio waves. Proc. IRE, 1 Vol. 46, 1958, p. 334.
2. Reyd, G. K. and K. Kollinz. Observations of anomalous absorption of radio waves in the ultrashort wave range at middle and higher latitudes. In: Pogloshcheniye radiovoln v polyarnoy shapke (Absorption of radio waves in the polar cap), Moscow, Mir Publishing House, 1965.
3. Ortner, J., B. Hultqvist, R. R. Brown, T. Hartz, O. Holt, B. Landmark, J. L. Hook, and H. Leinbach. Cosmic noise absorption accompanying geomagnetic storm sudden commencements. J. Geophys. Res., Vol. 67, No. 11, 1962, p. 4169.
4. Basler, R. Radio wave absorption in the auroral ionosphere. J. Geophys. Res., Vol 68, No. 16, 1963, p. 4665.
5. Ansari, Z. A. A peculiar type of daytime absorption in the auroral zone. J. Geophys. Res., Vol. 70, No. 13, 1965, p. 3117.
6. Ansari, Z. A. The aurorally associated absorption of cosmic noise at College Alaska. J. Geophys. Res., Vol. 69., No. 21, 1964, p. 4493.
7. Pugovkin, M. I., and O. I. Shumilov. Intensity of auroral absorption as a function of the time of day and type of geomagnetic disturbance. In Press.
8. Pudovkin, M. I., R. G. Skrynnikov, and O. I. Shumilov. Magneto-ionospheric disturbances in the zone of polar aurora. Geomagnetizm i Aeronomiya. Vol. 4, No. 6, 1964, p. 1094.
9. Berkey, F. T. and R. Parthasarathy. An investigation of selected types of radio wave absorption in auroral zone. Sci. Rept. Geophys. Inst. Alaska, 1964, UAG-R151.
10. Parthasarathy, R. and F. T. Berkey. Auroral zone studies of sudden-onset radio wave absorption events using multiple-station and multiple-frequency data. J. Geophys. Res., Vol. 70, No. 1, 1965, p. 89.
11. Brown, R. R. A study of slowly varying and pulsating ionospheric absorption events in the auroral zone. J. Geophys. Res., Vol. 69, No. 11, 1964, p. 2315.
12. Ortner, J., and W. Riedler. A smooth type of cosmic noise absorption. Nature, Vol. 204, No. 4964, 1964, p. 1181.
13. Chamberlain, J. Physics of Polar auroral and atmospheric studies, Moscow, Leningrad, 1963,.

14. Brown, R. R. and J. R. Barcus. Day-night ratio of auroral absorption events associated with negative magnetic bays. J. Geophys. Res., Vol. 68, No. 14, 1963, p. 4175.
15. Brown, R. R. Day-night ratio of auroral absorption for break-up events. J. Geophys. Res., Vol. 69, no. 7, 1964, p. 1429.
16. Brown, R. R., and R. J. Barcus. Balloon observations of auroral zone electron precipitation events. J. Geophys. Res., Vol. 68, No. 22, 1963.

MAGNETIC ACTIVITY AT HIGH LATITUDES OF THE NORTHERN  
HEMISPHERE DURING THE MAXIMUM AND MINIMUM OF THE SOLAR CYCLE

R. G. Afonina and Ya. I. Fel'dshteyn

**ABSTRACT.** The paper presents the results of the analysis of the space-time distribution of intensity of geomagnetic disturbances in the IGY - IQSY periods with the help of equivalent ranges of K-indices according to the data from the high-latitude observatories of the northern hemisphere. This analysis is premised by a summary of the main regularities of magnetic activity in high latitudes, obtained with the K-index application.

The results obtained are as follows:

1. At  $\Phi' > 70^\circ$  the magnetic activity remains at high level also in the years of the minimum of the solar activity cycle.
2. The region of the maximum values  $r_K$  in the coordinate system "corrected geomagnetic latitude<sup>K</sup> -- geomagnetic time" is of an oval form, located in higher latitudes by day and in lower ones at night.
3. With the increase of  $K_p$  the region of the maximum disturbance is removed to the lower latitudes, but in all cases it preserves an oval form.

The displacement of the oval of the maximum magnetic disturbance agrees well with the dynamics of the auroral belt.

A number of extensive investigations are devoted to the study of the space- /139  
time distribution of magnetic activity at high latitudes. The magnetic activity is measured by diverse indices; hence, their utilization naturally results in rather distinct deductions relative to the regularities of its distribution. The indices utilized in the literature can be separated into

two fundamental groups which differ in time resolution, three- or one-hour.

The index  $K$  is defined by the maximum amplitude of the oscillations of three geomagnetic field components in a three-hour interval adjusted for a quiet day and expressed in points. It was introduced into magnetic observatory practice in 1939 [1] for the total characteristics of the magnetic field variation. It is often utilized in analyzing disturbances because of the simplicity of the definition and the accessibility of data from a planetary network of magnetic observatories.

The most extensive investigations of the magnetic disturbances in terms of the index  $K$  are in [2 - 8]. Indexes with a one-hour time resolution ( $r_H$ ,  $Q$ ) have been utilized in investigations [9 - 13]. Application of hourly indices to study the diurnal variation in magnetic activity is an indisputable advantage [12, 14], and the fact that three-hour indices have been used in a number of researches up to now can be explained only by the fact that very few stations [15] publish the  $r_H$  and  $Q$  characteristics. Dissatisfaction with the description of diurnal changes in activity by the three-hour characteristics resulted in Canadian researchers' rejecting completely the recording of the  $K$  indices at the high-latitude Resolute Bay, Baker Lake and Churchill observatories, and going over to hourly amplitudes despite international recommendations.

In connection with some discrepancies in the morphology of the magnetic activity at high latitudes during the IGY—discrepancies which has been obtained on the basis of hourly indexes [12, 13] and three hour indexes [7, 8]—it would be interesting to clarify whether or not such a discrepancy results from the roughness of the methodology for determining the latitude and time distributions of the magnetic activity when utilizing the three-hour characteristics. We prefer a brief survey of the results of studying the regularities of magnetic activity at high latitudes, obtained by using the index  $K$ , to such an analysis. A survey of analogous results according to the hourly index  $r_H\gamma$  is presented in [12, 13].



Latitudinal changes in the amplitude and phase of the first and second harmonics were analyzed in [2] after the diurnal changes in K had been expanded into the harmonic series  $S_a = \sum C_n \cos (nt - \alpha_n)$ . It turned out that the first phase of the harmonic varied between  $0^\circ$  at  $\Phi \sim 65^\circ$  to  $150^\circ$  at  $\Phi \sim 80^\circ$ . The phenomenon hence proceeds in a sufficiently individual fashion, and will sometimes differ in close-lying observatories. Representing  $S_a$  as the sum of two terms dependent on universal and local time, respectively

$$S_a = S(t) + S(T),$$

the author [2] found that there is no component dependent on universal time in  $S_a$  (at least in the middle latitudes).

The magnetic activity in observatories located at identical geomagnetic latitudes, but at different longitudes, is sometimes quite substantially different. Hence, it was assumed that the "longitudinal terms" of  $S_a$  can be associated with singularities in the ionosphere, which is inhomogeneous along a geomagnetic parallel, and with the inhomogeneous conductivity of the Earth, which causes a dependence of the current induced in the Earth on the longitude. The "longitudinal terms" in  $S_a$  can be represented by series in universal time, but this representation will be formal in nature, without any specific physical meaning. The form of  $S_a$  at high latitudes is checked better by the distance of the observatory from the aurora borealis zone (the corrected geomagnetic latitude  $\Phi'$ ) than by the geomagnetic latitude. Seasonal changes in  $S_a$  occur as a result of seasonal oscillations in the part  $S(t)$  rather than because of the annual change in the slope of the geomagnetic dipole axis to the plane of the ecliptic (universal time effect).

Fundamental investigations of the magnetic activity at high latitudes have been performed in [3]. The change from the index K in points to equivalent amplitudes by means of the relation

$$r_K = \frac{\sum r_{iK} N_i}{\sum N_i},$$

(where  $r_K$  is the mean three-hourly equivalent amplitude of  $\gamma$ ;  $r_{iK}$  is the three-hour amplitude for the index  $K$  of point  $i$ ;  $N_i$  is the number of  $K$ -indices of points  $i$ ) gave a comparison between values of the magnetic disturbance for various observatories which utilized different scales to record the index  $K$ .

It has been shown that the calculated equivalent amplitudes do not differ by more than 5% from the three-hour amplitudes measured directly on magnetograms. Processing the magnetograms of a number of stations by using scales for which the lower boundary of the index  $K$  is 1000, 1500 and 2000  $\gamma$  showed that the magnitude of the equivalent amplitudes is independent of the scale choice.

Therefore, a methodological basis for measuring the magnetic disturbance in a three-hour period in absolute units by going from the indices  $K$  in points (tables are published regularly by the International Index Service) to equivalent amplitudes  $r_K$  has been developed in [3]. The magnetic disturbance of 49 magnetic observatories at high latitudes of the northern and southern hemispheres was analyzed by means of  $r_K$ , primarily in IPY (International Polar Year) I and II. Two kinds of magnetic activity were investigated in detail, the nocturnal and the diurnal, which are characterized by different seasonal changes which achieve the greatest intensity at declination of  $1 \sim 77^\circ$  at night and  $1 \sim 85^\circ$  during the day.

The time at which the activity maximum appears changes with latitude. It turns out that the latitudinal distribution of the average daily values of the activity, the time of appearance of the maxima, the separation of the stations into those having only daytime and those having only nighttime activity is ordered /141 essentially if the inclination at a 5000 km altitude is utilized in place of the geomagnetic latitude or the inclination at the Earth's surface. Presented in Figure 1 from [3] are changes in the average daily values of the equivalent amplitudes as a function of the inclination. The great difference in average daily values at observatories with approximately identical inclination, but located at different longitudes, is noticeable. The scatter of the points

indicates a considerable longitudinal effect in the average daily values of  $\bar{r}_K$ . The data from stations with the same kind of activity located at equal  $I$ , but at different longitudes were averaged to eliminate the longitudinal difference. This permitted obtaining the latitude history of  $r_K$  for which the disturbance varies smoothly with inclination.

Latitudinal changes of  $r_K$  are presented in [3] for individual seasons only for values averaged with respect to the longitude (Figure 2). The nocturnal disturbance achieves the highest values at the equinox, and the diurnal, in the summer. As the disturbance level increases, the nocturnal disturbance ( $I \sim 77^\circ$ ) is magnified sharply. It is much stronger than the diurnal disturbance (Figure 3).

Changes in the magnetic activity ( $S_a$ ) were investigated in [4], according to data from a planetary network of magnetic observatories. However, in contrast to [3], where the change from the indices  $K$  to the equivalent amplitudes had been accomplished, latitudinal changes in the phase and amplitude of  $S_a$  in fractions of the index  $K$  are considered in [4]. Since this makes the possibility of comparing the amplitudes of variations in stations at different latitudes difficult, we shall not consider the results obtained in [4] in detail, particularly since IGY data were again analyzed by the same authors in [7,8] with more material (with the change to equivalent amplitudes).

The latitudinal dependence of the geomagnetic disturbance according to the three-hour index along the midday and midnight meridians during the IGY and IPY has been obtained in [5]. It was calculated for definite cycles of inclination of the geomagnetic dipole axis with respect to the plane of the /142  
ecliptic. Therefore, a change in  $S_a$  due to the diurnal and seasonal change of this angle (influence of universal time) was excluded. The change in  $r_K$  with latitude has been obtained for a definite orientation of the geomagnetic dipole by superposition of the data of many observatories dispersed at different longitudes, with different universal time periods, and for different months, but all satisfying one demand — a definite orientation of the dipole axis relative to the plane of the ecliptic. Assuming that the polarity of the

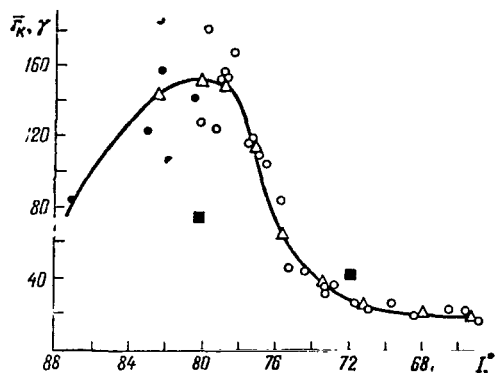


Figure 1. Change in  $\bar{r}_K$  for stations in the northern hemisphere during the Second IPY.

Magnetic declination is reduced to a 5000km altitude. Triangles show average data from a group of observatories through which a smooth curve has been drawn. Squares denote the Barrow and Yakutsk observatories, not part of the average.

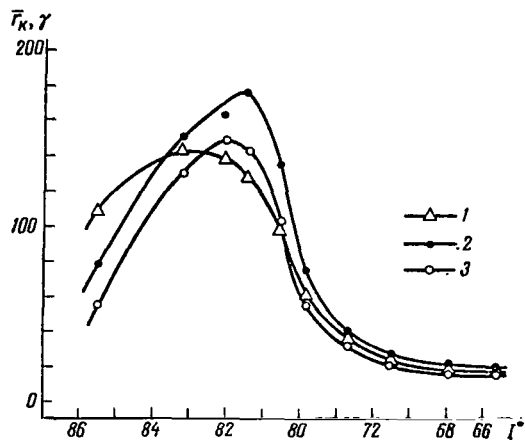


Figure 2. Seasonal changes in  $\bar{r}_K$   
1.- summer; 2-equinox; 3-winter

geomagnetic field does not influence the distribution of the geomagnetic disturbance, the author [5] utilized data from both hemispheres. The scatter of the points over the latitudinal sections is sufficiently great is due primarily to longitudinal effects. Hence, smoothed curves were drawn through points yielding a disturbance of stations within  $\pm 22.5^\circ$  longitudes from the geomagnetic meridian passing through the geographic and geomagnetic poles. It will later be shown [16] that the spread diminishes substantially if the corrected geomagnetic latitude ( $\phi'$ ) is utilized according to [17,18], instead of the geomagnetic latitude; however, it remains sufficiently substantial at  $70 - 80^\circ$  latitudes.

The dependence of  $r_K$  on  $\phi'$  for different geomagnetic dipole orientations for planetary indices of magnetic activity  $K_p = 0, 2, 4, 6$  is presented in Figure 4 from [16].

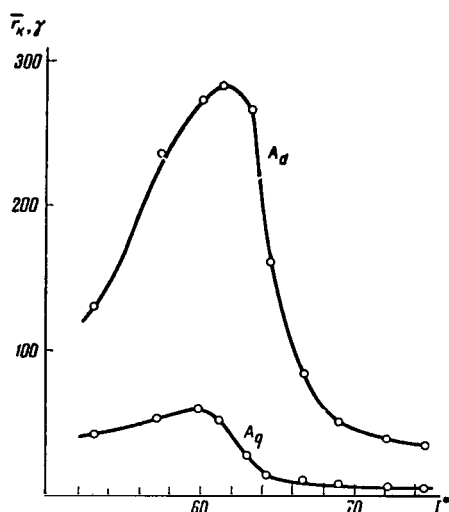


Figure 3. Changes in  $\bar{r}_K$  per year during international disturbed  $A_d$  and quiet  $A_q$  days.

It follows from the results presented:

1. The maximum disturbance on the night side is located at identical latitudes in both the summer and winter seasons (lower and upper part of the graph for a 11.5 and 23° slope angle, respectively). On the day side, the maximum disturbance is located at higher latitudes in summer than in winter.

2. For moderate  $K_p$  the latitude of the maximum disturbance region is greater in the daytime than at night in both summer and winter. The shift of the maximum disturbance region towards the equator as  $K_p$  increases is more substantial around the midday meridian than along the midnight meridian. Therefore, the maximum disturbance region is not a circle of constant latitude. It is an oval in a polar projection, even if the corrected geomagnetic latitude is used as a coordinate.

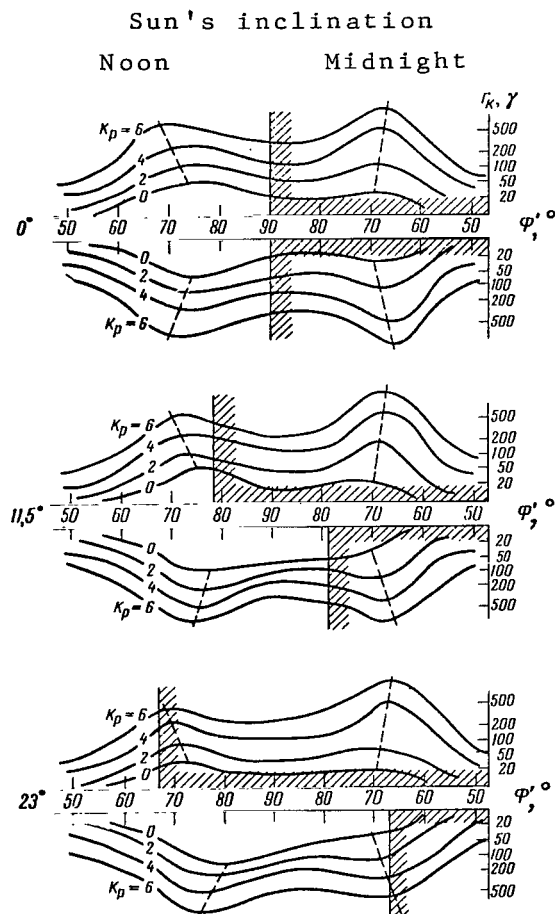


Figure 4. Dependence of the value of the geomagnetic disturbance on  $\phi'$  along the midday-midnight meridian for dipole axis declinations of 0, 11.5, and 23° relative to the plane of the ecliptic for  $K_p=0,2,4,6$ , during IGY.

It should be noted that the passage from K-indices to  $r_K$  in [5] was done by a method rather different from that utilized in [3, 6-8]. Graphs of the dependence of K on  $K_p$  at noon and midnight were first constructed for each month at each station for separate three-hour intervals. The value of K, which was transferred into the equivalent amplitude by means of the known point scale of the index K at a given observatory, was determined from these graphs for  $K_p = 0, 2, 4, 6$ .

An assumption of the existence of a functional relationship, or at least a correlation, between  $K_p$  and the local index K at a specific observatory underlies such a method of determining the equivalent three-hour amplitude. Such correlation dependences have been obtained in [5]. The index  $K_p$  is determined from the data of 12 observatories located at subarctic latitudes; hence, it characterizes primarily the intensity of nighttime magnetic disturbances, which are most intense at  $\phi' \sim 65^\circ$ . In the region near the pole, geomagnetic disturbances reaching tens of gammas and not connected with the nighttime disturbances [19 - 21] may appear in the summer in the daytime. Worsening of the correlation between  $K_p$  and K in observatories near the pole, which can result in a difference in the values of  $r_K$  determined by different methods, is explained by the appearance of the diurnal disturbances.

/143

The diurnal magnetic activity in  $r_K$  at the polar caps is analyzed in detail in [6]. It has been shown that the time of maximum magnetic activity, estimated by the equivalent amplitude  $r_K$  observed in the region near the pole (a polar distance  $\theta < 14^\circ$ ) at about noon, experiences a systematic deviation from local noon. The magnitude and direction of the shift depend on the longitude, and they change sign upon passage through the local noon hour at the southern "pole of invariance". (1)

/144

---

(1) The pole of invariance is understood to be the position of a point on the Earth's surface to which a line of force arrives from infinity when taking account of the real magnetic field of the Earth. The geographic coordinates of the pole of invariance are:  $\lambda = 125.08^\circ\text{E}$  and  $\phi = -74.84^\circ$  (southern hemisphere);  $\lambda = -81.61^\circ\text{W}$  and  $\phi = 80.11^\circ$  (northern hemisphere).

The deviations obtained are presented in Figure 5 are derived from [6]. Since the magnitude of the shift depends on the longitude, it is then possible, at first glance, to consider the activity caused by the action which depends on universal time, i.e., on the orientation of the geomagnetic dipole relative to the plane of the ecliptic. It has been shown in [6] that this shift, just like the seasonal variations in diurnal activity, is not due to the daily and annual changes in orientation of the geomagnetic dipole relative to the plane of the ecliptic. The maximum sets in at a time equidistant from the local and magnetic noon of the observatory, and it is due to the shift of the time of the maximum from the magnetic to the local noon because of the increase in ionosphere conductivity at local noon. Such an interpretation of seasonal changes in activity agrees with the results in [2], where it was assumed that seasonal changes are due mainly to the variations in the part of the activity component dependent on local time. A longitudinal shift in the maxima is due, exactly as in [6], to the influence of conductivity of the ionosphere or to local effects.

An estimate of the contribution of the various components to the resultant K-index showed that variations in the vertical component are quite essential in deducing the K-index in the region near the pole. The Z-contribution is magnified as the source of variation recedes from the observation point. Hence, annual changes in the ratio of the Z amplitude to the amplitudes of the X- and Y-components indicate recession of the source of variation from the circumpolar region in winter as compared with in summer. The essential contribution of Z to  $r_K$  must be taken into account in comparing results of the spatial activity distribution according to the indices K and  $r_H$  or Q.

The diurnal variation in activity at the Little America, Amundsen-Scott, Gauss Land ( $14^\circ < \theta < 17^\circ$ ) stations is characterized by two maxima which appear at hours which are symmetric to the hour of appearance of the single maximum in the  $\theta < 14^\circ$  region. As  $\theta$  increases, the discontinuity between the time of appearance of maximal  $r_K$  increases. The presence of one maximum in the circumpolar region and its bifurcation at lower latitudes are explained in [6] by the precipitation of high-energy particles into the oval zone enclosing the pole of invariance and located at higher latitudes in the daytime

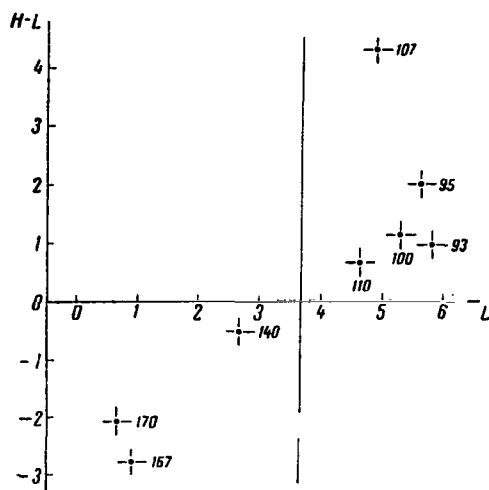


Figure 5. Difference between the hour of maximum magnetic activity and local midday H-L as a function of the hour of local midday for eight Antarctic stations of the center of the polar cap. Vertical line is the time of local noon for the southern "pole of invariance". Numbers—longitude of the observatory.

than at night.

The diurnal behavior of the magnetic activity and the position of the zone of maximum magnetic activity in magnetically-disturbed and magnetically-quiet days of 1957-1959, at 92 observatories, were investigated in [7,8]. The analysis was by equivalent amplitudes, to which the transition was made from K indices just as in [3]. It was assumed that  $S_a$  is of complex structure, and depends on both the local  $t$  and the universal time  $T$

$$S_a = S'(t) \pm S''(T) + S'''(T) = r' \cos(t - \psi) \pm r'' \cos(T - \eta) + r''' \cos(T - \gamma),$$

where  $S'(t)$  is the part of  $S_a$  dependent on local time,  $S''(T)$  is the asymmetric part of  $S_a$ ,  $S'''(T)$  is the symmetric part of  $S_a$ , and  $S''(t)$  and  $S'''(T)$  are checked by universal time. The plus sign in the second member refers to winter—and the minus, to summer. Therefore, in contrast to [2, 6], seasonal changes in  $S_a$  are connected both with the annual behavior of the slope of the dipole axis and with the change in conductivity of the ionosphere.

The separation of  $S_a$  into parts dependent on local and universal times was done by the method of harmonic analysis, as in [2]. Assuming that the first harmonic predominates in the diurnal behavior of most of the stations, the authors [7] limited themselves to the analysis of only the day waves. Representing  $S_a$  in a universal or local time reference system, it is possible to write, according to [7], that



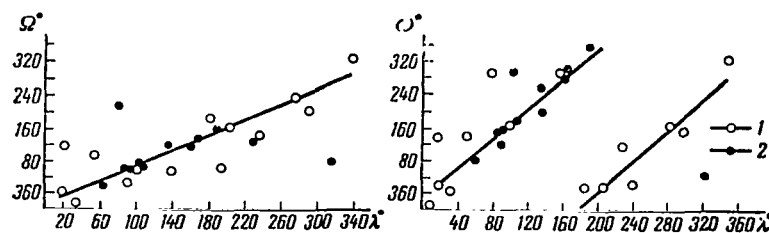


Figure 6. Dependence of the phase of maximum  $S_a(r_K)$  on the longitude  $\lambda$  in a universal time  $\Omega$  and local time  $\omega$  reference system according to [7]. 1-northern hemisphere stations; 2 - southern hemisphere stations.

$$S_a = r_1 \cos(T - \Omega^\circ) = r_1 \cos(t - \omega) = r' \cos(t - \psi) + r^{II} \cos(T - \delta),$$

where

$$t = T - \lambda.$$

If the contribution of universal time in  $S_a$  is comparable to the contribution of local time ( $r^{II} \sim r'$ ), then  $\Omega$  and  $\omega$  will change regularly with longitude. If it is considerably less than local time ( $r^{II} < r'$ ), then  $\Omega$  will vary with longitude, and the change in  $\omega$  as a function of  $\Omega$  is insignificant. To clarify the relationships of  $\Omega(\lambda)$  and  $\omega(\lambda)$ , it is necessary to utilize values of  $\Omega$  and  $\omega$  at stations located at approximately identical geomagnetic latitudes.

Presented in Figure 6 from [7] are dependences of  $\Omega$  and  $\omega$  of the first harmonic of  $S_a$  for high latitude stations ( $\Phi > 60^\circ$ ) in the summer season. The lines illustrate the dependence of the quantities  $\Omega$  and  $\omega$  on longitude. According to [7] the results presented in Figure 6 mean that two components in  $S_a$  are essential during the IGY -- a component controlled by the local time of day, and a component dependent on universal time. They yield equivalent contributions to  $S_a$ . A quantitative estimate made in [7] also shows that the ratio between amplitudes of components controlled by universal and by local times

$\sim 1$  at  $60^\circ < \phi < 65^\circ$ , and varies somewhat with the season. However, data from observatories which were not in a narrow latitude range but in the whole high latitude region  $\phi > 60^\circ$  were utilized in the construction of Figure 6. Hence, /146 they are not free of the latitude effects described in [2, 3, 6], including changes in  $\omega$  with latitude. The dependence of  $\omega$  on  $\phi$  is imposed on the dependence of  $\omega$  on  $\lambda$ , if it exists. In order to obtain in pure form the dependences  $\omega(\lambda)$  and  $\Omega(\lambda)$  it is necessary to reconstruct Figure 6 so that the lines connect the phase angles  $\Omega$  and  $\omega$  of stations located at approximately identical  $\phi$ , but different  $\lambda$ . Figure 7 illustrates the dependence of the phase angles of the first harmonic on the longitude, which we constructed from data in [7], for the summer and winter seasons of high latitude stations of the northern hemisphere. For convenience in comparison with Figure 6, values of  $\Omega$  and  $\omega$  for all stations with  $\phi > 60^\circ$  are superposed in Figure 7. The phase angles of  $S_a$  at observatories located in the latitude range  $60^\circ < \phi < 65^\circ$  are connected by lines.

In the summer season  $\Omega$  changes regularly with longitude. As the longitude increases, the activity maximum in a narrow latitude belt is manifested at earlier hours of universal time, i.e., the nature of the change in  $\Omega$  is opposite that pictured in Figure 6. Upon going over to local time in the summer season,  $\omega$  does not change with longitude in practice (the observatory at Lake Dikson is not included in this dependence), i.e., the activity maximum is manifested at the identical local time at stations of different longitudes. In winter there is a tendency toward a variation of  $\omega$  with  $\lambda$ , and the amplitude of the variation in the phase angle is  $\sim 110^\circ$  and  $\lambda$  changes by  $\sim 240^\circ$ . In changing to the corrected geomagnetic time, the amplitude  $\omega'$  diminishes to  $\sim 70^\circ$  and can be /147  $\sim 50^\circ$ , if it is taken into account that, as a rule,  $\omega$  at the observatory in College is  $\sim 200^\circ$  and not  $218^\circ$  as is assumed in [7]. Therefore,  $\omega$  changes substantially less than  $\Omega$  with longitude. Hence, a more exact analysis of the changes in the phase angles  $\Omega$  and  $\omega$  with longitude did not verify the dependences  $\Omega(\lambda)$  and  $\omega(\lambda)$  obtained in [7] and showed that the contribution of the component  $S(T)$  is substantially less than the contribution of  $S(t)$  at  $60^\circ < \phi < 65^\circ$  during the IGY. It follows from Table 2 in [7] that it is hardly possible to neglect the second harmonic at high latitudes. For example,

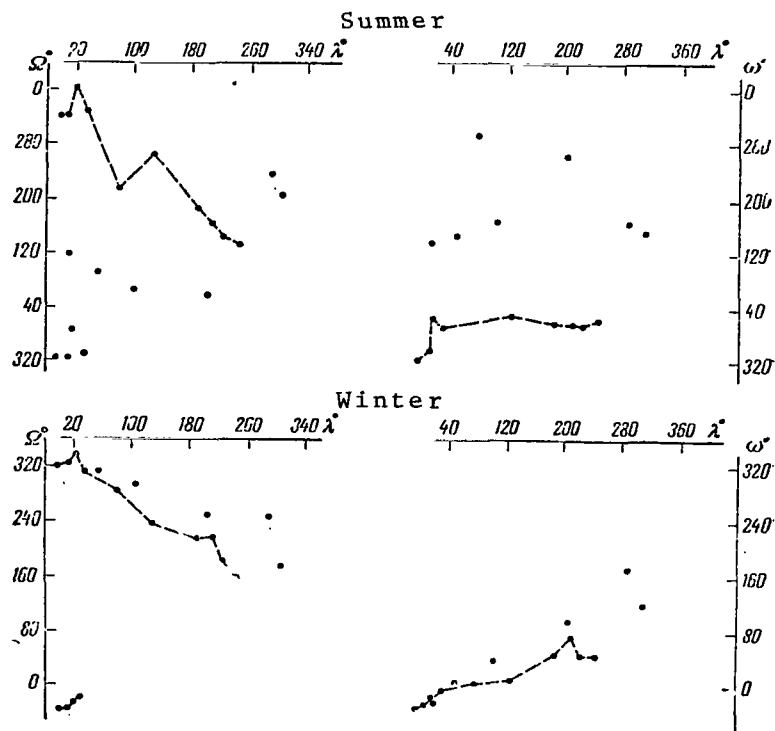


Figure 7. Dependence of the phase of the maximum  $S(r_K)$  on the longitude  $\lambda$  according to results in [7] in a universal  $\Omega$  and local  $\omega$  time reference system for northern hemisphere stations at  $\phi > 60^\circ$ . Lines connect phase angles of stations located at  $60^\circ < \phi < 65^\circ$ .

out of the 15 high latitude stations of the northern hemisphere with  $\phi > 60^\circ$  in the summer, six stations have a second harmonic contribution commensurate with the contribution of the first harmonic in the summer season.

In order to separate the activity variations into the parts  $S(t)$  and  $S(T)$  the stations having approximately equivalent geomagnetic latitudes but different longitudes were combined into groups. The amplitudes and phases of corresponding components were found by expansion in trigonometric series. To separate  $S(T)$  into the parts  $S''(T)$  and  $S'''(T)$ , the winter-summer differences and the winter-summer sums were analyzed. Latitude changes in the amplitudes and phases of all three components of  $S_a$  were presented in [7] as a function of the geomagnetic latitude.

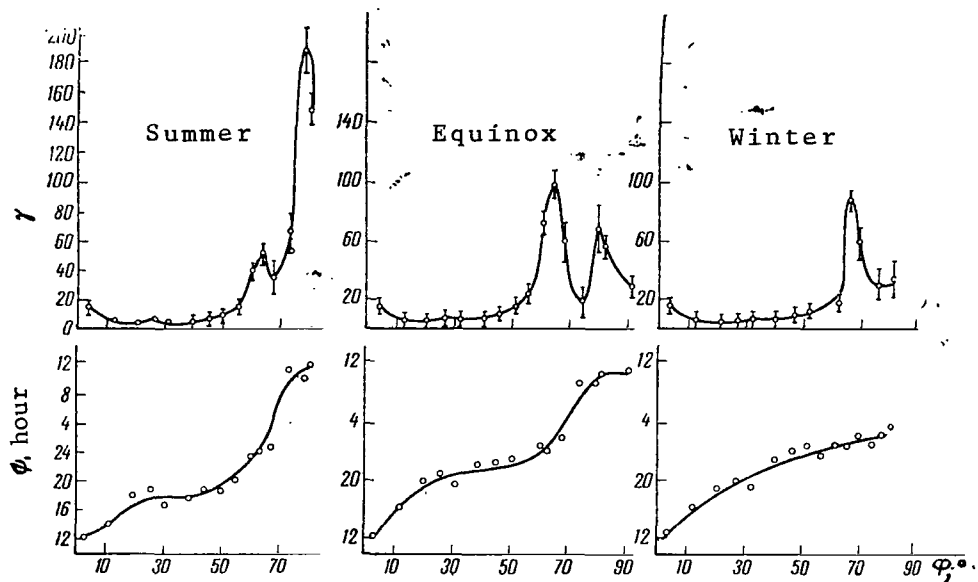


Figure 8. Dependence of the amplitude  $r'$  and phase  $\psi$  of the  $S'(t)$  component on the geomagnetic latitude  $\phi$  according to [7].

Given in Figure 8 are latitude changes of the parameters of the  $S'(t)$  component from [7], which are characterized by the following: 1) The amplitude  $r'$  reaches its greatest values in two zones at  $\phi = 63 - 67^\circ$  and at  $\phi \sim 78^\circ$ ; 2) the activity is maximum near noon at  $\phi \sim 0$  and  $\phi \sim 78^\circ$ ; 3) the activity predominates at  $\phi = 63 - 67^\circ$  in near midnight hours.

It should be noted that  $S_a$ , calculated according to [7] and observed at a number of high latitude observatories, differs noticeably.

By calculating the mean diurnal disturbance at each observatory for winter, the equinox, and summer, and taking the latitude behavior of the  $S'(t)$  parameters as shown in Figure 8, the authors [8] obtained the position of the zone of latitude maxima activity presented in Figure 9.

There are two zones of elevated activity at high latitudes in the summer. /148 Their shape at any instant of universal time is almost circular. The first corresponds to the standard Fritz zone ( $\phi \sim 63^\circ - 65^\circ$ ), and the second to

a ring at the latitudes  $75 - 78^\circ$ . In winter there is one ring zone at  $\phi \sim 63 - 65^\circ$ . The activity maximum in the first zone is observed at all hours of the day independently of the season. The presence of a magnetic disturbance at  $\phi = 63 - 65^\circ$  in the daytime is not confirmed by the results of A. P. Nikol'skiy [14] and M. S. Bobrov [20]. The disturbance in the second zone, which is greatest in the daytime, has a sharp maximum in the summer and is insignificant in winter. In summer the zones are separated by a region of relatively low activity. The maximum activity zones on magnetically-quiet days are located at the same latitudes as on disturbed days.

The deductions obtained in [8] relative to the position of the maximum magnetic activity zone contradict the results described above according to data in [6, 16], as well as data based on hourly indices of magnetic activity [11, 12, 13]. According to these latter, the region of maximum magnetic activity has the shape of an oval enclosing the geomagnetic pole and located during the daytime at higher latitudes than at night. On going from day to night hours, a smooth diminution in the latitude of the maximum activity zone is observed. The oval is fixed relative to the Sun, and is oriented so that it is located at  $\phi \sim 75^\circ$  in winter in the daytime, and at  $\phi \sim 67^\circ$  at night. Moreover, the maximum activity region shifts somewhat towards the equator as  $K_p$  increases. The existence of such an oval, observed at fixed instants of universal time, follows from aurora borealis observations [22 - 24] and is explained by the structure of the internal magnetosphere [25].

It is completely probable that the position of the zone of maximum magnetic disturbance in [8] is a result of utilizing the ordinary geomagnetic coordinate system in place of the corrected geomagnetic system, and a consequence of the methodology used which does not take account of the second harmonics and longitudinal effects in the mean diurnal values of the field, which may be quite substantial [26, 12, 3]. It is possible that in a more exact analysis taking account of all these factors, the difference between the position of the maximum magnetic activity zone found by the hourly indices in [11 - 13] and in [8] would diminish substantially, and would reflect only the

specifics of the indices themselves which were utilized (taking account of the more remote sources in the K-index, and of currents at the zenith in the  $r_H$  and Q-indices).

According to [7], the spiral-shaped part of the oval can be obtained according to the data in Figure 8 if latitude changes of the phase of the  $S'(t)$  component are pictured in a polar projection. Such a spiral from [7] is pictured in Figure 10. However (see Figure 8), for the winter season the phase of  $S'(t)$  changes within  $0^h < \psi < 4^h$  limits in the  $60^\circ < \phi < 80^\circ$  range, while the spiral includes 12 hours local time in this same range of latitudes. For the summer season, the phases of  $S'(t)$  equal  $\sim 0^h$  and  $\sim 12^h$  for  $60^\circ < \phi < 70^\circ$  and  $73^\circ < \phi < 80^\circ$ , respectively. Hence, the phases of  $S'(t)$  for the summer season are not pictured on the polar diagram as a spiral, but as two segments near the zone and twelve-hour meridians. /149

A spiral distribution can be obtained if  $S'(t)$  is represented as the superposition of two waves with a near-midday and near-midnight maximum whose phases do not change with latitude

$$S'(t) = r'_I \cos(t - \alpha) + r'_{II} \cos(t - \beta).$$

The time of the maximum is determined in local time from the relationship

$$\operatorname{tg} t = \frac{r'_I \sin \alpha + r'_{II} \sin \beta}{r'_I \cos \alpha + r'_{II} \cos \beta}.$$

in this case. Assuming  $\alpha = 180^\circ$  and  $\beta = 15^\circ$  according to [7], the changes in  $t$  in the  $60 - 78^\circ$  range can be computed for the summer season for a latitude change in the amplitudes  $r'_I$  and  $r'_{II}$  presented in [7]. It is found that the change in  $t$  is less than 2 hours, and not 12 as the spiral distribution requires. Small changes in  $t$  are in sharp contradiction to results on aurora borealis and magnetic activity with respect to hourly indexes, according to which the oval zone is included entirely within the  $60 - 78^\circ$  range of latitudes in the winter.

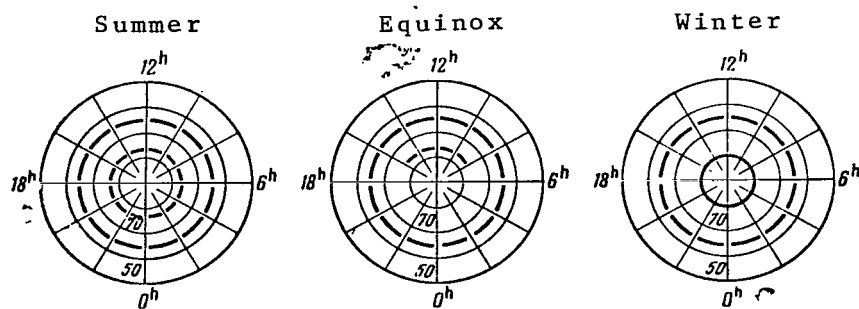


Figure 9. Location of the maximum magnetic activity zone in disturbed days in 1957 - 1959, in a polar projection.

This brief survey and comparison of data on the distribution of the K indices which are known in the literature indicate that to obtain a well-founded space-time distribution of the magnetic activity controlled by local time, it is necessary:

1. To have available data in the corrected geomagnetic coordinate system;
2. to exclude the possible contribution of components controlled by universal time as well as the significant longitude effects in the mean diurnal values;
3. to take account of not only the first but also higher harmonics in  $S'(t)$  in extracting the part of  $S_a$  controlled by local time.

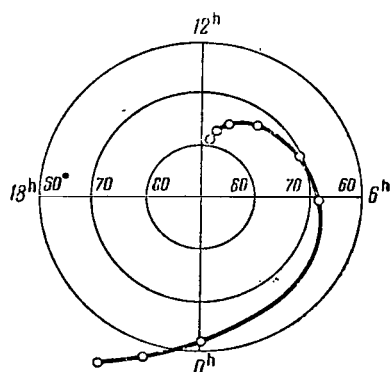


Figure 10. Latitude behavior of the phase of the  $S'(t)$  component according to [7].

#### ACTIVITY DURING THE IGY ACCORDING TO $r_K$

Results of observations of 22 high latitude stations of the northern hemisphere are utilized to clarify the space-time pattern of the magnetic activity estimated by the K index. Indicated in the table is the location of these observatories; i.e., their geographic ( $\phi, \lambda$ ), geomagnetic ( $\phi, \Lambda$ ) and corrected geomagnetic ( $\phi', \Lambda'$ ) coordinates are presented.

TABLE

Observatories	$\varphi$	$\lambda$	$\Phi$	$\Lambda$	$\Phi'$	$\Lambda'$
Eskdalemoor	55°19' N	03°12' W	58,5° N	83,2°	54,3° N	80,5°
Nurmijarvi	60 31	24 39 E	57,8	112,9	56,6	103,6
Agincourt	43 47	79 18 W	55,3	346,8	57,2	350,1
Larvik	60 08	01 11 W	62,5	88,8	58,9	84,3
Minook	54 37	113 20 W	61,9	300,8	62,5	301,2
Welland	66 10	169 50 W	61,7	232,8	62,6	243,0
Sodankylä	67 22	26 39 E	63,7	120,4	63,4	109,2
Murmansk	68 57	33 03 E	64,0	126,8	64,7	114,8
Colledge	64 52	147 50 W	64,6	256,3	64,9	260,3
Tiksi Bay	71 38	128 53 E	69,3	191,3	65,6	194,9
Tromsø	69 40	18 57 E	67,2	116,7	63,3	105,4
Dikson	73 33	80 34 E	62,8	165,5	63,0	154,9
Barrow	71 18	156 45 W	63,5	240,7	69,7	247,0
Churchill	53 30	94 12 W	68,6	322,5	70,0	326,0
Medvezhiy Island	74 31	19 01 E	71,1	124,0	70,9	110,9
Cape Chelyuskin	77 43	104 17 E	66,1	176,5	71,3	173,9
Tikhaya Bay	80 30	52 48 E	71,3	153,5	74,3	140,7
Baker Lake	64 18	96 00 W	73,8	314,8	75,1	320,4
Murchison	80 03	18 15 E	75,0	138,0	76,0	121,2
Godhavn	69 14	53 31 W	80,0	33,6	77,6	43,3
Resolute Bay	74 42	94 54 W	83,1	287,7	84,3	301,0
Thule	77 29	69 10 W	89,2	357,4	87,7	39,6

The K-indices of the majority of observatories considered are published in [150]. It has been remarked above that the magnetic activity is characterized by substantial longitudinal effects. To eliminate them, it is necessary to average the data of observatories located at identical latitudes but different longitudes. Consequently, it is extremely desirable to have the greatest possible number of points with different  $\lambda$ . However, there are no K-indices in [27] for a number of high latitude observatories located in the western hemisphere and on Spitsbergen. Since data from these observatories are needed to eliminate the effect of universal time in  $S_a$ , as well as to smooth the longitudinal differences, the K-indices of the Canadian observatories at Resolute Bay, Baker Lake and Churchill, as well as those of the observatory at Murchison, were recorded directly from magnetograms stored at the B2 World Data Center.



The transition from K-indices to equivalent amplitudes was made just as in [3]. The amplitude limits of each point were taken according to [28] depending on the scale used at the observatory. The calculations of  $S_a$  and the mean daily values of the magnetic activity were made separately for all days and periods with planetary magnetic activity  $K_p = 0 - 1, 3$  and  $5$  for November, December, 1957; January, February, 1958; and May - August, 1958 (respectively). A list of the daily changes in  $r_K$  at high latitude stations of the southern hemisphere is contained in [29].

Presented in Figure 11, is a latitudinal distribution of the mean diurnal  $\bar{r}_K$  for  $K_p = 3$  in winter and summer as a function of  $\phi$  and  $\phi'$ . For  $K_p = 3$  the volume of statistics is greatest, and the change in  $\bar{r}_K$  with latitude is the same as for calculations of  $\bar{r}_K$  for all days. The curves in Figure 11 are drawn through points representing the arithmetic mean of the values of  $\bar{r}_K$  within a  $2^\circ$  band in  $\phi'$  or  $\phi$ . The mean diurnal value of  $\bar{r}_K$  at each station is shown by a point, and the mean value by a circle. The vertical line equals the mean square deviation.<sup>(2)</sup> Figure 11 shows that the latitudinal distribution of  $\bar{r}_K$  /151 becomes more ordered in  $\phi'$  coordinates than in  $\phi$  coordinates. In particular, the magnitude of the dispersion in the winter season diminishes from  $53$  to  $38\gamma$  and in summer, from  $55$  to  $30\gamma$ .

In winter  $r_K$  increases from the middle latitudes to  $\phi' \sim 70^\circ$ , becoming a maximum at  $\phi' \sim 70^\circ \sim 260\gamma$ . At higher latitudes,  $\bar{r}$  decreases first rapidly, then slowly at  $\phi' \geq 76^\circ$ . At  $\phi' > 80^\circ$  in the region near the pole,  $\bar{r}_K$  is substantially greater than at  $\phi' \sim 56 - 58^\circ$ . Such a monotonic change in  $\bar{r}_K$  is described by the values of  $\bar{r}_K$  averaged within  $2^\circ$  limits in  $\phi'$ . If there is no averaging, and the curve of the latitude distribution is drawn directly through the  $\bar{r}_K$  of the specific observatories, three maximums can be computed (at  $\phi' \sim 64, 69$ , and  $71^\circ$ ). We assume that the curve drawn through the averaged data to be closer to the true latitude distribution of  $\bar{r}_K$ .

---

(2) The  $\bar{r}_K$  of Murmansk observatory were not averaged.

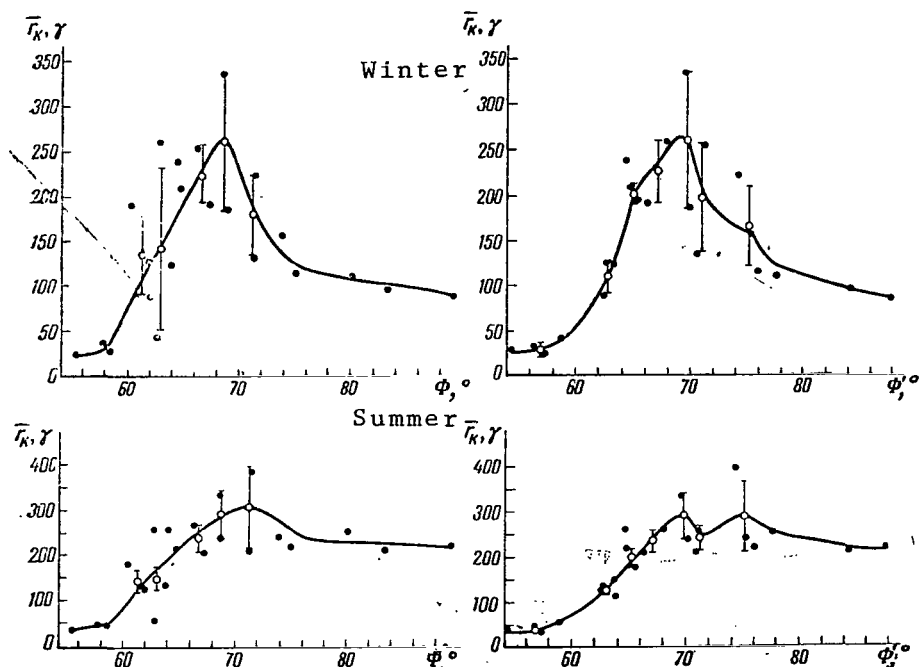


Figure 11. Latitude distribution of the mean diurnal values of magnetic activity in  $r_K$  for winter and summer as a function of the geomagnetic  $\phi$  and corrected geomagnetic  $\phi'$  latitude for  $K_p = 3$ .

The differences in the  $r_K$  of observatories located at approximately identical  $\phi'$  are due to local and longitude effects which sometimes result in substantial changes in  $\bar{r}_K$ . For example, the ratio is  $r_K = 1.8$  at Barrow and Churchill  $\Delta\phi' = 0.3^\circ$ , while the ratio is  $r_K = 1.9$  at Chelyuskin and Medvezhiy  $\Delta\phi' = 0.4^\circ$ . All four observatories are located at  $\phi' \sim 70^\circ$ , where night disturbances, which reach their highest intensity in this region, yield the greatest contribution to  $r_K$  in winter. In summer the magnitude of the ratio diminishes. The mean diurnal level of disturbance levels off to a considerable extent, which is apparently explained by the influence of remote sources of disturbance which are very intense in the daytime hours of the summer season in the region near the pole. The sharp difference in  $\bar{r}_K$  at observatories with identical corrected geomagnetic latitudes again makes it necessary to average  $\bar{r}_K$  over the latitude circle to eliminate quite significant longitudinal effects.

The latitude distribution in the summer period is characterized by a high level of activity in the circumpolar region which is twice the corresponding winter level. Moreover, a second increase in  $\bar{r}_K$  at  $\phi' \sim 75^\circ$  is observed on the curve of the latitude distribution of  $\bar{r}_K$  for the summer season. The averaged  $\bar{r}_K$  are identical in magnitude at  $\phi' \sim 70$  and  $75^\circ$ . The dispersion in the points at this part of the curve is such that it is difficult to verify definitely the existence of two maximum zones of magnetic activity at these latitudes in the summer. However, it is not excluded that the latitude change in  $\bar{r}_K$  will reach maximum values at  $\phi' \sim 70^\circ$  (nocturnal disturbances) and  $\phi' \sim 75^\circ$  (diurnal disturbances) in connection with the development of intense magnetic disturbances in the circumpolar region in the summer. The ratio  $\bar{r}_K(\text{summer})/\bar{r}_K(\text{winter})$  varies with latitude. The greatest changes occur at high latitudes at  $\phi > 74^\circ$ . Seasonal changes are small at  $\phi' \leq 70^\circ$ . Therefore, at latitudes where nocturnal disturbances predominate, the mean diurnal values of the activity do not change from the winter to the summer solstice, while its changes are significant in the circumpolar region. These data are in conformity with [3].

The fundamental features of the latitude distribution of  $\bar{r}_K$  are presented in Figure 12 for  $K_p \leq 1$  and  $K_p = 5$  (for  $K_p \leq 1$  the number of cases is small). The maximum values of  $\bar{r}_K$  are always observed at  $\phi' \sim 70^\circ$  in winter. However, for a weak disturbance ( $K_p = 0 - 1$ ), the  $\bar{r}_K$  at  $\phi' \sim 70^\circ$  are always 25% greater than the  $r_K$  in the circumpolar region. As  $K_p$  increases, the  $r_K$  increases at all latitudes, and particularly significantly at  $\phi' \sim 70^\circ$ . The latitude distribution takes on the customary bell-shape. In summer the  $\bar{r}_K$  vary relatively different manner as  $K_p$  increases at  $\phi' \sim 70^\circ$  and  $75^\circ$ . For  $K_p = 0 - 1/153$  the  $\bar{r}_K$  at  $\phi' \sim 75^\circ$  is 25% greater than the  $\bar{r}_K$  at  $\phi' = 70^\circ$ . For  $K_p = 3$  the  $\bar{r}_K$  at these latitudes are equal (see Figure 11) and for  $K_p = 5$  the disturbance at  $\phi' \sim 70^\circ$  is 100% greater than the  $\bar{r}_K$  at  $\phi' \sim 75^\circ$ . Such a redistribution of  $r_K$  with the change in  $K_p$  is explained by an abrupt increase in the intensity of the nocturnal disturbances when going from  $K_p = 0 - 1$  to  $K_p = 5$ , and the relatively weaker magnification of the diurnal disturbances in the circumpolar region.

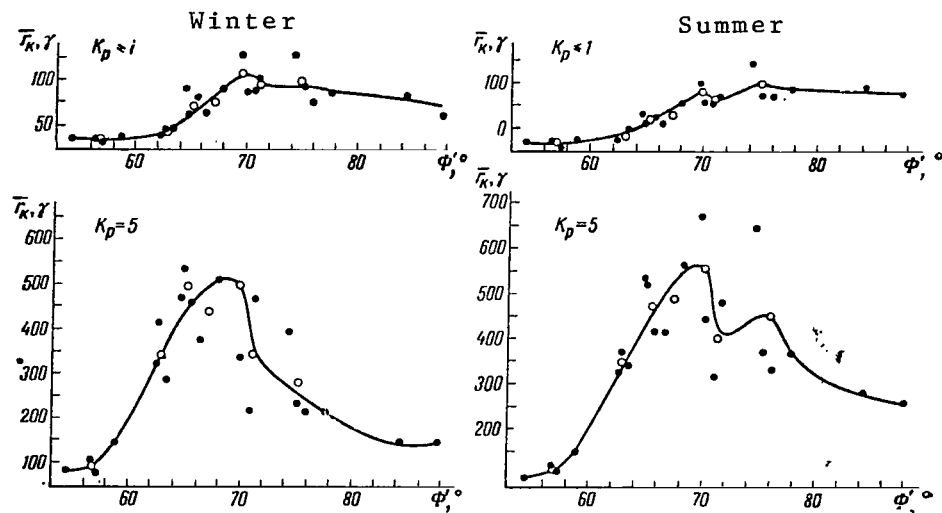


Figure 12. Latitude distribution of the mean diurnal values of magnetic activity in  $\bar{r}_K$  for winter and summer with  $K_p \leq 1$  and  $K_p = 5$ . Open circles - values of  $\bar{r}_K$  averaged every  $2^\circ$  in  $\Phi'$ , dark circles - values of  $\bar{r}_K$  at specific observatories.

On the whole, the results of the analysis of the latitude distribution of  $\bar{r}_K$  in summer and in winter verify the deductions obtained earlier [12, 13] in an analysis of the mean diurnal magnitudes of the Q-index and  $\bar{r}_H$ : In winter the mean diurnal values of the magnetic activity are maximal in the Fritz-Weston zone of the aurora borealis for any value of  $K_p$ . In summer the magnetic activity in the circumpolar region increases abruptly and is at a high level throughout the whole polar cap from the geomagnetic pole to the aurora borealis zone. Only during strong magnetic disturbances is a region with maximum magnetic disturbance at latitudes of the Fritz-Westin aurora borealis zone again manifested in the latitude distribution for the summer season. It is known that the diurnal changes in magnetic activity depend on the latitude of the observatory and the season. Pictured in Figure 13 are the  $S_a$  of several observatories for the winter and summer seasons. In winter  $S_a$  has a simple shape with a maximum in the nighttime at  $\Phi' \sim 65^\circ$  and in the daytime at  $\Phi' \sim 65^\circ$  (Sodankylä, Tromsø, Thule). At intermediate latitudes (Chelyuskin)  $S_a$  is represented by a more complex curve with two maxima in the pre-midnight and morning hours. Just like the latitude distribution of  $\bar{r}_K$ , the shape of  $S_a$  is determined to a greater extent by the corrected geomagnetic latitude than by the geomagnetic latitude of the central dipole. In the summer the daily

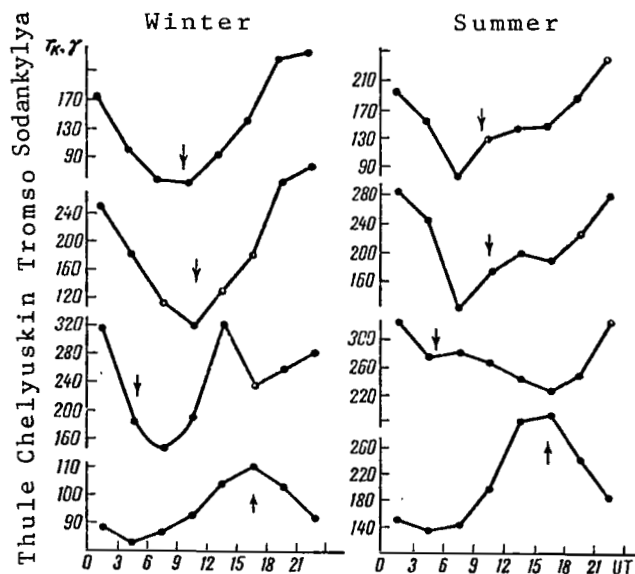


Figure 13. Diurnal changes in magnetic activity in winter and summer for all day observations. Arrows indicate local noon.

maximum also remains unique at  $\phi' > 75^\circ$ . At  $\phi' \sim 65^\circ$ , besides the maximum around midnight, there is a second maximum in the evening hours which is hardly noticed in Sodankylya and is clearly seen in Tromso. The rise in activity in the evening at these latitudes is even more clearly manifested in the hourly indices [11, 12]. The morning maximum is retained at the intermediate latitudes and, moreover, a second activity maximum is manifested in the post-midday hours in addition to the pre-midnight hours.

/154

The time of appearance and the number of  $r_K$  maxima in  $S_a$  depend on  $\phi'$ . In winter one maximum is observed in the near midnight hours from  $60$  to  $80^\circ$ ; the other sets in at later hours local time with the advance into higher latitudes: at  $2^h$  at  $\phi' \sim 62^\circ$  and  $12^h$  at  $\phi' \geq 80^\circ$ . In summer, the separation into two maxima becomes noticeable at  $\phi' \sim 62^\circ$ , where as the latitude increases, the morning maximum is manifested later, and the evening maximum at earlier local times. In a polar projection these dependences are spirals analogous to those described earlier for the hourly indices. As  $K_p$  increases the spirals are deformed somewhat. The change in the spirals with growth in activity can be determined more accurately on the basis of hourly activity indices hence, we do not consider this here.

The value of the magnetic activity which changes during the day can be determined from the general relationship

$$S_a = S_0 + S(T) + S(l),$$

where  $t = T + \lambda$ ,  $S_0$  is the mean diurnal value,  $S(T)$  and  $S(t)$  are parts of the diurnal behavior dependent, respectively, on universal and local time [2, 4].

The extraction from  $S_a$  of the part controlled by local time can be accomplished by averaging the  $S_a$  of stations located at the identical  $\phi'$  but at different longitudes, with respect to local time. The first harmonic of  $S(T)$  is eliminated when taking the average for two stations separated by  $180^\circ$  longitude. The first and second harmonics are eliminated for four stations with uniform longitudinal distribution, etc. But the  $S(t)$  part is conserved completely to the very highest harmonics. Moreover, taking the average of the mean diurnal value with respect to the longitude smooths out the longitudinal effect  $\bar{r}_K$ .

Therefore, taking the average with respect to local time of  $S_a$  of a number of observatories at identical latitudes leads to values of magnetic activity: a) free of the influence of universal time [the part  $S(T)$ ]; b) smoothed with respect to the longitudinal effect (in  $r_K$ ); c) retaining all harmonics up to the highest in the part  $S(t)$ .

A comparison of the  $S_a$  for local and local geomagnetic times showed that local geomagnetic time regulates the phenomenon best. Hence,  $S_a$  is averaged with respect to geomagnetic time ( $t'$ ). The  $S_a$  of the following observatories were utilized:

Nurmijarvi - Agincourt	56.9
Sodankylä - Minook	63.0
Tromsø - College	65.6
Churchill-Barrow-Cape Chelyuskin	
Medvezhiy Island	70.5
Tikhaya Bay-Baker Lake	74.7
Godhavn - Murchison	76.8

The  $\phi'$  of each observatory differed from the  $\phi'_{av}$  of the appropriate pair /156 by not more than several tenths of a degree. In the "corrected geomagnetic latitude - geomagnetic time" polar coordinates, Figure 14 gives the intensity

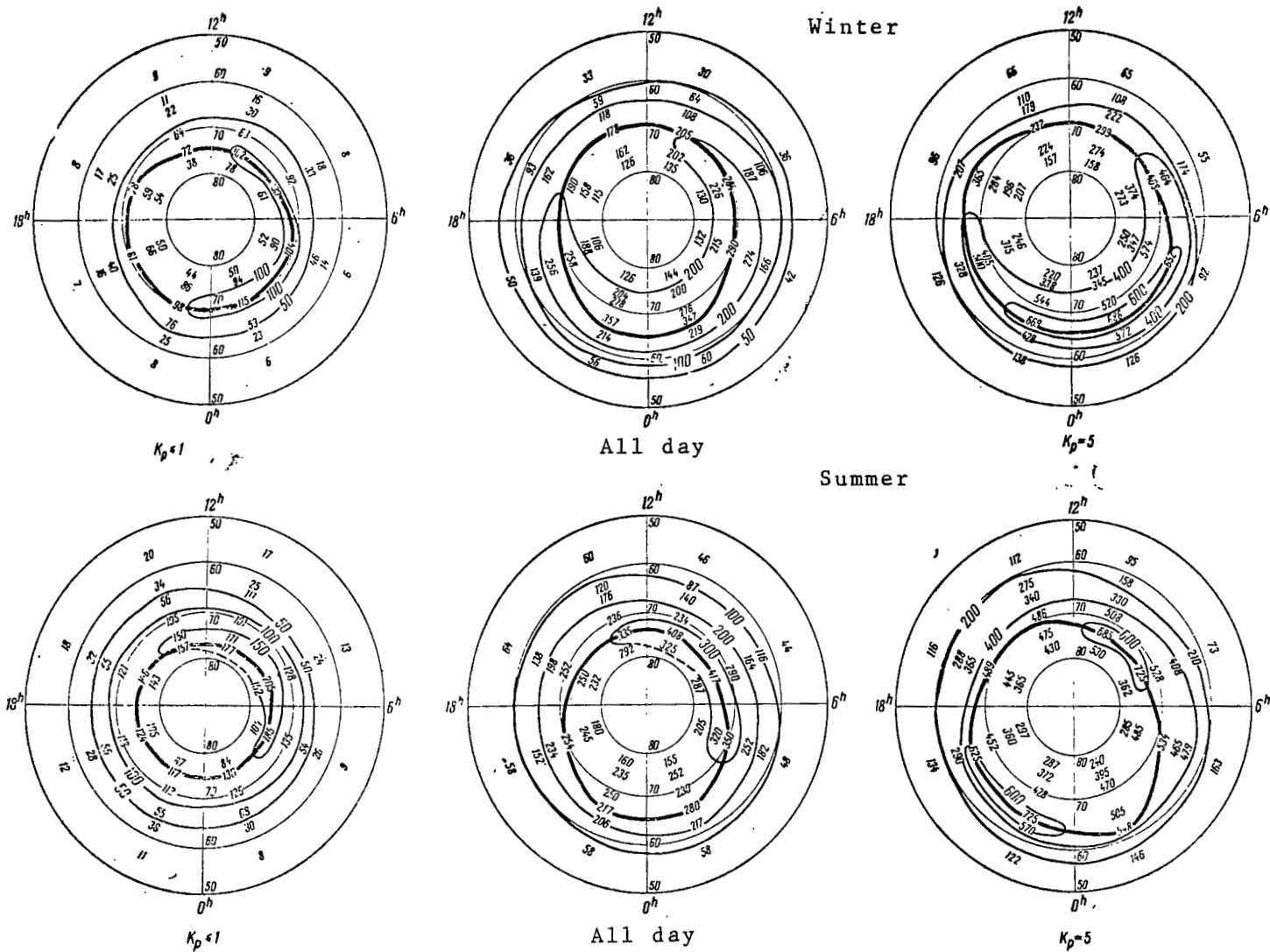


Figure 14. Change in  $r_k$  in three-hour local geomagnetic time intervals in a polar projection for pairs of observatories. Heavy line connects points at which the disturbance is a maximum for a given three hour interval.

distribution of  $r_K$  for the listed pairs of observatories for the winter and summer seasons for  $K_p \leq 1$ , and for all days for  $K_p = 5$ . Values of  $r_K$  of the part  $\bar{S}_0 + \bar{S}(t)$  for the appropriate three hour interval are indicated by numbers along the lines  $\Phi' = \text{const}$ . Isolines drawn by interpolating between appropriate numerical data yield a general representation of the distribution of the magnetic activity components dependent on local time. The heavy line in the shape of an oval in the  $\Phi', t'$  coordinates is the position of the maximum disturbance region. The location of the oval for different  $K_p$  characterizes the dynamics of the maximum disturbance region.

For  $K_p \leq 1$ , the greatest disturbance in the winter season is observed at  $\Phi' \sim 70.5^\circ$  at night, and  $\Phi' \sim 74.7^\circ$  by day. As  $K_p$  increases, the disturbance intensity grows strongly at all latitudes, and the region of maximum disturbance shifts towards the equator on both the day and the night sides of Earth. An analogous shift is also observed for the auroral bands as  $K_p$  increases [30, 31]. However, the ovalness of the region of maximum disturbance is conserved for all disturbance levels, because the disturbance reaches maximum values at higher latitudes on the dayside as compared with the nightside. The absolute value of the disturbance along the oval decreases from nighttime to daytime. An analogous result has been obtained according to hourly indices [12, 13].

In summer, in contrast to winter, the greatest disturbance is observed at  $\Phi' \sim 75 - 77^\circ$  in the forenoon. For  $K_p \leq 1$  the maximum disturbance in these hours is possibly located at still higher latitudes. As  $K_p$  increases, the nocturnal disturbance at  $\Phi \sim 65^\circ$  is magnified abruptly, and for  $K_p = 5$  the disturbance achieves maximum values at night and by day. In summer, as in winter, the maximum activity region forms an oval whose width increases with the passage from nighttime to daytime.

The presence of two elevated disturbance regions along the oval in the summer season indicates that the oval zone of maximum magnetic disturbance is inhomogeneous. Since the oval is located on the boundary of the region of magnetic lines of force forming the loop of the magnetosphere, the diurnal disturbance should then be connected with processes in the region of the high-



latitude neutral line on the dayside, and the nocturnal disturbance in the region of the neutral layer of the magnetosphere loop.

The abrupt magnification of the diurnal disturbance of the summer season is the reason for the second high-latitude maximum in  $\bar{r}_K^Y$  at  $\phi' \sim 75^\circ$  noted above. Therefore, one oval zone exists at high latitudes rather than two quasicircular zones of maximum disturbance at  $\phi = 63 - 65^\circ$  and  $\phi = 75 - 78^\circ$ . However, the disturbances in the diurnal and the nocturnal sectors of the oval are different, and can hence vary differently with disturbance level, season, etc.

In Figure 14, the region of maximum disturbance values was determined by the latitude of a pair of observatories at which the disturbance was a maximum within the given three-hour interval. The latitude and amplitude of greatest activity in this three-hour interval of local geomagnetic time can be determined more exactly if a parabola with a vertical axis is drawn through the maximum value of  $r_K$  and two points which frame it. Then the coordinates of the parabola's vortex define these two parameters. Shown in a polar projection in Figure 15 is the location of a maximum disturbance region calculated in this manner. The dynamics of the oval in the near-midday and near-midnight hours is in good agreement with [16] and with the dynamics of the aurora borealis bands.

Taking the average of  $S_a$  of a pair of observatories with respect to universal time, an attempt can be made to extract the component  $S(T)$ . A maximum is clearly apparent at 12 - 18<sup>h</sup> UT by pairs with  $\phi'_{av}$  65.6, 70.5, 74.7, 76.8° in the averaged patterns on all days in winter. In summer the changes in  $r_K$  with respect to UT are extremely irregular, and maxima can appear at any time. Hence, in winter the component  $S(T)$  introduces a contribution to  $S_a$  and the time of the maximum corresponds to that obtained in [7, 12]. However, the contribution of  $S(T)$  to  $S_a$  is slight. Otherwise it is difficult to explain why diurnal changes in  $r_K$  differ quite insignificantly in a number of observatories with identical  $\phi'$  but diverse longitudes. Presented in Figure 16 are changes in  $r_K$  in the winter season at observatories at Tiksi Bay, College,

/157

/158

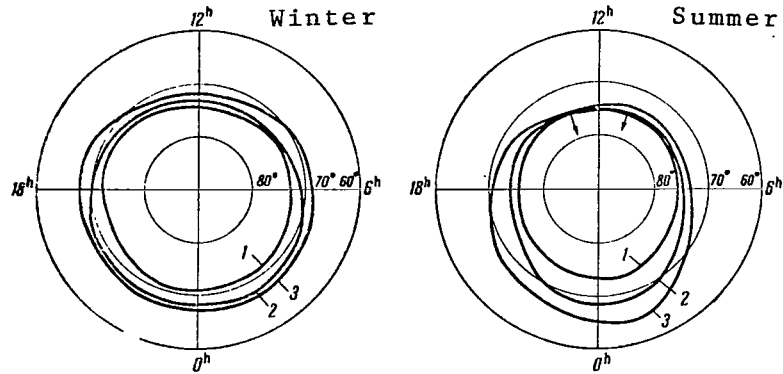


Figure 15. Location of maximum disturbance regions in winter and summer for  $K_p \leq 1$  (1);  $K_p = 3$  (2);  $K_p = 5$  (3).

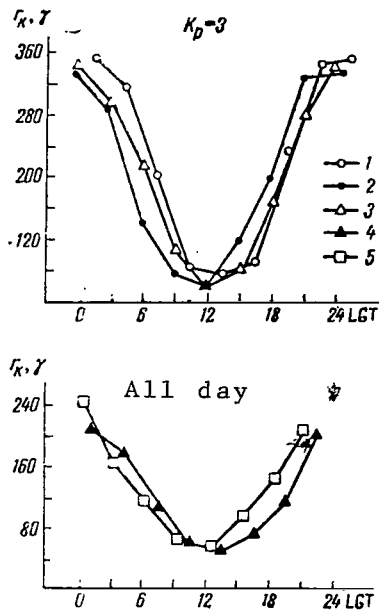


Figure 16. Change in  $r_K$  in the winter season. 1 - College, 2 - Tromso, 3 - Tiksi Bay, 4 - Minook, 5 - Sodankylä.

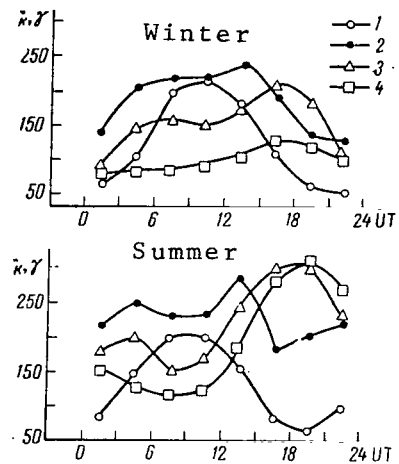


Figure 17.  $S_a$  for all day at Canadian observatories in winter and summer. 1 - Minook, 2 - Churchill, 3 - Baker Lake, 4 - Resolute Bay.

Tromso ( $K_p = 3$ ) and Minook, Sodankylä (all day). The almost total similarity of the diurnal changes indicates the insignificance of the component  $S(T)$  in this case; however, a difference is perceptible for other  $K_p$ .

Since the amplitude of  $S(T)$  at high latitudes is substantially less than the amplitude of  $S(t)$ , the latitudinal displacements of the maximum disturbance region should then result in a redistribution of relative values of  $r_K$  at observatories located at identical longitudes but different latitudes. In particular,  $r_K$  will be maximal at lower latitude stations in the nighttime, and at high-latitude stations in the daytime. The identical longitude of the observatories eliminates the longitude effect and makes it possible to compare the  $S_a$  in universal time.

There are two such chains of observatories at our disposal, in Canada and in Western Europe. Presented in Figure 17 are  $r_K$  for all day for the Minook, Churchill, Baker Lake, Resolute Bay stations. Since interruptions occurred in the recording of the magnetic field, time intervals during which there was no recording at a certain observatory were then excluded from the computations at all the observatories.

The disturbance is at a maximum at night in the winter between Minook and Churchill and drops at the pole. In the daytime, the  $r_K$  are maximal at the Baker Lake observatory. In summer at night, the disturbance is greater at the Minook and Churchill observatories at night, and at the high-latitude Baker Lake and Resolute Bay observatories during the day. These changes in the position of the maximum disturbance oval agree with the results obtained above by averaging  $S_a$  of pairs of observatories. Analogous diurnal changes in the relative values of  $r_K$  are also observed in the chain of European observatories.

#### $r_K$ ACTIVITY DURING THE IQSY

The regularities in the  $r_K$  distribution described above characterized the year of high solar activity. Observations during the IQSY period permitted a corresponding analysis in the year of the minimum. If the sun had been

extraordinarily active in 1957 - 1958 (mean monthly Wolf number  $\sim 200$ ), then the mean monthly Wolf numbers in 1964 were less than 10 for the major portion of the year.

The  $S_a$  and  $\bar{r}_K$  were calculated seasonally during the IQSY: winter (January-February and November - December 1964) and summer (May - August 1964) for all days and separately for  $K_p \leq 1$ ,  $K_p = 3$  and  $K_p = 5$ . With some exceptions, the K-indices of the same observatories as during the IGY were used. In particular, there was no material from magnetic observations at the Murchison observatory at the B2 World Data Center, but there was a possibility of using data from the Kirun and Reykjavik observatories.

In Figure 18 is the latitude distribution of  $\bar{r}_K$  for all day for  $K_p \leq 1$ ,  $K_p = 3$ , and  $K_p = 5$  as a function of  $\phi'$ . The curves have been drawn through points representing the mean values of  $\bar{r}_K$  for  $2^\circ$  intervals in  $\phi'$ . No curve was drawn for  $K_p = 5$ , because intense planetary disturbances were rarely manifested during the IQSY and hence the statistical confidence in results obtained for  $K_p = 5$  is slight.

The  $\bar{r}_K$  at the Reykjavik observatory is less for all disturbance levels than at Tiksi Bay and College. This is apparently a manifestation of the longitude effect, which consists of reduced values of the magnetic activity at the European observatories as compared with the Asiatic and American [12, 26].

In winter the  $\bar{r}_K$  is a maximum at  $\phi' \sim 71^\circ$  for all disturbance levels. It /159 diminishes towards the equator and towards the pole. The drop at the pole is sharper for intense disturbances. Despite the abrupt diminution in solar activity, the intensity of a disturbance at the maximum is kept at the same level as during the IGY. The position of the maximum is also shifted quite negligibly. Conservation of the magnetic activity at a high level during the minimum solar activity year has been noted earlier in [5, 33]. Thus, the mean diurnal disturbance level at  $\phi' \sim 70 - 71^\circ$  experiences no noticeable cyclic changes, remaining  $\sim 100\gamma$  for  $K_p \leq 1$  and  $\sim 300\gamma$  for  $K_p = 3$ . In the region near

the pole  $r_K$  increases in 1964 as  $K_p$  grows. The ratio  $\bar{r}_K$  is  $\sim 2$  for  $K_p \leq 1$  and  $\sim 1$  for  $K_p = 3$  during the maximum and minimum years.

Therefore, a sufficiently intense magnetic disturbance, comparable in magnitude to the disturbance in the maximum year, is observed at high latitudes even in the year of the minimum solar activity cycle. The difference in the  $\bar{r}_K$  /160 distributions during the IGY and IQSY for all day is slight in connection with the relative redistribution of the number of intervals with  $K_p \leq 1$ ,  $K_p = 3$  and  $K_p = 5$ , and is less than two. In 1957-1958, intervals with  $K_p = 3$  appeared most often, and with  $K_p \leq 1$  in 1964.

The disturbance in the circumpolar region is magnified sharply in summer. For  $K_p \leq 1$  the  $\bar{r}_K$  is approximately identical in the whole range of latitudes  $\phi' \sim 70^\circ$ , but as  $K_p$  increases a more intense magnification of  $\bar{r}_K$  is observed at  $\phi' \sim 70^\circ$ , as compared with the polar region. All these singularities of the latitude distribution of  $r_K$  were also characteristic for the year of the maximum.

The  $S_a$  retain the basic features of the IQSY period in 1964: one maximum at night at  $\phi' \sim 65^\circ$  in winter and at  $\phi' > 80^\circ$  during the day, and two maxima in the evening and morning hours at intermediate latitudes. There is a difference in that in 1957-1958 two maxima were clearly observed in the Cape Chelyuskin observatory, while there is just one night maximum at this observatory in 1964 and a two-humped curve appears at higher latitudes. Two maxima are seen clearly at the Tikhaya Bay observatory in Figure 19. The cyclic changes in the shape of  $S_a$  at the Cape Chelyuskin observatory can be explained by the fact that the Cape Chelyuskin observatory was within the oval zone of maximum magnetic disturbance in the all-day observations in the winter of 1957-1958, and in the zone itself in 1964.

The part controlled by local time was extracted from  $S_a$  by the method described above, and space-time distributions of  $\bar{r}_K$ , presented in Figure 20 for  $K_p = 1$ ,  $K_p = 3$ , and  $K_p = 5$ , were constructed in a polar projection.

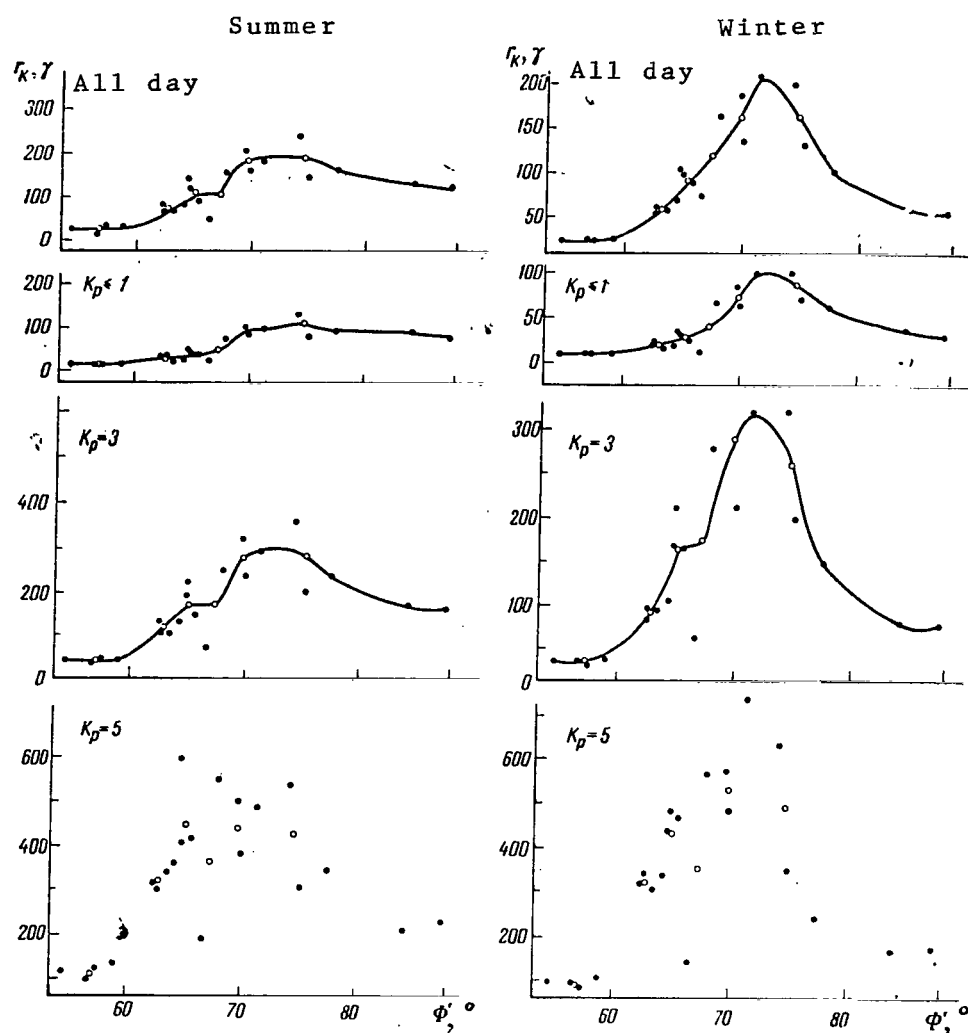


Figure 18. Latitude distribution of the mean diurnal values of magnetic activity in  $\bar{r}_K$  for winter and summer for  $K_p \leq 1$ ,  $K_p = 3$ ,  $K_p = 5$ , and all day in 1964.

Circles - mean value of  $r$  every  $2^\circ$  in  $\phi'$

The  $S_a$  data, averaged with respect to geomagnetic time for the observatories, are presented below:

/162

Nurmijarvi - Agincourt 56.9

Sodankylä - Minook 63.0

College - Reykjavik - Kiruna - Tiksi Bay 65.4

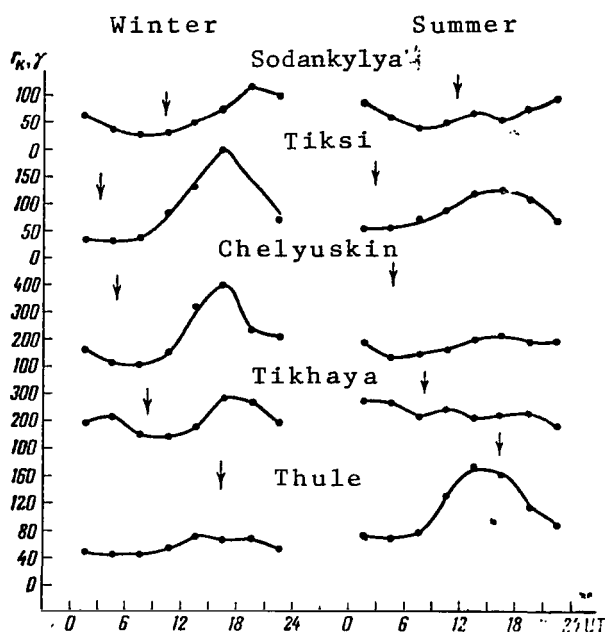


Figure 19. Diurnal changes in  $r_K$  for winter and summer according to all-day observations in 1964.

Arrows show local noon.

the position of the maximum disturbance region. The position of the oval for different  $K_p$  characterizes the dynamics of the maximum disturbance region.

Just as for the IGY period, the position and intensity of the maximum disturbance were calculated in a parabolic approximation. In contrast to the IGY (see Figure 15), when the maximum disturbance is observed at night in winter at lower latitudes as  $K_p$  increases ( $\phi' \sim 71^\circ$  for  $K_p = 1$  and  $\phi' \sim 67^\circ$  for  $K_p = 5$ ), the maximum disturbance is retained at  $70 - 71^\circ$  latitudes in the IQSY as  $K_p$  varies between 1 and 5. An analogous phenomenon was noted earlier also in the distribution of the aurora borealis [32]. The calculated position of the maximum disturbance region for all day observations in the years of the maximum and minimum solar activity cycle is presented in Figure 21. Both in winter and in summer, independently of the phase of the cycle, it is an oval in shape, located at higher latitudes in the daytime than at night. The oval is

Cape Chelyuskin - Churchill 70.6

Tikhaya Bay - Baker Lake 74.7

In addition  $S_a$  from the Godhavn and Resolute Bay observatories near the pole were utilized (without averaging).

Values of  $r_K$  of the part  $\overline{S_0} + S(t)$  are indicated along the isolines  $\phi' = \text{const}$  in Figure 20 for the corresponding three hour interval. The isolines drawn by interpolating between corresponding numerical results yield a general concept of the distribution of the magnetic activity component dependent on local time. The heavy line in the shape of an oval in the  $\phi', t'$  coordinates represents

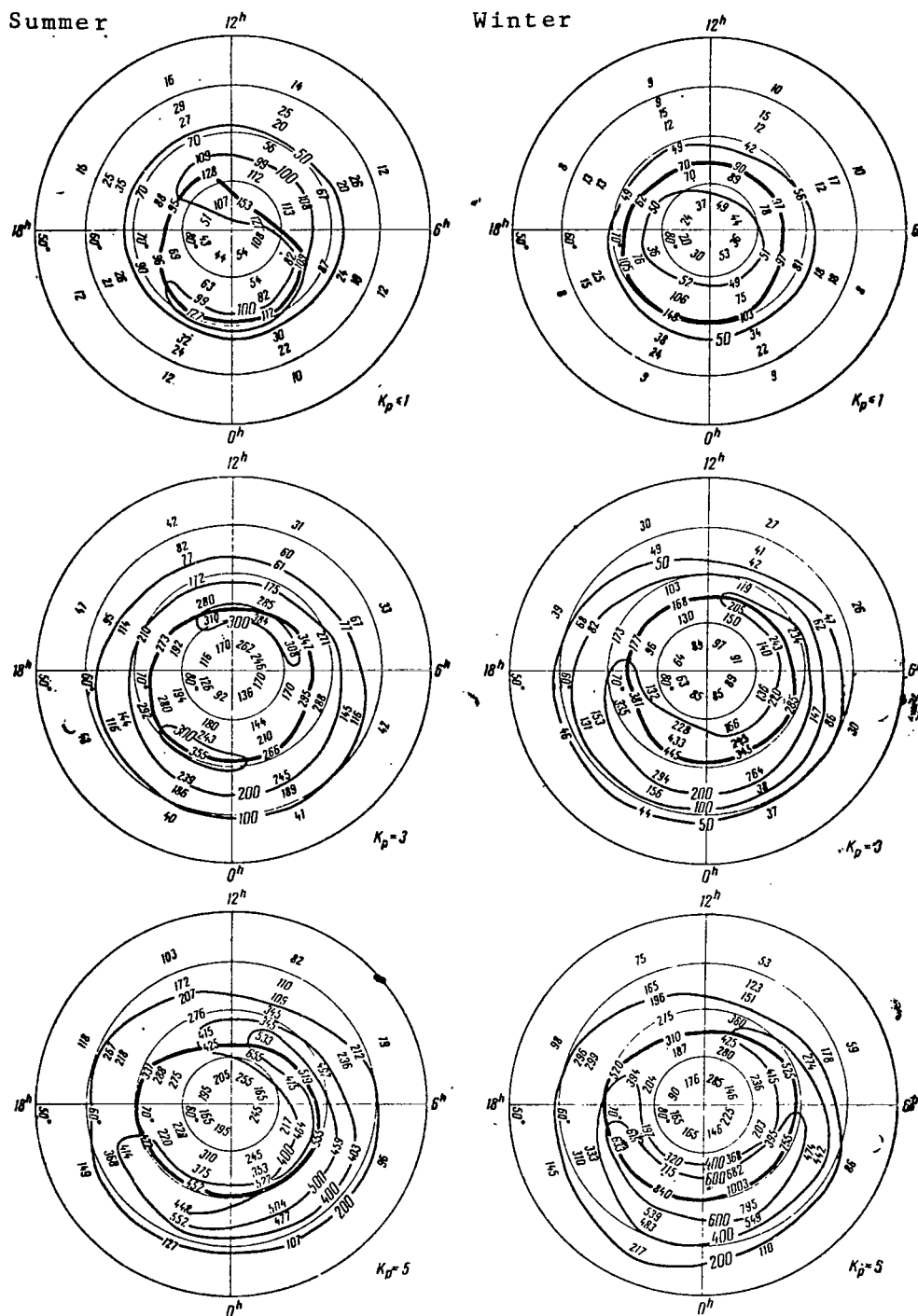


Figure 20. Changes in  $r_K$  in three-hour local geomagnetic time intervals in a polar projection for pairs of observatories. Heavy line connects points at which the disturbance is a maximum for the given three-hour interval.



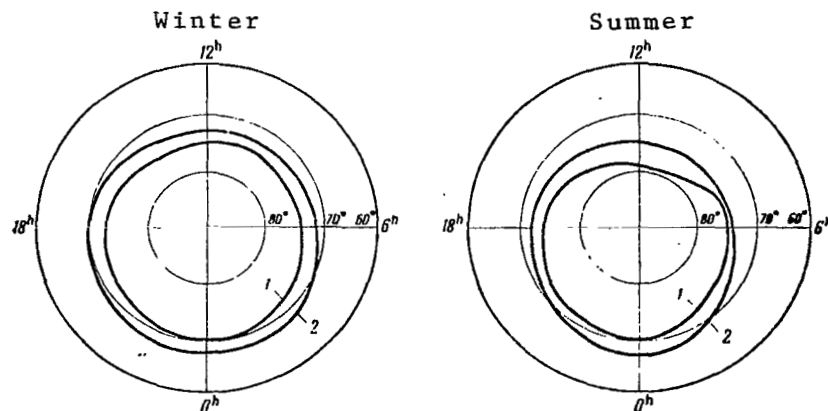


Figure 21. Location of the maximum disturbance region for all day observations in winter and summer. 1 - IQSY, 2 - IGY.

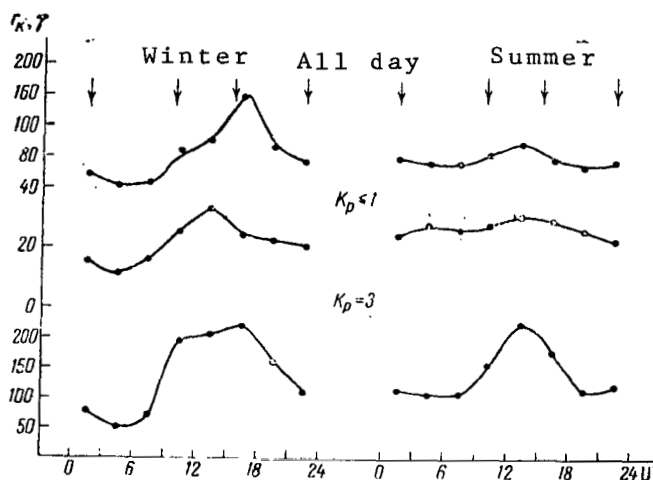


Figure 22. Averaging of  $S_a$  over chains of observatories at College, Reykjavik, Kurina, Tiksi with respect to UT. Arrows note local midnight at each observatory.

located at lower latitudes in the years of the maximum, which is explained by the predominance of disturbed intervals in these periods, characterized by larger values of  $K_p$  than the years of the minimum.

As during the IGY, the  $S(T)$  component is extracted by averaging the  $S_a$  values of the observatories with respect to universal time. In 1964, we had data of four observatories located approximately uniformly in longitude for  $\phi' \sim 65^\circ$ .

Presented in Figure 22 are results of the averaging for the winter and /163

summer seasons during the periods when there were sufficient statistics. The diurnal changes in  $r_K$  at these latitudes are of simple shape; and hence, the data from the four observatories are adequate for a reliable extraction

of the  $S(T)$  portion. In winter  $S(T)$  is at a maximum in the  $12 - 18^h$  UT range, and at  $12 - 15^h$  UT in summer. Therefore, the phase of the  $S(T)$  component changes somewhat from winter to summer. The ratio between the amplitudes of the components  $S(T)/S(t)$  changes during the solar cycle, increasing at the minimum. This agrees with the results obtained in [15]. An analysis of the winter-summer differences in  $S(T)$  verified the presence of an  $S(T)$  portion during the IQSY, which attains a maximum value at  $15 - 18^h$  UT [4].

### CONCLUSIONS

Space-time patterns of the magnetic activity during the maximum and minimum solar activity cycle are considered herein for different planetary disturbance levels and all day. The following fundamental results are obtained.

1. The magnetic activity is kept at a high level at high latitudes even in years of minimum solar activity. The mean diurnal values of  $\bar{r}_K$  are approximately identical in the IGY and IQSY at  $\phi' \sim 70^\circ$ , while their ratio depends on  $K_p$  in the region near the pole, but also is  $\sim 1$ .

2. The region of maximum values of  $\bar{r}_K$  in a "corrected geomagnetic latitude-geomagnetic time" coordinate system is oval in shape and located at higher latitudes by day and lower latitudes at night. The magnetic disturbance in the diurnal and nocturnal parts of the oval has a different physical nature by day and by night.

3. As  $K_p$  increases, the maximum disturbance region shifts towards lower latitudes, but retains its oval shape in all cases.

4. For a quiet magnetic field ( $K_p \leq 1$ ) the oval is located at  $\phi' \sim 71^\circ$  in the nighttime in winter both for IGY and IQSY. For  $K_p = 5$  in the minimum years, the oval is at  $\phi' \sim 70^\circ$ , while it is at  $\phi' \sim 67^\circ$  in the maximum years. /164

These results on the dynamics of the magnetic disturbance oval are in good agreement with the dynamics of the aurora borealis belt.

5. The oval arrangement of the maximum disturbance region is much more clearly expressed in summer than in winter.

# REFERENCES

1. Bartels, J., N. H. Heck, and H. F. Johnston. The three hour range index measuring geomagnetic activity. Terr. Magn. Atmos. Electr., Vol. 44, No. 3, 1939, p. 411.
2. Ben'kova, N. P. Diurnal magnetic activity behavior. Trudy NIIZM, No. 3 (13), 1948, p. 15.
3. Mayaud, P. N. Activité magnetique dans les regions polaires. Resultats scientifiques, expeditions Antarctiques. (Magnetic activity in the circumpolar regions. Scientific results, Antarctic expeditions, Terre Adelie, 1951 - 1952). Magnetisme Terrestre, fasc. II. Paris, 1955.
4. Mishin, V. M. On the structure and nature of the diurnal magnetic activity behavior. Trudy, IZMIRAN SSSR, No. 20 (30), 1962, p. 148.
5. Fukushima, N. Gross character of geomagnetic disturbance during the International Geophysical Year and Second Polar Year. Rept. Ionosphere Space Res. Japan. Vol. 16, No. 1, 1962, p. 37.
6. Lebeau, A. Sur l'activity magnetique diurne dans les calottes polaires. (Diurnal magnetic activity at the Polar caps). Ann. Geophys. Vol. 21, No. 2, 1965, p. 167.
7. Bazarzhapov, A. D., V. M. Mishin, E. I. Nemtsova, and O. A. Troshichev. Diurnal magnetic activity behavior during the IGY (disturbed days). In: Geomagnitnyye issledovaniya (Geomagnetic investigations), No. 8, Series "IGY Results", Moscow, Nauka, 1966, p. 63.
8. Mishin, V. M., O. A. Troshichev, and V. D. Urbanovich. Magnetic activity distribution at high latitudes. In: Geomagnitnyye issledovaniya (Geomagnetic investigations), No. 8, Series "IGY Results", Moscow, Nauka, 1966, p. 96.
9. Nikol'skiy, A. P. On the second zone of elevated magnetic disturbance intensity in the circumpolar region. Trudy AANII, Vol. 83, 1956, p. 5.
10. Nikol'skiy, A. P. On the planetary distribution of magnetic-ionospheric disturbances. Trudy AANII, Vol. 223, 1960, p. 5.
11. Burdo, O. A. On the relationships between regular and irregular variations in the geomagnetic field at high latitudes. Trudy AANII, Vol. 223, 1960, p. 21.
12. Fel'dshteyn, Ya. I. Space-time distribution of magnetic activity at high latitudes of the northern hemisphere. Geomagnetic investigations, No. 5, Series "IGY results", Moscow, AN SSSR Press, 1963.

13. Zhigalov, L. N. Neregulyarnyye magnitnyye vozmushcheniya v Antarktike (Irregular magnetic disturbances in the Antarctic). Dissertation, Leningrad, 1965.
14. Nikol'skiy, A. P. On the connection between magnetic activity and disturbances in the F2 layer of the ionosphere. Geomagnetizm i Aeronomiya, Vol. 6, No. 1, 1966, p. 40.
15. Mishin, V. M. and E. I. Nemtsova. Diurnal magnetic activity behavior during the IGY. I. S"(T) Component. Geomagnetizm i Aeronomiya, Vol. 4, No. 4, 1964, p. 1089.
16. Fukushima, N. Seasonal change of auroral zone in corrected geomagnetic latitudes. Rept. Ionosphere Space Res. Japan, Vol. 19, No. 3, 1965, p. 367. /165
17. Hultqvist, B. The geomagnetic field lines in higher approximation. Arkiv geofys., Vol. 3, No. 4, 1958, p. 63.
18. Hakura, Y. Tables and maps of geomagnetic coordinates corrected by higher order spherical harmonic terms. Rept. Ionosphere Space Res. Japan, Vol. 19, No. 2, 1965, p. 121.
19. Nagata, T., and S. Kokubun. An additional geomagnetic daily variation field, ( $S_q^p$ -field) in the polar region on geomagnetically quiet day. Rept. Ionosphere Space Res. Japan, Vol. 16, No. 2, 1962, p. 256.
20. Bobrov, M. S. Total planetary picture of geomagnetic disturbances of corpuscular origin. In: Solnechnyye korpuskulyarnyye potoki, lokalizatsiya ikh istochnikov i svyaz' s geomagnitnymi vozmushcheniyami (Solar corpuscular fluxes, localization of their sources, and connection with geomagnetic disturbances). No. 1, Series "IGY Results", AN SSSR Press, 1961.
21. Zaytsev, A. N., and Ya. I. Fel'dshteyn. Quiet solar diurnal variations during the IGY. Present collection, p. 128.
22. Fel'dshteyn, Ya. I. Geographic distribution of aurora borealis and arc azimuths. In: Polyarnyye siyaniya i svecheniye nochnogo neba (Aurora Borealis and Glow of the Night Sky), No. 4, Series "IGY Result", Moscow, AN SSSR Press, 1960, p. 62.
23. Fel'dshteyn, Ya. I. Some questions on the morphology of aurora borealis and magnetic disturbances at high latitudes. Geomagnetizm i aeronomiya, Vol. 3, No. 2, 1963, p. 227.
24. Khorosheva, O. V. Diurnal drift of a closed ring of aurora borealis. Geomagnetizm i aeronomiya, Vol. 2, No. 5, 1962, p. 839.

25. Akasofu, S. I. The auroral oval, the auroral substorm and their relations with the internal structure of the magnetosphere. Planet Space Sc., Vol. 14, No. 7, 1966, p. 587.
26. Nikol'skiy, A. P. On the dependence of the mean magnetic activity level on latitude and longitude. In: Problemy Arktiki i Antarktiki (Problems of the Arctic and Antarctic), No. 3, 1960, p. 85.
27. IAGA Bulletin, No. 12, 1961 - 1962.
28. Belousova, M. A. Mery magnitnoy aktivnosti (Magnetic Activity Measurements) Manuscript. IZMIRAN, 1962.
29. Mansurov, S. M., and L. G. Mansurova. Atlas Antarktiki (Antarctic Atlas). Vol. I, "Terrestrial Magnetism" Division, 1966.
30. Starkov, G. V., and Ya. I. Fel'dshteyn. Dynamics of the oval auroral zone. Geomagnetizm i aeronomiya, Vol. 7, No. 1, 1967, p. 62.
31. Fel'dshteyn, Ya. I. and G. V. Starkov. Dynamics of auroral belt and polar geomagnetic disturbances. Planet. Space Sci., Vol. 15, No. 2, 1967, p. 209.
32. Fel'dshteyn, Ya. I., N. F. Shevnina, and L. V. Lukina. Aurora borealis in magnetically disturbed and magnetically quiet periods. Geomagnetizm i aeronomiya, Vol. 6, No. 2, 1966, p. 312.
33. Milyayev, N. A. On the mean magnetic disturbance level in the Central Arctic. In: Problemy Arktiki i Antarktiki (Problems of the Arctic and Antarctic). No. 12, 1963.

NATIONAL AERONAUTICS AND SPACE ADMINISTRATION

WASHINGTON, D. C. 20546

OFFICIAL BUSINESS

PENALTY FOR PRIVATE USE \$300

FIRST CLASS MAIL



POSTAGE AND FEES PAID  
NATIONAL AERONAUTICS AND  
SPACE ADMINISTRATION

09U 001 38 51 3DS 71166 00903  
AIR FORCE WEAPONS LABORATORY /WL0L/  
KIRTLAND AFB, NEW MEXICO 87117

ATT E. LOU BOWMAN, CHIEF, TECH. LIBRARY

POSTMASTER: If Undeliverable (Section 158  
Postal Manual) Do Not Return

*"The aeronautical and space activities of the United States shall be conducted so as to contribute . . . to the expansion of human knowledge of phenomena in the atmosphere and space. The Administration shall provide for the widest practicable and appropriate dissemination of information concerning its activities and the results thereof."*

— NATIONAL AERONAUTICS AND SPACE ACT OF 1958

## NASA SCIENTIFIC AND TECHNICAL PUBLICATIONS

**TECHNICAL REPORTS:** Scientific and technical information considered important, complete, and a lasting contribution to existing knowledge.

**TECHNICAL NOTES:** Information less broad in scope but nevertheless of importance as a contribution to existing knowledge.

**TECHNICAL MEMORANDUMS:**  
Information receiving limited distribution because of preliminary data, security classification, or other reasons.

**CONTRACTOR REPORTS:** Scientific and technical information generated under a NASA contract or grant and considered an important contribution to existing knowledge.

**TECHNICAL TRANSLATIONS:** Information published in a foreign language considered to merit NASA distribution in English.

**SPECIAL PUBLICATIONS:** Information derived from or of value to NASA activities. Publications include conference proceedings, monographs, data compilations, handbooks, sourcebooks, and special bibliographies.

**TECHNOLOGY UTILIZATION PUBLICATIONS:** Information on technology used by NASA that may be of particular interest in commercial and other non-aerospace applications. Publications include Tech Briefs, Technology Utilization Reports and Technology Surveys.

*Details on the availability of these publications may be obtained from:*

**SCIENTIFIC AND TECHNICAL INFORMATION OFFICE**

**NATIONAL AERONAUTICS AND SPACE ADMINISTRATION**

**Washington, D.C. 20546**